12

AFWAL-TR-84-2001

LUBRICANT FOAMING AND AERATION STUDY, PART I

Sydney Ross

Rensselaer Polytechnic Institute
Troy NY 12181

April 1984

Final Report for Period September 1980 - August 1983

Approved for Public Release; Distribution Unlimited

AERO PROPULSION LABORATORY
AIR FORCE WRIGHT AERONAUTICAL LABORATORIES
AIR FORCE SYSTEMS COMMAND
WRIGHT-PATTERSON AIR FORCE BASE OH 45433

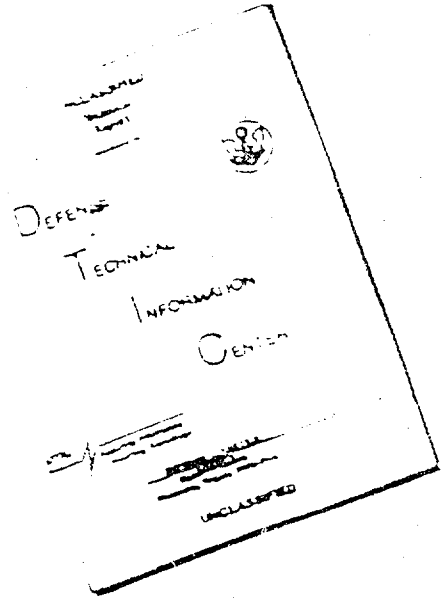
Defense
Technical
Information
Center
UNCLASSIFIED

NOTICE

This report has been reviewed by the Office of Public Affairs (ASD/PA) and is releasable to the National Technical Information Service (NTIS). At NTIS, it will be available to the general public, including foreign nations.

This technical report has been reviewed and is approved for publication.

Phillip W. Centers	Howard F. Jones
PHILLIP W. CENTERS	HOWARD F. JONES
Project Engineer	Chief, Lubrication Branch

FOR THE COMMANDER

Robert D. Sherrill

ROBERT D. SHERRILL
Chief, Fuels and Lubrication Division

UNCLASSIFIED
SECURITY CLASSIFICATION OF THIS PAGE

REPORT DOCUMENTATION PAGE

1a. REPORT SECURITY CLASSIFICATION
UNCLASSIFIED

1b. RESTRICTIVE MARKINGS

2a. SECURITY CLASSIFICATION AUTHORITY

2b. DECLASSIFICATION/DOWNGRADING SCHEDULE

3. DISTRIBUTION/AVAILABILITY OF REPORT
Approved for public release; distribution unlimited.

4. PERFORMING ORGANIZATION REPORT NUMBER(S)

5. MONITORING ORGANIZATION REPORT NUMBER(S)
AFWAL-TR-84-2001

6a. NAME OF PERFORMING ORGANIZATION
Rensselaer Polytechnic Inst.

6b. OFFICE SYMBOL (If applicable)

7a. NAME OF MONITORING ORGANIZATION
Aero Propulsion Laboratory (AFWAL/POSL)
Air Force Wright Aeronautical Lab (AFSC)

6c. ADDRESS (City, State and ZIP Code)
Troy, N.Y. 12181

7b. ADDRESS (City, State and ZIP Code)
Wright-Patterson Air Force Base, OH 45433

8a. NAME OF FUNDING/SPONSORING ORGANIZATION

8b. OFFICE SYMBOL (If applicable)

9. PROCUREMENT INSTRUMENT IDENTIFICATION NUMBER
F33615-80-C-2017

8c. ADDRESS (City, State and ZIP Code)

10. SOURCE OF FUNDING NOS.

PROGRAM ELEMENT NO.	PROJECT NO.	TASK NO.	WORK UNIT NO.
62203F	3048	06	14

11. TITLE (Include Security Classification)
LUBRICANT FOAMING AND AERATION STUDY, PART I

12. PERSONAL AUTHOR(S)
Sydney Ross

13a. TYPE OF REPORT
Final

13b. TIME COVERED
FROM 80/9/1 TO 83/8/31

14. DATE OF REPORT (Yr., Mo., Day)
83/11/23

15. PAGE COUNT
220

16. SUPPLEMENTARY NOTATION

17. COSATI CODES

FIELD	GROUP	SUB. GR.
11	08	
14	02	

18. SUBJECT TERMS (Continue on reverse if necessary and identify by block number)
Foam Aeration Lubricant Foam Testing
Lubrication Surface Viscosity Surface Tension

19. ABSTRACT (Continue on reverse if necessary and identify by block number)

This research is directed toward the investigation of the mechanisms associated with lubricant foaming and aeration. Theories of the cause of foaming were reviewed, for the purpose of testing the applicability of suggested mechanisms to the present problem. The experimental studies were of basestock ester and ester-additive systems. The foaming of these systems was investigated with respect to the following variables or conditions: temperature; viscosity of the bulk liquid; viscosity of the surface layer; solubility of additives; mixtures of additives; surface-tension lowering at equilibrium; surface-tension changes on expansion or contraction of surface; rate of gas injection; gas solubility; geometrical shape of the foam container; and electrical properties. Results obtained demonstrate that total additive concentration and synergistic effects of additives are important variables, either affecting the surface tension under dynamic conditions, or promoting electrical surface potentials, both of which effects conduce to the foaminess of ester solutions.

20. DISTRIBUTION/AVAILABILITY OF ABSTRACT
UNCLASSIFIED/UNLIMITED ☒ SAME AS RPT. ☐ DTIC USERS ☐

21. ABSTRACT SECURITY CLASSIFICATION
UNCLASSIFIED

22a. NAME OF RESPONSIBLE INDIVIDUAL
PHILLIP W. CENTERS

22b. TELEPHONE NUMBER (Include Area Code)
(513)255-6608

22c. OFFICE SYMBOL
AFWAL/POSL

EDITION OF 1 JAN 73 IS OBSOLETE.

UNCLASSIFIED

PREFACE

This final report contains the results of an effort to investigate foaminess and gas retention of turbine-engine lubricants to obtain a fundamental understanding of the causes of such effects. The work was performed in the Colloid and Surface Chemistry Laboratories, Department of Chemistry, Rensselaer Polytechnic Institute, Troy, N.Y. 12181, by Professor Sydney Ross, Dr Yaakov Suzin, Mr D.F. Townsend, and Mrs Tammar Suzin during the period September 1980 to August 1983. The effort was sponsored by the Aero Propulsion Laboratory, Air Force Wright Aeronautical Laboratories, Air Force Systems Command, Wright-Patterson AFB, Ohio, under Contract F33615-80-C-2017. The work was accomplished under Project 3048, Task 304806, Work Unit 30480614, Foaming and Aeration Characteristics of Turbine Lubricants, with Mr H.A. Smith and Mr Phillip W. Centers as Project Engineers.

TABLE OF CONTENTS

LIST OF ILLUSTRATIONS

FIGURE PAGE

FIGURE PAGE

FIGURE PAGE

FIGURE PAGE

FIGURE PAGE

FIGURE PAGE

FIGURE PAGE

LIST OF TABLES

SECTION I

INTRODUCTION

In the functioning of a lubricating oil in engines and in various types of other mechanisms, it is not unusual to come across the formation of oil foam. Severe foaming of a turbine-engine lubricant can lead to breakdown of the normal operation of aircraft lubricating systems. Difficulties that can arise include fluctuations of oil pressure, oil-pump cavitation, decrease in lubrication and cooling efficiencies and, in extreme cases, loss of oil overboard through the breathers. Therefore, measures to combat foam are necessary. The problem has proved to be stubborn, as different types of oil respond differently to antifoam additives; and it is further complicated by the presence of proprietary compounds (additives) used to enhance lubricity, thermal stability, and extreme-pressure characteristics of the oils. These additives include oxidation inhibitors, viscosity-index improvers, pour-point depressants, dispersing agents and oil-soluble detergents. In addition, in order to neutralize corrosive acids, which are produced by the burning of petroleum fuels, colloidal dispersions of alkali-earth carbonates, in which the particles are stabilized by adsorbed layers of surface-active agents, are sometimes provided in mineral oils. Furthermore, oils can change during use or even during storage and produce undesirable results: in some cases used or stored oils have lost their antifoam additives; again, the oils may leach out organic products from sealants and elastomers, or they may generate oxidized or decomposition products that cause foaming. As the outcome of so many different causes, the problem of foam presents itself frequently. The basic mechanisms of foam formation, foam collapse, and foam inhibition are not sufficiently well understood to anticipate problems, to diagnose difficulties and to develop lubricants with improved foam properties. Unless such an understanding is reached of the fundamental principles that govern foam formation in a solution, each problem as it arises has to be tackled *de novo*. The purpose of this research project is to study the basic mechanisms that affect and control the foaming of turbine-engine lubricants.

The experimental approach is to select a typical synthetic lubricant and then to discover circumstances that cause it to foam. The nature of the foam thus produced is then to be studied as a function of pertinent variables, such as temperature, or the presence and amount of contaminants or additives present. The altered physical properties of the lubricant introduced by these controlled conditions are next to be studied, guided by the best available theories of the stability of liquid films, to find possible correlations with, and hence causes for, the formation and stabilization of foam.

SECTION II

LITERATURE SURVEY

1. Rayleigh-Gibbs Theory of Foam

Pure liquids do not form stable foams, but allow entrained air to escape with no delay other than what is inseparable from the Stokesian rate of rise, which is controlled by the diameter of the bubble of dispersed air and the viscosity of the bulk liquid. Certain solutes are able to stabilize thin sheets (or lamellae) of liquid: if these solutes are present the escape of entrained bubbles is more or less retarded, and a head of foam is produced. Theories of foam postulate plausible mechanisms to account for this behavior, with the ultimate objective of understanding the phenomenon so thoroughly that predictions can be made about expected behavior of a given solute prior to actual observation. One may say at the outset that this final goal is not yet completely attained.

The earliest of these theories, the one usually designated the Rayleigh-Gibbs theory[1, 2] has best withstood criticism through the years. This theory refers the stability of foam to an elasticity or restoration of liquid lamellae, which depends on the existence of an adsorbed layer of solute at the liquid surface and the effect of this adsorbed layer in lowering the surface tension of the solution below that of the solvent. The two effects, surface segregation, or adsorption, and the lowering of the surface tension, are concomitant: a reduction of surface tension due to the addition of a solute is evidence, admittedly indirect but no less certain than were it given by direct observation, that the solute is segregated at the surface. The degree of the segregation is measured as excess moles of solute per square centimeter of surface, designated Γ_2 , and is proportional to the variation of the surface-tension lowering with concentration of solute; i.e.,

$$\Gamma_2 = d\Pi / RT\ d\ \ln a_2 \qquad [1]$$

where Π is the lowering of the surface tension caused by a thermodynamic activity a_2 of solute in the solution. Equation [1] is based on thermodynamics, derived for a two-component system. In this report, the term "surface-active solute" denotes a solute that reduces the surface tension of a liquid to any appreciable extent, even by as little as 1 mN/m.

When local areas of a foam lamella are expanded, as would happen for example when a bubble of air pushes through a liquid surface, new areas of surface are created where the instantaneous surface tension is large, because the adsorbed layer has not had sufficient time to form. The greater surface tension in these new areas of surface exerts a pull on the adjoining areas of lower tension, causing the surface to flow toward the region of greater tension. The viscous drag of the moving surface carries an appreciable volume of underlying liquid along with it, thus offsetting the effects of both hydrodynamic and capillary drainage and restoring the thickness of the lamella.[3] Gibbs elasticity is defined as the ratio of the increase in the tension resulting from an infinitesimal increase in the area and the relative increase of the area. For a lamella with adsorbed solute on both sides, the elasticity E is given by:[4]

$$E = 2\, d\sigma / d \ln A \qquad [2]$$

where σ is the surface tension and A is the area of the liquid surface. The factor 2 is required because the stretching of the lamella increases the area on both of its sides.

In general, the elasticity arising from the variation of the surface tension during deformation of a liquid lamella may be manifested both in equilibrium (when a surface layer under forces leading to deformation is in equilibrium with its bulk phase) and in non-equlibrium conditions. The first case refers to the Gibbs elasticity and the second to the Marangoni elasticity.[5] The Marangoni elasticity is a dynamic, non-equilibrium property, normally larger in value than the Gibbs elasticity that could be obtained in the same system.

Attempts to test equation [2] have been made by measuring the dynamic (i.e., non-equilibrium) surface tension as the surface of a solution is abruptly extended, or pulsated. Some investigators have found dynamic surface tensions occurring at rather low frequencies of dilatation-compression cycles, from one per minute to one every thirty minutes; others[6] have used frequencies as high as 15 to 135 Hz (cycles/second), although such disturbances are far from corresponding to the expansion-contraction cycles occurring in an actual foam. The measurement must be made coincidentally with the extension of the surface. Quite a different measurement is the rate of decline of the surface tension of the undisturbed liquid surface with time. This property may be less significantly related to foam stability: the times required for equilibrium to be established at the surface are often so long compared to the lifetime of a bubble, that they can have little relevance to the phenomenon of foam creation and decay.

The Rayleigh-Gibbs theory depends therefore on a combination of two physical properties of the solution: the solute should be capable of lowering the surface tension of the medium; but this alone is not enough: a rate process is also required, by which a freshly created liquid surface retains its initial, high, non-equilibrium surface tension long enough for surface flow to occur. Many instances are known in which the mere reduction of surface tension by the solute does not lead to the stabilization of foam, presumably because it is not accompanied by the relatively slow attainment of equilibrium, after a fresh surface is made, which is the second requirement for the ability to stabilize bubbles.

The foregoing theory was developed bearing in mind chiefly the behavior of aqueous solutions; but water is a peculiar solvent inasmuch as its high surface tension depends upon hydrogen bonding between molecules, and so is readily reduced in the presence of solutes that are not able to take part in hydrogen bonding with water molecules, and that, as a result, interfere with and disrupt the hydrogen bonding between the water molecules. An oil solvent, lacking the ability to hydrogen bond, at least to the same degree, and so unable to produce the same effects, has a lower surface tension than water: the presence of a solute therefore does not usually reduce the surface tension of an oil, even though the solvent molecules may be only partially able to enter into an heteromolecular interaction with the solvent molecules. If a change of conditions, either of concentration or of temperature, decreases the heteromolecular interaction the solute will approach phase separation; and as a portent of its insolubility will begin to segregate at the surface and to manifest surface activity. (This behavior is named Lundelius' Rule.) But even then, the overt manifestation of surface activity, that is, the reduction of the surface tension, is not as pronounced in oil solutions as in aqueous solutions. Dilatation of the surface of an oil solution would not, therefore, create as pronounced a dilution of the surface concentration of the solute, with its consequent increase of surface tension, as is observed in aqueous solutions of adsorbed solutes. What has been reduced only slightly in the first instance cannot be expected to increase by much when conditions are reversed. In oil solutions, however, contraction of a surface in which a solute is adsorbed does much more to magnify the effect of its presence than does expansion; for while there is barely any scope for the surface tension to rise, there is less limitation for it to decline. Liquid lamellae of oil solutions, therefore, typically manifest elasticity on contraction; whereas with aqueous solutions, the elasticity of lamellae is manifest typically on dilatation.

2. Enhanced Viscosity or Rigidity at the Liquid-Gas Interface

A single surface-active species in solution does not usually confer any increase of the viscosity, much less rigidity, in the surface layer of the solution. Although foam is capable of being produced by such a solute, the foam is of brief duration. That kind of foam is called "evanescent foam," but it can nevertheless be a cause of concern; because if produced rapidly it can reach a large expansion ratio and so flood any container. Much more stable foam is created if, in addition to the Rayleigh-Gibbs effect described above, the surface layer of the solution has an enhanced viscosity or rigidity.[7] This phenomenon is known to occur in water with certain mixtures of solutes or with certain polymers, both natural and synthetic. The best known examples in aqueous systems are solutions of water-soluble proteins, such as casein or albumen. Common examples are the stable foams produced with whipping cream, egg white, beer, or rubber latex. In many other examples the highly viscous surface layer is made by having present one or more additional components in the solution. An example is the increase in surface viscosity of a mixture of tannin and heptanoic acid in aqueous solution, compared to the effect of the two constituents separately. In non-aqueous liquids, particularly in bunker oils and crude oils, surface layers of high viscosity have been observed; porphyrins of high molecular weight have been indicated as a possible source of this effect. In a hydrocarbon lubricant, the additive calcium sulfonate, for example, has been identified as creating a plastic skin (or two-dimensional Bingham body) at the air interface; it also acts as a foam stabilizer.[8] These viscous or rigid layers in non-aqueous liquids enhance the stability of foam, just as they do in aqueous solutions.[9,10,11]

Different kinds of surface viscosity are also distinguished:

a. Innate surface viscosity: This viscosity is the resistance to flow that is innately associated with the presence of a liquid surface, whether or not there are additional sources of resistance such as those described below.[12]

b. Surface-shear viscosity: This viscosity is associated with the presence of a pellicle or skin, such as an insoluble monolayer, but not restricted to that example, at the liquid surface. A layer of denatured protein that stabilizes the foam of meringue, or of whipped cream, or of beer, is a common example.

c. Dilatational or compressional viscosity: The surface elasticity that arises from local differences of surface tension is simultaneously associated with a resistance to surface flow. The local difference of surface tension is caused by dilatation or compression of the surface of the solution, so the resistance to flow that results from Marangoni counterflow is known as dilatational (or compressional) surface viscosity.

3. Mutual Repulsion of Overlapping Double Layers

The adsorption of ionic surfactants into the surface layer is evident in aqueous solutions and readily leads to the formation of charged surfaces of the lamellae in foams.[13] The counter-ions in the liquid interlayer of the lamella are the compensating charges. When the thickness of the lamella is of the order of magnitude of twenty times the Debye thickness of the electrical double layer, the counter-ions adjacent to the two opposite surfaces repel each other more or less according to an exponential decline of electric potential with distance. This repulsion prevents further thinning of the lamella, and so preserves it from imminent rupture.

The mechanism of charge separation that operates in water cannot occur in non-ionising solvents. Until relatively recently the conclusion was maintained, therefore, that electrostatic repulsion of overlapping electrical double layers could not be a factor in the stabilizing of liquid lamallae in oil foams. But we now recognize that other mechanisms of charge separation are possible, and indeed must operate; for zeta potentials of 25 to 125 millivolts have been observed for various kinds of particle dispersed in non-aqueous media of low conductivity.

Nevertheless no evidence has yet been reported to suggest that foam may be stabilized by charged surfaces in non-aqueous solutions.

4. Effect of Dispersed Particles on Foam Stability

It was found experimentally by Ottewill *et al.*[14] that the presence of colloidally stable, suspended, solid particles increases the tendency to form stable foams over and above that of the matrix in the absence of such particles. The increase in foam stability is linked to the increased bulk viscosity of the dispersion with solids content, which is described by a relation of the following form:

$$\eta_d = \eta_0 \, (1 + k_1 \phi + k_2 \phi^2 \ldots .) \qquad [3]$$

where η_0 = viscosity of the liquid matrix, η_d = viscosity of the dispersion, and ϕ = volume fraction of dispersed solid. The coefficient k_2 was larger than predicted by purely hydrodynamic factors, being enhanced by the electrostatic repulsions between the solid particles, which effectively enlarges each particle and so creates a larger volume fraction of solids than is calculated from the density of the solid. In addition, the presence of a minimum in the pair-interaction energy curve introduces some association between the particles with increase in volume fraction, which leads to a viscosity enhancement at the low rates of shear experienced in a slowly draining lamella. The effect of bulk-dispersion viscosity on the ripples formed in the lamella surface by thermal fluctuations is not known with certainty, but it seems likely that this would have a damping effect on the magnitude of the ripples and thus lead to further enhancement of foam stability.

5. Solution Theory of Surface Activity

While accepting the Rayleigh-Gibbs theory as an operative mechanism underlying the stability of liquid lamellae, it still gives no guidance to the character of a surface-active solute. To that end a theory of solubility is required.[15,16] Solution occurs when solute-solvent interaction (or adhesional force) is strong enough to overcome the cohesion of the solvent molecules to themselves and the cohesion of solute molecules to themselves. When adhesional forces are markedly larger than cohesional forces, negative deviations from Raoult's law are observed, and the two components are found to be miscible in all proportions. Such a condition is not conducive to surface activity, as solute has a lower potential energy (i.e., more interaction) in the bulk-phase solution than in the surface-phase solution. But when the adhesional forces are weaker than cohesional forces, the position is reversed; and the solute does not have its lowest potential energy in the bulk-phase solution. This condition offers a possibility for surface activity, as there is now an opportunity for more adhesional interaction with the solvent in the surface-phase solution than in the bulk-phase solution. We look, therefore, according to this theory, for positive deviations from Raoult's law as the first indicator of potential surface activity. If the positive deviations from Raoult's law are large, the system of solvent + solute may separate into two immiscible solutions. In such systems of partial miscibility were found correlations between surface activity, composition, and temperature. The partial miscibility by itself is not the cause of the surface activity, but is merely an indicator of the presence of positive deviations from Raoult's law, which in turn may also be considered as an indicator of weak adhesional forces between solvent and solute molecules.

This theory has promising and still unexplored corollaries. A binary system consisting of a Lewis acid and a Lewis base would have large adhesional interaction and so would lead to negative deviations from Raoult's law. This has been observed, for example, with the systems: chloroform (Lewis acid) + acetone (Lewis base); methyl ether (Lewis base) + hydrogen chloride (Lewis acid); pyridine (Lewis base) + acetic acid (Lewis acid); and water (Lewis base) + formic, nitric, hydrochloric, or hydrobromic acids (Lewis acids.) These solutions all show negative deviations from Raoult's law, and so would not be expected to have any significant surface activity. On the other hand, the combination of two Lewis acids or two Lewis bases leads to weak adhesional interaction and so is conducive to surface activity. The synthetic esters used as lubricants are weak Lewis bases and we should therefore be on the lookout for the possibility of surface activity (and foaminess) when they are combined with additives that are also Lewis bases. A future activity is the identification of lubricant additives in terms of Lewis acids or bases.[17]

SECTION III

STUDIES INVOLVING POLYDIMETHYLSILOXANE

Most of the studies performed to date have been on the synthetic lubricant ester designated Base Stock 704, which is a practical grade of trimethylolpropane heptanoate (a more systematic name would be 2-2-diheptanoyloxymethyl-*n*-butyl heptanoate) and mixtures of this ester with various additives. This ester is designated tmp-heptanoate in this report.

1. Physical Properties of Tmp-Heptanoate.

Physical properties of interest to us are: (a) The variation of density with temperature, which is reported in Figure 1, along with a comparison of the same property of water. (b) The variation of the surface tension with temperature, which is reported in Figure 2. (c) The variation of the viscosity with temperature, which is reported in Figure 3.

2. Solubilities of Polydimethylsiloxane in Tmp-Heptanoate

Measurements of solubilities of polydimethylsiloxane fractions, by whatever techniques they are determined, are subject to a peculiarity of the material, namely, that if the range of molecular weights in the sample is too wide, the higher members will register insolubility while the lower members will not yet have reached their saturation solubility. Consequently at concentrations well above the apparent solubility limit, some fraction of the material continues to be extracted into the solution. We have observed the effects of this phenomenon in the foaminess data, where the foaminess increases with concentration of added polydimethylsiloxane, although the latter is well above its apparent limit of solubility. If this had been a single molecular species the foaminess would have become constant when maximum solubility was reached, leaving out of account the possible foam-inhibiting effects of the insoluble residue.

The determination of solubility is important because it is normally related to surface activity and hence to foaminess. As a solute that interacts only slightly with the solvent approaches its solubility limit it tends to concentrate in the surface phase in preference to the bulk phase; because in the surface region more interaction with the solvent is possible. The concentrating of solute in the surface phase is a manifestation of surface activity; and to a close first approximation it is accompanied by an increase of foaminess. As soon as nucleation and separation of solute occurs, the dispersed phase, if it is of lower surface tension than the medium, may act to inhibit foam. We have yet to find the proper conditions for this behavior with polydimethylsiloxane in tmp-heptanoate solutions; in fact we observe an increase in foaminess as concentrations are increased even beyond the solubility-point limit. This behavior may be explained by two effects: the increase in concentration in the solution of soluble polydimethylsiloxane of low molecular weight and the failure of the

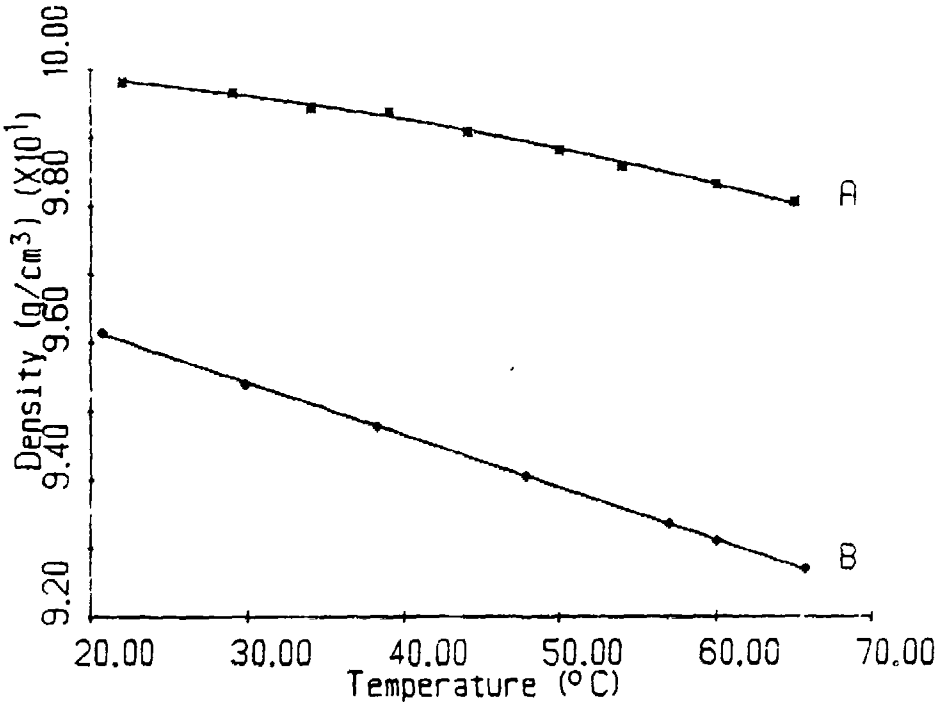

Figure 1 Variation of Density with Temperature for (A) Water and (B) Tmp-Heptanoate

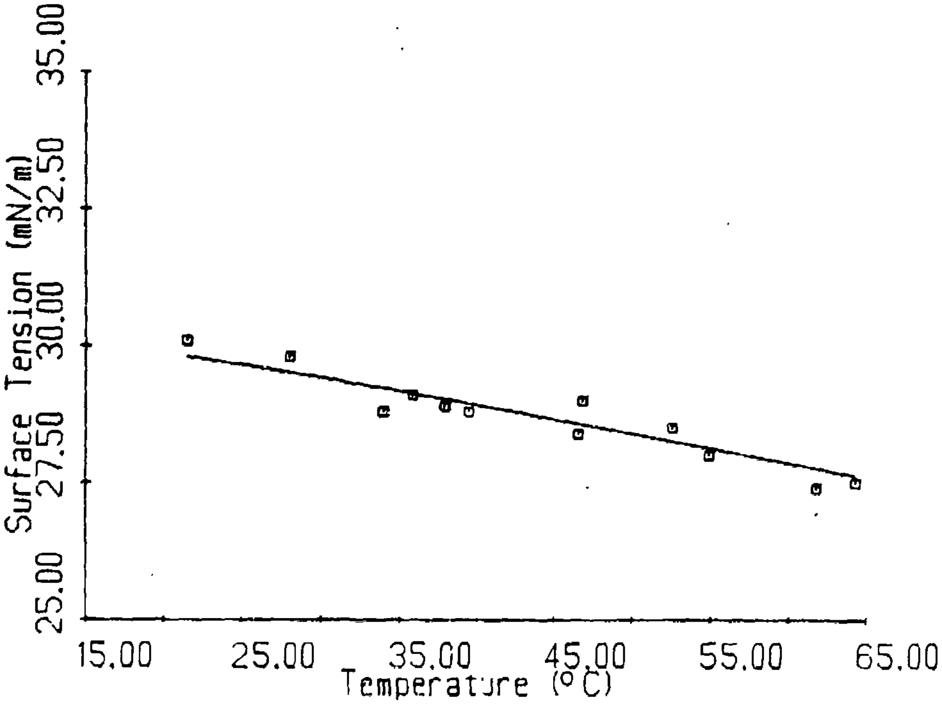

Figure 2 Variation of Surface Tension with Temperature for Tmp-Heptanoate

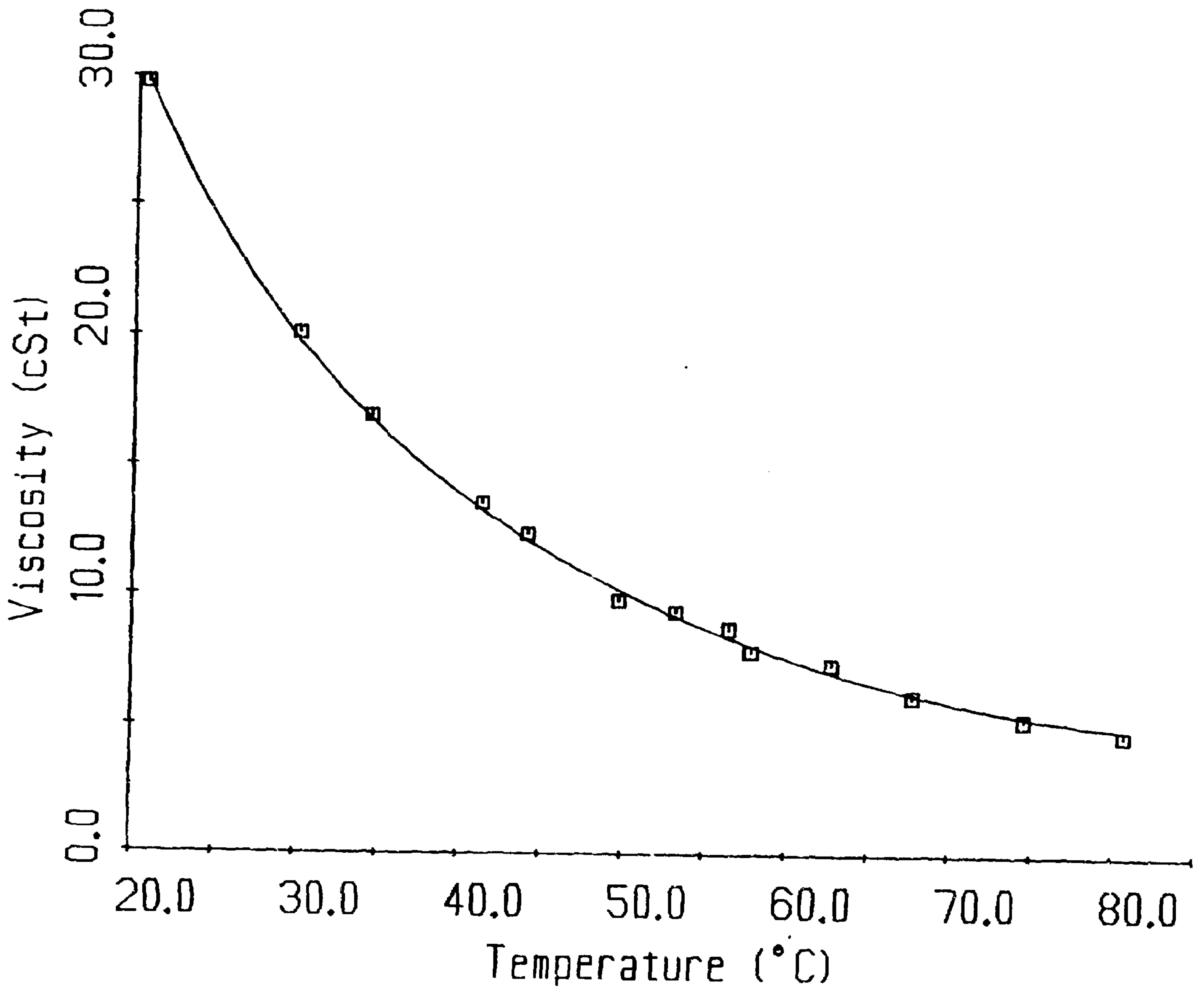

Figure 3. The Kinematic Viscosity (CentiStokes) of Tmp-Heptanoate, from 20 to 80°C

insoluble polydimethylsiloxane to behave as an antifoam because of its unsuitable degree of dispersion. Polydimethylsiloxane, or silicone oil, is a linear polymer that can be obtained commercially in a number of different viscosities. Each such sample is not of uniform molecular weight, but represents a distribution of molecular weights. The number average molecular weight of the mixture is related to the kinematic viscosity by the equation:

$$\log \text{viscosity (centiStokes at } 25^{\circ}\text{C)} = 1.00 + 0.0123\ M^{1/2} \qquad [4]$$

This equation is reported to be reasonably valid for values of M above 2500.[18] Values of M calculated by this equation for some of the samples of polydimethylsiloxane used in this work are reported below:

Viscosity in cSt at 25°C	Number average mol. wt.
500	19,000
1000	26,000
10,000	60,000

The solubility in tmp-heptanoate of various polydimethylsiloxane fractions, distinguished from each other by the value of their kinematic viscosity, was determined by means of the Faraday-Tyndall effect (scattered light) and is reported in Figure 4. The solubility decreases with increasing molecular weight. Tmp-heptanoate to which various amounts (volume percent) of toluene have been added makes a better solvent, as is also shown in Figure 4.

The variation with temperature of the solubilities in tmp-heptanoate of polydimethylsiloxane fractions of 500, 1000, and 5000 centiStokes viscosity is reported in Figure 5.

3. Foaminess of Polydimethylsiloxane in Tmp-Heptanoate

When dissolved in tmp-heptanoate, polydimethylsiloxane of low molecular weight is a surface-active solute. This fact is demonstrated in Figure 6, which shows the variation with temperature of the surface tension of a solution of polydimethylsiloxane (100 centiStokes viscosity) in tmp-heptanoate at a concentration of 30 ppm. The curve for the solution lies below that of the solvent, showing a lowering of the surface tension by about 6 mN/m at temperatures between 35°C and 85°C.

Although polydimethylsiloxane is a foam inhibitor in hydrocarbon lubricants, it only acts as such when it is present at concentrations above its solubility limit, and even then only when it is suitably dispersed. In the absence of the foam inhibiting action of the insoluble fraction, which has not shown up yet in our experiments in tmp-heptanoate, we find the following:

Solutions of various concentrations of polydimethylsiloxane (1000 centiStokes) in tmp-heptanoate, in the range of 53 to 646 ppm were tested for foam with an apparatus consisting of a 60x3 cm jacketed glass cylinder having a flat chromatographic glass frit of 3.00 cm diameter at the bottom. Foam was generated with nitrogen

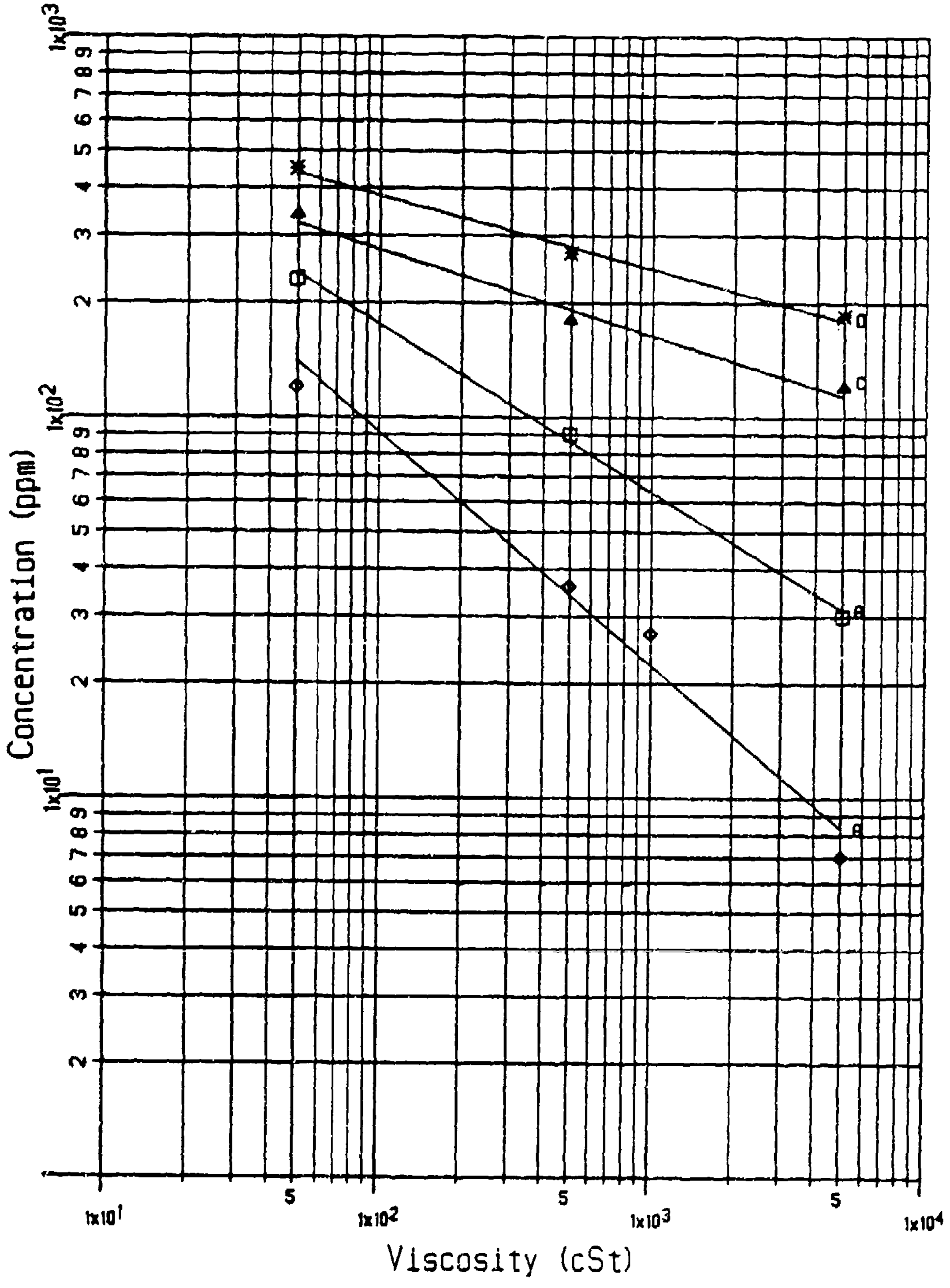

Figure 4 Variation of Solubility of Polydimethylsiloxane in Various Solvents at 20°C as a Function of its Kinematic Viscosity. Solvents are: A = Tmp-Heptanoate; B = Tmp-Heptanoate containing 10% Toluene (v/v); C = Tmp-Heptanoate containing 20% Toluene (v/v); D = Tmp-Heptanoate containing 30% Toluene (v/v)

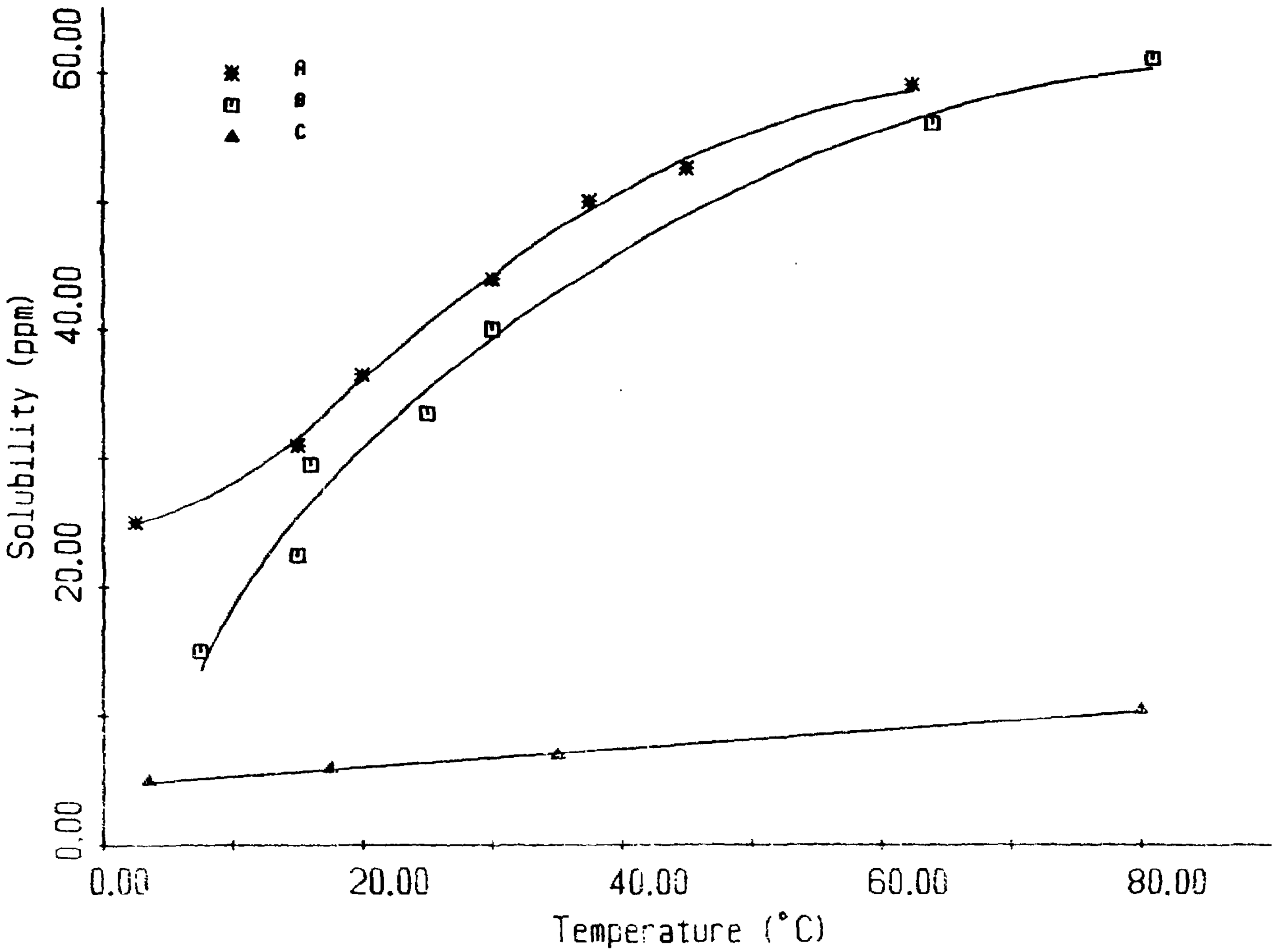

Figure 5. The Solubility of Polydimethylsiloxane of Different Viscosities in Tmp-Heptanoate, at Various Temperatures.
A = Polydimethylsiloxane of 500 cSt
B = Polydimethylsiloxane of 1000 cSt
C = Polydimethylsiloxane of 5000 cSt

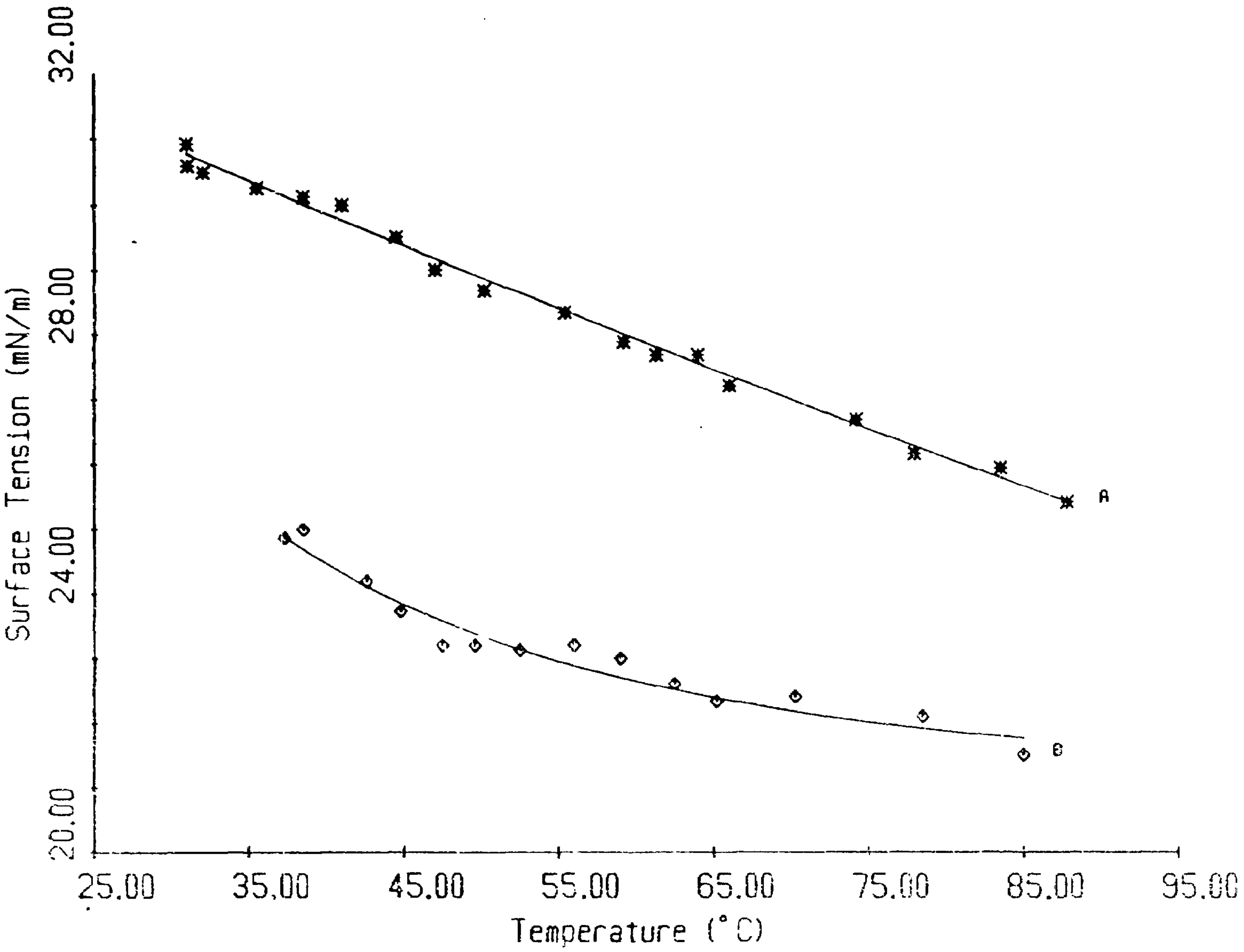

Figure 6 Variation of Surface Tension with Temperature of Tmp-Heptanoate (A) and of a Solution of Polydimethylsiloxane (100 cSt), 30 ppm in Tmp-Heptanoate(B)

gas, with flow rates up to 600 ml/minute and at temperatures of 25 to 95°C. The test results are reported in Figures 7, 8, and 9. A summary of results follows:

a. No significant foam is observed at concentrations less than 51 ppm at the temperatures and flow rates studied.
b. In the range of concentrations of 50 to 324 ppm the foaminess increases with concentration of polydimethylsiloxane.
c. In the range of concentrations of 324 to 646 ppm the foaminess no longer shows an increase with concentration of polydimethylsiloxane.
d. In the range of temperatures from 25 to 95°C the foaminess increases with temperature at all concentrations of solute.

Foaminess is reported in Figures 7, 8, and 9 in terms of the "Foam Height". Other units used in this report are "Foam Volume" and "Volume Ratio" (or "Foam Volume Ratio"). The latter is the most readily obtained and least doubtful of any reading that can be made of the amount of foam in a foam column, as it does not require an estimate to be made of the position of the solution/foam interface -- an interface that is often obscure and impossible to identify with certainty. The foam volume is given by the topmost reading at the foam/air interface; from this volume subtract the volume of solution originally present in the vessel, to get the volume of gas retained in the foam; the volume ratio is the ratio of gas to liquid volumes in the foam column, at constant temperature, and at a rate of flow of nitrogen gas of 1000 ml/minute. Volume ratios are calculated from the measured volume of foam obtained from a known volume of liquid. The volume ratio is calculated by the equation:

Volume Ratio = {(Foam volume) - (Liquid volume)}/(Liquid volume)

The volume of liquid in every test is 200 ml; with this datum other units, such as:
Expansion Factor = (Foam volume / Liquid volume)
may be calculated from the numbers for Volume Ratio.

At the higher concentrations reported, the polydimethylsiloxane is beyond its solubility limit and turbidity is evident in the solutions. Nevertheless, the advent of insolubility and the presence of undissolved spherical droplets of silicone oil in the medium is not accompanied by the onset of foam inhibition, as has been our experience with many other binary systems. The inhibition of foam is well known to occur in hydrocarbon lubricants with silicones of viscosity from 1,000 to 60,000 centiStokes. The observed effect in the synthetic lubricant, which is a better solvent for polydimethylsiloxane, may be due to silicone polymer of low molecular weights, which are profoamant, dissolved in the system to a level at which the antifoamant action of the dispersed particulate silicone is not effective.

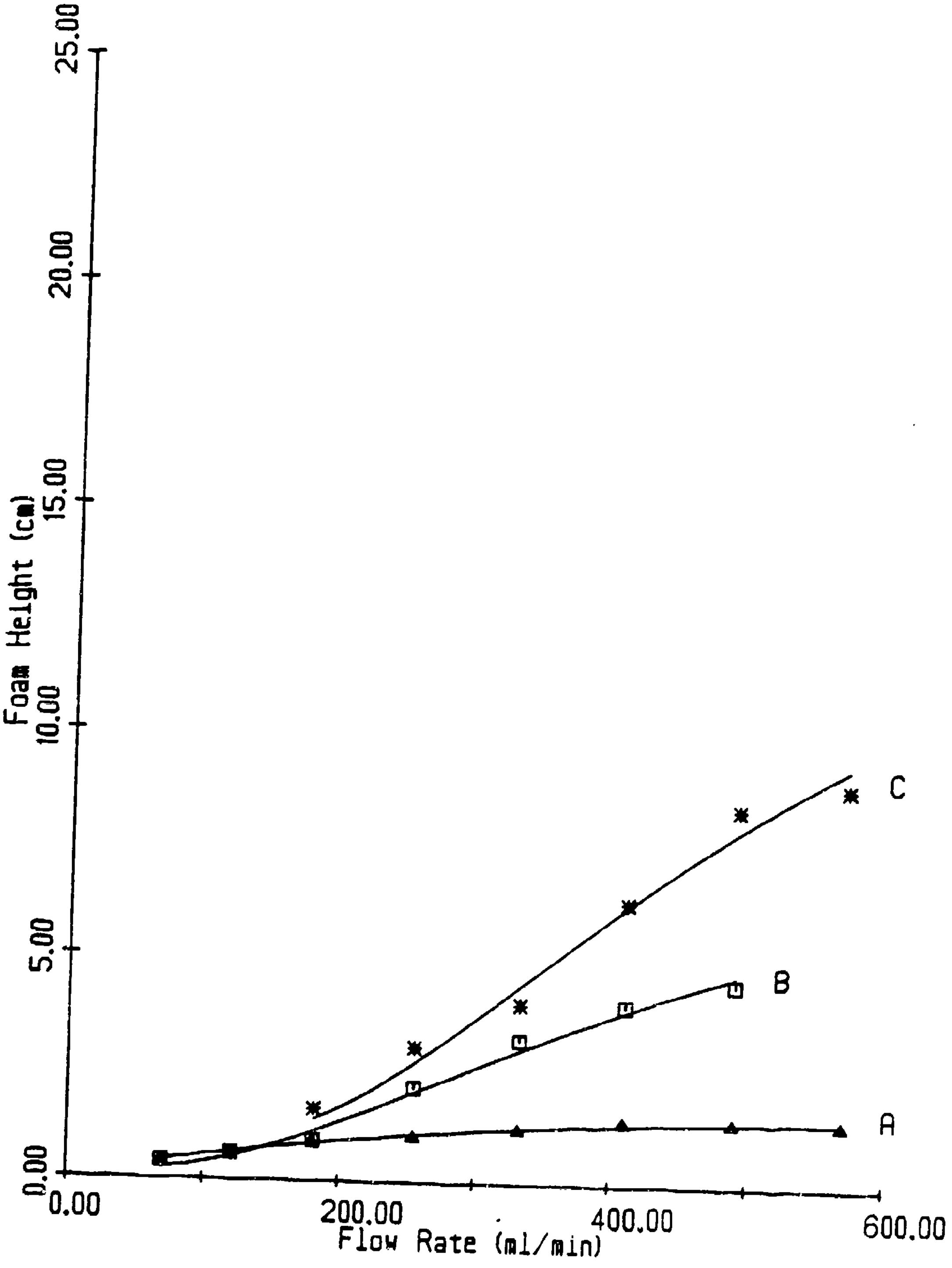

Figure 7 Variation of Foam Height with Flow Rate of Nitrogen Gas (ml/minute) through a Solution of Polydimethylsiloxane (1000 cSt) at a Concentration of 89.2 ppm in Tmp-Heptanoate at different Temperatures.
A is 85°C; B is 90°C; C is 94.5°C.

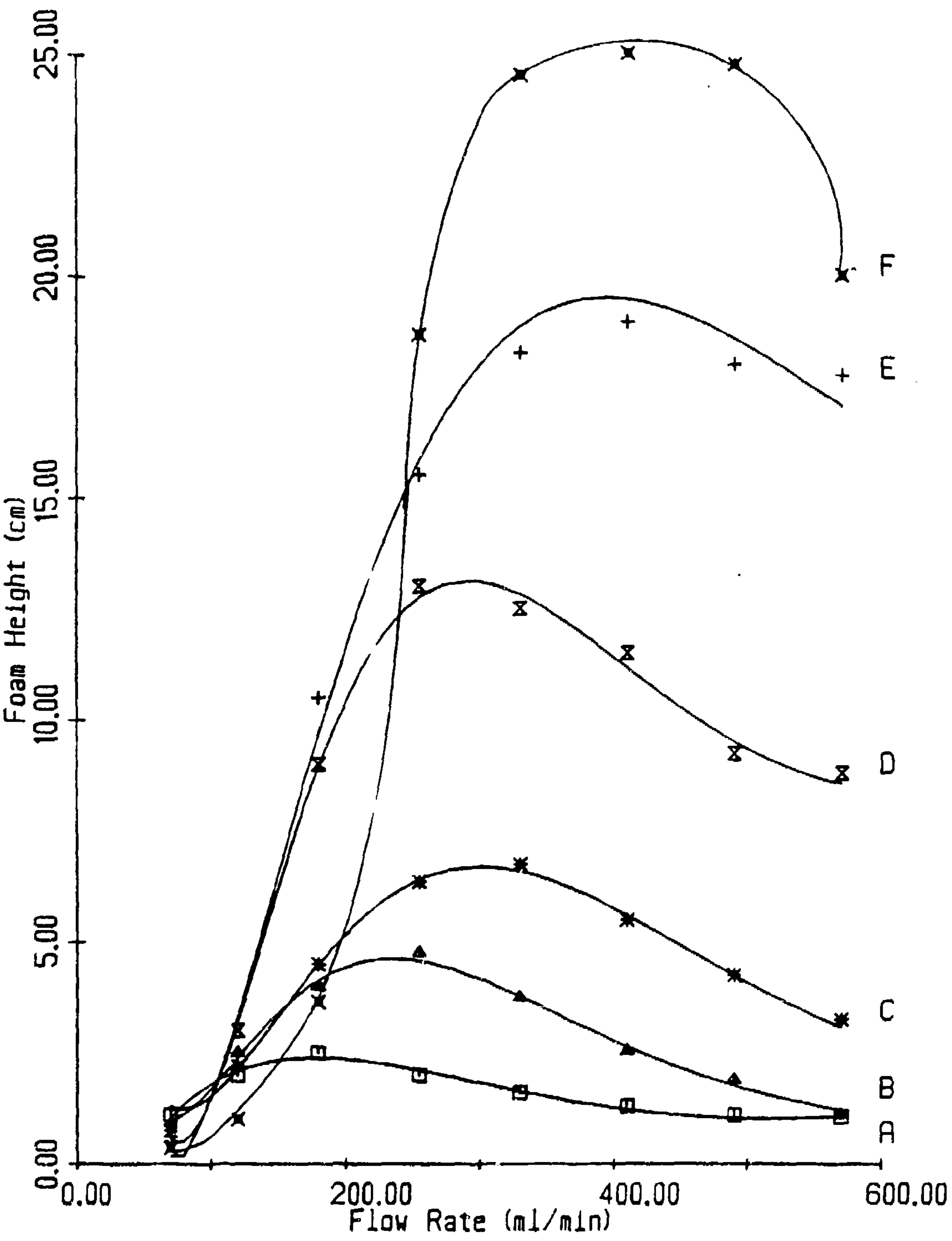

Figure 8 Variation of Foam Height with Flow Rate of Nitrogen Gas (ml/minute) through a Solution of Polydimethylsiloxane (1000 cSt) at a Concentration of 324.3 ppm in Tmp-Heptanoate at different Temperatures.
A is 32°C; B is 42°C; C is 52°C; D is 61°C; E is 71°C; F is 82°C.

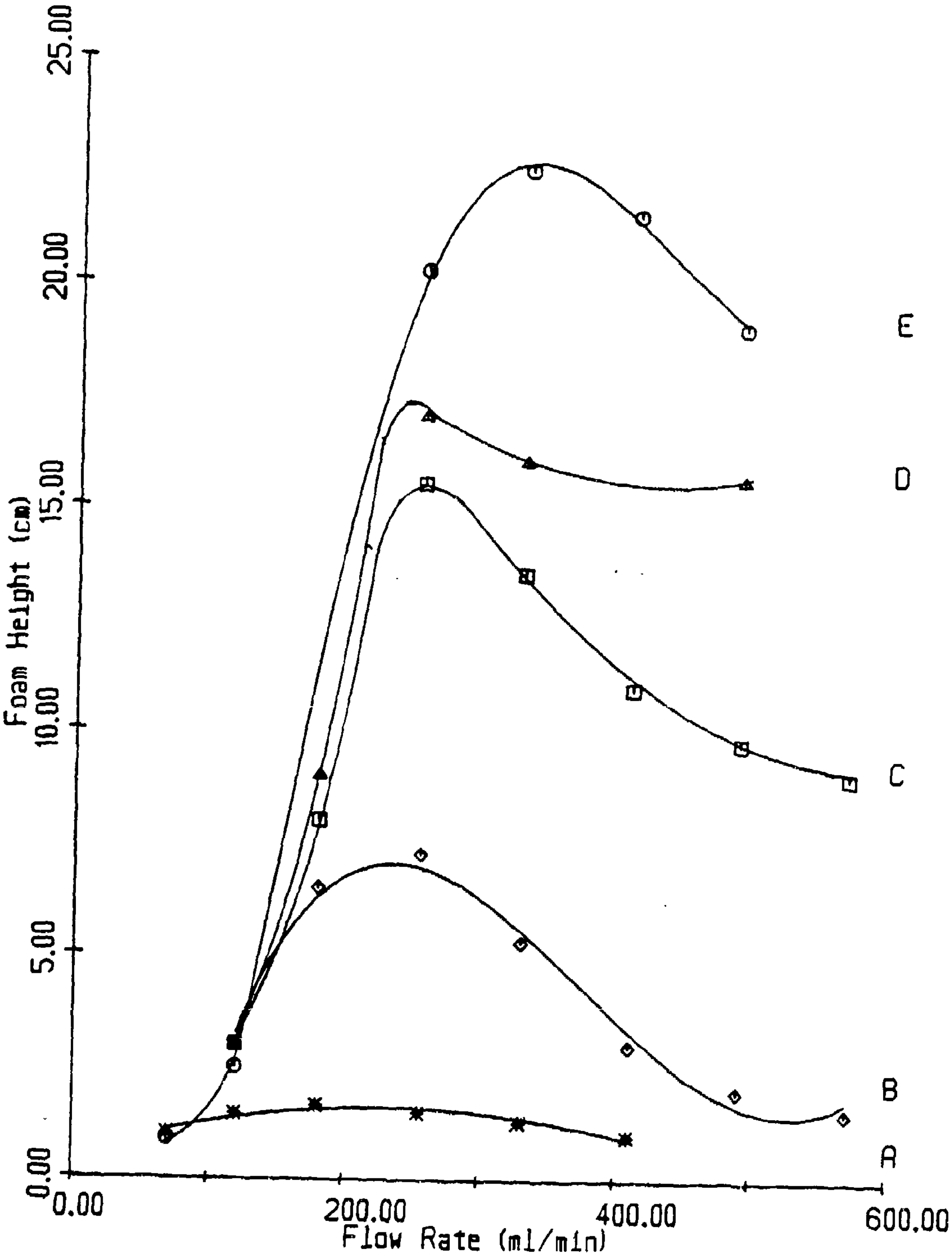

Figure 9 Variation of Foam Height with Flow Rate of Nitrogen Gas (ml/minute) through a Solution of Polydimethylsiloxane (1000 cSt) at a Concentration of 646 ppm in Tmp-Heptanoate at different Temperatures.
A is 33.5°C; B is 43.5°C; C is 53.5°C; D is 63°C; E is 73°C.

Although we have not yet observed polydimethylsiloxane act as an inhibitor for foamable solutions of this synthetic lubricant, we have found other materials that can inhibit their foaminess. Of these the most effective, without evidence of "fatigue" in its action even after continual bubbling for 24 hours, is G.E. FF-150, a fluoro-silicone fluid of viscosity = 10,000 cSt.

4. Foaminess of Different Concentrations of Polydimethylsiloxane (1000 centiStokes) in Tmp-Heptanoate, Measured by ASTM D892 Foam Test at 80°C

In Figure 10 we report both the foam volumes and the foam-collapse times of solutions of polydimethylsiloxane (1000 centiStokes) in tmp-heptanoate in concentrations from 1 to 400 ppm, measured by ASTM D892 Foam Test (Test Method 3213),[19] at 80°C. The limit of apparent solubility of this sample of polydimethylsiloxane at 80°C by the Tyndall-Faraday effect is 60 ppm, but it is clear from Figure 10 that the foaminess continues to increase at concentrations greater than 60 ppm. The presence of soluble lower-molecular-weight fractions in the 1000 centistokes fraction is the most probable cause of this effect.

5. Foaminess of 1000 cSt Polydimethylsiloxane in Tmp-Heptanoate

The foam tests of 1000 cSt polydimethylsiloxane in tmp-heptanoate reported above have been extended. The tests now include more concentrated mixtures of the 1000 cSt polydimethylsiloxane in order to support correlations between foaminess and other physical properties. The appended results describe the relation between foam height and concentration of polydimethylsiloxane at several temperatures in the range of 25 to 75°C, and at flow rates of 300 ml/min and 500 ml/min (Figures 11A and 11B respectively.)

6. Foaminess of Silicones of various Viscosities in TMP-Heptanoate

We intend to test the possibility of using silicones, in the range of viscosities 10,000 to 600,000 centiStokes, as foam-inhibiting agents for tmp-heptanoate + additive(s) solutions. Preliminary tests included measurements of the foaminess of mixtures in tmp-heptanoate of the silicones in question, to find an optimal molecular weight and suitable concentration range for the silicone. Tables 1, 2, and 3 report the foam volumes measured for three silicones (100, 26,000, and 600,000 cSt respectively) at various concentrations and temperatures. These tables show that of the three polydimethylsiloxanes (pdms) tested, only the one with the highest viscosity can be used as a foam-inhibiting agent in the range of concentrations of 0 to 100 ppm, at all the temperatures investigated.

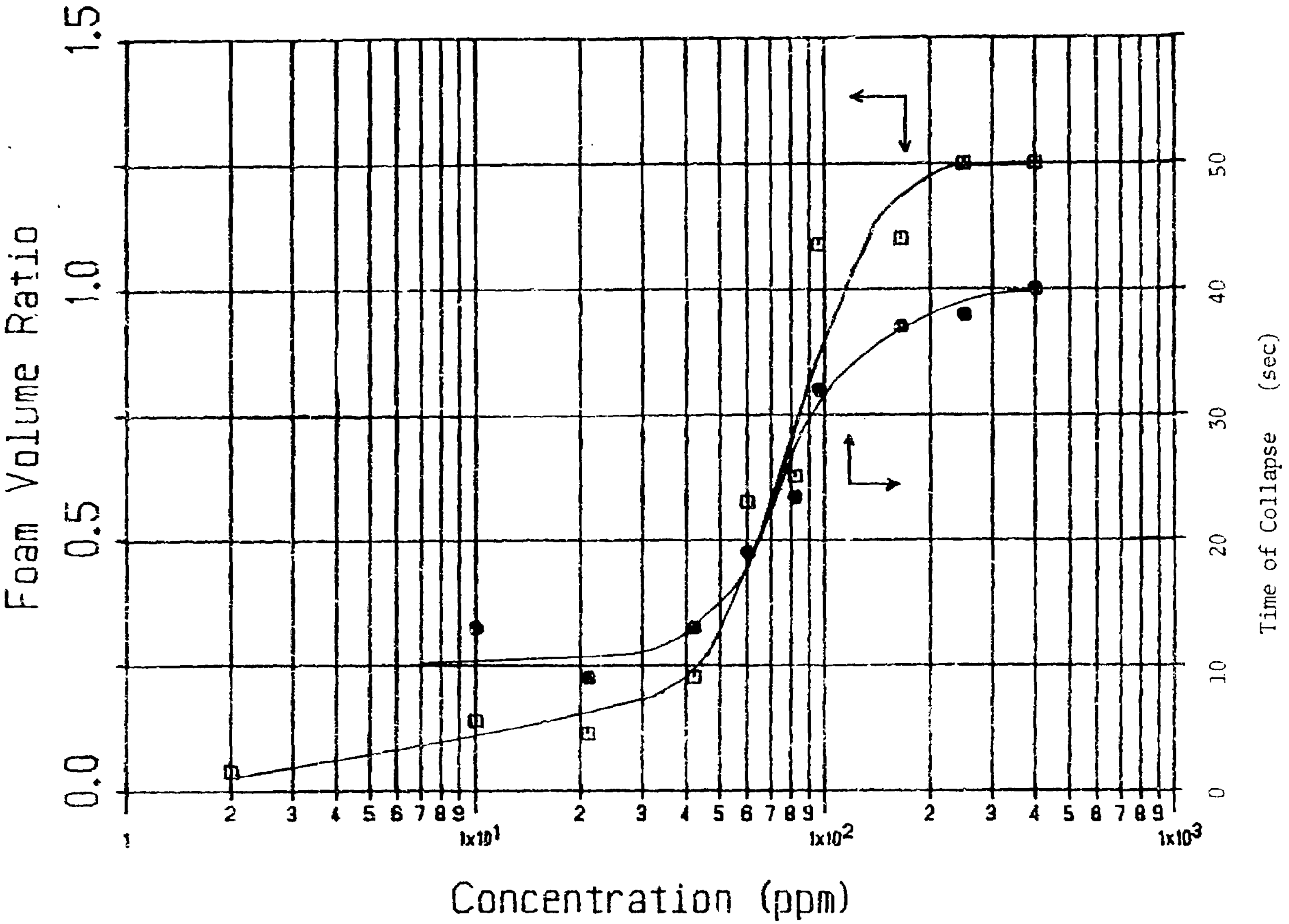

Figure 10. Foam Volume Ratios and Collapse Times (seconds) of Solutions of Polydimethylsiloxane (1000 cSt) at Various Concentrations In Tmp-Heptanoate, at 80°C, with Test Method 3213.

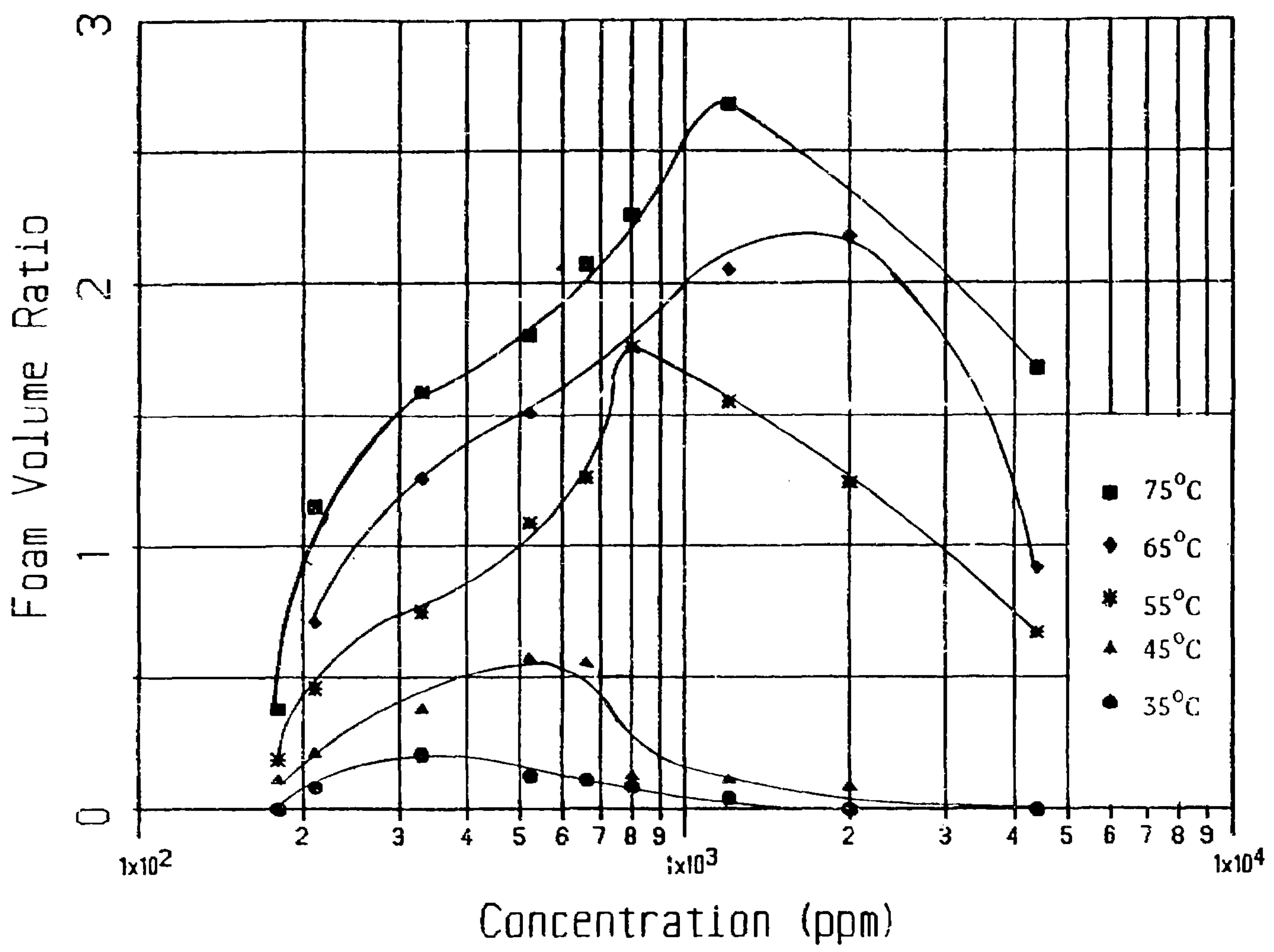

Figure 11a. Foam Volume Ratio of Solutions of Polydimethylsiloxane (1000 cSt) in Tmp-Heptanoate at Various Concentrations and Temperatures, measured in a Cylindrical Apparatus, with Flow Rate of Nitrogen Gas of 300 cm³/minute.

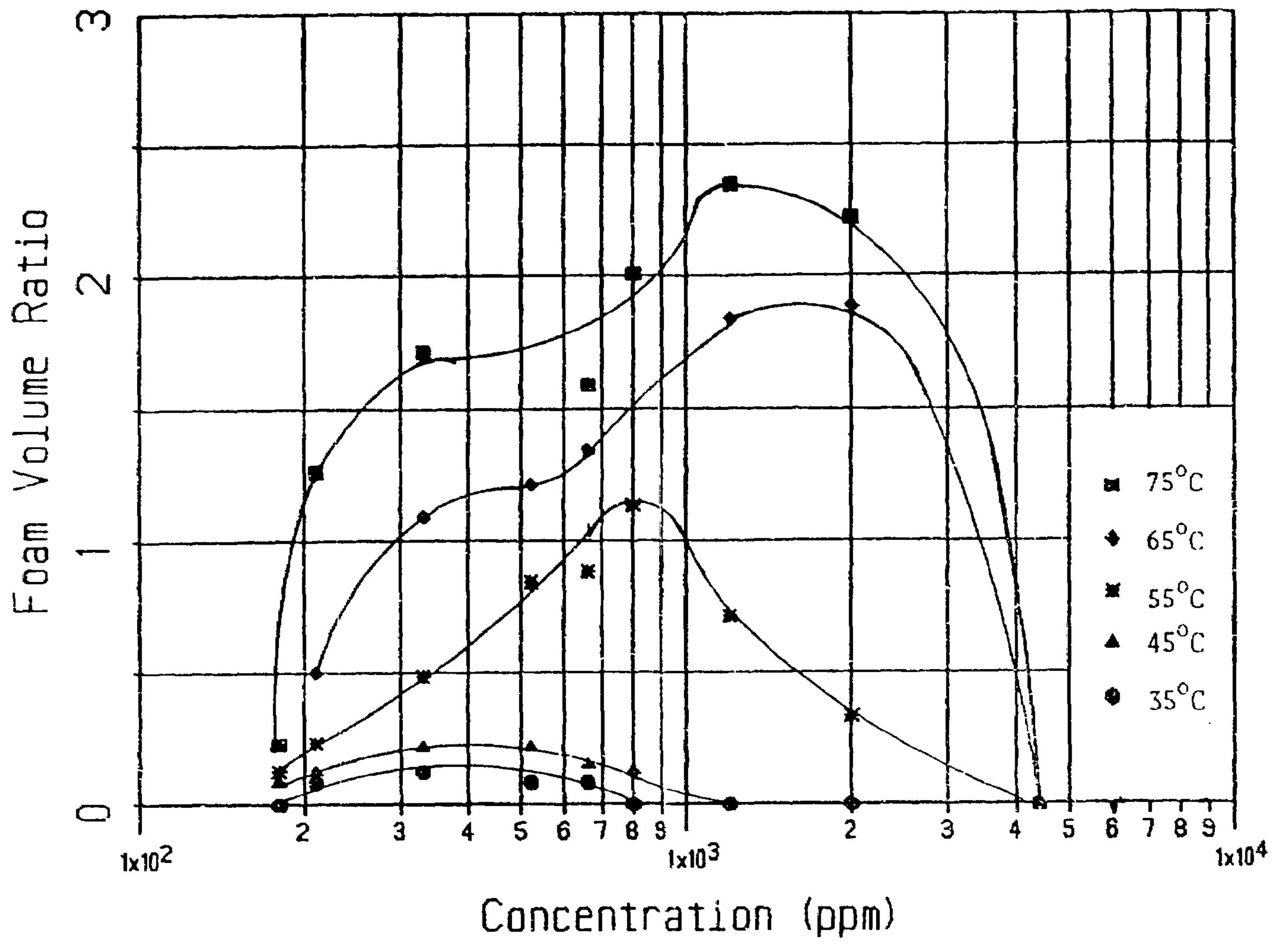

Figure 11b. Foam Volume Ratio of Solutions of Polydimethylsiloxane (1000 cSt) in Tmp-Heptanoate at Various Concentrations and Temperatures, Measured in a Cylindrical Apparatus, with Flow Rate of Nitrogen Gas of 500 cm^3/minute.

Table 1. Foam Volumes (cm^3) of 100 cSt PDMS in Tmp-Heptanoate, at Various Concentrations and Temperatures.

	Concentration				
T°C	10 ppm	50 ppm	100 ppm	1,000 ppm	10,000 ppm
40	0	340	500	500	500
60	10	500	500	500	500
80	20	500	500	500	500

Table 2. Foam Volumes (cm^3) of 26,000 cSt PDMS in Tmp-Heptanoate, at Various Concentrations and Temperatures.

	Concentration			
T°C	10 ppm	100 ppm	1,000 ppm	10,000 ppm
40	0	10	500	500
60	0	85	500	500
80	10	170	500	500

Table 3. Foam Volumes (cm^3) of 600,000 cSt PDMS in Tmp-Heptanoate, at Various Concentrations and Temperatures.

	Concentration			
T°C	10 ppm	100 ppm	500 ppm	1,000 ppm
40	0	0	20	25-30
60	0	0	150	60-450
80	0	0	>200	500

We have previously reported the results of foam measurements of solutions of polydimethylsiloxane, 1000 cSt, in tmp-heptanoate by Test Method 3213, at 80°C as per standard requirements. To relate foaminess of these solutions to gas entrainment, to surface viscosity, and to our projected measurements of dynamic surface tension, all at 25°C, we require data on foaminess at lower temperatures, down to ambient temperatures. Other than temperature, all the parameters and conditions of the test are according to the standard procedure. All the solutions tested were heated to 60°C for three hours, cooled to room temperature, and then blended three times with a hand homogenizer. Figure 12 reports the results obtained at four temperatures: 25°C, 40°C, 60°C, and 80°C; with solutions varying in concentration in the range 0.1 to 500 ppm. Figure 12 confirms results previously reported with a slightly different apparatus.

7. Foaminess of Solutions of Polydimethylsiloxane in a White, Refined Mineral Oil

To extend the base of these studies beyond a particular solvent, we include data on solutions in a hydrocarbon oil. The present Section is devoted to foam measurements: these are collected here for comparisons with solutions of polydimethylsiloxane in tmp-heptanoate, and also will be referred to when correlations between foaminess and other physico-chemical properties of a solution are considered. Foaminess was measured, using the Test Method 3213. Table 4 and Figure 13 show the results obtained at four temperatures, 25, 40, 60, and 80°C.

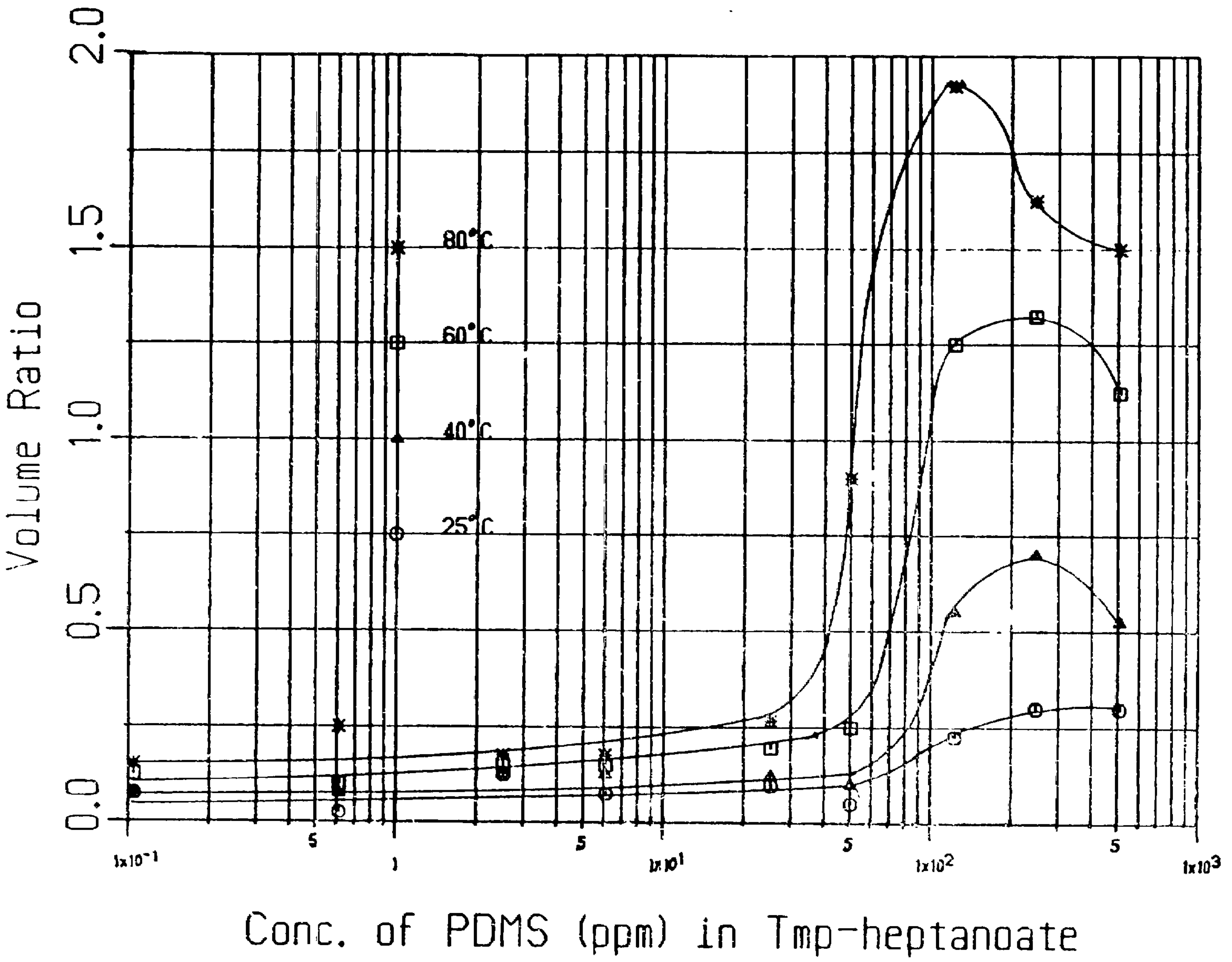

Figure 12. Foaminess of Solutions of Polydimethylsiloxane (1000 cSt) in Tmp-Heptanoate at 25°C, 40°C, 60°C, and 80°C, Measured by Test Method 3213.

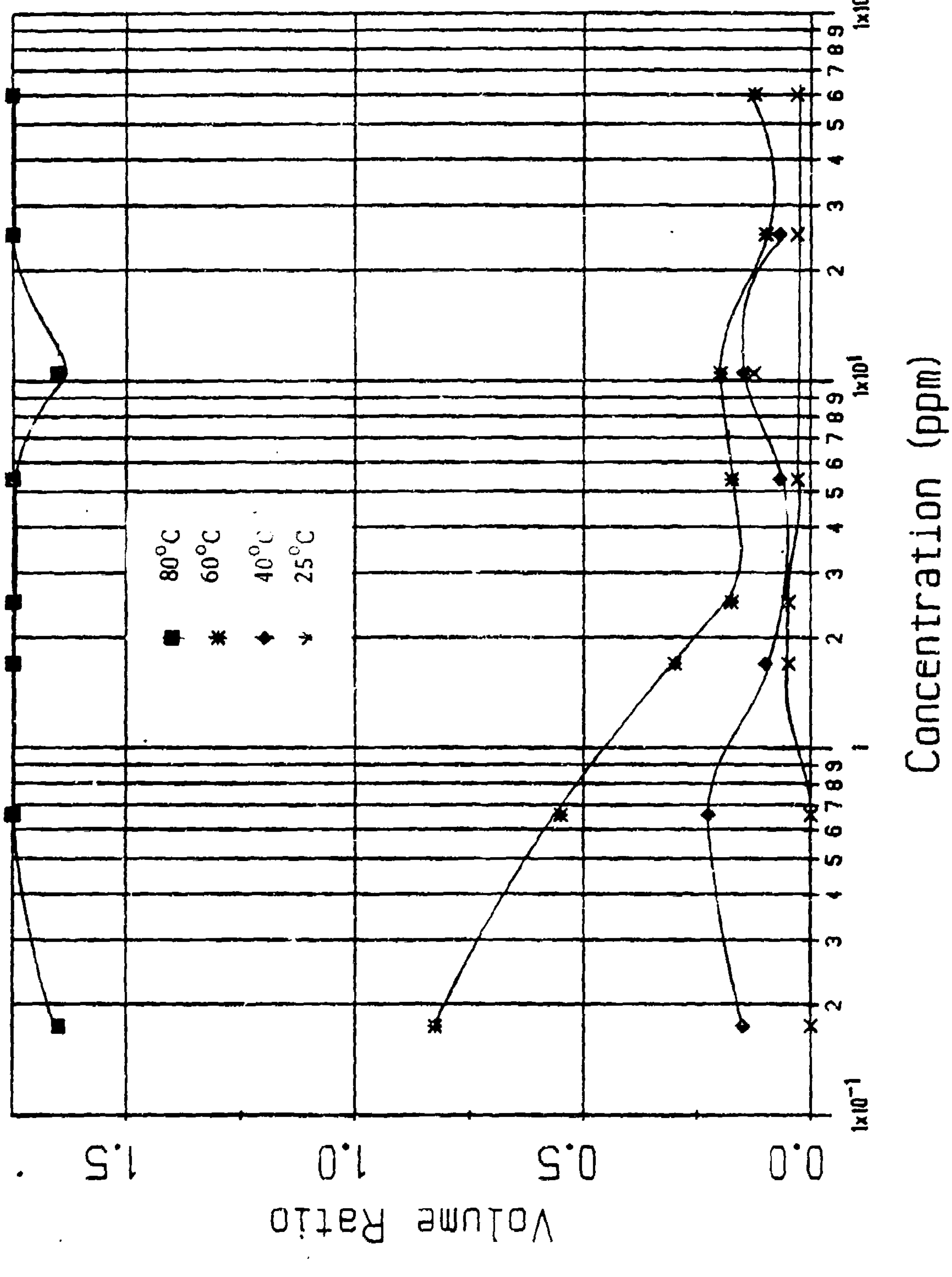

Figure 13. Foaminess of Solutions of Polydimethylsiloxane (1000 cSt) in Mineral Oil at Various Temperatures Measured by Test Method 3213.

Table 4. The Volume Ratios (Gas/Liquid Volumes) of Foams Obtained in Polydimethylsiloxane Solutions in Mineral Oil

Concentration (ppm)	Volume Ratio			
	25°C	40°C	60°C	80°C
0.173	0	0.15	0.825	1.65
0.67	0	0.225	0.55	>1.90
1.69	0.05	0.10	0.30	>1.90
2.52	0.05	0.05	0.175	>1.90
5.50	0.05	0.075	0.20	>1.90
10.4	0.125	0.15	0.20	1.65
23.75	0.05	0.075	0.10	>1.90
59.98	0.05	0.05	0.125	>1.90
88.9	0.05	0.05	0.125	>1.90

The volume ratios given in the table and the diagram refer to the ratio of gas to liquid in a given foam column at constant temperature and flow rate of nitrogen gas. The use of these values, instead of absolute foam volumes, is less uncertain as it does not require us to make the difficult distinction between the liquid phase (containing entrained gas) and the foam phase. Table 4 and Figure 13 show that in the whole range of concentrations tested no significant foam occurs at 25°C and 40°C. On the other hand, the volumes of foam produced at 80°C are large and mostly above the measurable limit of the instrument. At 60°C the foaminess is concentration dependent as shown in Figure 13. Since the mineral oil in itself shows a large foaming ability the conclusion of these results is that at the lower temperatures the smallest polydimethylsiloxane concentrations used sufficed to inhibit the foaminess, while at the highest temperature the profoaming effects are in evidence, the silicone concentration being below its solubility limit at 80°C.

SECTION IV

FOAMINESS OF SOLUTIONS OF VARIOUS OIL ADDITIVES

Solutions of the following oil additives were made in tmp-heptanoate:
A: N-Phenyl-1-naphthylamine with maximum concentration of 2% (w/w)
B: Phenothiazine with maximum concentration of 2% (w/w)
C: Quinizarin with maximum concentration of 0.05% (w/w)
D: Tricresyl phosphate with maximum concentration of 2% (w/w)

The variation with temperature of the density of solutions of A, of B and of D are reported in Figures 14, 15, and 16.

The variation with temperature of the surface tension of solutions of A, of B, of C, and of D are shown in Figures 17, 18, 19, 20, and 21. For comparison, the surface tension of the solvent is also shown on each of these diagrams.

The surface tensions of some other oil-soluble surface-active solutes as a function of concentration are shown in Figure 22. These surface tensions reach equilibrium very slowly; the data reported in the diagram are equilibrium measurements made after ten to twenty hours of surface aging. Span 20, which is a solute based on a fatty-acid alkyl chain, lowers the surface tension of a mineral oil by a mere 2 mN/m; whereas polydimethylsiloxane, a more powerful agent, lowers the surface tension of mineral oil and of tmp-heptanoate by as much as 7 or 8 mN/m, and does so at concentrations only one-hundredth of those required by Span 20.

The variation with temperature of the kinematic viscosity (centiStokes) of solutions of B, of C, and of D are shown respectively in Figures 23, 24, and 25.

1. Foaminess of Tmp-Heptanoate with Various Oil Additives

Tmp-heptanoate mixtures with various additives were tested for foaminess using method 3213 of federal Test Method standard 791.[19] The four additives tested were:
A: N-Phenyl-1-naphthylamine with maximum concentration of 2%(w/w)
B: Phenothiazine with maximum concentration of 2%(w/w)
C: Quinizarin with maximum concentration of 0.05%(w/w)
D: Tricresyl phosphate with maximum concentration of 2%(w/w)
Compositions made of different combinations of additives A to D were tested, using the foam test apparatus of Method 3213, nitrogen gas flow rate of 1000 ± 20 ml/minute; Temperature = 80 ± 1°C. The results of the foaminess tests are reported in Table 5. The apparatus does not give readings of foam volumes larger than 500 cm^3.

Table 5 shows:
a. The mixtures containing a single additive at maximum concentration(2% w/w) do not foam.
b. Three out of the six combinations of two additives show

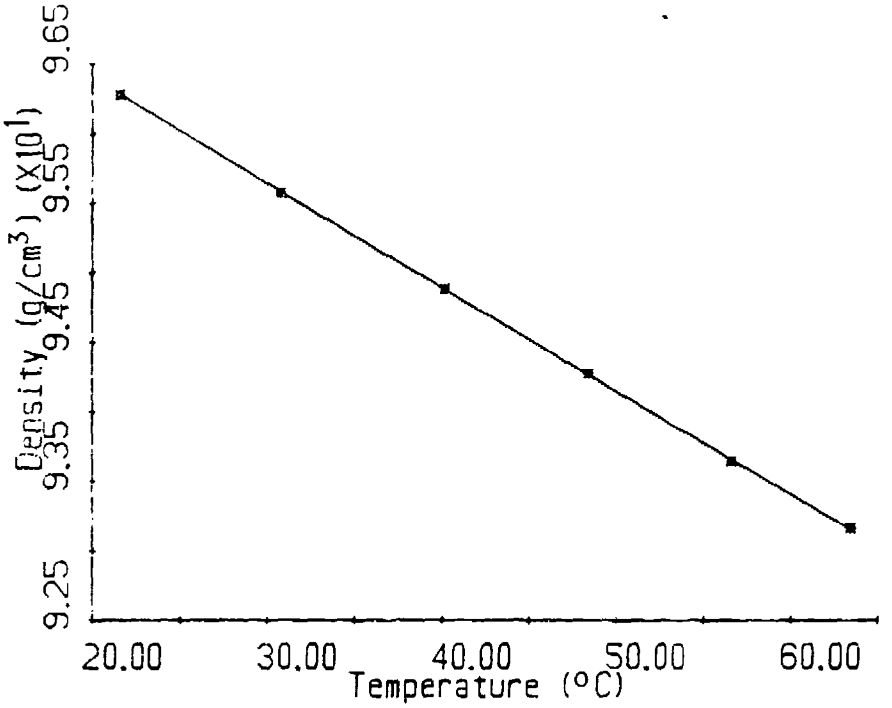

Figure 14. Variation of Density with Temperature for Tmp-Heptanoate Containing N-Phenyl-1-Naphthylamine (1.96% w/w)

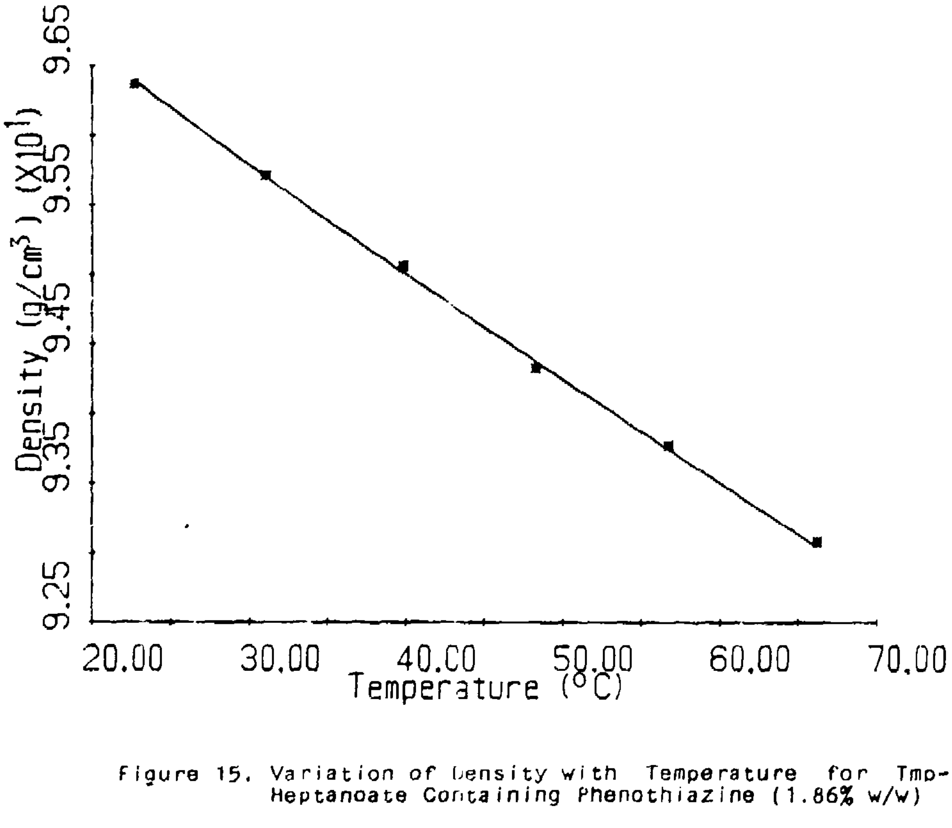

Figure 15. Variation of Density with Temperature for Tmp-Heptanoate Containing Phenothiazine (1.86% w/w)

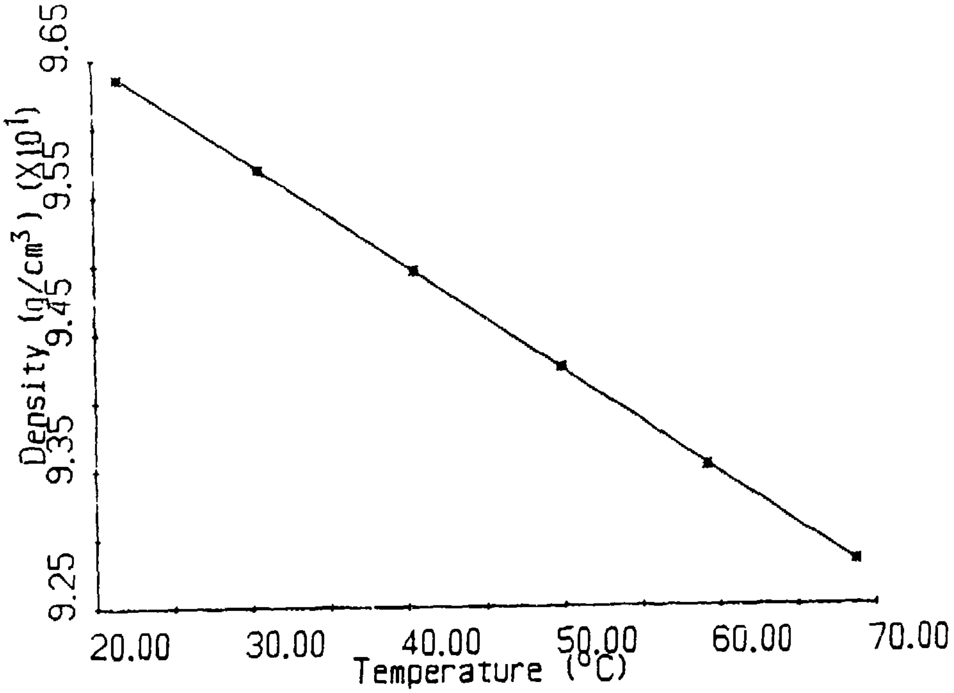

Figure 16. Variation of Density with Temperature for Tmp-Heptanoate Containing Tricresyl Phosphate (2.05% w/w)

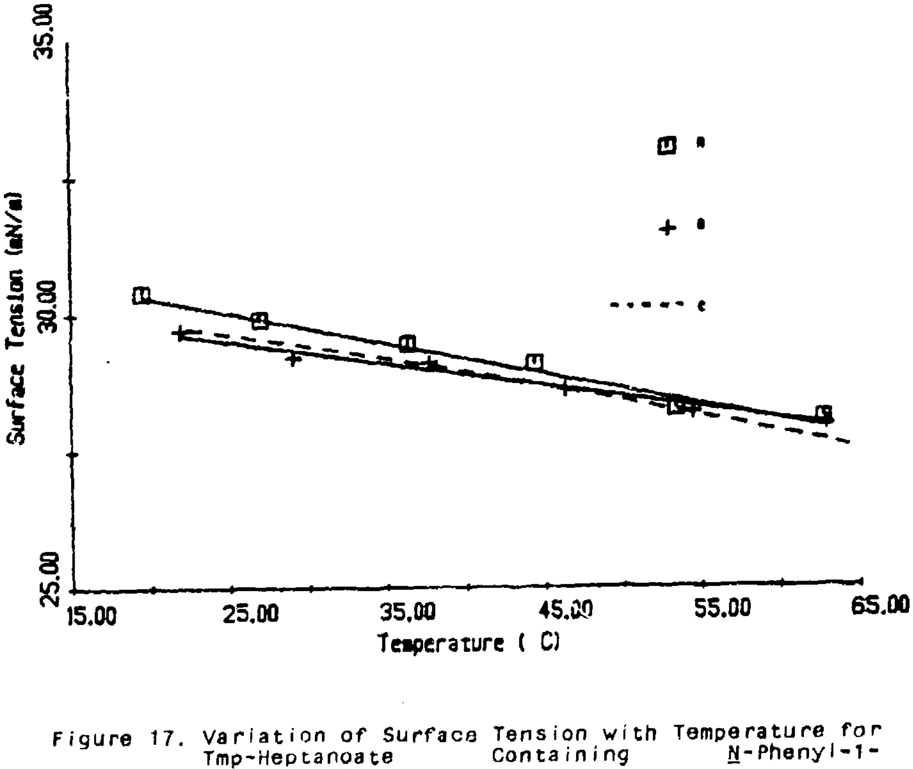

Figure 17. Variation of Surface Tension with Temperature for Tmp-Heptanoate Containing *N*-Phenyl-1-Naphthylamine
<u>Broken Line</u> is Solvent Alone; A is 1.86% (w/w) *N*-Phenyl-1-Naphthylamine; B is 0.96% (w/w) *N*-Phenyl- 1-naphthylamine

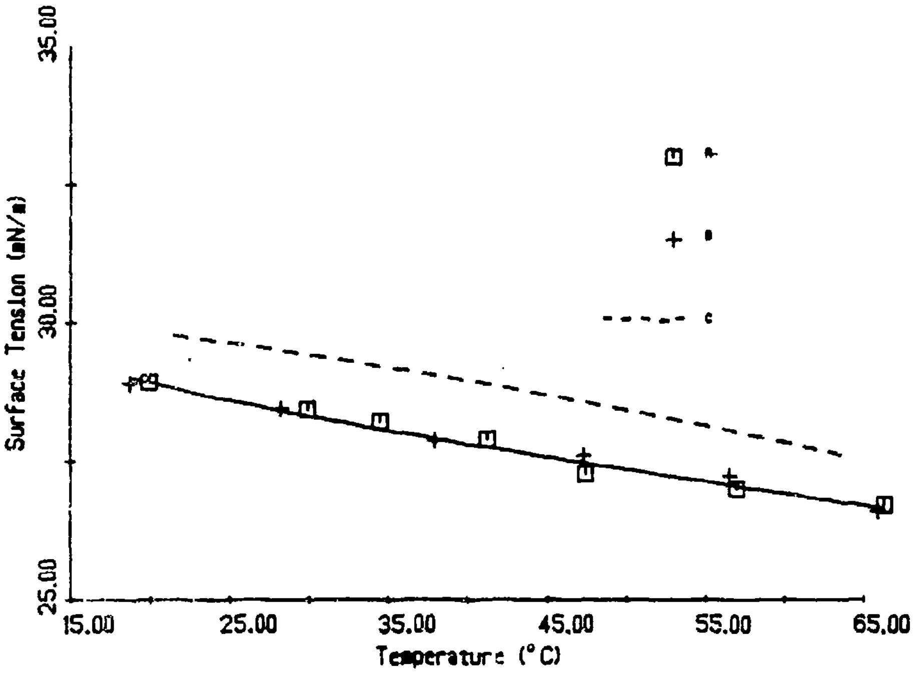

Figure 18. Variation of Surface Tension with Temperature for Tmp-Heptanoate Containing Phenothiazine Broken Line is Solvent Alone; A is 1.86% (w/w) Phenothiazine; B is 0.935% Phenothiazine (w/w)

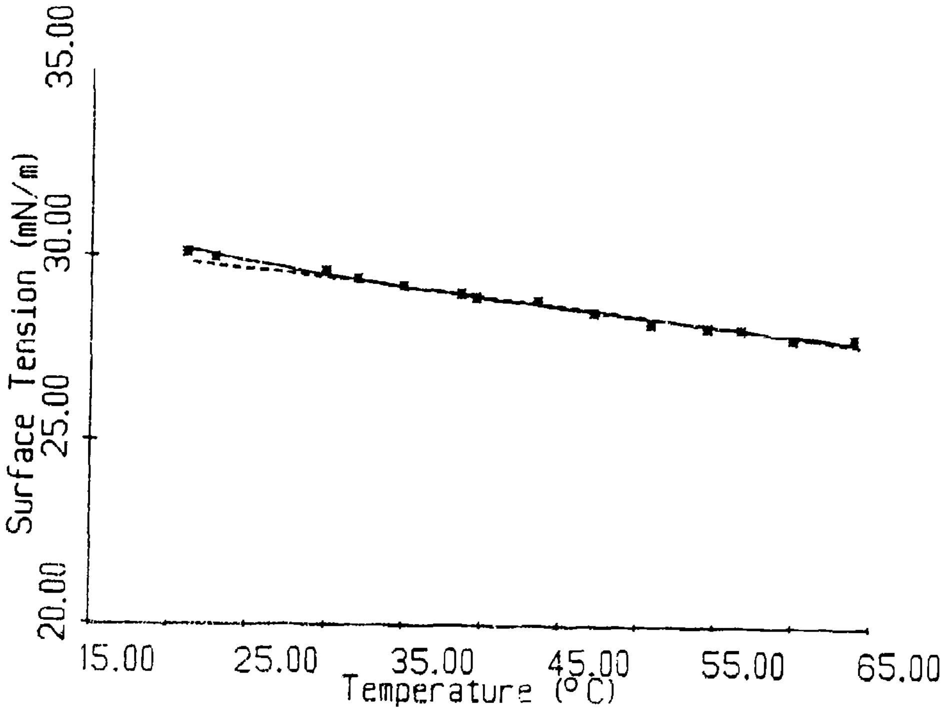

Figure 19. Variation of the Surface Tension with Temperature for Tmp-Heptanoate Containing Quinizarin Broken Line is Solvent Alone; Continuous Line is 0.0238% (w/w) Quinizarin

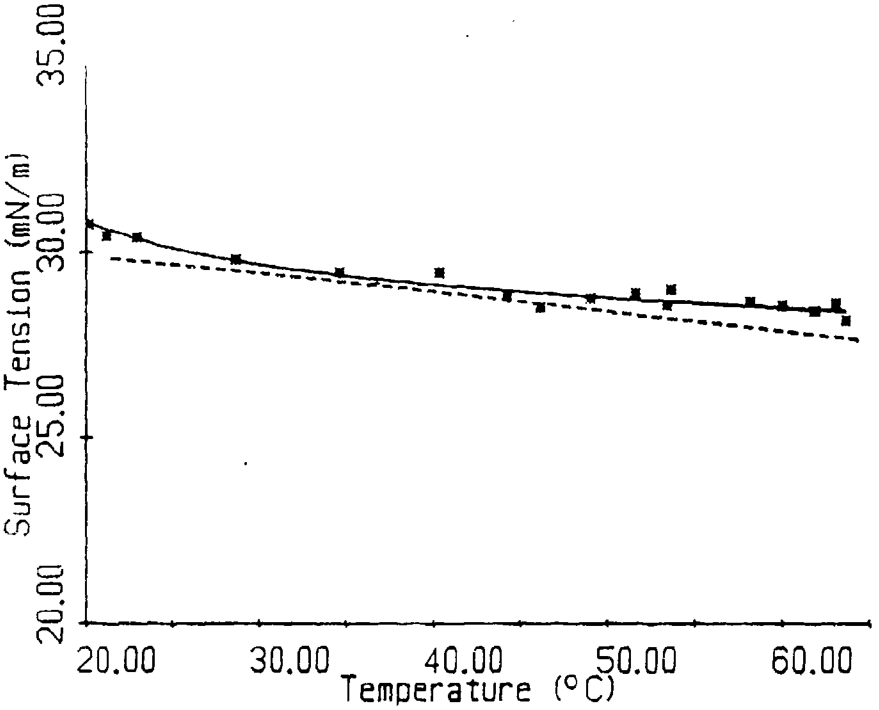

Figure 20. Variation of the Surface Tension with Temperature for Tmp-Heptanoate Containing Quinizarin <u>Broken Line</u> is Solvent Alone; <u>Continuous Line</u> is 0.0477% (w/w) Quinizarin

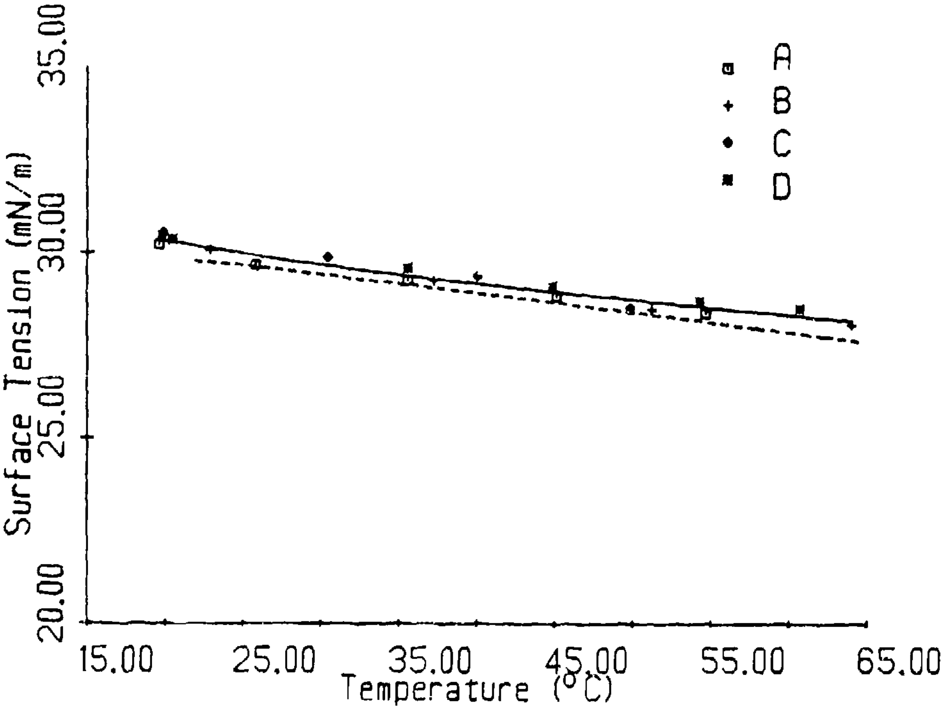

Figure 21. Variation of the Surface Tension with Temperature for Tmp-Heptanoate Containing Tricresyl Phosphate <u>Broken Line</u> is Solvent Alone; A is 2.05% (w/w) Tricresyl Phosphate; B is 1.99% (w/w) Tricresyl Phosphate, Temperature Increasing; C is 1.99% (w/w) Tricresyl Phosphate, Temperature Decreasing; D is 0.858% (w/w) Tricresyl Phosphate

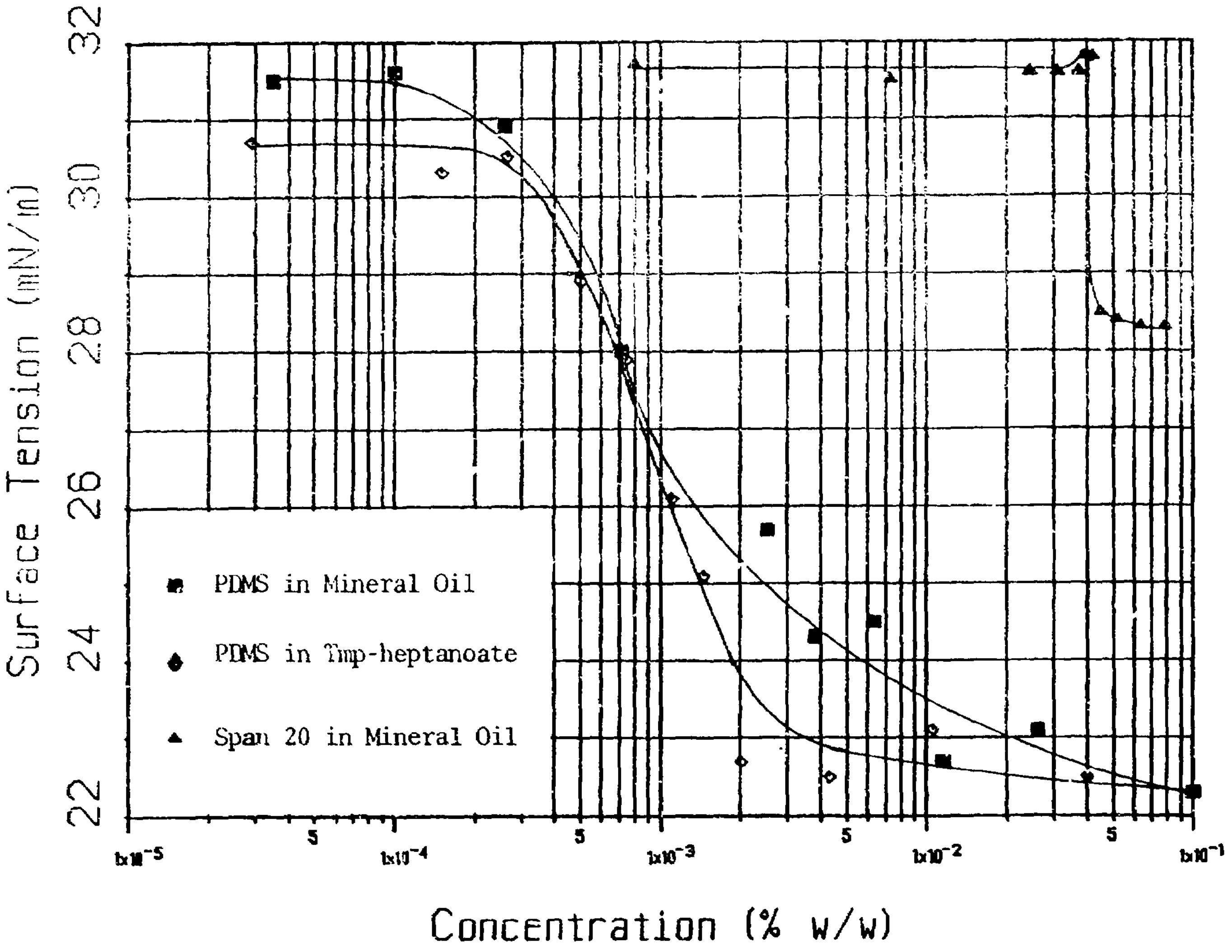

Figure 22. Equilibrium Surface Tension *versus* Concentration of Oil Solutions.
Polydimethylsiloxane (1000 cSt) in Mineral Oil at 23°C.
Polydimethylsiloxane (1000 cSt) in Tmp-Heptanoate at 23°C.
Span 20 in Mineral Oil at 23°C.

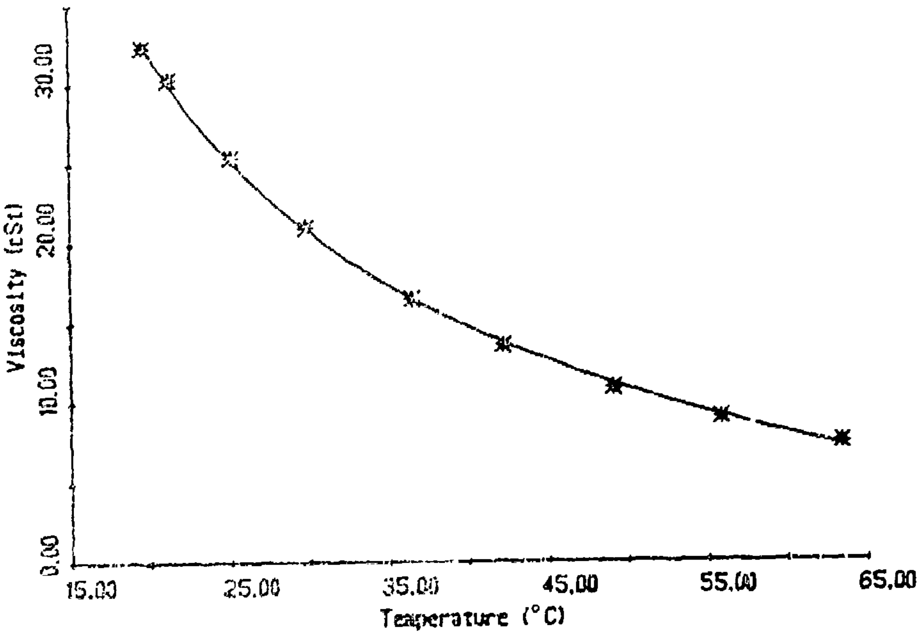

Figure 23. Variation of the Kinematic Viscosity (cSt) with Temperature for Tmp-Heptanoate Containing 1.86% (w/w) Phenothiazine

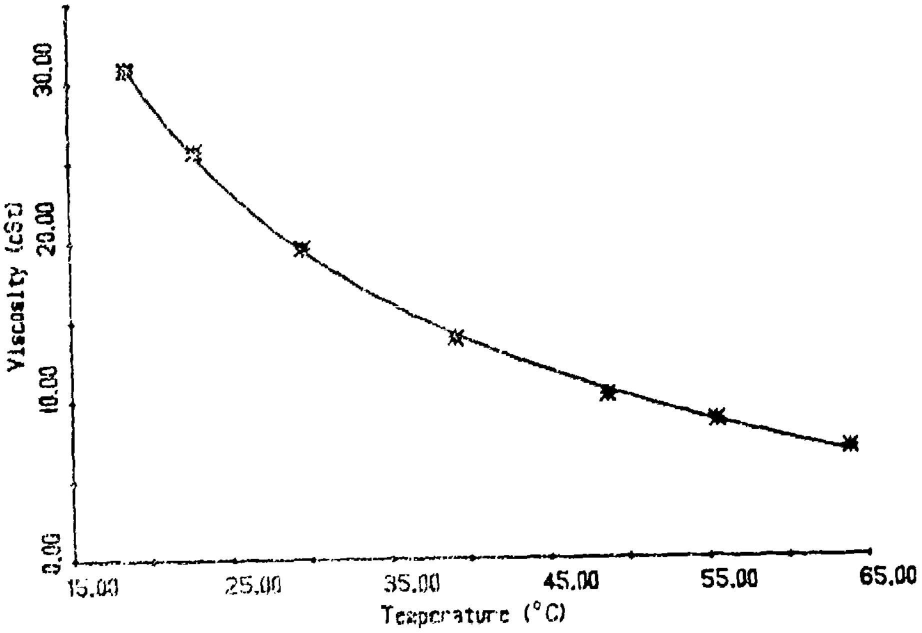

Figure 24. Variation of the Kinematic Viscosity (cSt) with Temperature for Tmp-Heptanoate Containing 0.0477% (w/w) Quinizarin

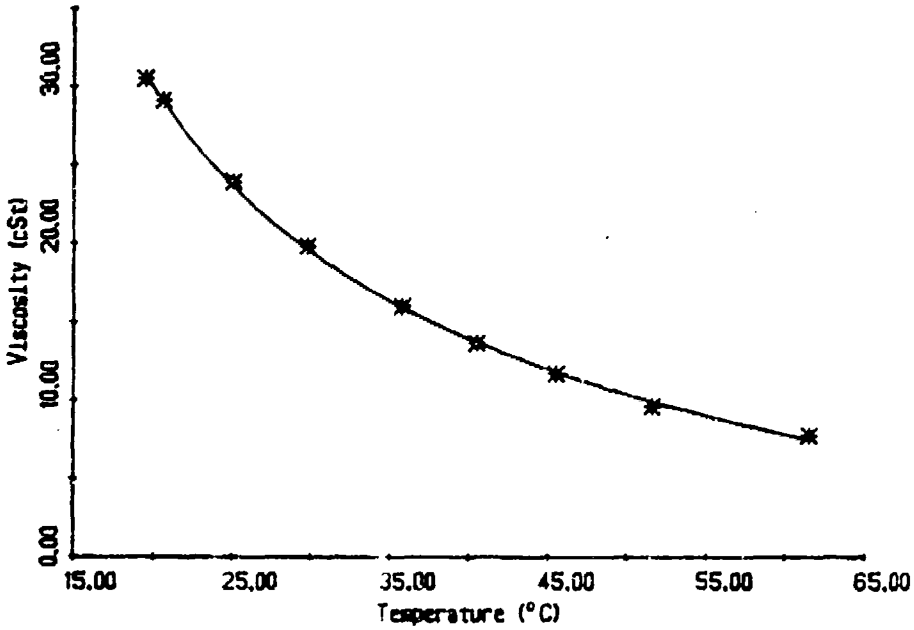

Figure 25. Variation of the Kinematic Viscosity (cSt) with Temperature for Tmp-Heptanoate Containing 1.99% (w/w) Tricresyl Phosphate

Table 5. Foaminess of Tnp-heptanoate Solutions with Various Oil Additives, by Test Method 3213.

NO.	COMBINATION	CONCENTRATIONS (%W/W) A	B	C	D	TEMP. (°C)	VOLUME RATIO	FOAM COLLAPSE TIME (sec)
1	A	1.99				80.2	0	
2	B		1.93			80.4	0	
3	C			0.050		79.8	0	
4	D				2.03	79.6	0	
5	AD	1.96			2.04	79.9	>2.50	18-24
6	AD	2.07			1.99	26.1	1.55	52
7	AD	2.07			1.99	39.3	2.15	49-60
8	AD	2.07			1.99	50.0	2.33	41
9	AD	2.07			1.99	61.1	2.50	31
10	AD	2.07			1.99	78.6	>2.50	30
11	AD	1.03			1.13	80.0	0	
12	AD	1.12			1.07	21.3	0	
13	AD	1.12			1.07	29.9	0	
14	AD	1.12			1.07	44.1	0	
15	AD	1.12			1.07	64.2	0	
16	AD	1.12			1.07	71.9	0	
17	AD	1.12			1.07	80.0	0	
18	AC	2.06		0.049		47.0	0	
19	AC	2.06		0.049		63.8	0	
20	AC	2.06		0.049		79.9	0	
21	AC	1.94		0.050		81.0	0	

Table 5.-Continued

NO.	COMBINATION	CONCENTRATIONS (%W/W) A	B	C	D	TEMP. (°C)	FOAM VOLUME (ml)	FOAM COLLAPSE TIME (sec)
22	AB	2.03	1.89			25.2	2.48	63
23	AB	2.03	1.89			61.0	>2.50	32
24	AB	2.03	1.89			80.0	>2.50	22
25	BC		2.01	0.052		79.8	0	
26	BD		2.03		2.01	79.8	>2.50	17
27	BD		2.03		2.01	27.0	2.10	51
28	BD		2.03		2.01	45.4	2.38	33
29	BD		2.03		2.01	58.1	2.13	27
30	BD		1.02		1.01	79.0	0	
31	CD			0.049	1.90	80.0	0	
32	BCD		1.97	0.051	2.03	79.8	2.50	16
33	ABC	1.90	2.03	0.049		80.0	>2.50	17
34	ABD	1.98	1.85		2.05	30.0	2.50	78
35	ABD	1.98	1.85		2.05	56.0	>2.50	46
36	ACD	1.97		0.048	1.87	80.0	>2.50	13
37	ABCD	1.76	2.03	0.032	2.51	80.2	>2.50	39
38	A	4.01				79.6	>2.50	17
39	AD	2.03			1.12	80.0	0.88	10
40	AD	1.11			2.07	80.0	0.33	7
41	AB	1.02	2.01			80.0	2.28	21
42	ACD	1.97	1.00			79.8	>2.50	14
43	B		3.94			79.8	>2.50	18

Table 5.-Continued

NO.	COMBINATION	CONCENTRATIONS (%W/W) A	B	C	D	TEMP. (°C)	FOAM VOLUME (ml)	FOAM COLLAPSE TIME (sec)
44	BD		2.00		1.13	79.8	>2.50	15
45	DB		0.93		2.05	79.9	0.15	
46	D				4.04	79.9	0.25	5
47	A	3.01				79.8	>2.50	14
48	B		3.01			80.0	>2.50	14
49	D				3.01	80.1	0	
50	AD	2.98			1.03	80.2	>2.50	15
51	AD	1.00			3.04	79.8	>2.50	14
52	BD		1.03		2.98	80.0	1.98	11
53	BD		2.97		1.20	79.8	>2.50	18
54	AD	2.46			0.52	79.9	>2.50	12
55	AD	0.50			3.59	79.8	2.30	12
56	BD		0.50		3.58	80.2	0.65	8
57	BD		1.50		1.59	79.8	0.50	7
58	BD		0.98		1.01	79.8	0	
59	AB	1.11	0.97			80.2	0	
60	AD	1.01			1.01	80.2	0	

foaminess: namely, AD, AB, BD.

c. With these, foam is stabilized even at room temperature and the foam height increases further with temperature.

d. The foam height is concentration dependent. On increasing the total concentration of additive composition made up of any two or all three components selected from A, B, and D, the onset of foaminess is abrupt, moving without much prior indication from non-foaming to off-scale on the foam test. This occurs at a <u>total</u> concentration of about 2.5% (w/w).

e. The foam collapse time decreases with increasing temperature.

f. All four different combinations of the four additives, cause the tmp-heptanoate to foam.

Further foam tests of additives were carried out by Test Method 3213 in the temperature range of 39°C to 80°C. The results are reported in Table 6.

Table 6. Foam tests with A, N-Phenyl-1-Naphthylamine; B, Phenothiazine; C, Quinizarin; D, Tricresyl Phosphate; E, Benzotriazole.

No.	Combination	Concentration (%w/w)					Temp (°C)	Foam Volume (cc)
		A	B	C	D	E		
1	E					0.049	59.0	None
2	E					0.049	60.0	None
3	E					0.049	79.3	None
4	E					0.099	80.2	None
5	BE		1.97			0.099	40.0	None
6	BE		1.97			0.099	60.1	30
7	BE		1.97			0.099	80.0	30
8	DE				1.94	0.097	40.0	None
9	DE				1.94	0.097	61.4	None
10	DE				1.94	0.097	49.8	None
11	BDE		1.98		1.98	0.120	39.5	360
12	BDE		1.98		1.98	0.120	60.4	495
13	BDE		1.98		1.98	0.120	49.6	430

Table 6 shows that no foaminess appears in solutions of tmp-heptanoate containing only benzotriazole within the applicable range of concentrations. Neither does addition at its maximum concentration to solutions of other additives change their foam properties; the only exception being the reduction of foam volume in the combination BDE (Number 13 of Table 6.)

Further foam tests of additives were carried out by Test Method 3213 in the temperature range of 39.8°C to 80.2°C. The results are reported in Table 7. That Table shows that no foaminess appears in solutions of p-nonyl phenol in tmp-heptanoate within the relevant range of concentrations. Neither does addition of its maximum concentration to solutions of other oil additives in tmp-heptanoate

Table 7. Foam, Surface Viscosity and Electrical Conductivity Tests with Various Solutions of Additives in Tmp-Heptanoate.

Combination	Concentration (% W/W)						Foam		Surface Viscosity (Slope)	Relative Conductivity
	A	B	C	D	E	F	Temp (°C)	Volume Ratio		
F						0.050	40.0 60.2 80.1	None None None	0.101 (0.098)	1.04
F						0.100	40.0 60.8 80.2	None None None	0.098 (0.098)	1.04
FA	1.99					0.100	39.8 60.3 79.9	None None 0.05	0.100 (0.098)	1.02
FB		2.02				0.100	40.0 60.0 80.0	0.05 0.10 0.125	0.112 (0.10[illegible]	68.2
FC			0.100			0.100	40.0 60.0 79.9	None None None	0.096 (0.098)	0.99
FD				1.99		0.100	40.0 60.0 80.0	None None None	0.098 (0.100)	0.86
FE					0.100	0.100	40.0 60.0 79.9	None None None	0.100 (0.097)	1.02
FAD	1.99			2.15		0.111	40.2 59.8 79.8	1.50 >2.50 2.35	0.115 (0.108)	1.10
FBD		1.98		1.98		0.100	40.0 60.0 79.9	1.88 2.63 1.98	0.115 (0.120)	38.6

A-	N-Phenyl-1-Naphthylamine	D-	Tricresyl Phosphate
B-	Phenothiazine	E-	Benzotriazole
C-	Quinizarin	F-	p-Nonyl Phenol

significantly affect their foam properties. (Compare with data reported in Tables 5 and 6 above.)

2. Synergism of Tricresyl Phosphate Additive in Promoting Foaminess of Other Additives in Solutions of TMP-heptanoate

The foaminess at 80°C of solutions of A in tmp-heptanoate is reported as a function of weight percent in Figure 26a. No foam is observed at concentrations below 2.5%, but a great increase of foaminess occurs at concentrations only slightly above 2.5%. Almost identical behavior for solutions of B in tmp-heptanoate is reported in Figure 26b. Both these solutes A and B display essentially the same behavior when combined with D (tricresyl phosphate) in solutions of tmp-heptanoate as solvent; that is, they will begin to show foaminess at lower concentrations by weight as tricresyl phosphate replaces either A or B in solution. For example:

1% concentration of A normally does not foam; neither does 3% concentration of tricresyl phosphate; but combined they produce enough foam to go off-scale on the test.

1% concentration of B normally does not foam; neither does 3% concentration of tricresyl phosphate; but combined they produce enough foam to go off-scale on the test.

These combinations, (A + tricresyl phosphate; B + tricresyl phosphate), at various compositions, at a total concentration of 4% are reported on the foam test at 80°C in Figures 27a and 27b. The foaminess of the same compositions at a total concentration of 3%, at a temperature of 80°C., are reported in Figures 28a and 28b.

The same compositions at a total concentration of 2% or less do not foam at all on the foam test at 80°C.

The results of the foregoing experiments allow us to make the following statement about the nature of the synergism of tricresyl phosphate in tmp-heptanoate solutions.

By itself in solution tricresyl phosphate is not a profoamer, even at concentrations as high as 4%, but when combined with either A or B in a solution in non-foaming concentrations of A or B as low as 1%, it behaves, as far as foam is concerned, as if it were some additional A or B; and when the combined concentration of A + tricresyl phosphate, or B + tricresyl phosphate, is raised to levels above 2.5% (w/w), copious foam is produced.

3. Foaminess of Solutions of Span 20 in Mineral Oil, by Test Method 3213

Table 8 below reports foaminess by Test Method 3213 of solutions of Span 20 in mineral oil, in the range of concentrations of 20 ppm to 5010 ppm.

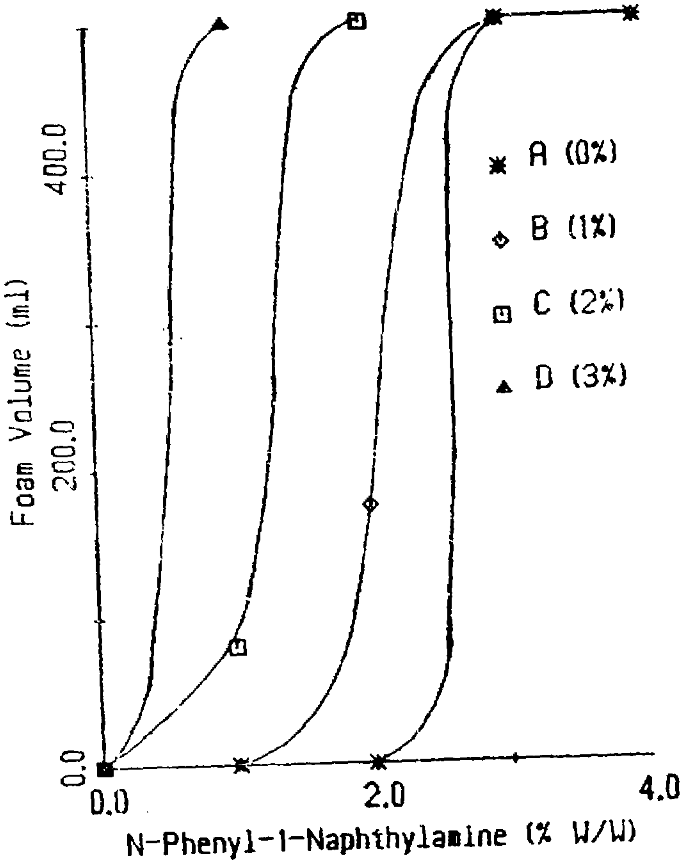

Figure 26a Foaminess Measured by Test Method 3213 at 80°C of N-Phenyl-1-Naphthylamine Dissolved in Tmp-Heptanoate up to a Concentration of 4% (w/w) (A); also Foaminess of Various Concentrations of N-Phenyl-1-Naphthylamine Combined with 1% (B), 2% (C), 3% (D), Added Tricresyl Phosphate in Tmp-Heptanoate

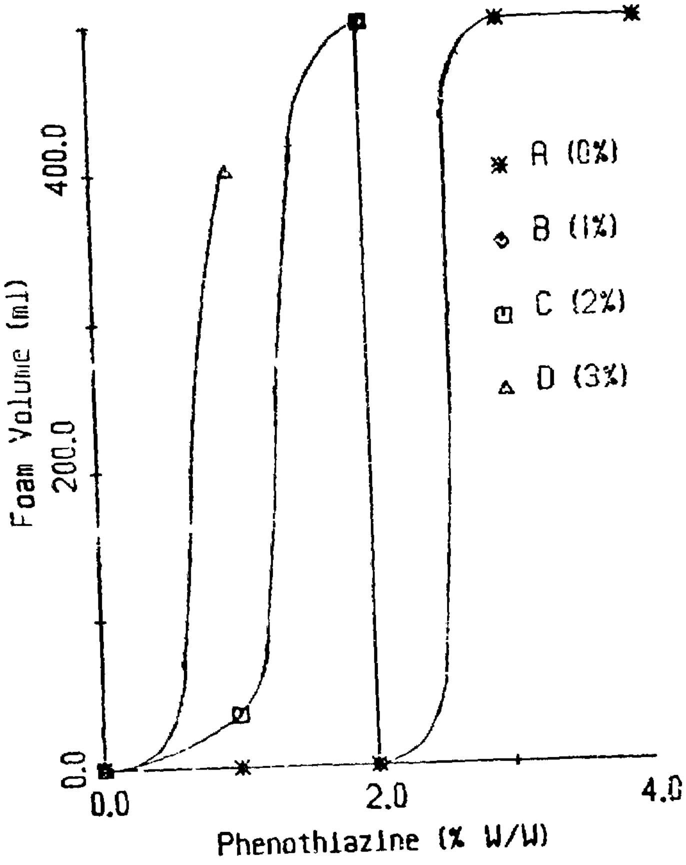

Figure 26b Foaminess Measured by Test Method 3213 at 80°C of Phenothiazine Dissolved in Tmp-Heptanoate up to a Concentration of 4% (w/w) (A); also Foaminess of Various Concentrations of Phenothiazine Combined with 1% (B), 2% (C), and 3% (D) Added Tricresyl Phosphate in Tmp-Heptanoate

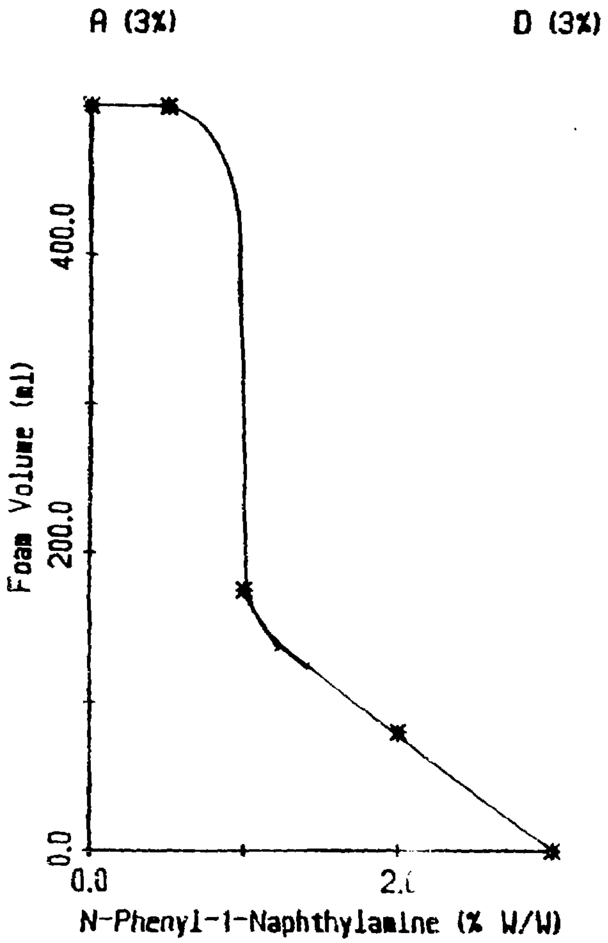

Figure 27a Foaminess of Solutions in Tmp-Heptanoate Measured by Test Method 3213 at 80°C as a Function of Mixtures of N-Phenyl-1-Naphthylamine (A) Combined with Tricresyl Phosphate (D) at Total Concentrations of 4% (w/w) of each Composition from 4% A to 4% D

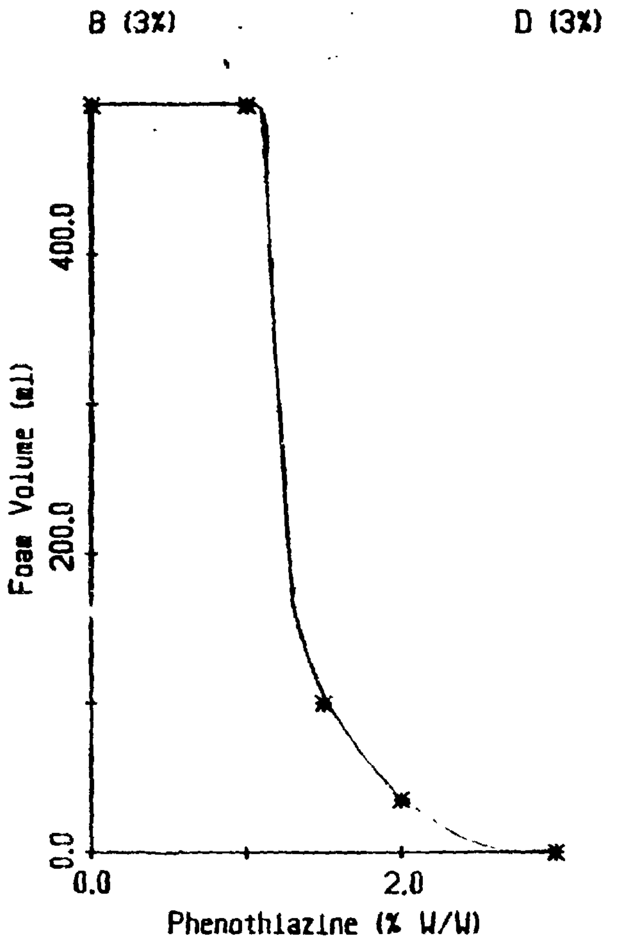

Figure 27b Foaminess of Solutions in Tmp-Heptanoate Measured by Test Method 3213 at 80°C as a Function of Mixtures of Phenothiazine (B) Combined with Tricresyl Phosphate (D) at Total Concentrations of 4% (w/w) of each Composition from 4% B to 4% D

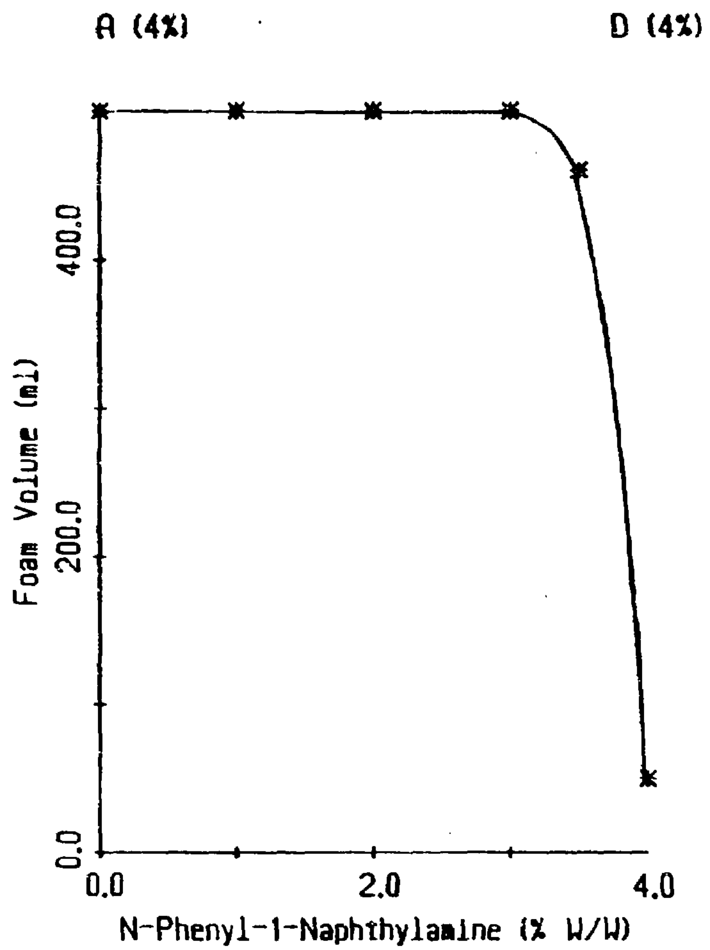

Figure 28a Foaminess of Solutions in Tmp-Heptanoate Measured by Test Method 3213 at 80°C as a Function of Mixtures of N-Phenyl-1-Naphthylamine (A) Combined with Tricresyl Phosphate (D) at Total Concentrations of 3% (w/w) of each Composition from 3% A to 3%D

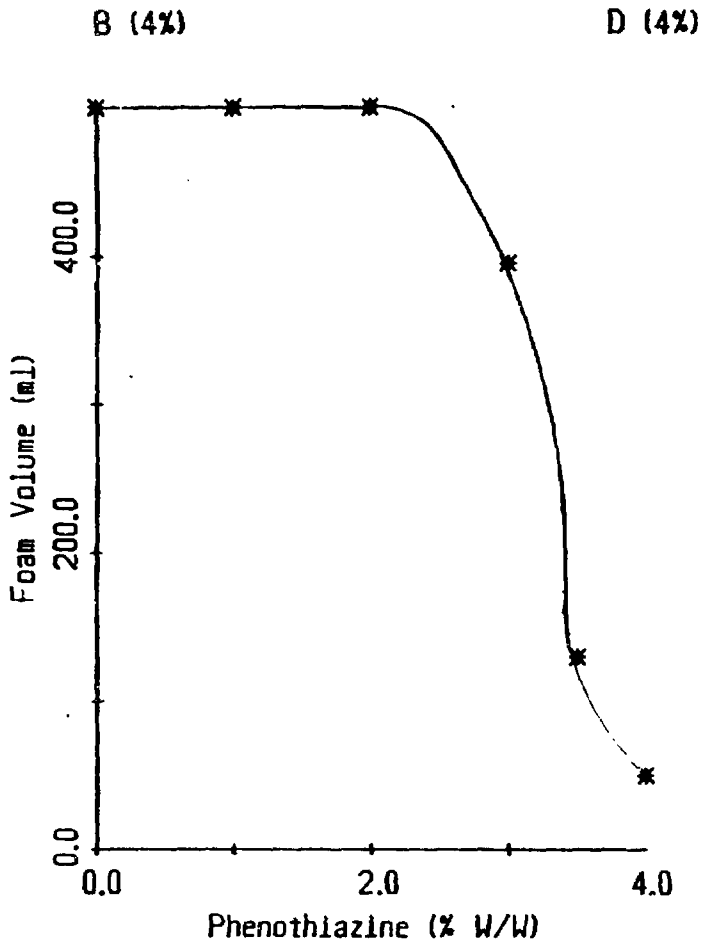

Figure 28b Foaminess of Solutions in Tmp-Heptanoate Measured by Test Method 3213 at 80°C as a Function of Mixtures of Phenothiazine (B) Combined with Tricresyl Phosphate (D) at Total Concentrations of 3% (w/w) of each Composition from 3% B to 3% D

Table 8. The Volume Ratios (Gas/Liquid Volumes) of Foams of Span 20 Solutions in Mineral Oil

Concentration (ppm)	Volume Ratio			
	25°C	40°C	60°C	80°C
0	0.65	0.95	>2	>2
20.1	0.65	0.65	>2	>2
69.9	1.75	0.95	>2	>2
81.1	1.75	1.37	>2	>2
251.6	1.75	1.75	>2	>2
601.3	>2	>2	>2	>2
5010.	>2	>2	>2	>2

Table 8 shows that at temperatures above 60°C the maximum measurable values of Volume Ratio are obtained with these solutions. At lower temperatures, the Volume Ratio increases with concentration in the range 0 to 600 ppm; above that concentration, the Volume Ratios are beyond the measurable limit.

The increase of the Volume Ratio with temperature cannot be related to variation in the amount of entrained nitrogen gas, since that decreases with temperature. The increase of the Volume Ratio with concentration of solute is parallel to the increased volume of nitrogen gas that is entrained at higher concentrations (see below Section V.5) : both effects reflect the increase of foaminess that develops with increasing concentration of Span 20.

4. Foaminess of Petronate L (Witco)

Petronate L (Witco) is described as "highly refined petroleum sulfonate." As an oil-soluble detergent it seemed likely to be a pro-foamer, and so was included in our series of tests. A solution of 1.2% w/w Petronate L in tmp-heptanoate was tested by Foam Test Method 3213. No foam was observed in the range of temperatures 25 to 80°C.

5. Foam Tests with Various Additives

Some additives used in hydrocarbon oils, received from various sources, were tested as solutions in tmp-heptanoate, by Test Method 3213.

a. OLOA 1200 (Chevron Chemical Company)
Mixtures of this additive in tmp-heptanoate at concentrations of 0.50, 1.00 and 2.03 % (w/w) were tested at 25°C, 40°C, 60°C and 80°C. No foaminess was found in that range of concentration at these temperatures.

b. OS#56119 (The Lubrizol Corporation)
The material is a formulated gear-oil blend which has been studied by Lubrizol chemists in relation to the effectiveness of various antifoamers. Mixtures in tmp-heptanoate at concentrations of 0.10, 0.50 and 1.00 % (w/w) were tested in the temperature range of 25.0 to 80.0°C. No foaminess was observed; therefore no indication of profoaming properties of this solute in tmp-heptanoate.

c. OS#60387A and OS#7160F (The Lubrizol Corporation)
The two samples tested are poly[alkyl acrylate] antifoamers denoted as OS#60387A -- 50% polymer in toluene; and OS#7160F -- 40% polymer in kerosene. Mixtures in tmp-heptanoate of 0.10, 0.50 and 1.0% (w/w) of each of the samples were tested at 25°C, 40°C, 60°C and 80°C. No foam was obtained from these solutions of either sample in the range of temperatures tested.

Tables 9 and 10 report the results with the two samples as foam inhibitors in foamy solutions of tmp-heptanoate (Table 9) and mineral oil (Table 10.) Table 9 reports that no antifoam effect was obtained in tmp-heptanoate solutions of phenothiazine (B) + tricresyl phosphate (D) or in tmp-heptanoate solutions of N-phenyl-1-naphthylamine (A) + tricresyl phosphate (D)with agent concentrations up to 2% (w/w). On the contrary, the foam volumes increased slightly as well as the rate of foam formation. (The data on rate are not included in the Tables.)

Table 10 reports that the sample OS#60387A has a small antifoaming effect at 25°C and no measurable effect at higher temperatures, when used in mineral oil at concentrations up to 2% w/w. The other sample, OS#7160F, on the other hand, proved itself a powerful antifoamer in the whole range of temperatures tested, if used at a concentration of about 2% w/w.

Table 9. Foam Volumes (cm^3) of Solutions of Additives in Tmp-Heptanoate Solutions with and without OS#60387A and OS#7160F by Test Method 3213

	2.0% w/w B + 2.0% w/w D		2.0% w/w A + 2.0% w/w D	
	No Antifoamer	2.0% w/w OS#60387A	No Antifoamer	2.0% w/w OS#7160F
25°C	330	340	255	315
40°C	390	410	400	425
60°C	550	>550	500	550
80°C	500	>550	430	525

A = N-Phenyl-1-Naphthylamine
B = Phenothiazine
D = Tricresyl Phosphate

Table 10. Foam Volumes (cm^3) obtained in Mineral Oil and Solutions of OS#60387A and OS#7160F in Mineral Oil by Test Method 3213

	Mineral Oil	OS#60387A		OS#7160F	
		0.49% w/w	1.97% w/w	0.53% w/w	1.99% w/w
25°C	>550	>550	390	255	235
40°C	>550	>550	>550	>550	245
60°C	>550	>550	>550	>550	245
80°C	>550	>550	>550	>550	250

The Aerosol OT used in these experiments was used as supplied without further purification, in spite of clear evidence of adsorbed water. The solution produced was completely transparent, the water probably solubilized in the micelles that are known to exist in nonaqueous solutions of this solute. Foam-volume ratios, flow rate of gas input = 1000 ml/minute, were obtained at four temperatures in the range 26 to 80°C, and with two concentrations of solute, 1.93% w/w, and 0.96% w/w. The data are presented in Table 11, and show that Aerosol OT is a potent profoamer in tmp-heptanoate in the range of concentration 1 to 2%.

Table 11. Volume Ratios of Foam Tests in Aerosol OT Solutions in Tmp-Heptanoate

Temp. (°C)	Volume Ratios	
	0.96% w/w	1.93% w/w
26	0.38	0.68
40	0.45	0.83
60	0.80	1.7
80	0.93	>1.7

SECTION V

AERATION, OR DETERMINATION OF ENTRAINED GAS

The IP 313/74 Method for the determination of air release value[20] was applied to measure entrained nitrogen in oil. The method is based on a controlled bubbling of nitrogen through the oil under test, and, after stopping the flow of gas, measuring the time dependence of the density of the fluid as the entrained bubbles escape from the oil.

1. Apparatus

The IP313/74 Method was slightly modified as follows:

a. Dry nitrogen gas from a gas cylinder was used instead of compressed air, which would have had to be carefully filtered and dried.

b. A mercury manometer and a gas flowmeter were added to improve the control of the gas flow.

2. Gas Release from Mineral Oil

The oil used in this experiment was a heavy white mineral oil (Albany Laboratories, Lot F1-2961). The time dependence of the gas volume (%v/v) dispersed in the oil, at five different temperatures, in the range of 25°C to 65°C, is reported in Figure 29. Figure 29 shows:

a. The volumes of dispersed gas decrease rapidly with time, as gas escapes from the oil.

b. The volumes of the dispersed gas at a given time decrease with increasing temperature in the range of 35-55°C, which is a straight reflection of the decrease of the viscosity of the oil with temperature. But at 25°C the entrained gas is less than at 35°C, though more than at 45°C. The curve for the data at 65°C overlaps --within the experimental error -- with the one at 55°C. Another sample of mineral oil from a different source did not show this complex behavior, but showed a regular decrease of entrained gas with decreasing viscosity of oil.

c. The gas release value is the time required for gas entrained in the oil to reduce in volume to 0.2% under the test conditions and at the specified temperature. For the heavy mineral oil under discussion the gas release values are a complex function of temperature (see Figure 30) with a maximum. These results indicate that temperature affects gas entrainment by a more complex mechanism than the mere change of viscosity.

3. Determination of Entrained Nitrogen in Solutions of Polydimethylsiloxane in Mineral Oil

The same oil with 27.5 ppm of polydimethylsiloxane (1000 cSt) dispersed in it provided the data reported in Figure 31. This diagram shows :

a. The presence of the silicone drastically reduces the volume of dispersed gas at a given temperature and time. This decrease

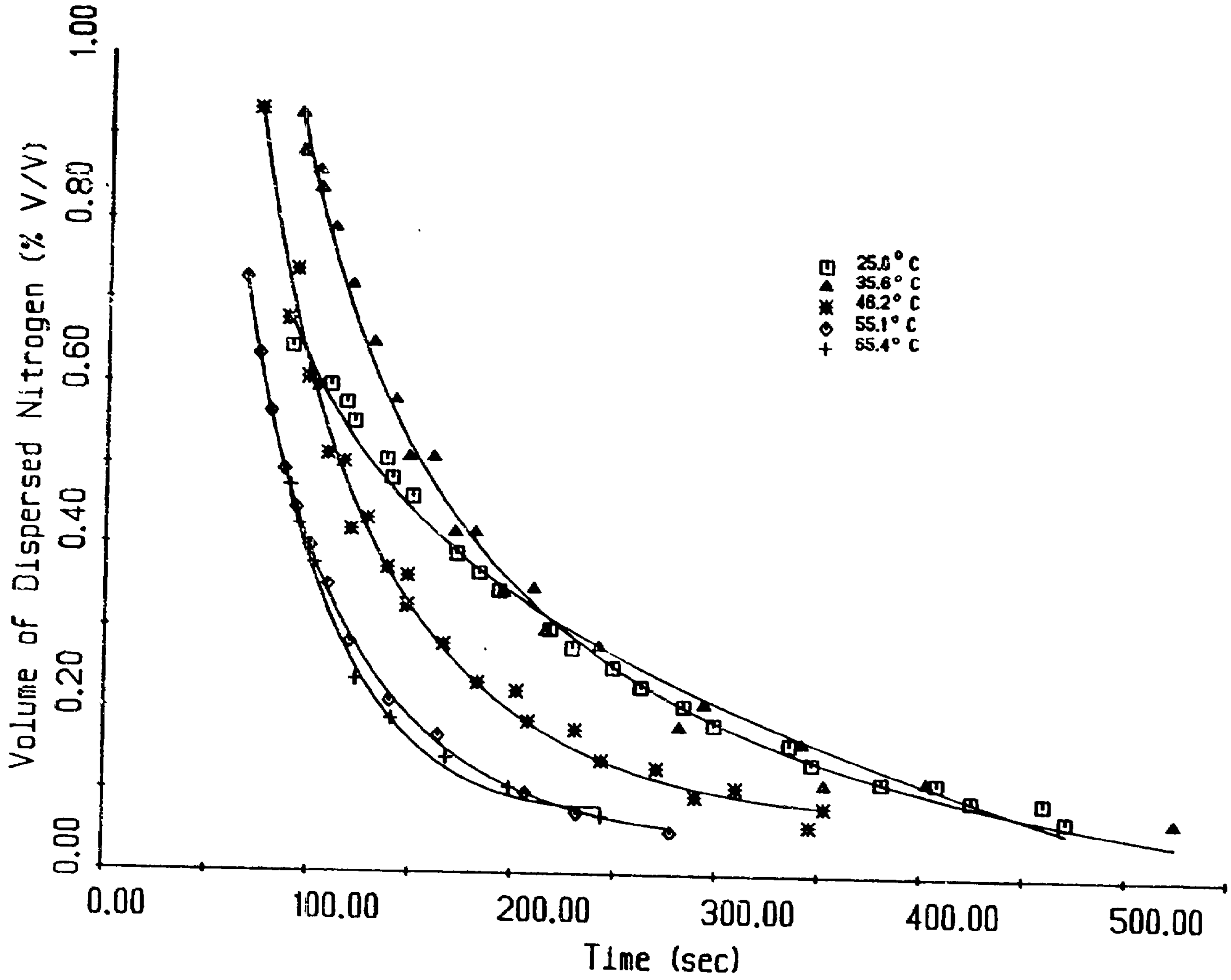

Figure 29. The Time Dependence of the Volume of Nitrogen Gas Dispersed in Mineral Oil at Various Temperatures.

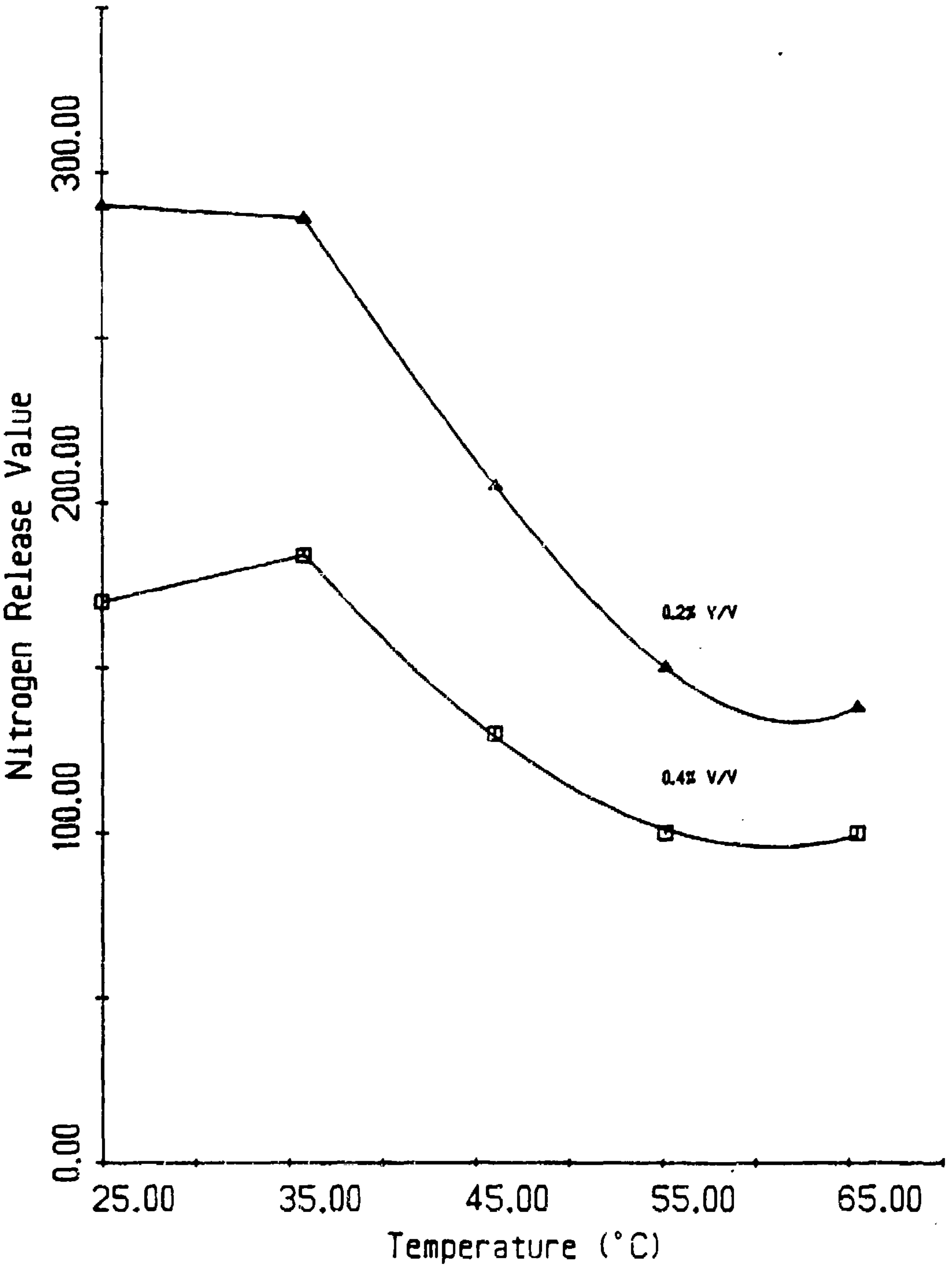

Figure 30. The Variation of the Nitrogen Gas Release Values, with Temperature, in Mineral Oil for 0.2% v/v and 0.4% v/v gas volumes.

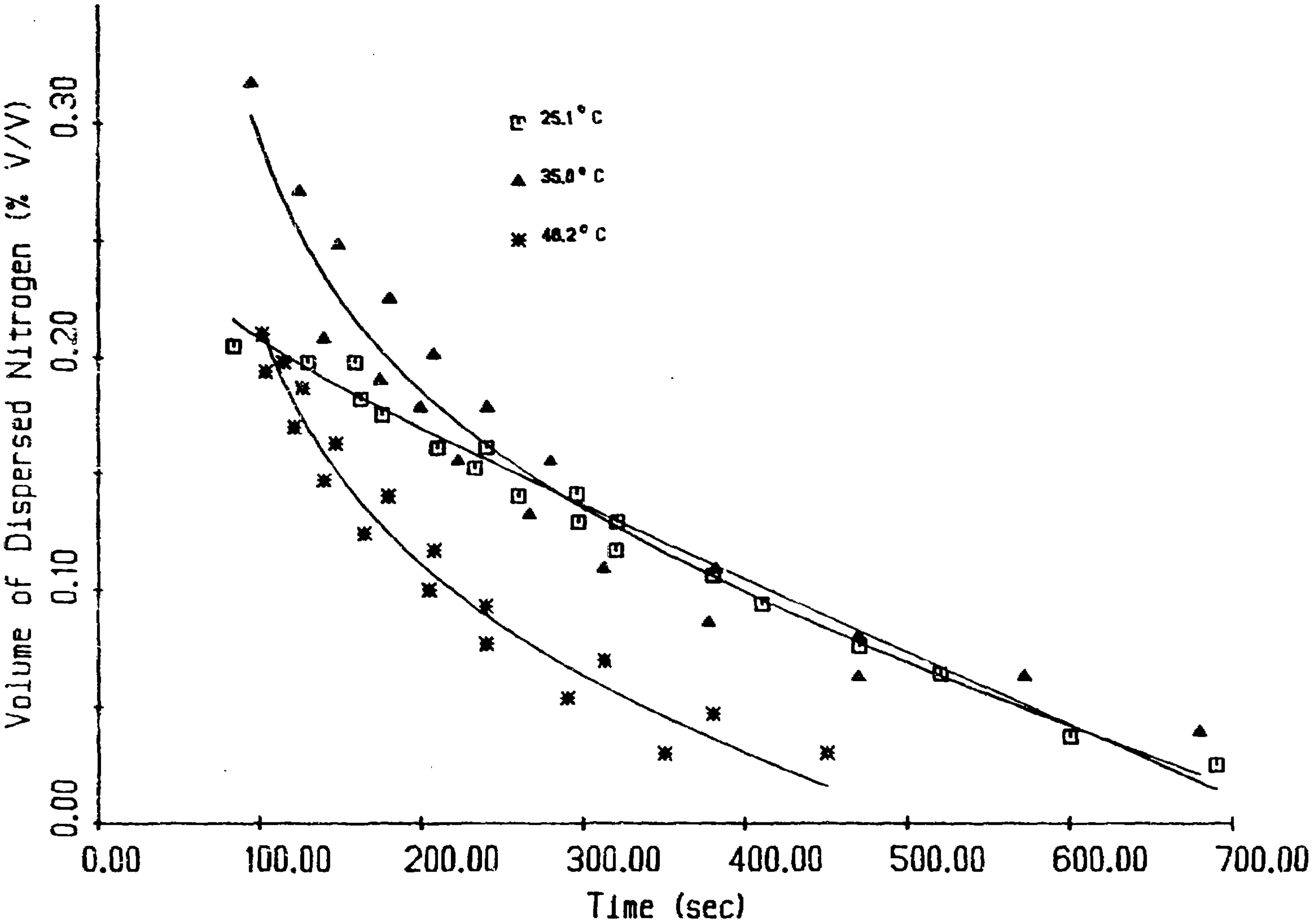

Figure 31. The Time Dependence of the Volume of Nitrogen Gas Dispersed in a 27.5 ppm Solution of Polydimethylsiloxane (1000 cSt) in Mineral Oil at Various Temperatures.

obscures the expected increase of entrainment due to the lowering of the rate of bubble rise by one-third (see below Section XIV.4.) The greatly decreased amount of entrained air in the silicone solution is probably due to the antifoaming or film-rupturing effect of the dispersed silicone in mineral oil.

b. The rate of change of the dispersed gas volume at a given temperature is lower in the silicone oil solution than in the solvent, indicating the effect of the larger number of bubbles of smaller size that was clearly visible in this solution compared to the oil without solute.

c. The same peculiar variation with temperature was repeated in the silicone oil solution as was observed in the oil solvent. The gas release curve for 25°C is located intermediately between those for 35°C and for 45°C.

The described behavior of the silicone solution may be explained by the significant reduction of surface tension by the polydimethylsiloxane (1000 cSt) at the concentration of 27.5 ppm (see above Figure 22.) At this concentration the silicone is above its limit of solubility in mineral oil, and acts as an effective foam inhibitor by destroying liquid lamellae as they are formed during the initial bubbling period of the test Method. That accounts for the much lower volume of gas that remains in the oil after the initial period of seven minutes of bubbling. On the other hand, the silicone dissolved in the oil, which is responsible for the observed lowering of the surface tension, is a surfactant and an effective dispersing or emulsifying agent for the gas phase. The presence of this solute changes the bubble size distribution in the marked way that was observed by producing a large number of tiny bubbles that require a prolonged time to depart from the solution.

Nitrogen entrainment in solutions of polydimethylsiloxane (1000 cSt) in heavy white mineral oil, in the concentration range of 0.1 to 60 ppm, was measured at 25°C, according to the method IP 313/74. Each solution was previously heated to between 60 and 70°C for several hours, cooled at room temperature while stirring, and then blended three times by means of a hand homogenizer. The measurements were carried out 40 to 45 minutes after the last pass through the hand homogenizer, to allow time for the escape of air entrained during the blending. Figure 32 describes the concentration dependence of the nitrogen-release value. Figures 33 and 34 report the volumes of entrained nitrogen after 100 seconds and 150 seconds respectively as a function of concentration. These diagrams indicate a difference in the concentration dependence in two ranges, one of 0 to 1 ppm and the other of 1.25 to 60 ppm, which correspond to values below and above the solubility of polydimethylsiloxane (1000 cSt) in this sample of mineral oil at 25°C. Below the solubility limit the nitrogen release values increase in the range of 290 to 400 seconds, that is, by a factor of 1.40, which corresponds to the retarding effect measured in the rate of rise of a gas bubble in solutions of polydimethylsiloxane in mineral oil in this range of concentration and at this temperature (see below figure 123.) Above the solubility limit, the dispersed droplets of insoluble polydimethylsiloxane show a pronounced "anti-

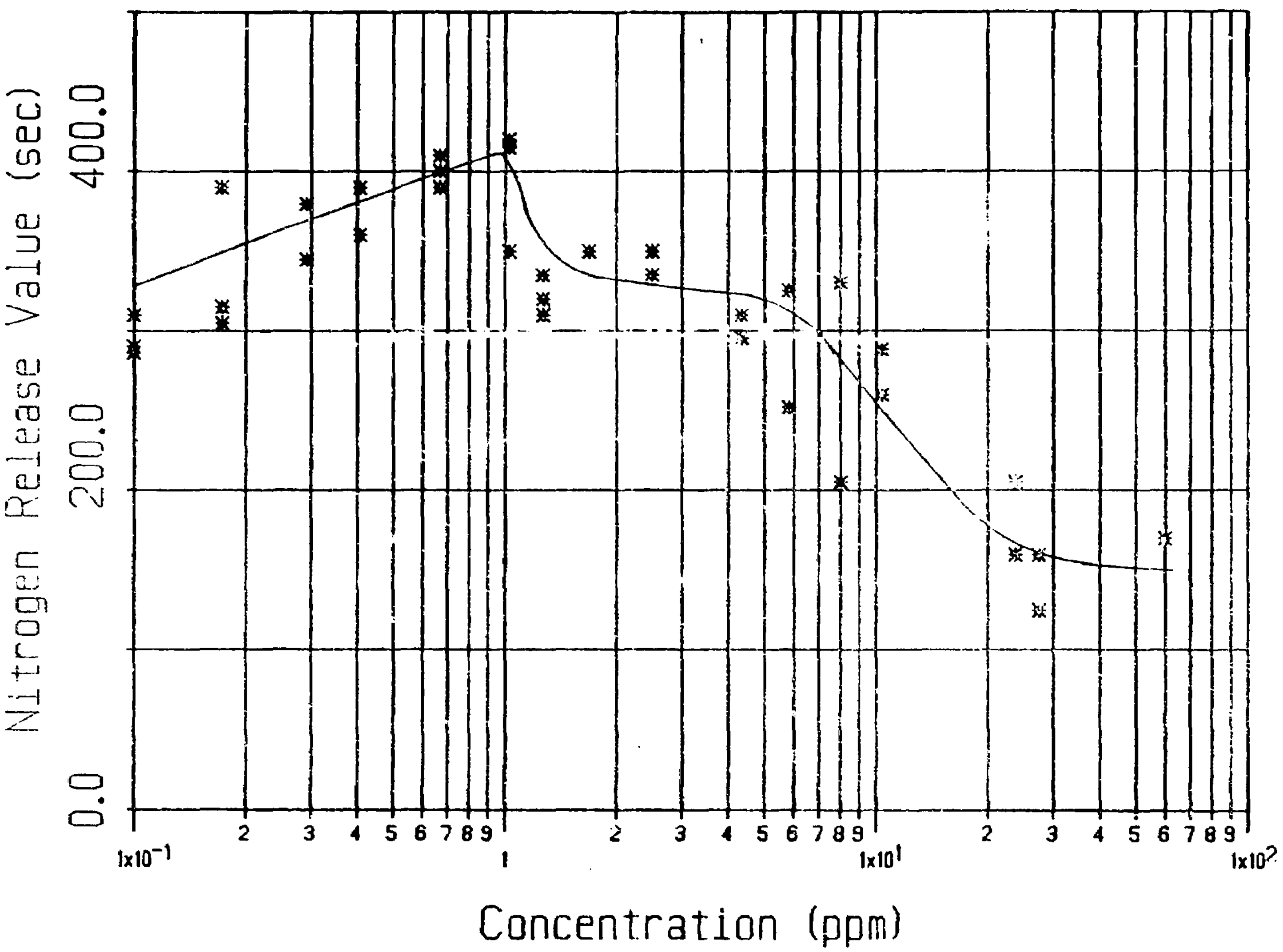

Figure 32. Nitrogen Release Values (in seconds) at 25°C as a Function of Concentration of Polydimethylsiloxane in Mineral Oil.

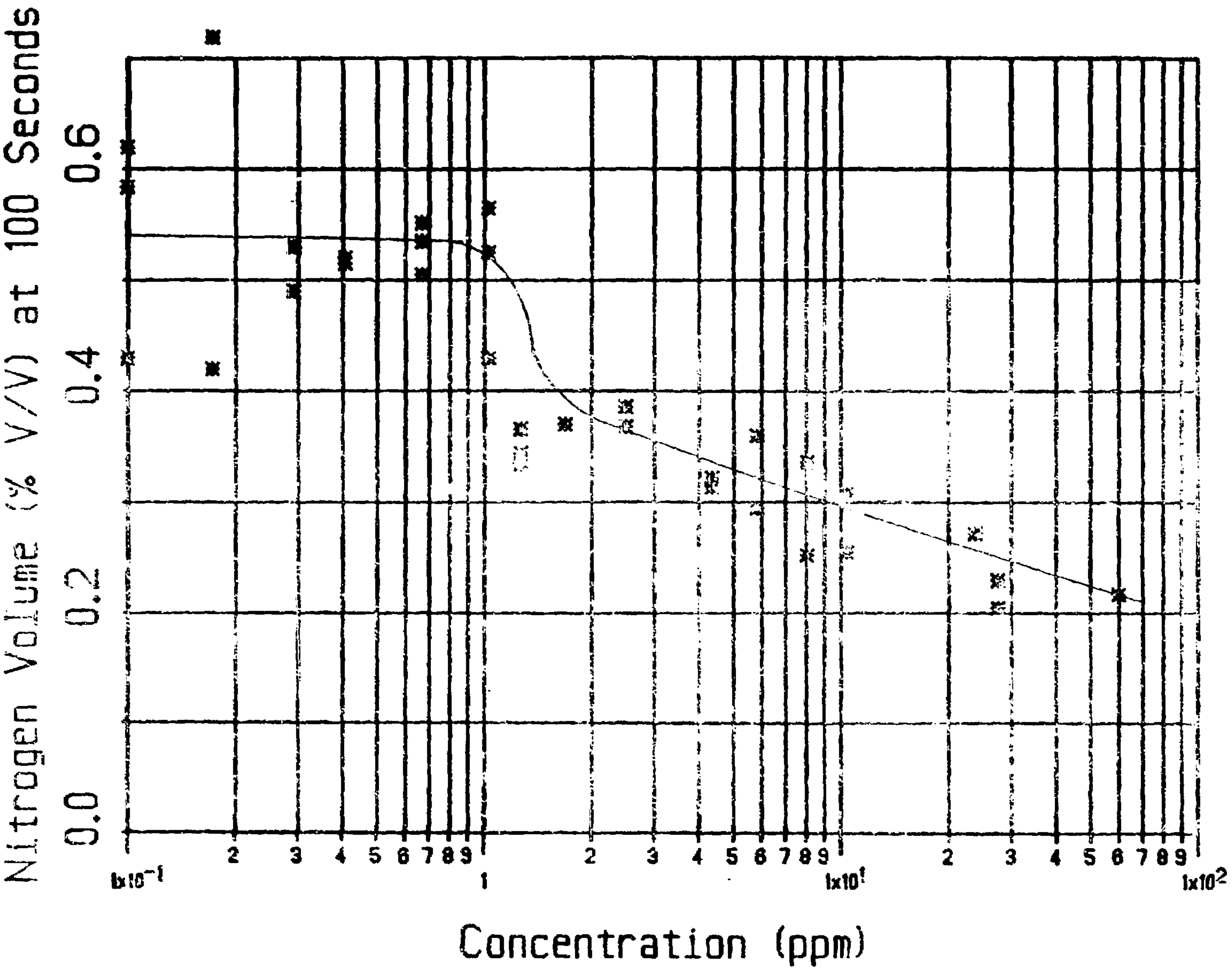

Figure 33. Retained Volume (% v/v)of Entrained Nitrogen at 100 Seconds at 25°C as a Function of Concentration of Polydimethylsiloxane in Mineral Oil.

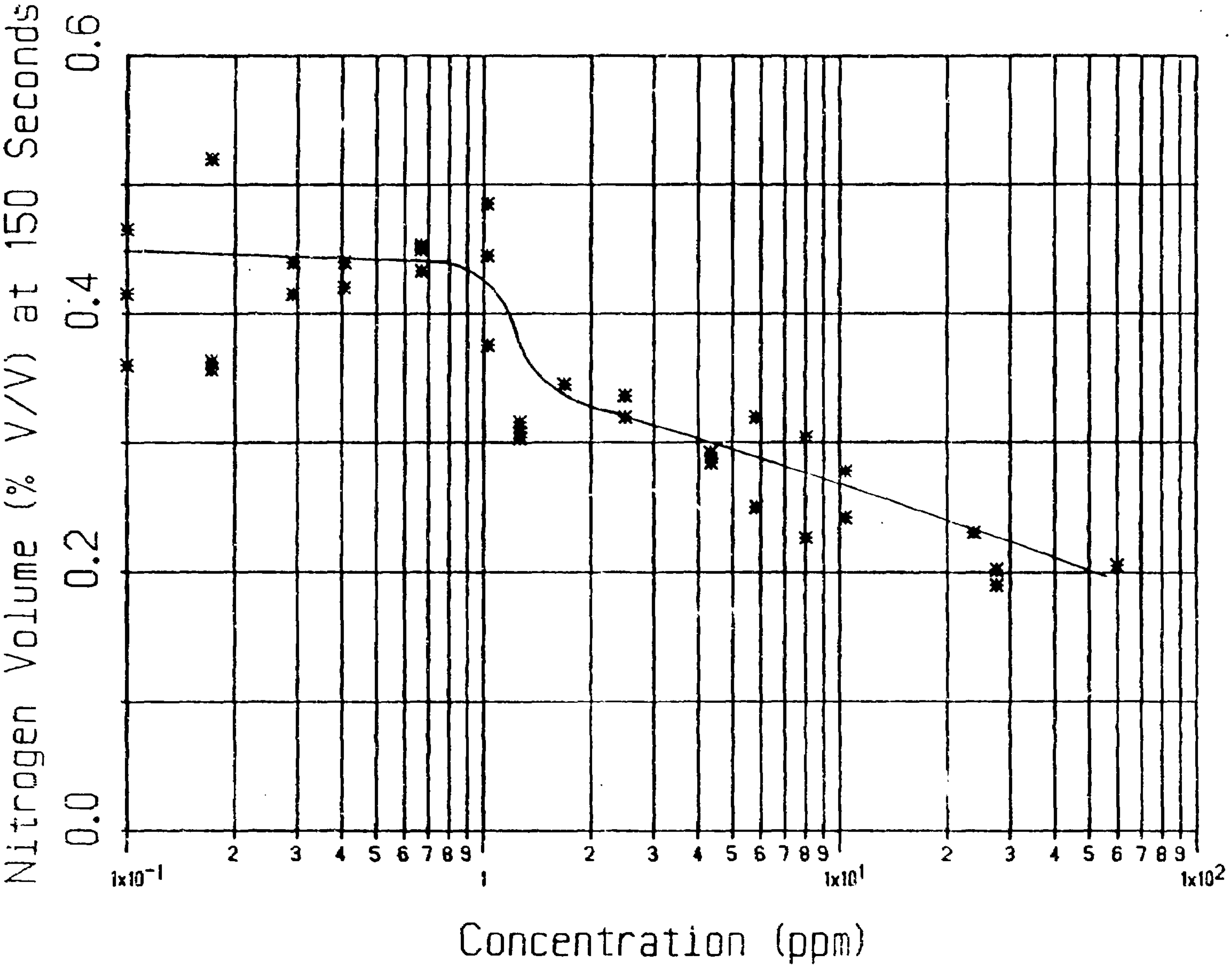

Figure 34. Retained Volume (% v/v) of Entrained Nitrogen at 150 Seconds at 25°C as a Function of Concentration of Polydimethylsiloxane in Mineral Oil.

entrainment" effect, demonstrated by the abrupt decrease of the nitrogen entrainment at a concentration of 1.0 - 1.27 ppm, from 400 to 320 seconds. At concentrations above 1.27 ppm the nitrogen release continues to decline in value, probably due to further anti-entrainment effect as more insoluble droplets of polydimethylsiloxane appear in the solution. These results clearly show that:

a. At concentrations below its solubility limit, polydimethylsiloxane promotes entrainment of gas in oil solutions;
b. Polydimethylsiloxane when insoluble has an anti-entrainment effect, probably by means of the same mechanism by which it can rupture liquid lamellae in a foam;
c. The anti-entrainment effect is concentration dependent.

4. The Dependence of the Anti-Entrainment Activity upon Particle Size

In a series of experiments we tested the effect of the quality of the silicone dispersion on the anti-entrainment properties. Solutions of given concentration were measured three times for nitrogen entrainment by the IP 313/74 Method, each time after a different treatment, namely:

a. Stirring at room temperature with a magnetic stirrer for sixty minutes;
b. Heating at 60 - 70°C for several hours, cooling with stirring at room temperature, followed by three passes through the hand homogenizer;
c. As above in (b) except for passing through the homogenizer six times instead of three times.

Figure 35 shows the time dependence of nitrogen entrained volumes in a solution of 1.27 ppm polydimethylsiloxane in mineral oil. The diagram shows that no anti-entrainment activity is shown by solutions that are merely stirred. Therefore, as with foam-inhibiting activity, a prerequisite for anti-entrainment activity is a fine dispersion.

5. Determination of Entrained Nitrogen in Solutions of Span 20 in Mineral Oil

The mineral oil used in the foregoing experiments came from a different batch (Albany Laboratories) than the one used previously, which was no longer available to us.

The time dependence of the gas volumes (% v/v) dispersed in the oil, at 25°C, 35°C, and 45°C, is reported in Figure 36. Comparison of this diagram with Figure 28, containing similar curves for the mineral oil used previously, shows:

a. In the second batch used, the volumes of dispersed gas are smaller;
b. The volumes of dispersed gas decrease regularly with temperature, reflecting the parallel changes of viscosity of the oil. The peculiarity observed with the batch of oil used previously, namely, that the entrainment curve for 25°C is located between those for 35°C and 45°C, is not repeated with this batch of oil.

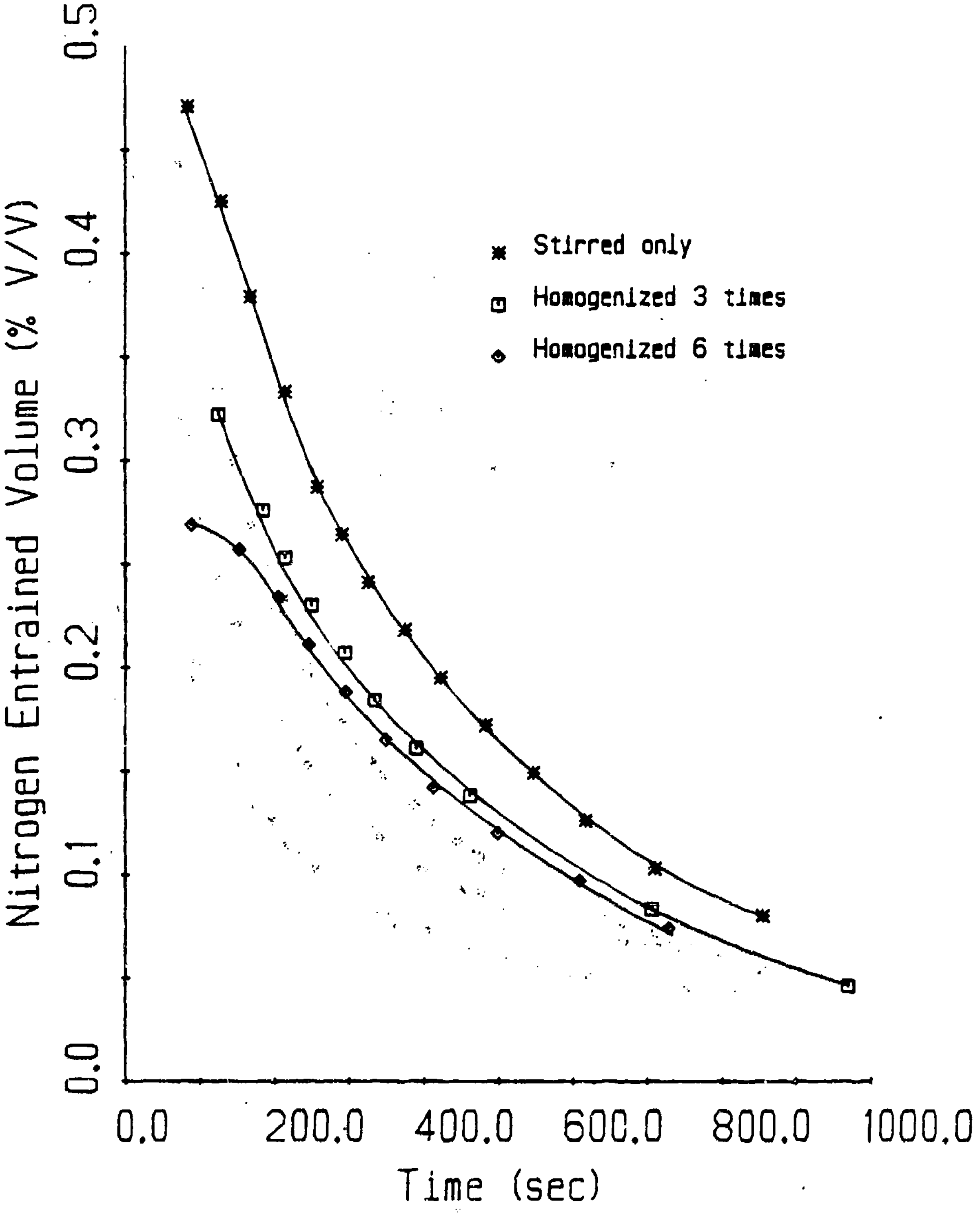

Figure 35. Rate of Loss of Retained Volume (% v/v) of Entrained Nitrogen in a 127 ppm Solution of Polydimethylsiloxane in Mineral Oil at 25°C.

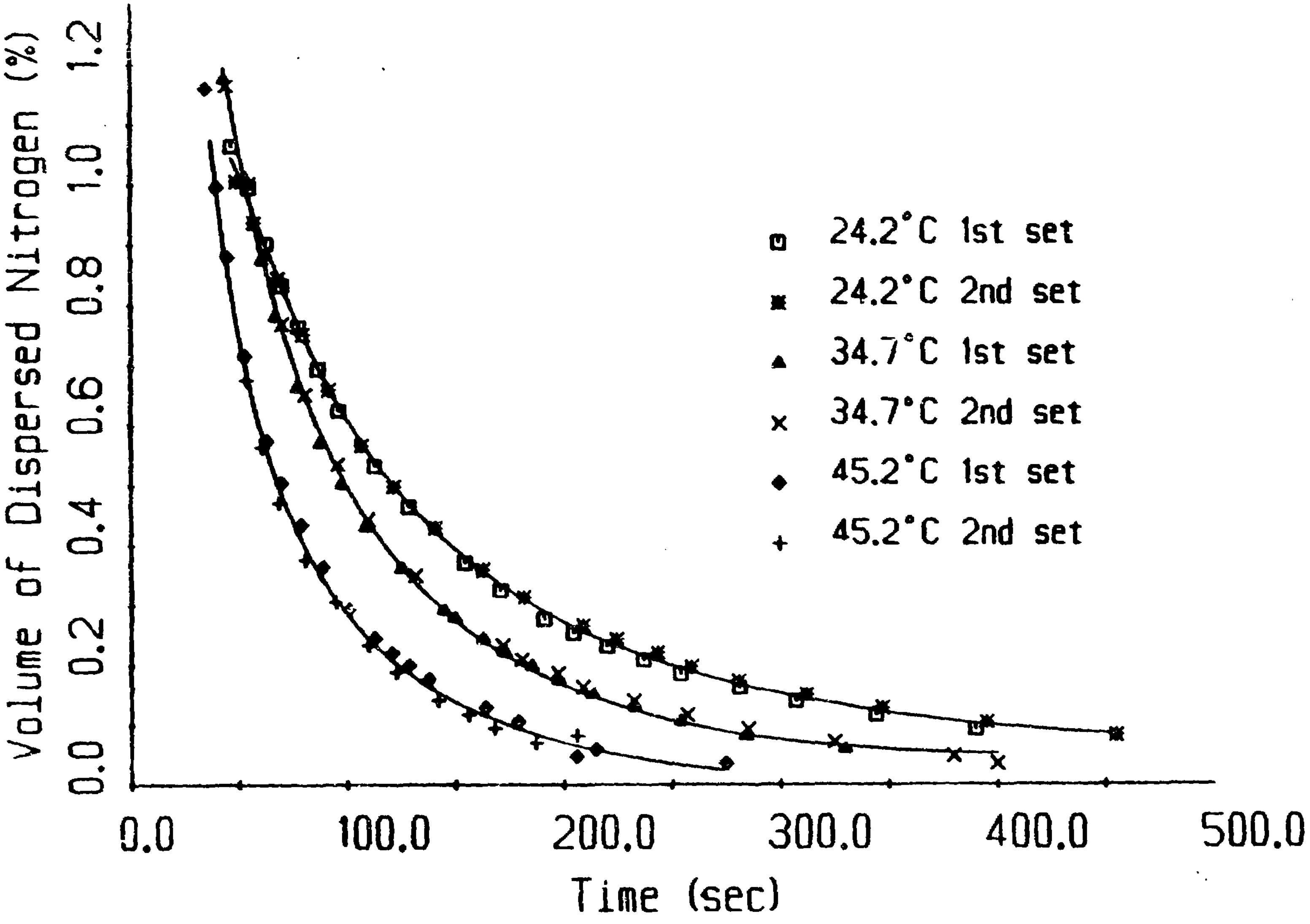

Figure 36. Time Dependence of Concentration of Entrained Nitrogen (% v/v) in Mineral Oil (batch no. 2) at Various Temperatures.

Entrainment of nitrogen in solutions of Span 20 in mineral oil,in the range of concentrations of 20 to 5010 ppm, was measured at 25°C using the method IP 313/74 and procedures described previously. Figures 37 and 38 describe the variation with concentration of the values of Nitrogen Release (in seconds) and of Nitrogen Volume at 100 Seconds (in %v/v,) respectively. The diagrams indicate that at low concentrations of Span 20, up to 70 ppm, the volumes of dispersed gas are small and independent of concentration; at greater concentrations the volumes of dispersed gas rapidly increase. A possible reason for the increased entrainment, which goes far beyond the relatively slight decrease in the rate of rise of a single bubble with greater concentration of surface-active solute (see below Figure 123,) is the production of smaller bubbles with greater concentration of solute. The measurement of the rate of rise of a single bubble were all done with equal-sized bubbles. The appearance of smaller bubbles in the gas-entrainment tests at greater concentrations is, indeed, a visual observation. The production of smaller bubbles is related (at least qualitatively) to the reduction of surface tension of these solutions, which occurs rather abruptly near the range of concentrations where the enhanced entrainment of gas is observed. (See Figure 22.)

6. Determination of Entrained Nitrogen in Solutions of Polydimethyisiloxane (1000 cSt) in Tmp-Heptanoate

The volumes of nitrogen gas entrained at 25°C by solutions of polydimethylsiloxane (1000 cSt) in tmp-heptanoate were measured by Test Method IP 313/74. Within the range of concentration of 0.3 to 500 ppm the measurable volumes of entrained nitrogen gas are very small, not exceeding 0.160 %(v/v) after an interval of 45 seconds from cessation of bubbling (45 seconds is the minimum time required after bubbling before the first reading can be obtained.) Figure 39 shows the concentration dependence of the entrained gas volume fifty seconds after stopping the flow of nitrogen gas. The amount of entrained gas increases with concentration of polydimethylsiloxane up to 120 ppm, then decreases sharply.

The curves reported in Figures 12 and 39 show identical behavior of the foaminess and the gas entrainment in these solutions, with respect to concentration. Plans for future work include similar measurements on other systems to test the generality of this correlation.

The decline of foaminess and of gas entrainment that is evident in Figures 12 and 39 occurs at a concentration (120 ppm) of polydimethylsiloxane in tmp-heptanoate that is far above the limit of solubility of the solute in this solvent, which is only about 5 ppm. In another solvent, mineral oil, a similar decline of gas entrainment with concentration of polydimethylsiloxane was observed, as reported in Figures 33 and 34; but there the anti-entrainment effect takes place at a concentration only slightly greater than the solubility limit. This difference in behavior in the two solvents is linked to our observation that polydimethylsiloxane is more

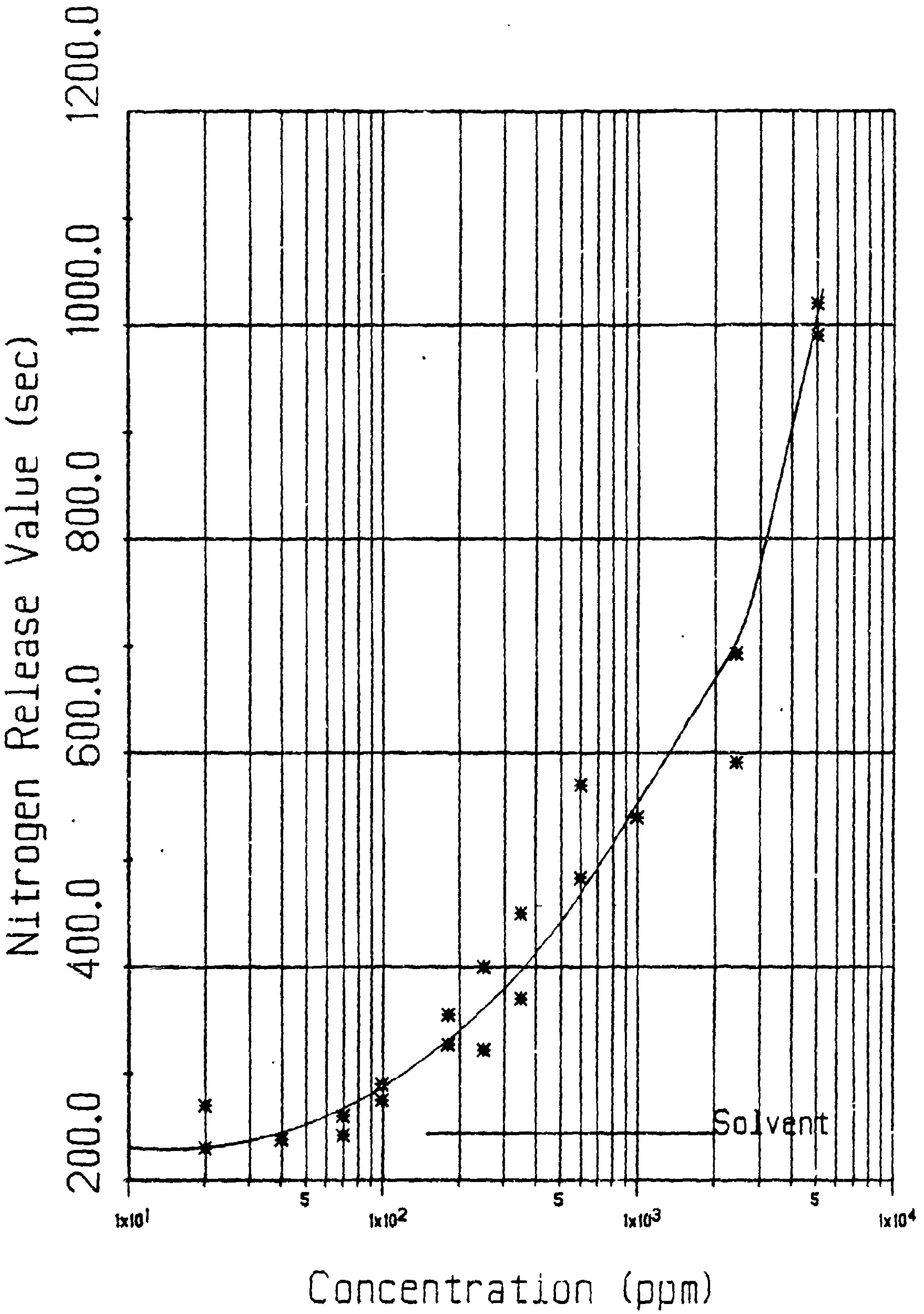

Figure 37. Nitrogen Release Value (Time Required for Concentration of Nitrogen in the Liquid to Reach 0.2% v/v) *Versus* Concentration of Span 20 in Mineral Oil at 25°C.

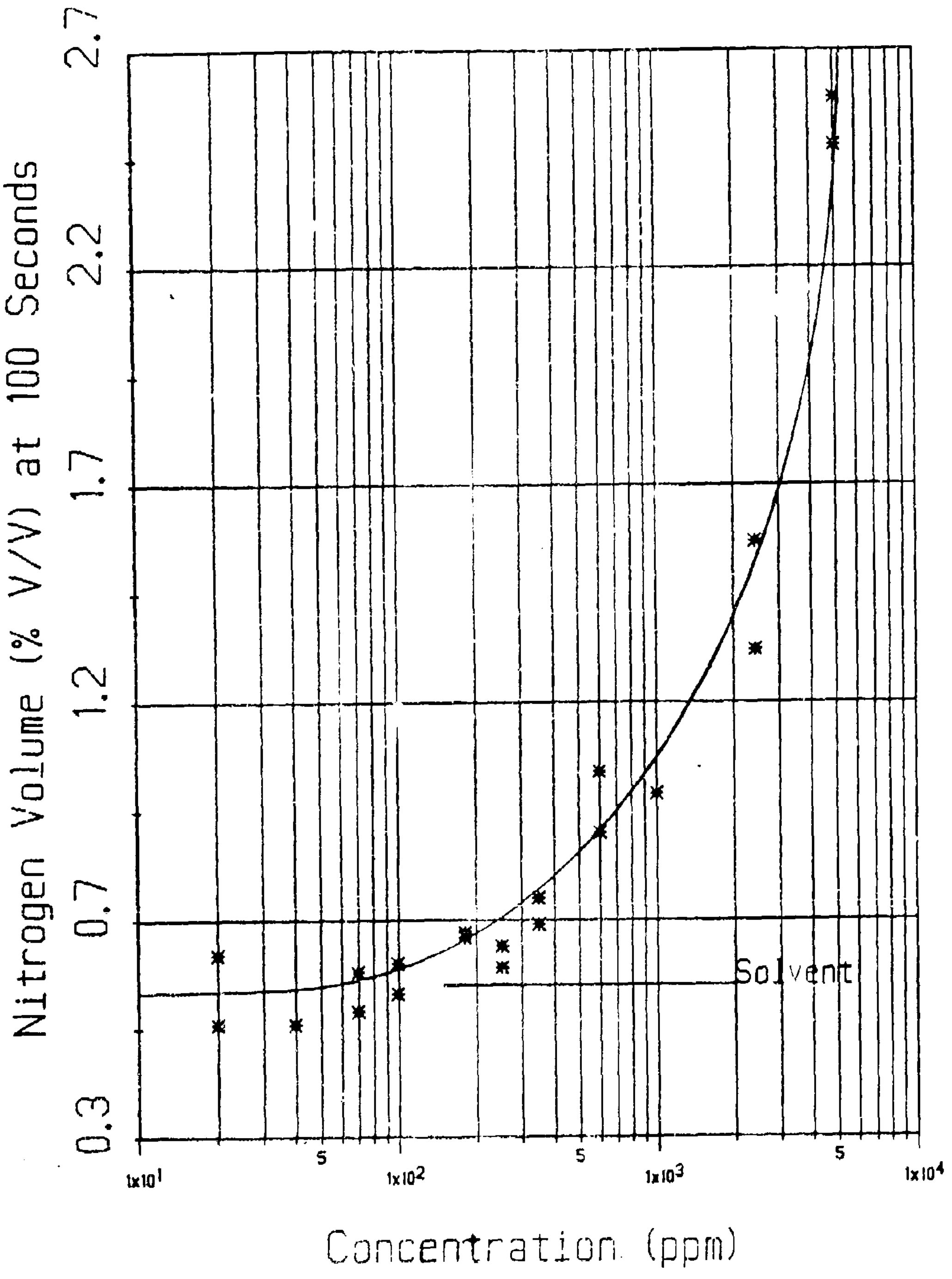

Figure 38. Nitrogen Entrainment Value (Concentration of Nitrogen in the Liquid % v at 100 sec) Versus Concentration of Span 20 in Mineral Oil at 25°C.

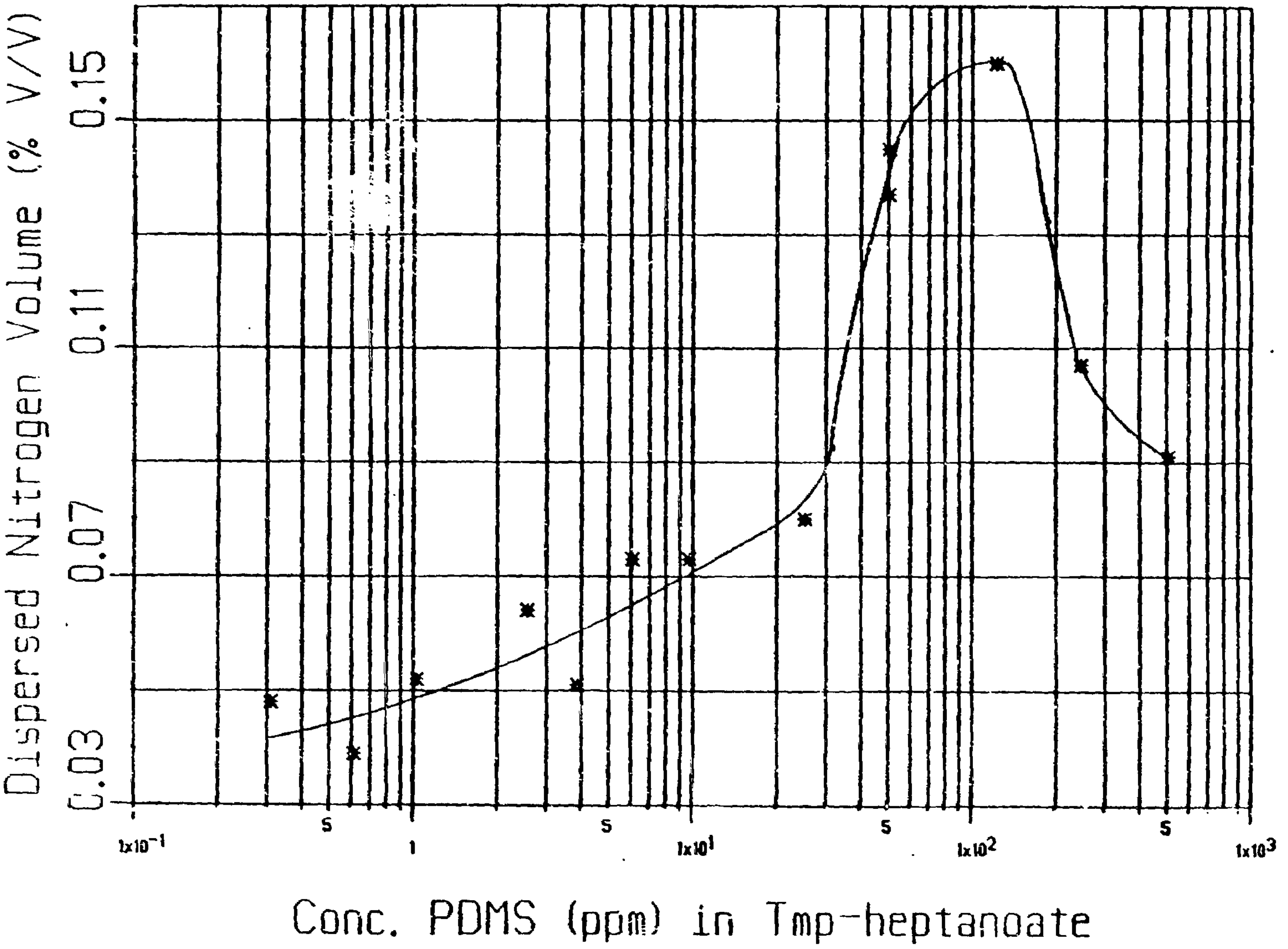

Figure 39. Volume of Nitrogen Gas Entrained at 25°C by Solutions of Polydimethylsiloxane (1000 cSt) in Tmp-Heptanoate, by Test Method IP 313/74.

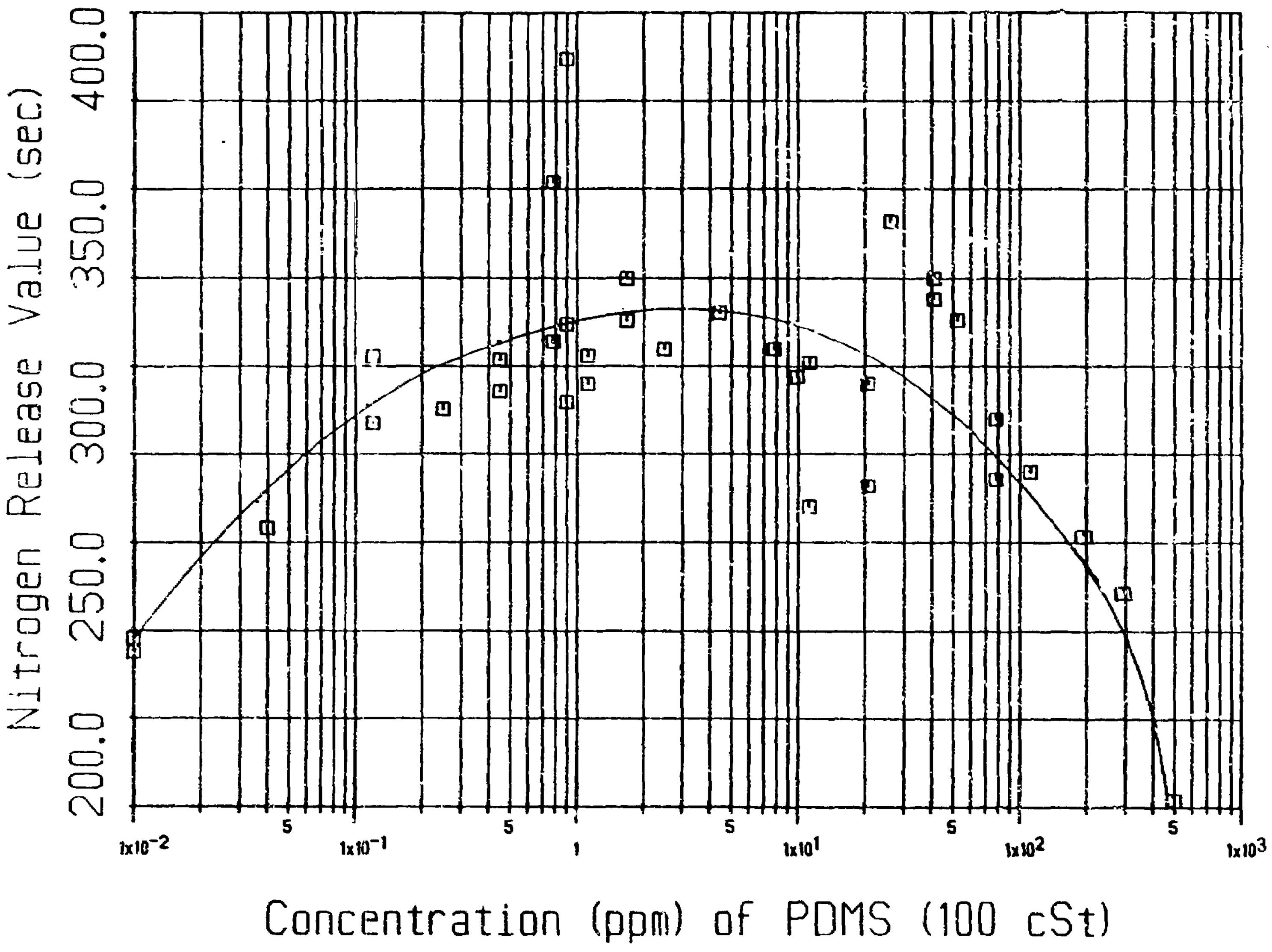

Figure 40. Entrainment of Nitrogen Gas by Solutions of Polydimethylsiloxane (100 cSt) in Tmp-Heptanoate at 25°C.

effective as an antifoam in hydrocarbon oils than it is in a synthetic lubricant.

Figure 40 shows the nitrogen-gas release values for the polydimethylsiloxane (100 cSt) solutions, at 25°C, in the range of concentrations 0.01 to 500 ppm. Like the results obtained with the corresponding solutions of polydimethylsiloxane (1000 cSt) in mineral oil, Figure 40 shows a range of concentration (< 4ppm) at which the volumes of entrained nitrogen gas increase with concentration, followed by a decrease. In the lower range of concentration, where the increasing entrainment occurs, the values of the nitrogen-release times rise from 245 to 345 seconds, i.e., by a factor of 1.4, which probably corresponds to the retarding effect of the adsorbed solute on the rate of rise of a gas bubble.

We report in Figure 41 the foaminess of the polydimethylsiloxane (100 cSt) solutions in mineral oil, in the same range of concentrations as those reported in Figure 40, at temperatures of 25°C, 40°C, and 60°C. The diagram shows the same general behavior pattern for the polydimethylsiloxanes in mineral oil solutions (compare Figure 13) though with much less antifoam activity of the lower molecular weight solute. But the presence of the polydimethylsiloxane (100 cSt) causes the foaminess to decrease continuously from a Volume Ratio of 1.75 at 10^{-2} ppm to 0.5 at 100 ppm, so that no definite concentration can be singled out as the critical point at which antifoaming begins; thus a close correlation between antifoam and anti-entrainment effects is not observed with this solute.

7. Aeration Study (Aerosol OT in Tmp-heptanoate)

Aeration tests were carried out according to the standard test IP 313/74 at 25°C. Figure 42 reports the concentration of nitrogen gas (% v/v) as a function of time for three solutions of Aerosol OT in tmp-heptanoate: 0.51%, 0.96%, and 2.04% (w/w). These data show a marked increase in the aeration of the solvent between one and two percent concentration of the solute.

8. Foam and Gas Entrainment of Polydimethylsiloxane (500 cSt) in Tmp-Heptanoate

We have reported above an observed parallelism in behavior between the effects of polydimethylsiloxane (1000 cSt) solutions in tmp-heptanoate and in mineral oil, on foam inhibition and on anti-entrainment of gas. We extended the investigation to polydimethylsiloxane (100 cSt) dissolved in mineral oil, where we found that the parallelism was less in evidence. These effects are now investigated further with solutions of polydimethylsiloxane (500 cSt) in tmp-heptanoate.

The volumes of entrained nitrogen gas were determined at 25°C by Test Method IP 313/74. The foaminess was measured by Test Method 3213 at temperatures of 25°C, 40°C, 60°C, and 80°C. Prior treatment of the samples (heating, blending, etc.) was identical for both series of tests.

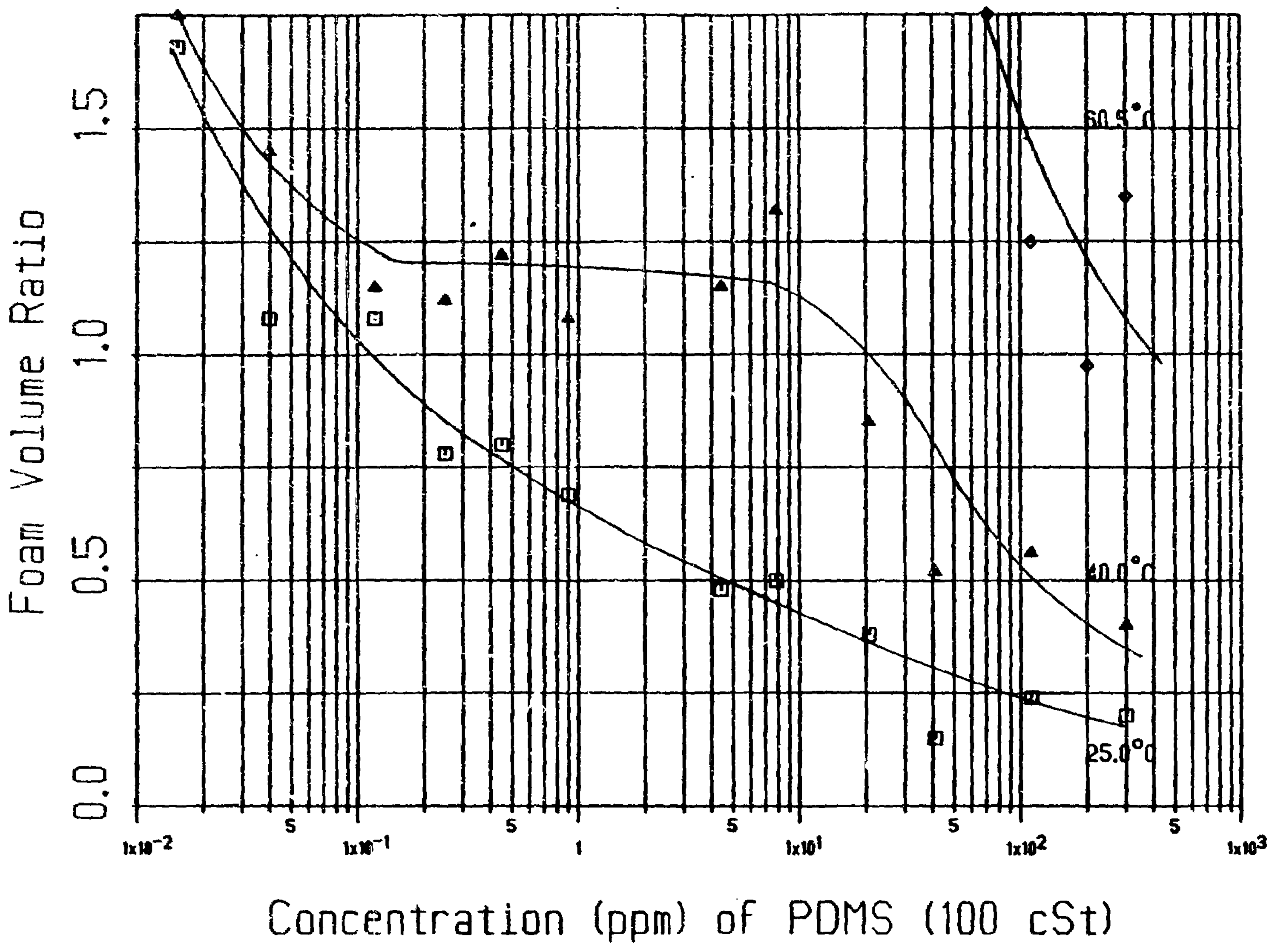

Figure 41. Foaminess of Solutions of Polydimethylsiloxane (100 cSt) In Tmp-Heptanoate at 25°C, 40°C, and 60°C, Measured by Test Method 3213.

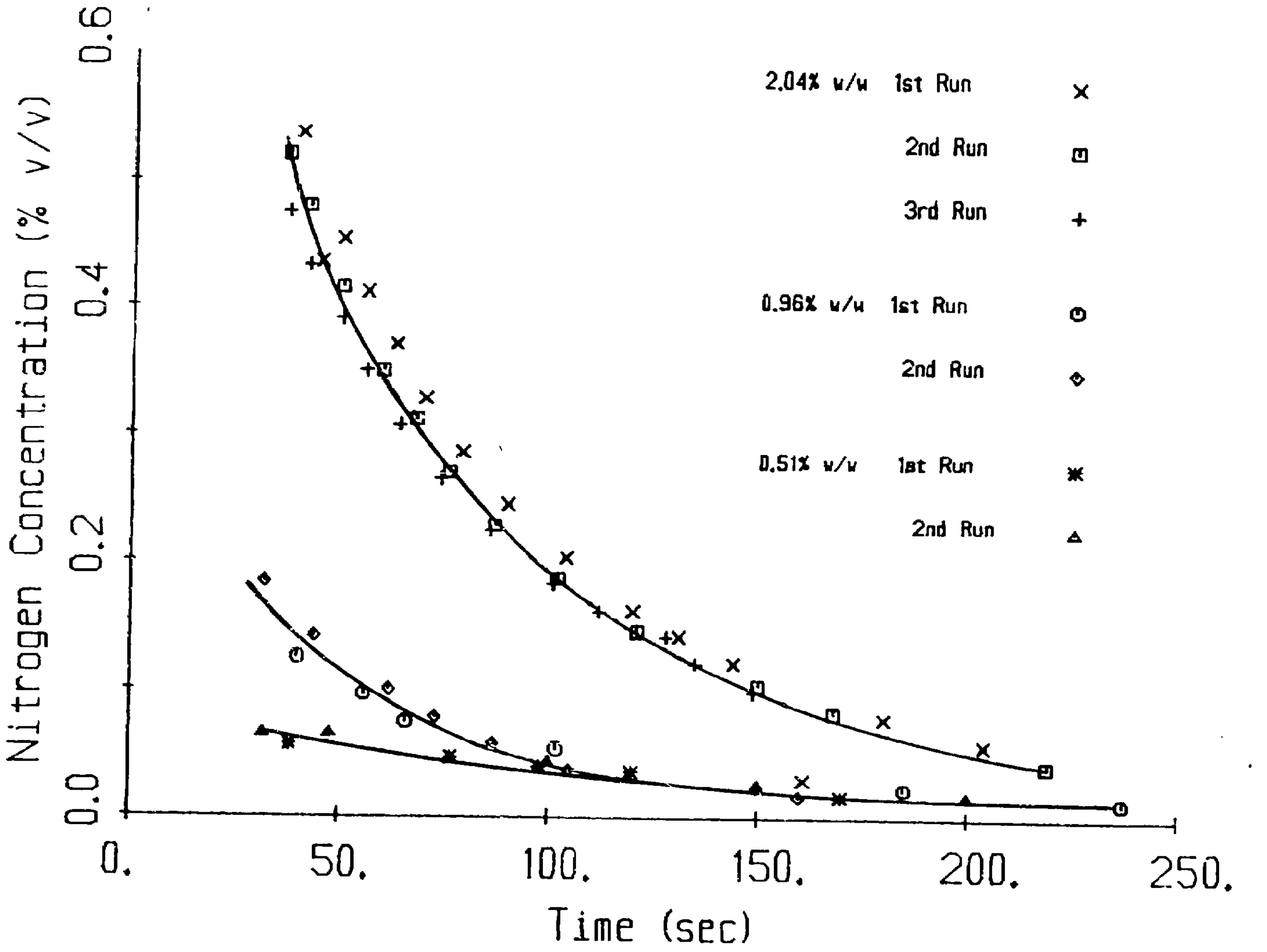

Figure 42. Time Dependence of Concentration of Entrained Nitrogen (% v/v) in Solutions of Aerosol OT in Tmp-Heptanoate at 25°C.

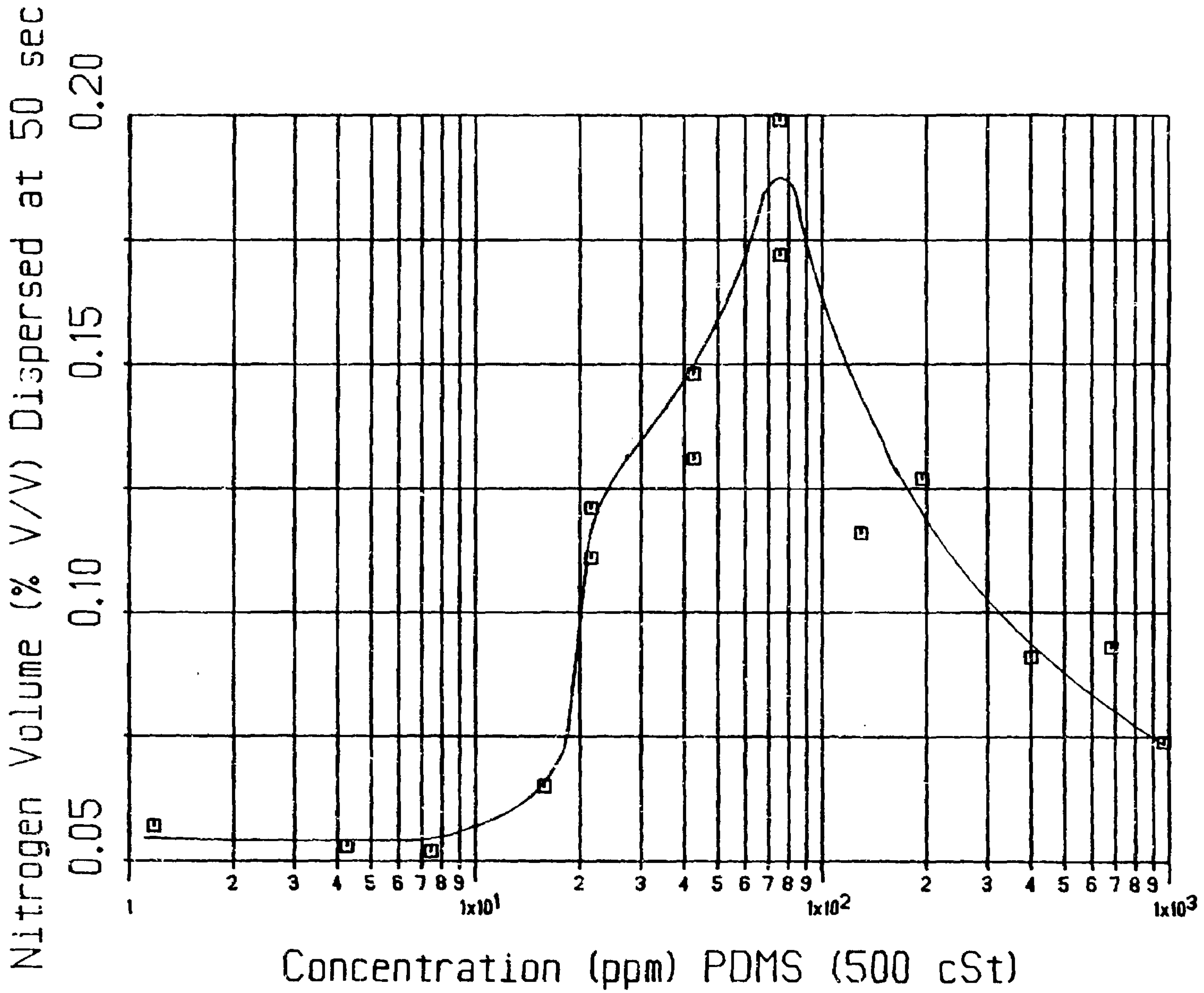

Figure 43. Volume of Nitrogen Gas Entrained at 25°C by Solutions of Polydimethylsiloxane (500 cSt) in Tmp-Heptanoate, by Test Method IP 313/74.

Figure 43 shows the concentration dependence of the entrained-gas volumes 50 seconds after stopping the flow of nitrogen gas into the solution, at 25°C. The amount of entrained gas increases sharply in the concentration range of 10 to 80 ppm of solute, then decreases. Figure 44 shows the results of the foam measurements at four temperatures, with the same solutions that were used in the entrainment tests.

Figures 43 and 44 show similar behavior for gas entrainment and for foaminess in these solutions as a function of the concentration, establishing the parallelism already noted with the higher molecular weight polydimethylsiloxane. It is worth noting that the concentration of solute at which these effects maximize is larger for the longer-chain polymer than for the shorter-chain polymer, suggesting that about the same molar concentration is required in each case. For both polymers, that concentration is above the solubility limits that we previously reported for polydimethylsiloxanes in tmp-heptanoate.

9. Foam and Gas Entrainment of Polydimethylsiloxane (5000 cSt) in Tmp-Heptanoate

We reported above the observed parallelism in behavior between the effects of two polydimethylsiloxanes (1000 and 100 cSt) with solutions in tmp-heptanoate and in mineral oil, on foam inhibition and on anti-entrainment of gas. These effects were further investigated with solutions of polydimethylsiloxane (500 cSt) in tmp-heptanoate. It was noted there that the concentration of solute at which the effects of foaminess and entrainment maximize, shifts to higher concentrations with the longer-chain polymer. These effects are now investigated further with solutions of polydimethylsiloxane (5000 cSt) in tmp-heptanoate.

The volumes of entrained nitrogen gas were determined at 25°C by Test Method IP 313/74. The foaminess was measured by Test Method 3213 at temperatures of 25°C, 40°C, 60°C, and 80°C. Prior treatment of the samples (heating, blending, etc.) was identical for both series of tests.

Figure 45 shows the concentration dependence of the entrained gas volumes 50 seconds after stopping the flow of nitrogen gas into the solution, at 25°C. The amount of gas increases in the concentration range 4 to 260 ppm, then decreases. Figure 46 shows the results of the foam measurements at three temperatures with the same solutions that were used in the entrainment tests.

Figures 45 and 46 confirm the similar behavior for gas entrainment and for foaminess as a function of concentration. It also shows a shift to a higher concentration of the value at which the effects have their maximum, compared to the shorter chain polymers previously investigated.

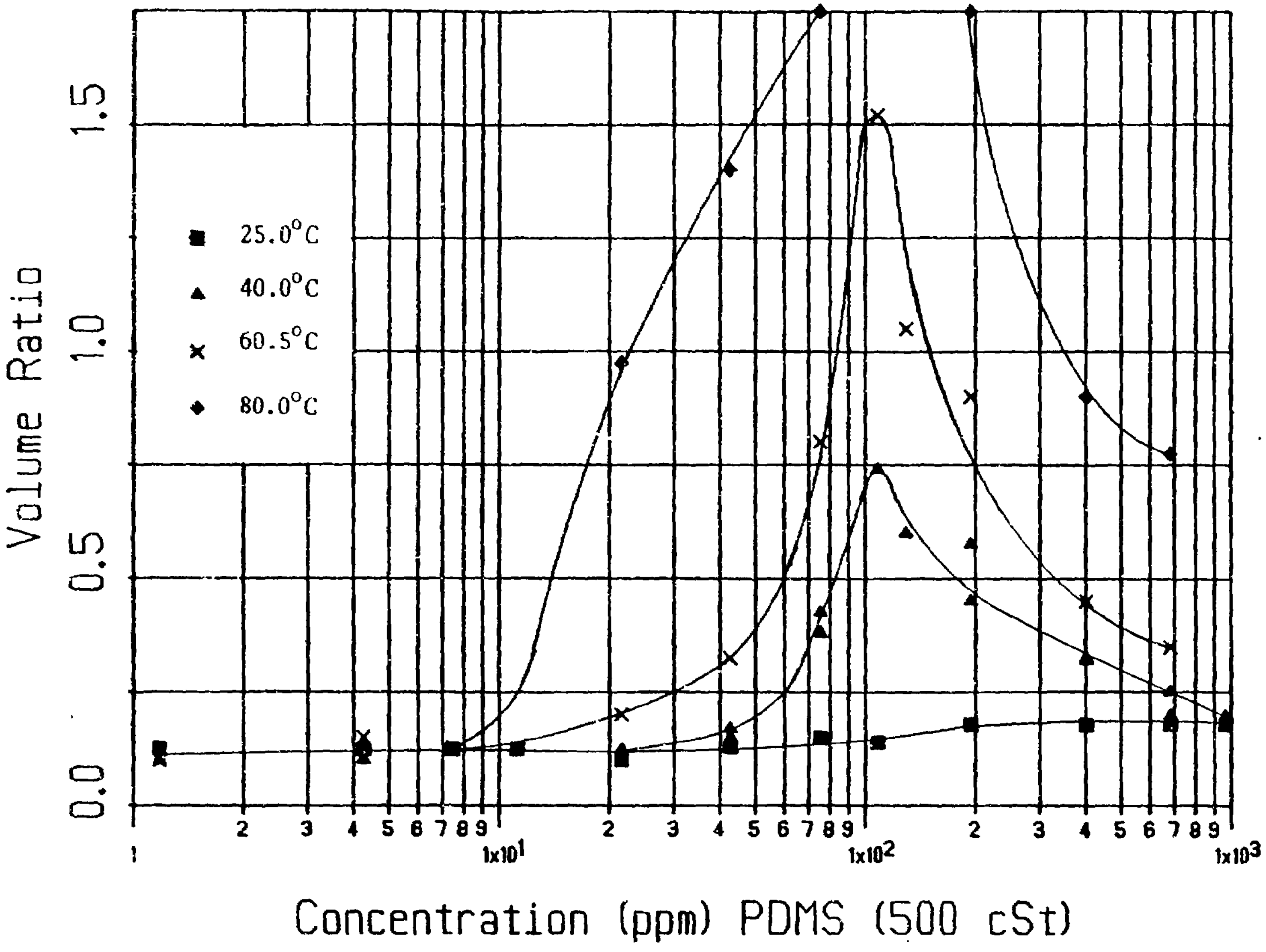

Figure 44. Foaminess of Solutions of Polydimethylsiloxane (500 cSt) in Tmp-Heptanoate at 25°C, 40°C, 60°C, an 80°C, measured by Test Method 3213.

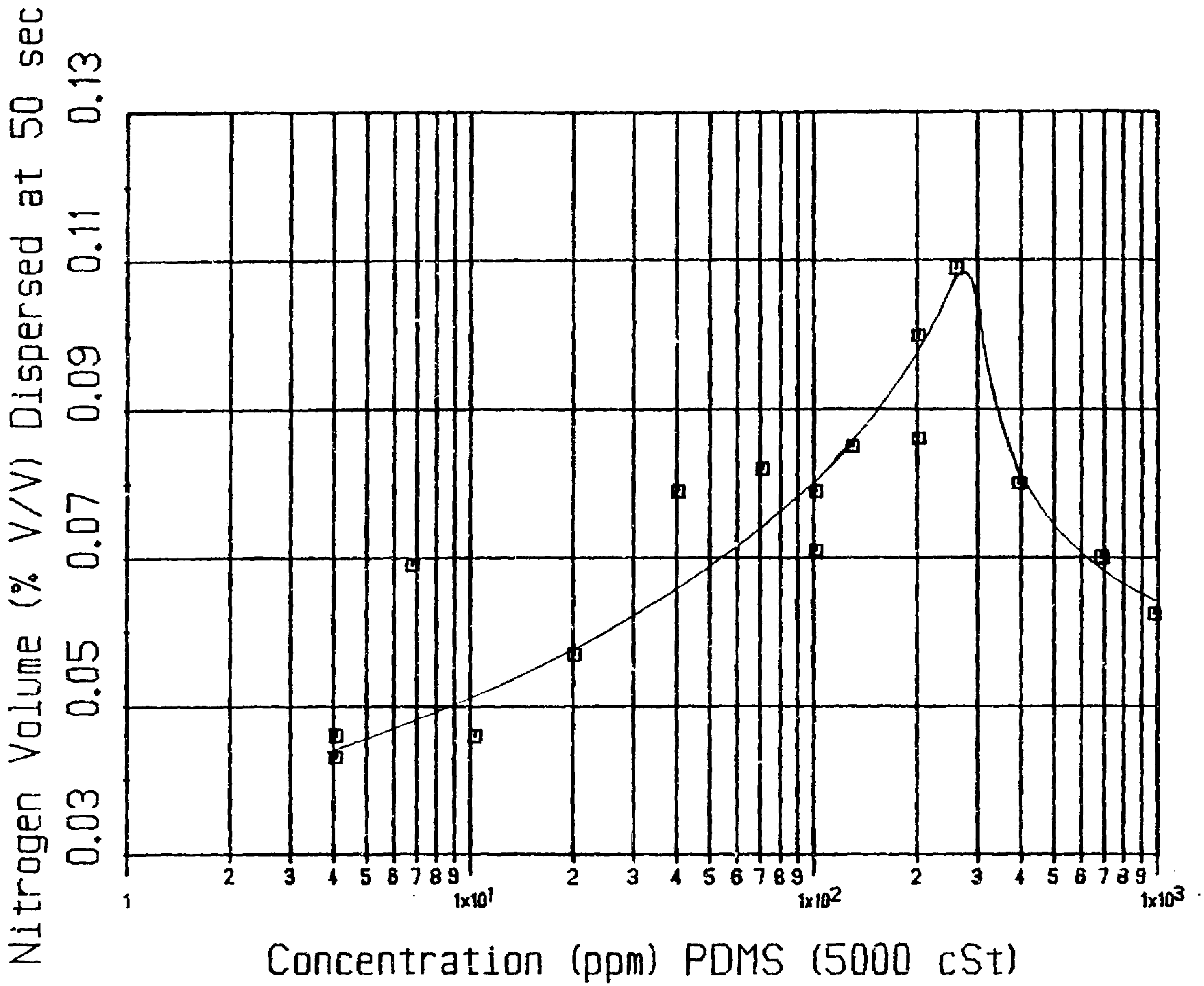

Figure 45. Volume of Nitrogen Gas Entrained at 25°C by Solutions of Polydimethylsiloxane (5000 cSt) in Tmp-Heptanoate, by Test Method IP 313/74.

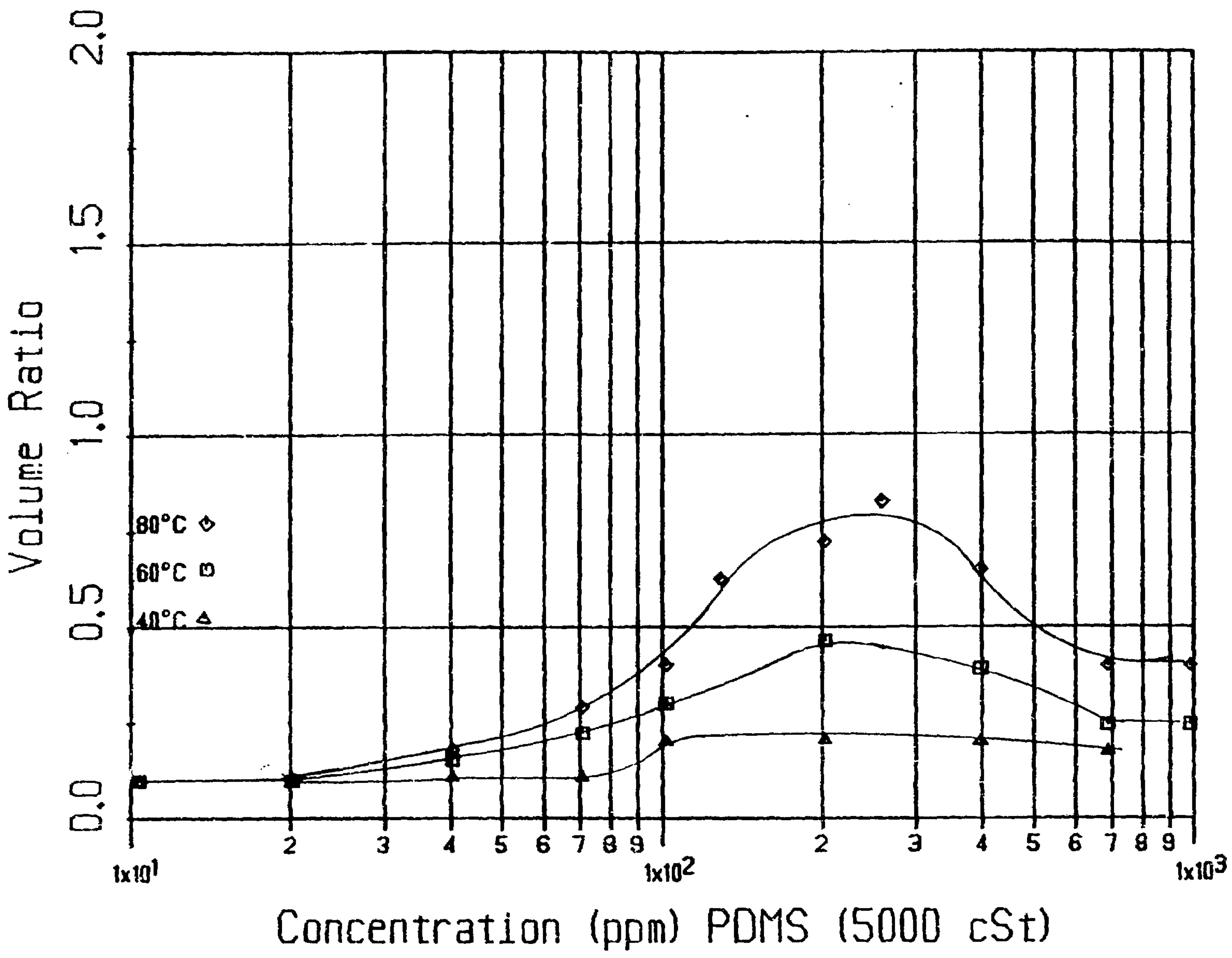

Figure 46. Foaminess of Solutions of Polydimethylsiloxane (5000 cSt) in Tmp-Heptanoate at 25°C, 40°C, 60°C, an 80°C, Measured by Test Method 3213.

SECTION VI

ACTION OF ANTIFOAMS

1. Antifoaming Action of Polydimethylsiloxane (600,000 CentiStokes)

Polydimethylsiloxane (600,000 centiStokes) in the range of concentration of 13.5 to 252 ppm was tested as an antifoaming agent for solutions of various additives in tmp-heptanoate. Table 12 reports the foam volumes, at 40°C and 60°C, measured by Test Method 3213, using two different compositions of additives in tmp-heptanoate, namely:

a. 3.1%(w/w)N-phenyl-1-naphthylamine plus 0.98%(w/w) tricresyl phosphate;

b. 3.0%(w/w) phenothiazine plus 0.97%(w/w) tricresyl phosphate.

The measurements show no antifoam effect of polydimethylsiloxane (600,000 centiStokes) in these solutions at any of the concentrations tested.

Table 12. Foam Volumes (cm^3) of Solutions of Additives in Tmp-Heptanoate, using Polydimethylsiloxane (600,000 centiStokes) as Antifoam

Solutions Tested	Concentration of Polydimethylsiloxane 13.5 ppm		95 ppm		252 ppm	
	40°C	60°C	40°C	60°C	40°C	60°C
3.1% w/w N-Phenyl-1-Naphthylamine and 0.98% w/w Tricresyl Phosphate	313	>500	300	>500	340	>500
3.0% w/w Phenothiazine and 0.97% w/w Tricresyl Phosphate			375	>500	375	>500

2. Tests of Polydimethylsiloxane (600,000 centiStokes) as a Foam Inhibitor in Foamable Solutions of TMP-Heptanoate

Polydimethylsiloxane (600,000 centiStokes) in the range of concentrations of 5.1 to 254 ppm was tested as a foam inhibitor for solutions of approximately 2%(w/w) phenothiazine plus 2%(w/w) tricresyl phosphate in tmp-heptanoate. Figure 47 reports the foam volumes, measured at 40°, 60°, and 80°C by Test Method 3213. We have reported similar experiments previously; on this occasion the tmp-heptanoate contained solutes that make it foam, whereas previous tests were made on tmp-heptanoate without additives.

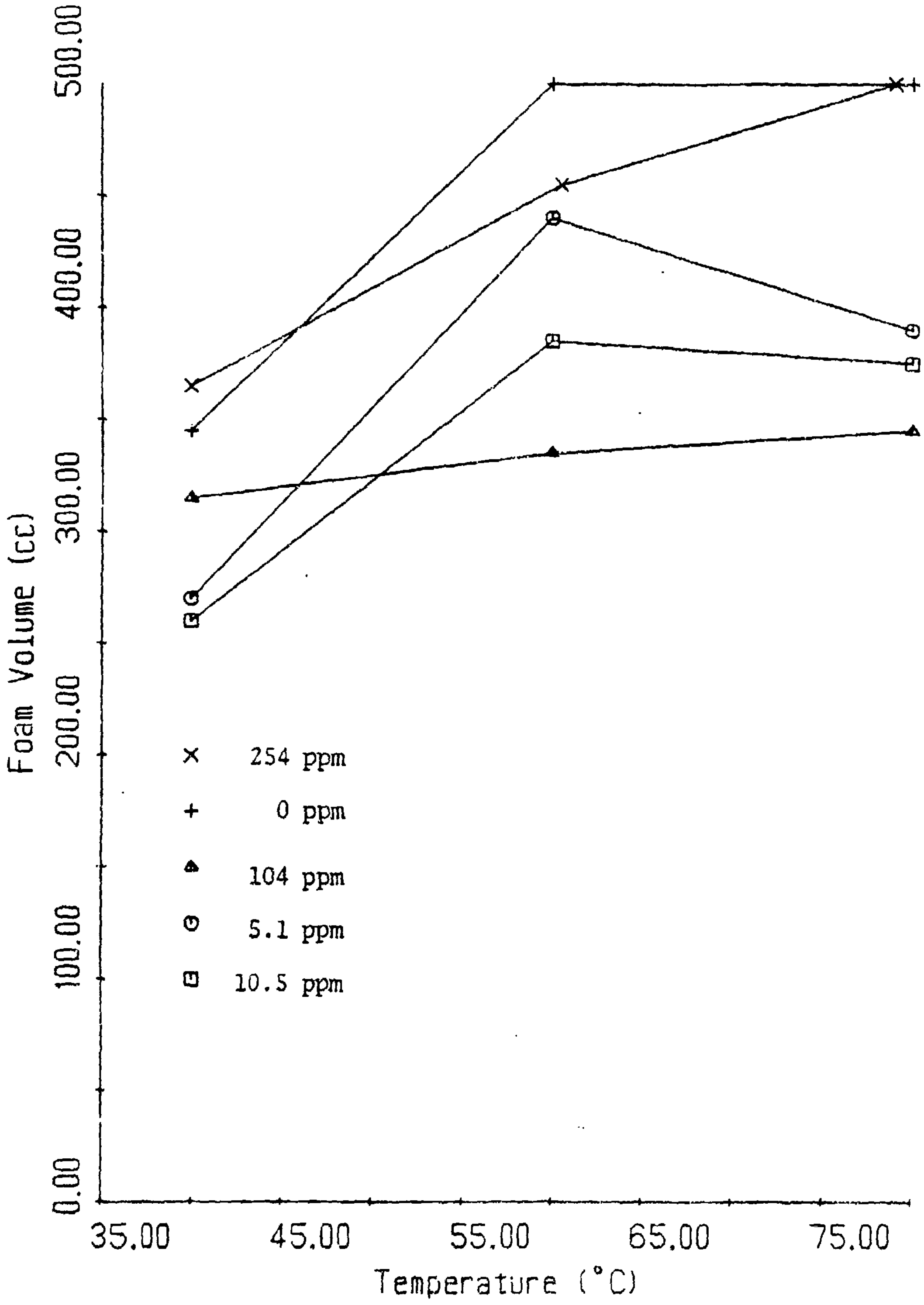

Figure 47. Foam Volumes *Versus* Temperature of Solutions of Phenothiazine (2% w/w) *Plus* Tricresyl Phosphate (2% w/w) in Tmp-Heptanoate, with Polydimethylsiloxane (600,000 cSt) Tested as a Foam Inhibitor.

The measurements show no foam-inhibiting action of the polydimethylsiloxane (600,000 centiStokes) on these solutions at any of the concentrations or temperatures tested.

3. Tests of GE FF-150 (10,000 centiStokes) as a Foam Inhibitor in Foamable Solutions of TMP-Heptanoate

GE FF-150 (10,000 centiStokes) is a fluorosilicone polymer with the formula $Me_3SiO(CF_3CH_2SiMeO)_nSiMe_3$. It was tested as a foam inhibitor in the range of concentrations 11 to 983 ppm in solutions of approximately 2%(w/w) phenothiazine plus 2%(w/w) tricresyl phosphate dissolved in tmp-heptanoate. Figure 48 reports foam volumes measured at 40°C, 60°C, and 80°C by Test Method 3213. The method of preparing samples for measurement was the same as that described above, i.e., prior dissolution of the profoaming solutes before dispersing the insoluble foam inhibitor in the solution. The measurements show no foam-inhibiting action of the GE FF-150 (10,000 centiStokes.)

4. Effect of Reduction of the Particle Size of Dispersed GE FF-150 (10,000 centistokes)

Taking dispersions of GE FF-150 (10,000 centiStokes), in tmp-heptanoate containing the solutes described above, at concentrations of dispersate of 90 and 252 ppm, further comminution of the immiscible-liquid dispersate was made by means of a hand homogenizer, to reduce the size of the liquid droplet and to make the droplets more uniform. The same profoamer solutes at the same concentrations were used as in the tests reported above. Foam volumes were measured at 40°C, 60°C, and 80°C by Test Method 3213. The results are included in Figure 48 to allow comparisons to be drawn. An appreciable decrease in foam volume is the result. Reducing the size of the dispersed liquid enhances the foam-inhibiting action of the GE FF-150 fluorosilicone.

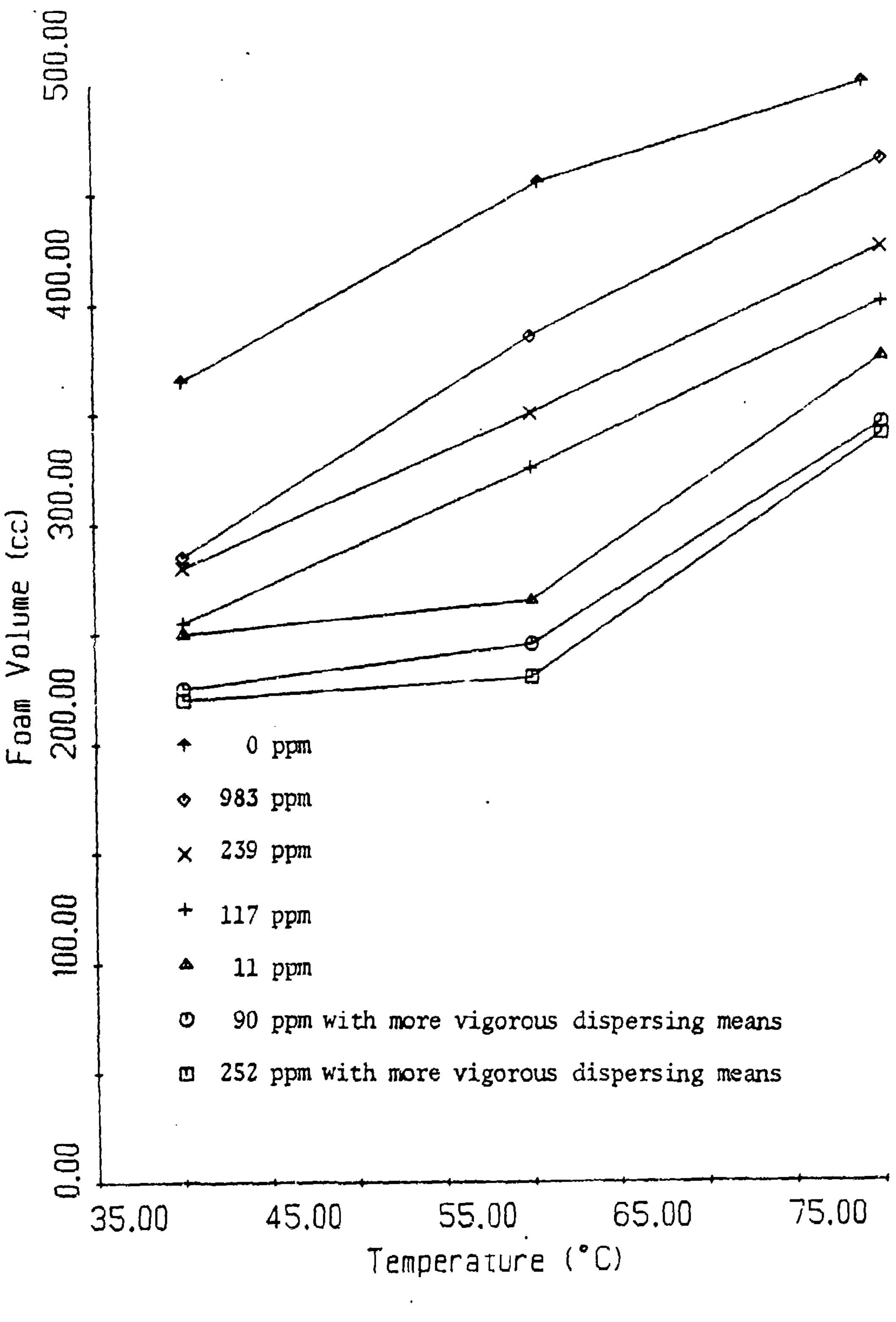

Figure 48. Foam Volumes *Versus* Temperature of Solutions of Phenothiazine (2% w/w) *Plus* Tricresyl Phosphate (2% w/w) in Tmp-Heptanoate, with Fluorosilicone Fluid FF-150-10M Tested as a Foam Inhibitor.

SECTION VII

SURFACE VISCOSITY MEASUREMENTS

1. Introduction

J.A.F. Plateau[11] introduced the concept of surface viscosity, and referred the stability of foam lamellae to its influence. This property is the two-dimensional analog of ordinary viscosity and its coefficient is analogously defined and determined. The coefficient of surface viscosity is the force in dynes that must be applied per centimeter of length along a surface to maintain a gradient of surface flow (between two parallel lines one centimeter apart) of one cm. $sec.^{-1}$. The unit is the surface poise with dimensions MT^{-1}. Weakly foaming solutions have little surface viscosity, soap solutions a moderate amount, and some solutions of proteins, saponin, etc., a high surface viscosity amounting to a non-Newtonian plasticity.

The simplest instrument to detect surface viscosity is the oscillating-disc viscosimeter.[21] The logarithmic decrement of its torsional oscillations is determined with and without the surface film of adsorbed solute. Figure 49 shows the details of the apparatus. The torsion wire is supported at the end of a shaft that can be given a rotational twist by means of an external lever. The damping of the oscillations is measured by a light beam whose intensity varies as it passes across a polariser that is attached to, and moves with, the torsion wire. The source of the light beam is a red light-emitting-diode. The intensity of the light is regulated and stabilized by a feed-back mechanism. The variation of the light intensity is transferred to a receiving photo-diode that is connected to a recorder through a variable-gain amplifier. The electronic circuit diagram is shown on Figure 50, and a record of the output is shown on Figure 51 (surface damping of tmp-heptanoate.) The damping curve shown in Figure 51 is typical of a perfectly Newtonian liquid surface, inasmuch as the logarithmic decrement is linear with time (Figure 52).

Further measurements of surface viscosity were carried out with the oscillating-disc viscosimeter. Various solutions, in the range of 0 to 500 ppm, of polydimethylsiloxane (1000 centiStokes) were tested at 23.90 ± 0.05°C. To estimate the kinetics of film formation, each solution was measured immediately after mixing and thereafter at stated time intervals. Figures 53, 54, and 55 illustrate some of our 46 measurements of surface viscosity. In each diagram the straight line represents the behavior of tmp-heptanoate without additive, and the different symbols represent measurements made at various time intervals after mixing. These measurements show that the original Newtonian liquid surface of the tmp-heptanoate remains essentially unchanged by the presence of the silicone, regardless of its concentration and the time interval after mixing. Therefore, no evidence of film formation was found, thus excluding the contribution of surface-shear viscosity to the foam stability of polydimethylsiloxane dissolved in tmp-heptanoate.

Schematics of the Surface Viscosity Apparatus

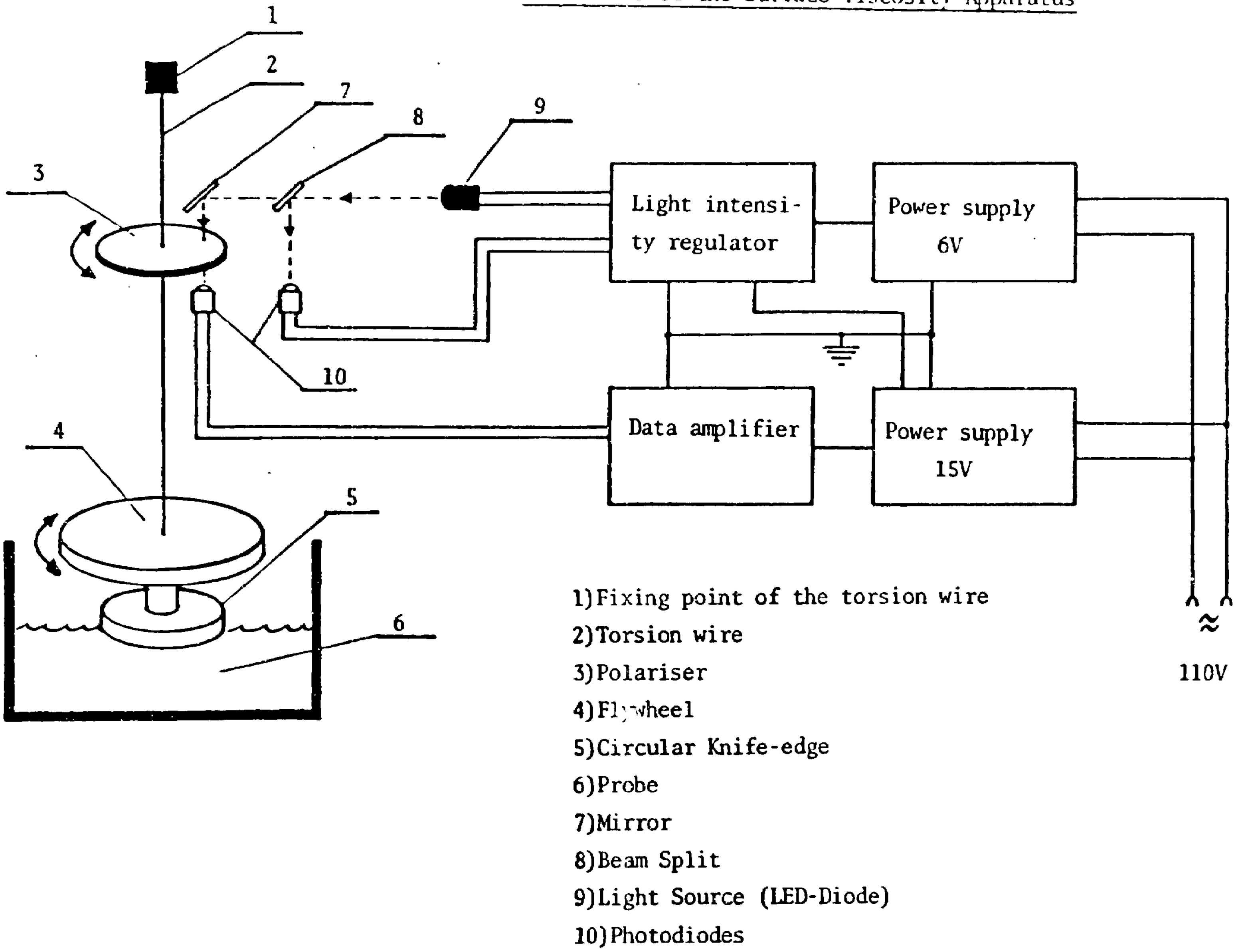

1)Fixing point of the torsion wire
2)Torsion wire
3)Polariser
4)Flywheel
5)Circular Knife-edge
6)Probe
7)Mirror
8)Beam Split
9)Light Source (LED-Diode)
10)Photodiodes

Figure 49. Schematics of the Oscillating-Disc Surface Viscosimeter

Electronic Circuits of the Surface Viscosity Apparatus

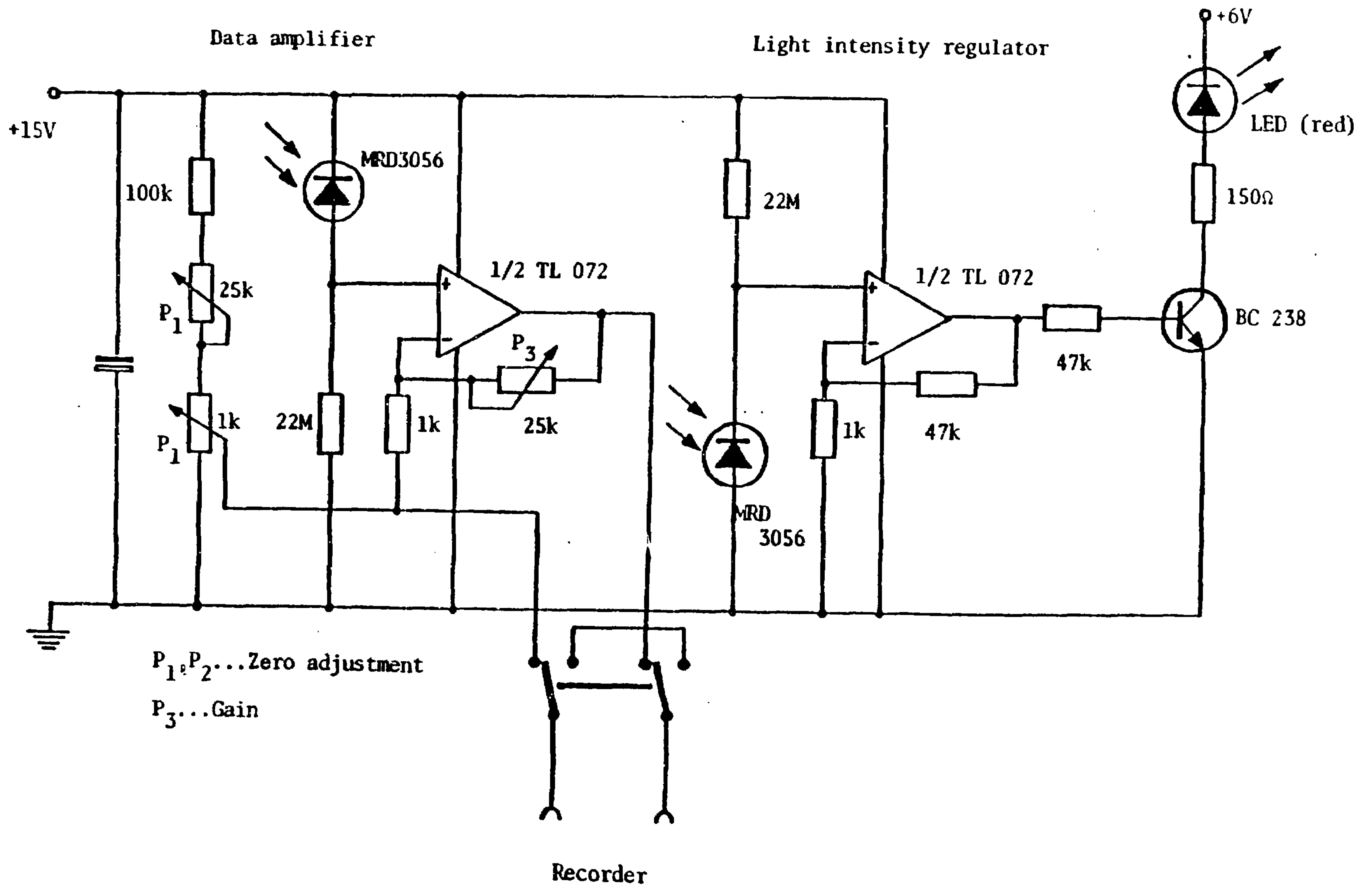

Figure 50. Electronic Circuits of the Oscillating-Disc Surface Viscosimeter

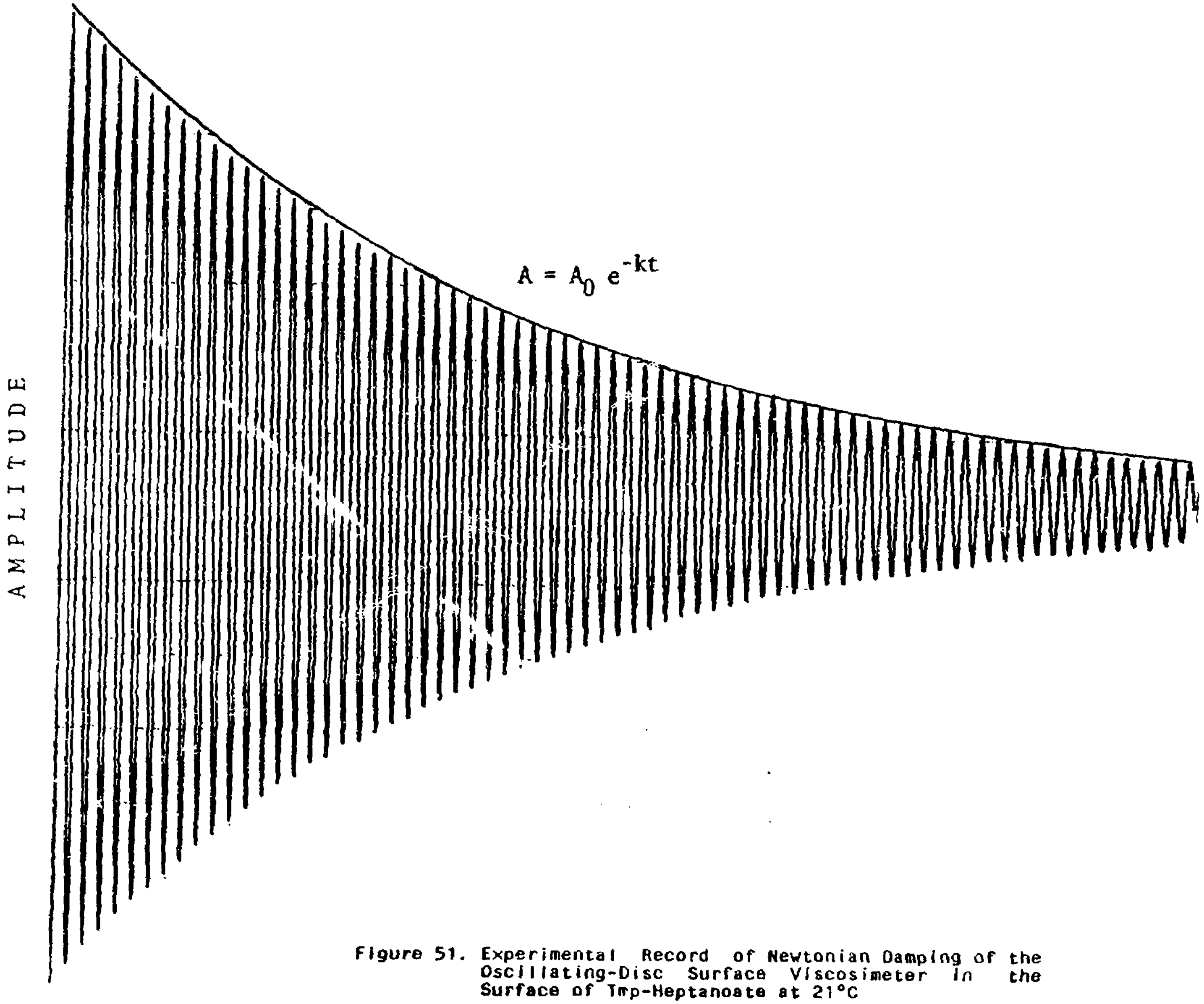

Figure 51. Experimental Record of Newtonian Damping of the Oscillating-Disc Surface Viscosimeter in the Surface of Tmp-Heptanoate at 21°C

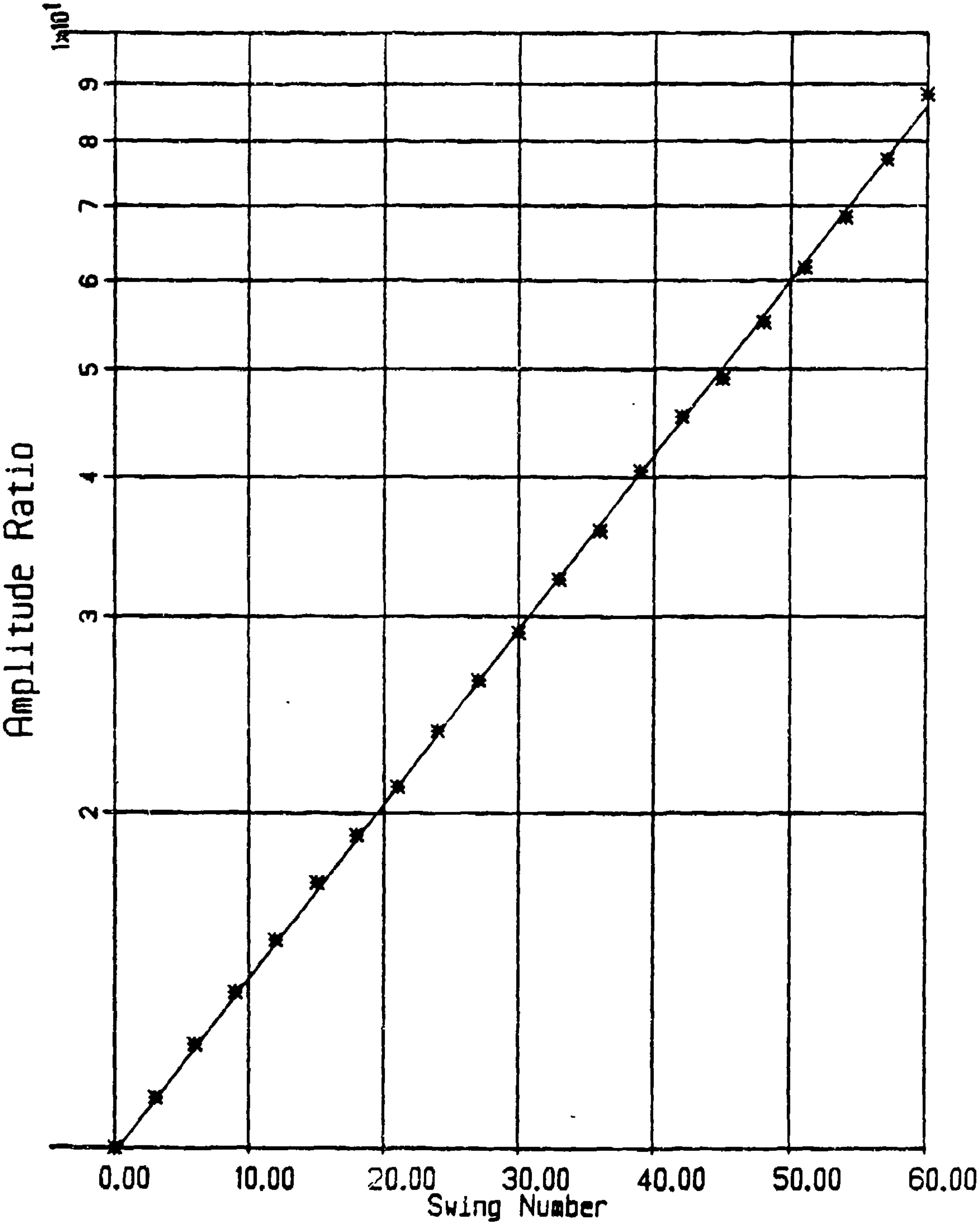

Figure 52. Linear Logarithmic Decrement of Amplitude with Time (Measured by Swing Number,) Calculated from the Experimental Record shown in Figure 51.

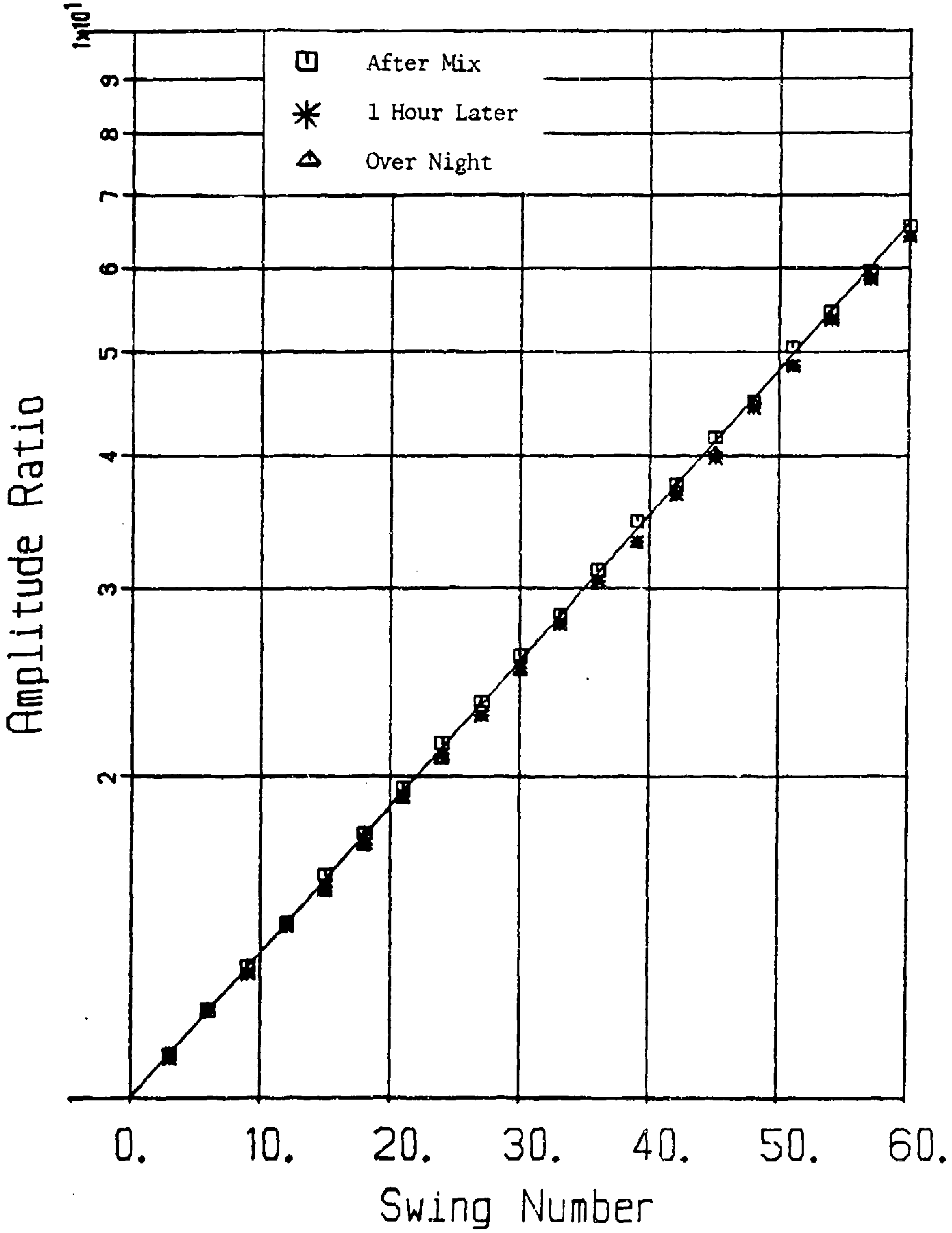

Figure 53. Surface Viscosity of Tmp-Heptanoate (Amplitude Ratio *Versus* Swing Number) Containing 2.96 ppm Polydimethylsiloxane (1000 cSt) to Determine Possible Effects of Aging of the Surface.

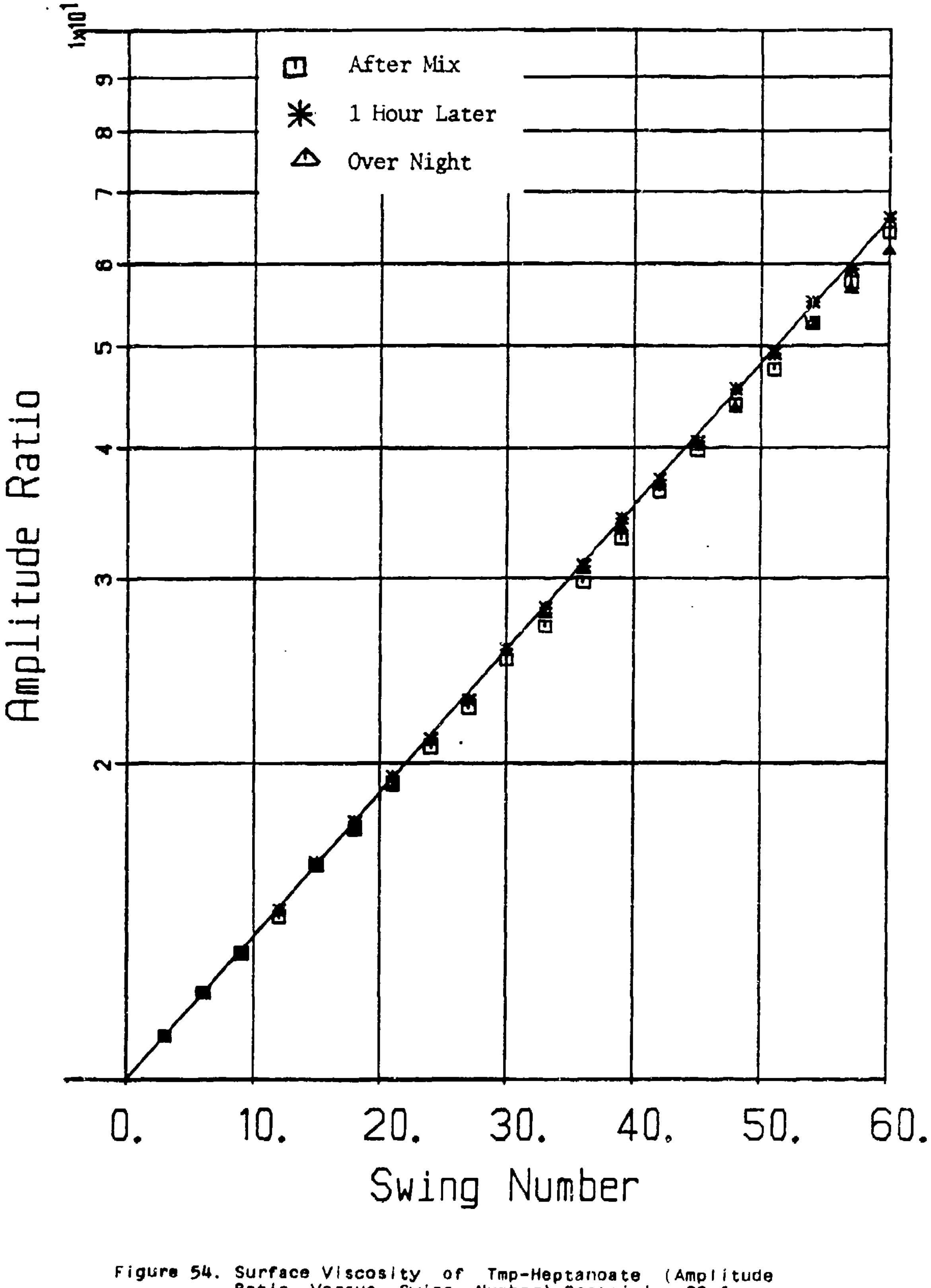

Figure 54. Surface Viscosity of Tmp-Heptanoate (Amplitude Ratio *Versus* Swing Number) Containing 29.3 ppm Polydimothylsiloxane (1000 cSt) to Determine Possible Effects of Aging of the Surface.

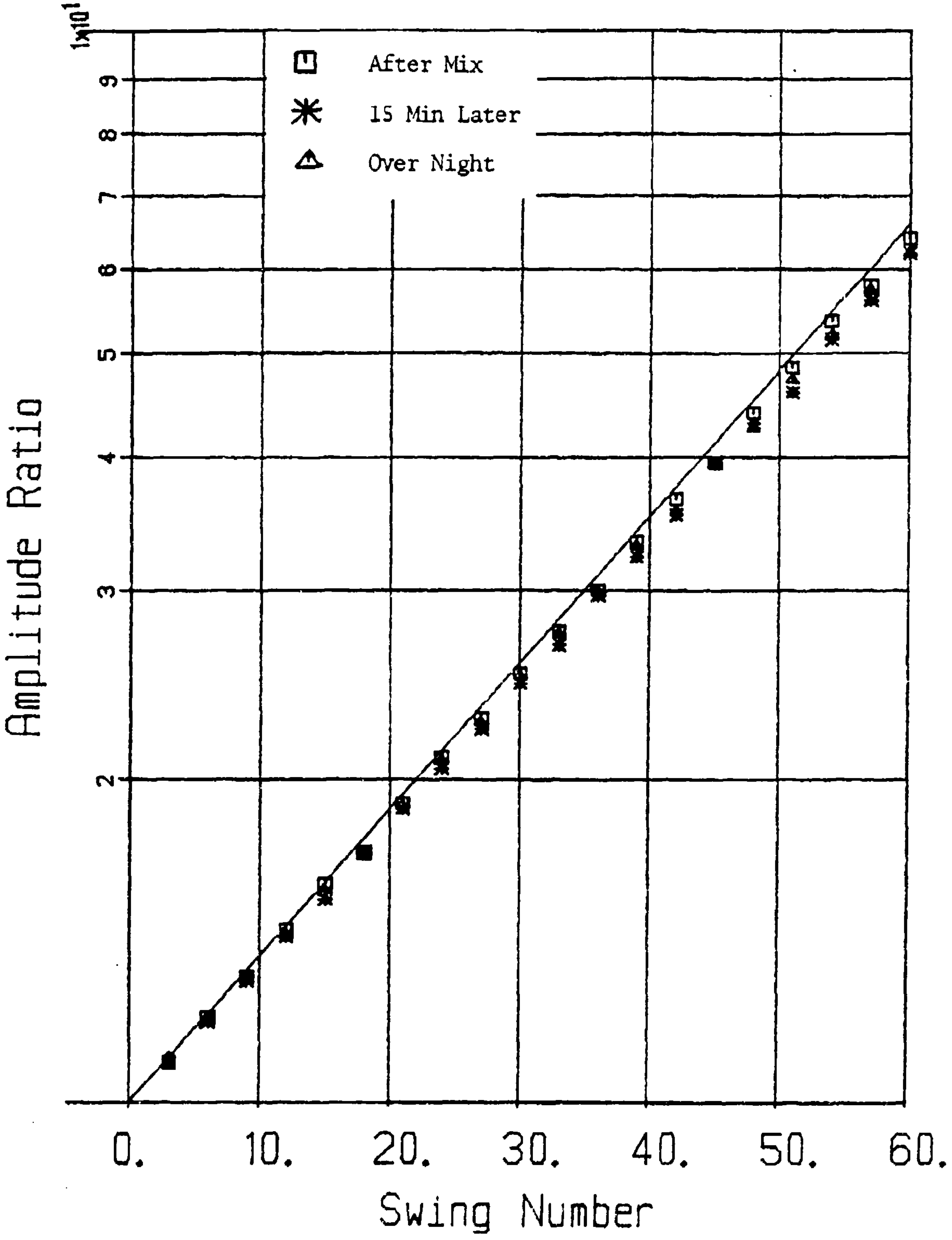

Figure 55. Surface Viscosity of Tmp-Heptanoate (Amplitude Ratio *Versus* Swing Number) Containing 501 ppm Polydimethylsiloxane (1000 cSt) to Determine Possible Effects of Aging of the Surface.

2. Surface Viscosities in Dry Nitrogen Atmosphere

The changes found in the bulk properties of tmp-heptanoate and its solutions on exposure to the air, suggest that similar changes might occur in the surface properties. All surface viscosities previously reported had been measured while the solutions had been exposed for short periods of time to room atmosphere (i.e., during preparation, mixing, measurement, and time intervals between consecutive measurements.) To investigate possible effects of exposure during handling, measurements were made under an atmosphere of dry nitrogen. Figure 56 illustrates the results obtained with fresh tmp-heptanoate, and with a sample of tmp-heptanoate after exposure to room atmosphere for a few hours. Figure 56 shows:

a. No significant difference exists between the results previously reported for the surface viscosity of tmp-heptanoate and those carried out under an atmosphere of dry nitrogen.

b. Exposure of the tmp-heptanoate to room atmosphere for a few hours causes a reduction of 10% in the surface viscosity.

These observations may explain the slight reduction of surface viscosity found in various solutions of polydimethylsiloxane (1000 centiStokes) in tmp-heptanoate, which occurs at large intervals of time after mixing.

3. Surface Viscosity of Additives in Solutions of TMP-Heptanoate

Surface viscosities were measured with the oscillating-disc viscosimeter, temperature control of ±0.1°C., dry nitrogen atmosphere above the surface. A slight modification was the use of solvent that had previously been equilibrated with dry nitrogen, by bubbling the gas through the oil for sixty minutes at 25°C.

The results of the measurements of surface viscosity show that the surface viscosity of the solvent oil is not affected by the presence of phenothiazine at a concentration of 2.03%(w/w), nor by the presence of tricresyl phosphate at a concentration of 1.96% (w/w), taken separately; but when these two additives are combined to give a single solution in tmp-heptanoate containing phenothiazine, 2.03% (w/w), plus tricresyl phosphate, 1.96% (w/w), there occurs a significant increase in the surface viscosity.

Figure 57 reports the damping curves of the disc in the surfaces of tmp-heptanoate, tmp-heptanoate + phenothiazine, 2.03%(w/w), and tmp-heptanoate + tricresyl phosphate, 1.96% (w/w). The data in this diagram were obtained after an interval of time of thirty minutes, which was required to reach thermal equilibrium. Additional measurements were made after one hour and two hours (not shown in diagram,) giving identical results. Figure 57 gives no evidence of any enhancement of the viscosity at the surface; the slight differences shown are related to corresponding slight increases in the viscosities of the bulk solutions.

Figure 58 reports the damping curves of the disc in the surfaces of tmp-heptanoate by itself and of a mixture of the two

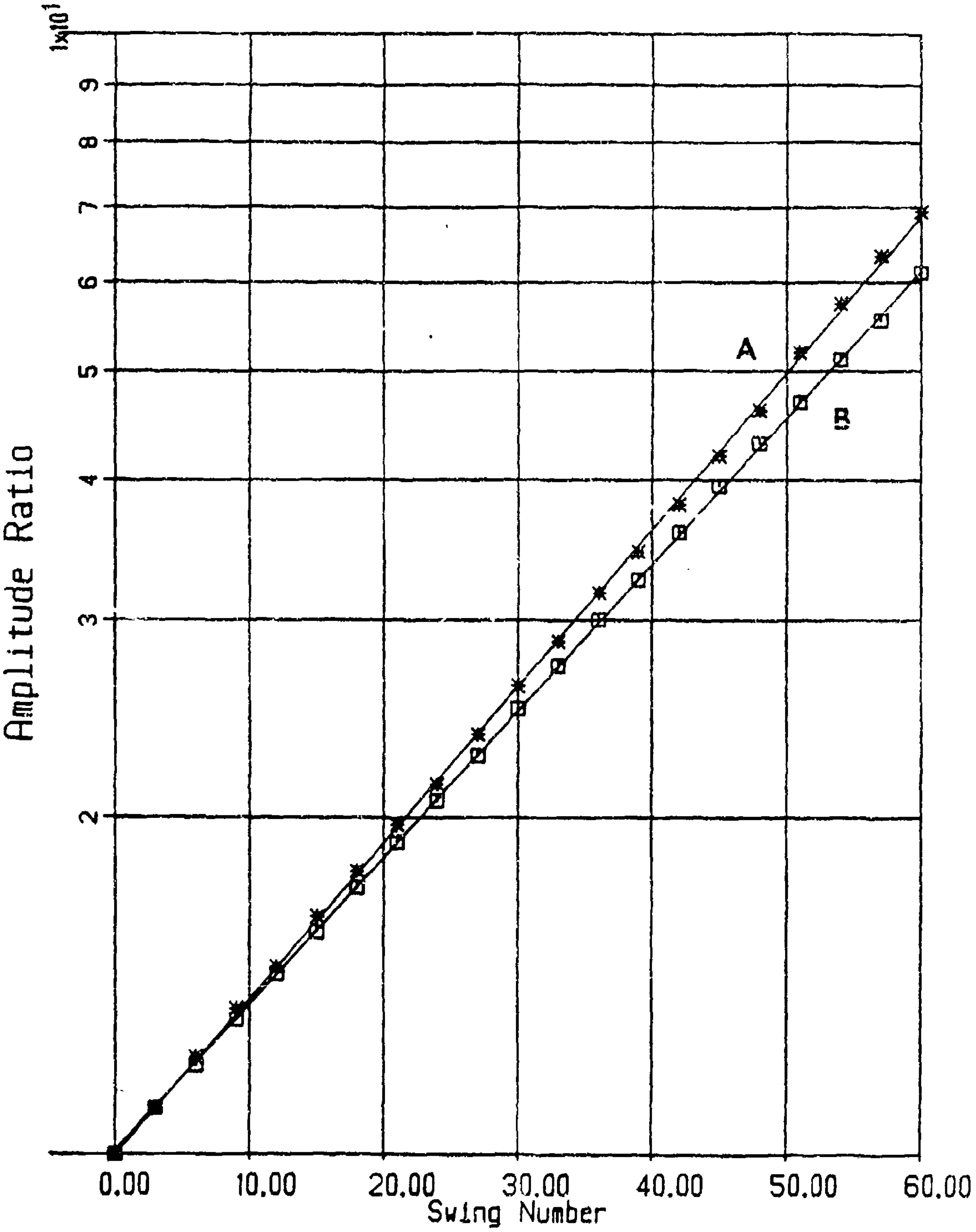

Figure 56. Records of Amplitude Ratio vs Swing Number from the Surface Vicosimeter, Measured on Fresh Tmp-Heptanoate (A) and on Tmp-Heptanoate After Exposure of a Few Hours to Room Atmosphere (B), both Measured under an Atmosphere of Dry Nitrogen. Curve A also Includes Data Previously Reported for Measurements on Fresh Tmp-Heptanoate, not Measured under an Atmosphere of Dry Nitrogen.

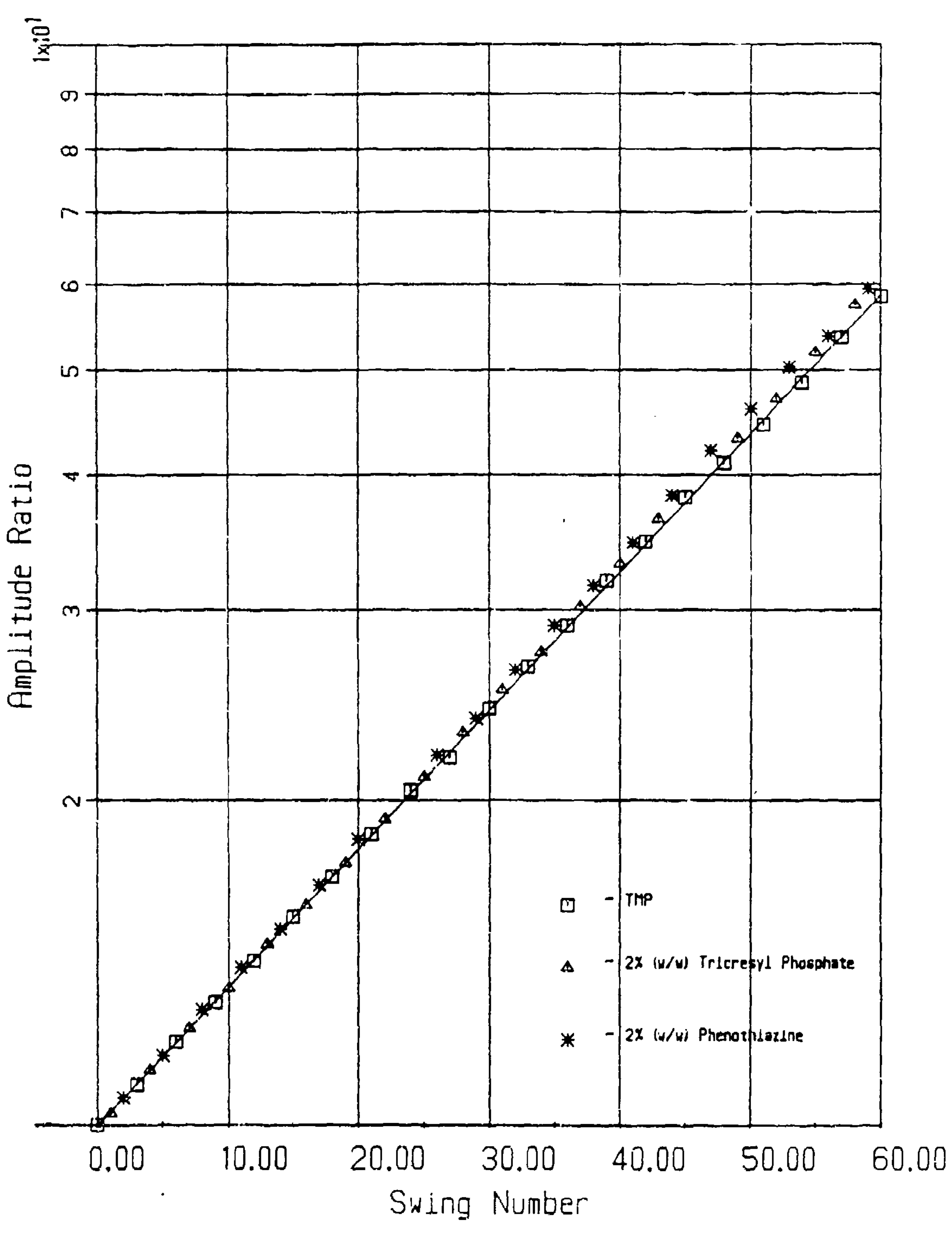

Figure 57. Damping Curve of Oscillating Disc in the Surface of Tmp-Heptanoate and Solutions of Additves in Tmp-Heptanoate at 25.0°C.

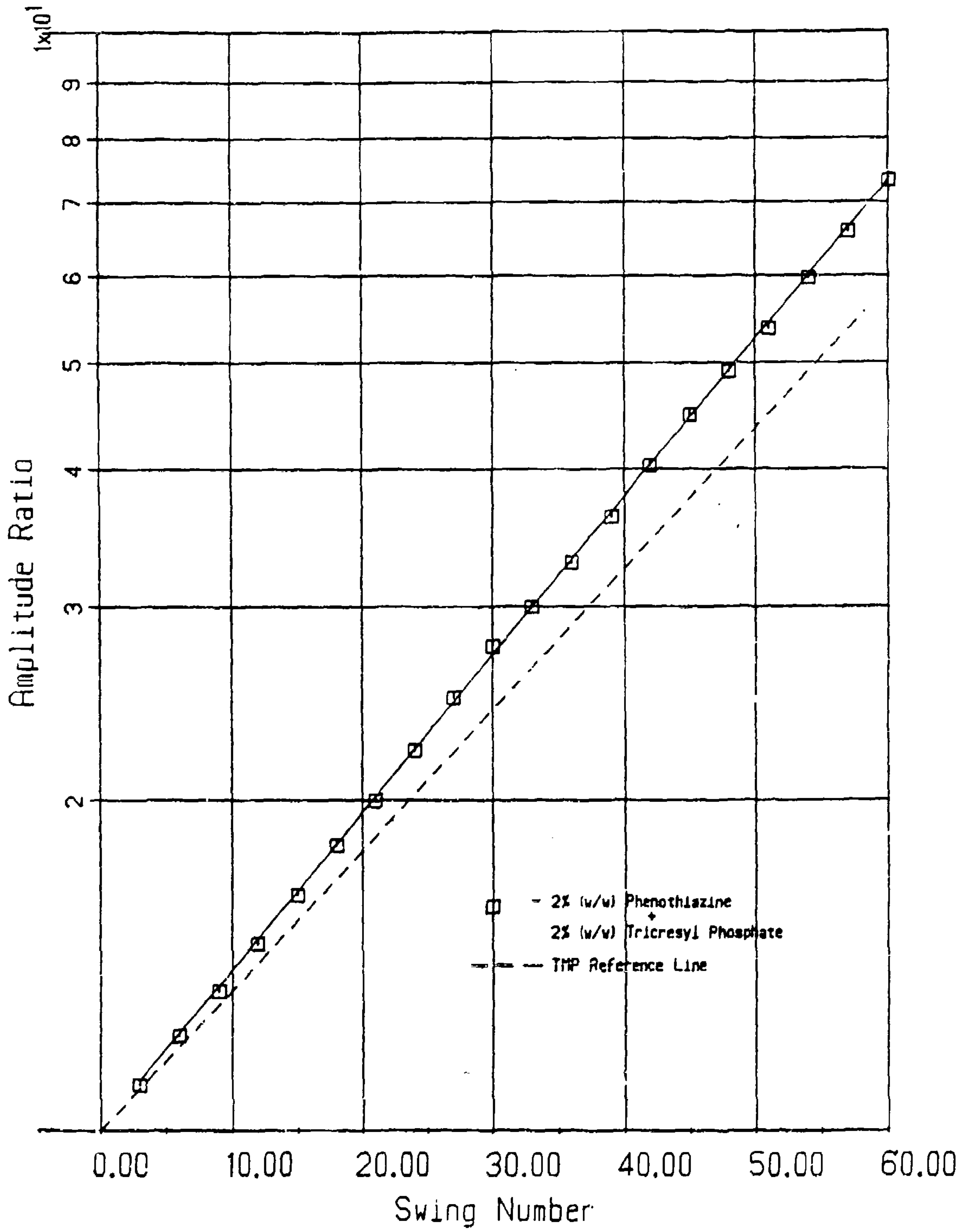

Figure 58. Damping Curve of Oscillating Disc in the Surface of Tmp-Heptanoate (Dotted Line) and a Solution of Two Additves Combined in Tmp-Heptanoate at 25.0°C.

additives dissolved in tmp-heptanoate; namely, phenothiazine, 2%, plus tricresyl phosphate, 2%. The diagram shows a significant increase in the surface viscosity of the ternary mixture. The magnitude of this increase is far larger than the corresponding increase in the bulk viscosities of the two liquids, which is an increase of only 4%, compared to an increase of 26% in the surface viscosity. Further measurements of surface viscosity made after longer time intervals, as much as two-and-a-half hours, gave identical results, showing that the surface structure was complete within the first time interval of thirty minutes.

4. Solutions Containing Benzotriazole

Surface viscosities were measured using the oscillating-disc viscosimeter, at the temperature 25.0 ± 0.1°C. The tests show (Figure 59) that solutions containing up to 0.1%(w/w) benzotriazole in tmp-heptanoate have the same surface viscosity as the solvent. The surface viscosity was also unchanged in a solution in tmp-heptanoate of 1.94%(w/w) tricresyl phosphate plus 0.1%(w/w) benzotriazole. Figure 59 reports the damping curve in the two solutions; the solid line, referring to tmp-heptanoate, is given as a reference. Figure 60 shows the damping curve of the disc in the surface of a solution of 0.10%(w/w) benzotriazole plus 1.97%(w/w) phenothiazine in tmp-heptanoate. The solid line refers to a solution containing only the phenothiazine, at the same concentration. Figure 60 clearly shows that the presence of the benzotriazole does not affect the surface viscosity. However, a decrease of surface viscosity is observed (Figure 61) when 0.12%(w/w) benzotriazole is present in a solution containing the synergistic mixture of 1.98%(w/w) phenothiazine plus 1.98%(w/w) tricresyl phosphate, to the extent of eliminating the synergistic increase previously reported. It is significant that the foam-depressing action of 0.12% bezotriazole in a given solution (entry no. 13 in Table 6) should be paralleled by its acting to inhibit the formation of a surface film in the same solution.

5. Solutions Containing p-Nonyl Phenol

Surface viscosities of solutions of p-nonyl phenol in tmp-heptanoate, and p-nonyl phenol in combination with other additives in tmp-heptanoate as solvent, were measured using the oscillating-disc viscosimeter at the temperature of 25.0 ± 0.1°C and are reported in Table 7 along with other properties of these solutions. The numbers under surface viscosity refer to the slopes of the lines that describe the logarithm of the amplitude ratio as a function of the swing number. The numbers given within parentheses in Table 7 refer to solutions of identical compositions but without the p-nonyl phenol. Some of the detailed data obtained are reported in Figures 62, 63 and 64.

Table 7 shows that the changes in surface viscosities taking place in the solutions of the various oil additives when the relevant maximum concentration of p-nonyl phenol is added thereto, are insignificant and usually within the experimental error.

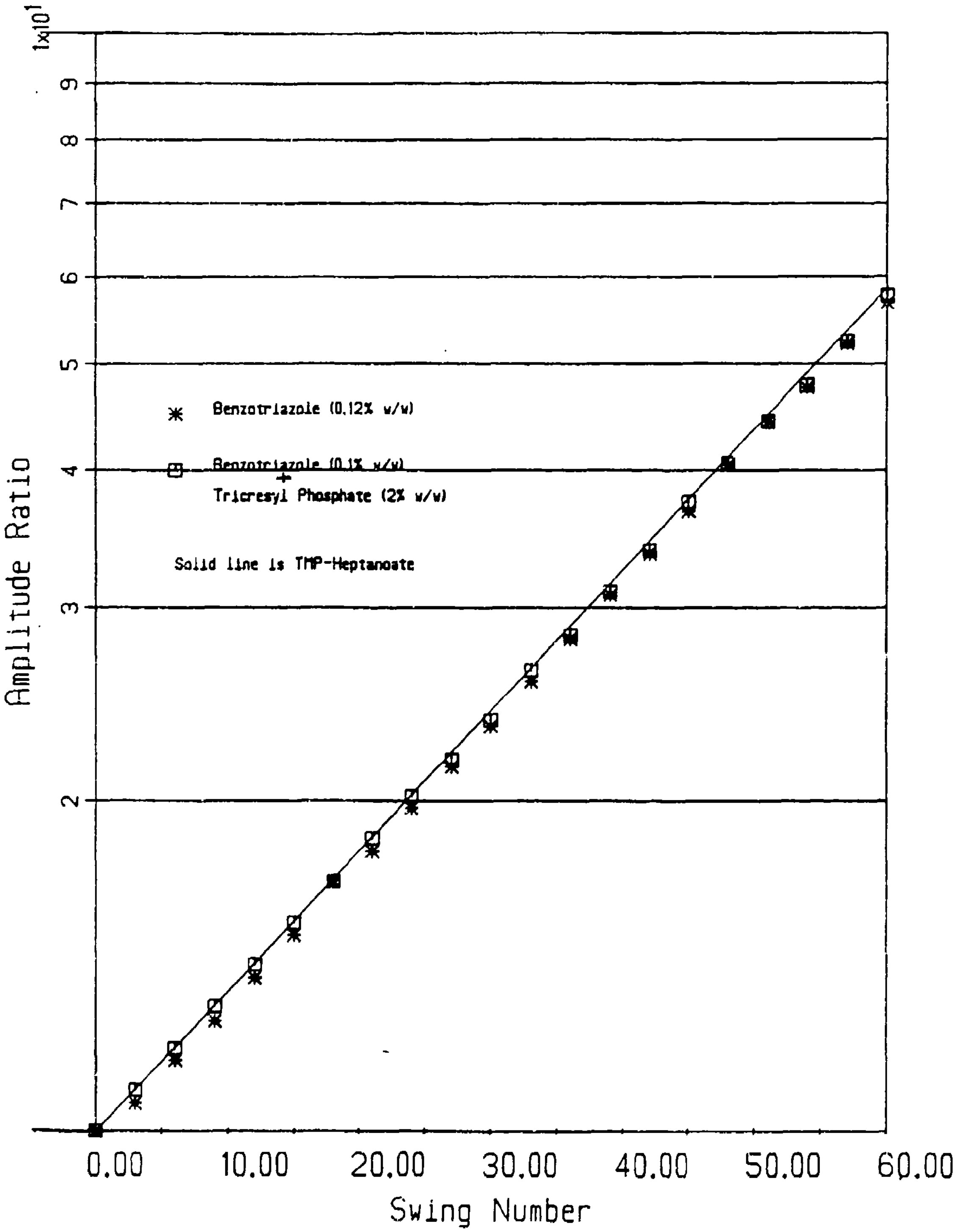

Figure 59. Damping Curve of Oscillating Disc in the Surface of Tmp-Heptanoate (Solid Line) and Solutions of Additves in Tmp-Heptanoate at 25.0°C.

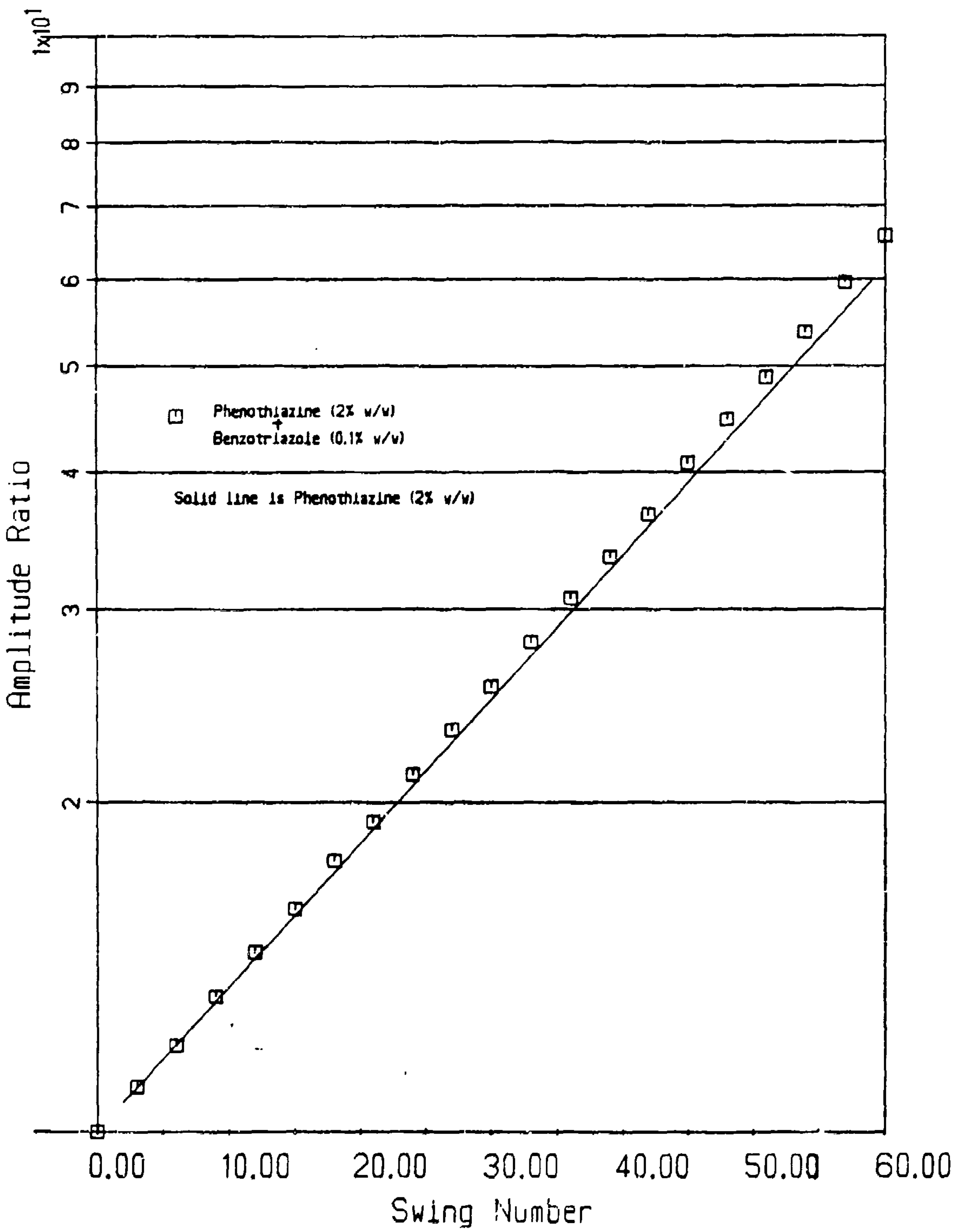

Figure 60. Damping Curve of Oscillating Disc in the Surface of a Solution of Phenothiazine in Tmp-Heptanoate (Solid Line) and a Solution of Two Additves in Tmp-Heptanoate at 25.0°C.

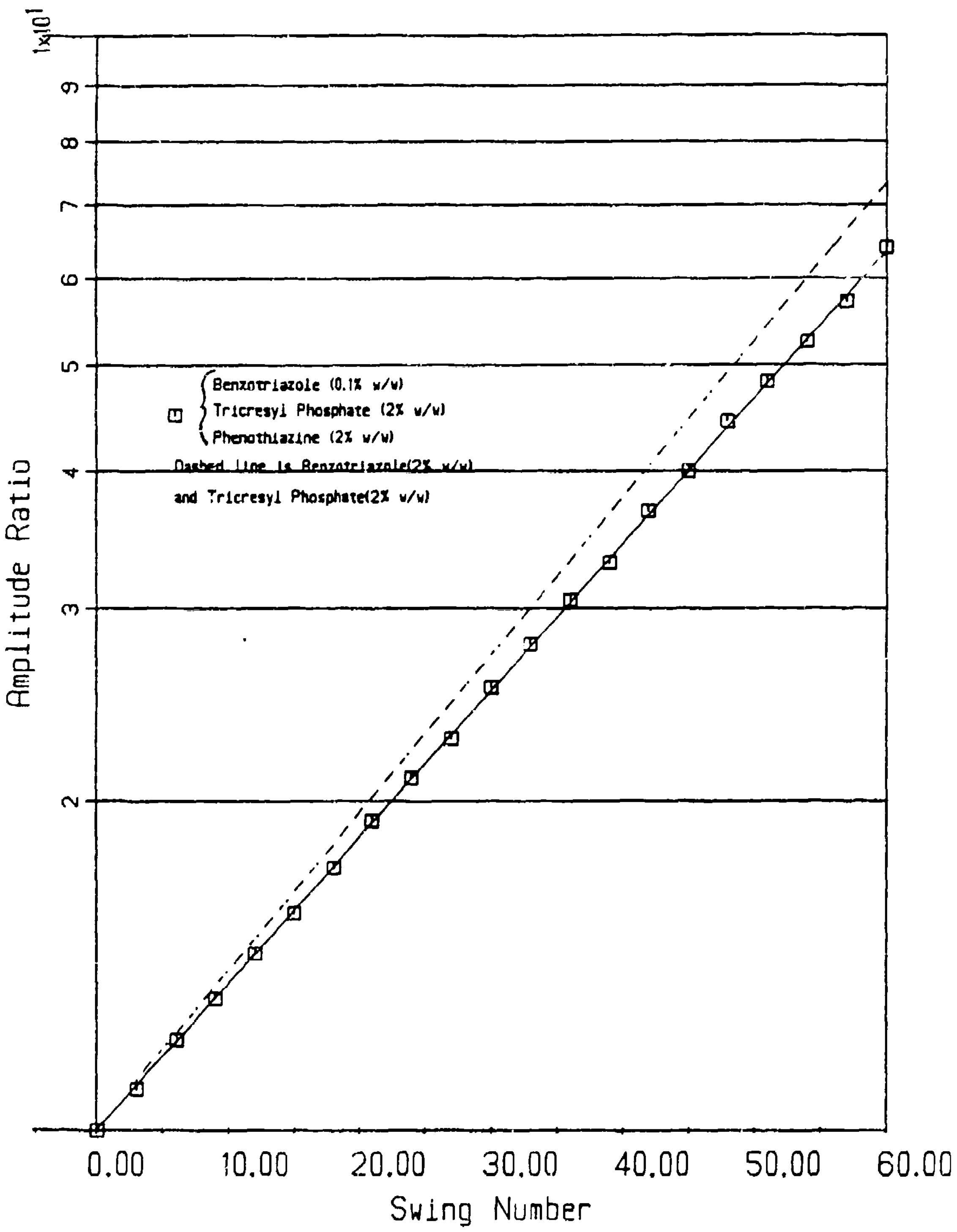

Figure 61. Damping Curve of Oscillating Disc in the Surface of Two Additves Combined in Tmp-Heptanoate (Dotted Line) and Three Additves Combined in Tmp-Heptanoate (Solid Line) at 25.0°C.

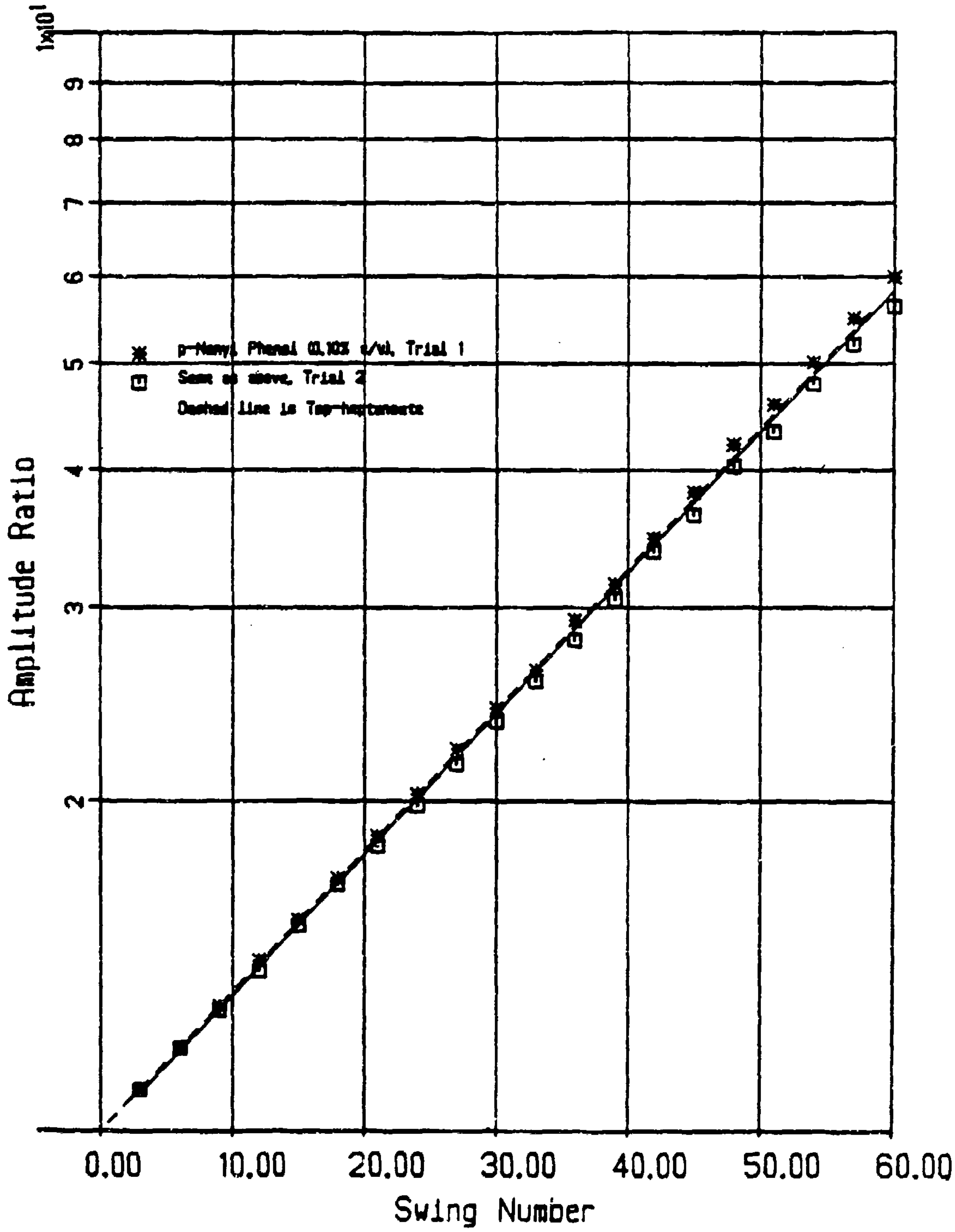

Figure 62. Damping Curve of Oscillating Disc in the Surface of Tmp-Heptanoate (Dashed Line) and Solutions of Additves in Tmp-Heptanoate at 25.0°C.

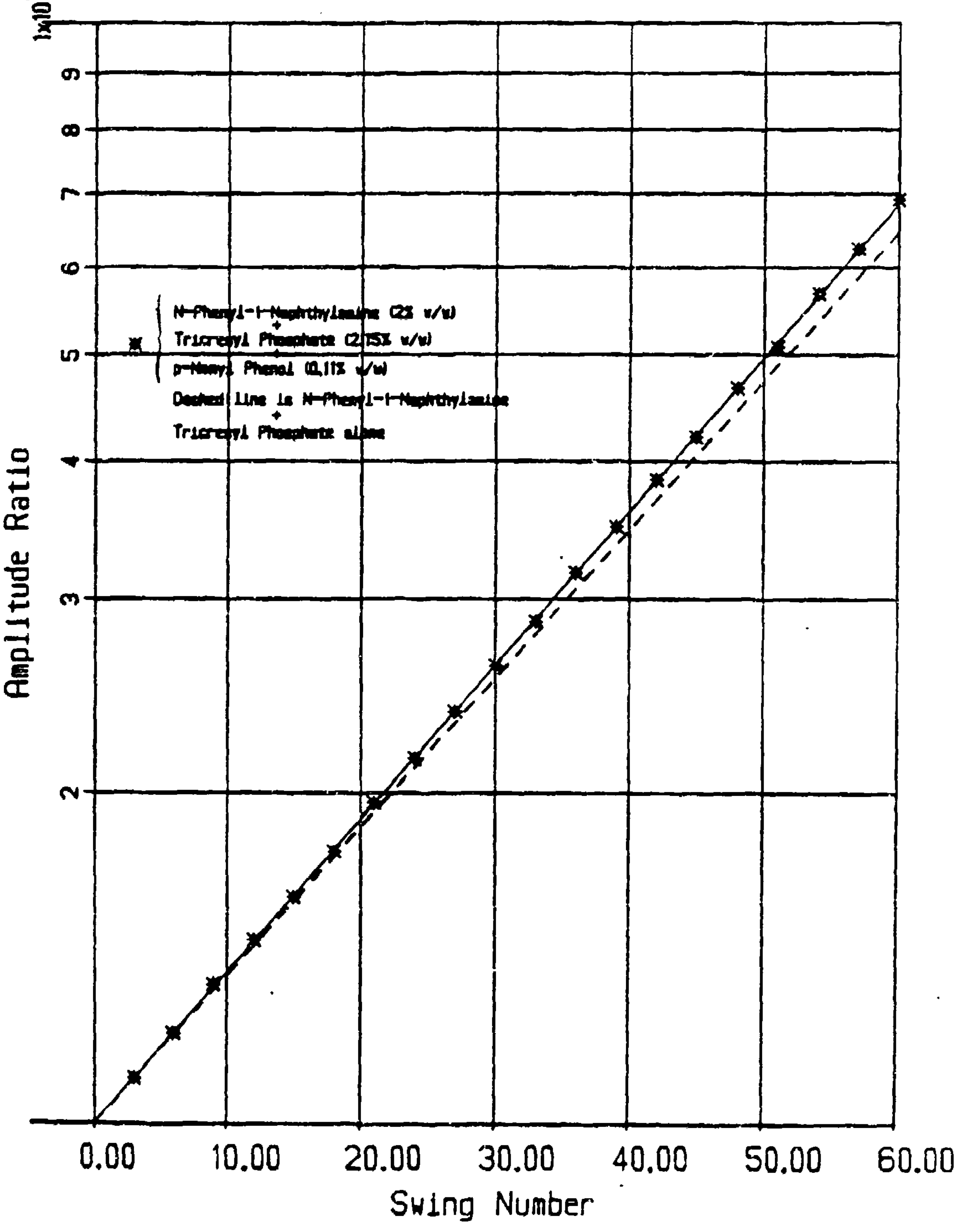

Figure 63. Damping Curve of Oscillating Disc in the Surface of a Solution of N-Phenyl-1-Naphthylamine with Tricresyl Phosphate in Tmp-Heptanoate (Dashed Line) and the same Two Additves plus p-Nonyl Phenol in Tmp-Heptanoate (Solid Line) at 25.0°C.

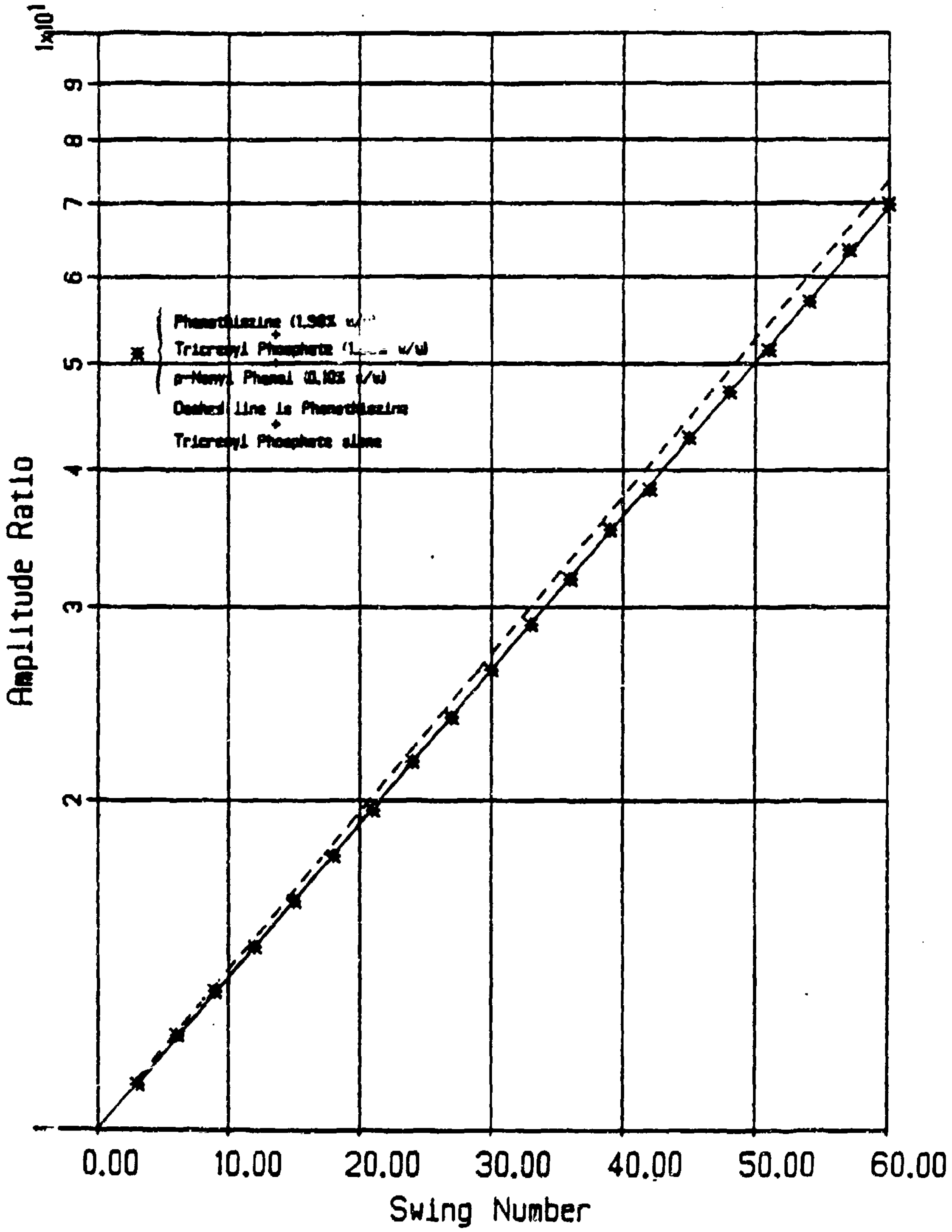

Figure 64. Damping Curve of Oscillating Disc in the Surface of a Solution of Phenothiazine with Tricresyl Phosphate in Tmp-Heptanoate (Dashed Line) and the same Two Additves <u>plus</u> p-Nonyl Phenol in Tmp-Heptanoate (Solid Line) at 25.0°C.

6. Polydimethylsiloxane (1000 cSt) in Mineral Oil

Surface viscosities were measured with the oscillating-disc viscosimeter, at 25° ± 0.1°C, with dry nitrogen gas flowing across the surface.

Figure 65 illustrates the damping curves of the disc in the surface of solutions of concentration 0.408 ppm and of 4.07 ppm polydimethylsiloxane in mineral oil. The continuous line in the diagram refers to the solvent. The reported results in Figure 65 show no change of surface viscosity due to the presence of polydimethylsiloxane at either concentration. Similar behavior was found in all tested solutions of polydimethylsiloxane in mineral oil, up to a concentration of 27.5 ppm.

7. Span 20 Solutions in Mineral Oil

Surface viscosities were measured with the oscillating-disk viscosimeter, at 25°C, with dry nitrogen gas flowing across the surface.

The results of all the measurements carried out with these solutions in the range of concentrations 0 to 5010 ppm show that the surface viscosity is not affected by the presence of Span 20 in solution. Figure 66 illustrates the damping curves of the disk in the surface of solutions of concentration 69.9 ppm and 5010 ppm of Span 20 in mineral oil. The continuous line in the diagram refers to the solvent. The diagram shows the invariability of the surface viscosity with the concentration, in the range tested.

8. Aerosol OT Solution in Tmp-Heptanoate

The surface-shear viscosity of a solution of Aerosol OT (2.04% w/w) in tmp-heptanoate was measured and compared with that of the solvent. The measurements were made according to the usual procedure: oscillating-disc surface viscosimeter; flow of dry nitrogen gas across the surface; temperature of 25°C. Figure 67 reports the amplitude ratio versus swing number for tmp-heptanoate and for the Aerosol OT solution in tmp-heptanoate, fifteen minutes and one hundred and fifty minutes after the agitation was stopped. The diagrams show no indication of the formation of a surface film; thus eliminating the mechanism of foam stabilization that depends on the presence of such a film.

9. Foaminess versus Surface Viscosity of Solutions of Additives in Tmp-Heptanoate

We have demonstrated (Figure 58) that a correlation exists between the measured foaminess of solutions of oil additives in tmp-heptanoate and the presence of a layer of enhanced viscosity at the surface of the solution; and the absence of such an effect in solutions that do not foam. Thus, in solutions that did not show a propensity to foam (2% (w/w) phenothiazine or 2% (w/w) tricresyl phosphate) the viscosity of the surface layer was found to be

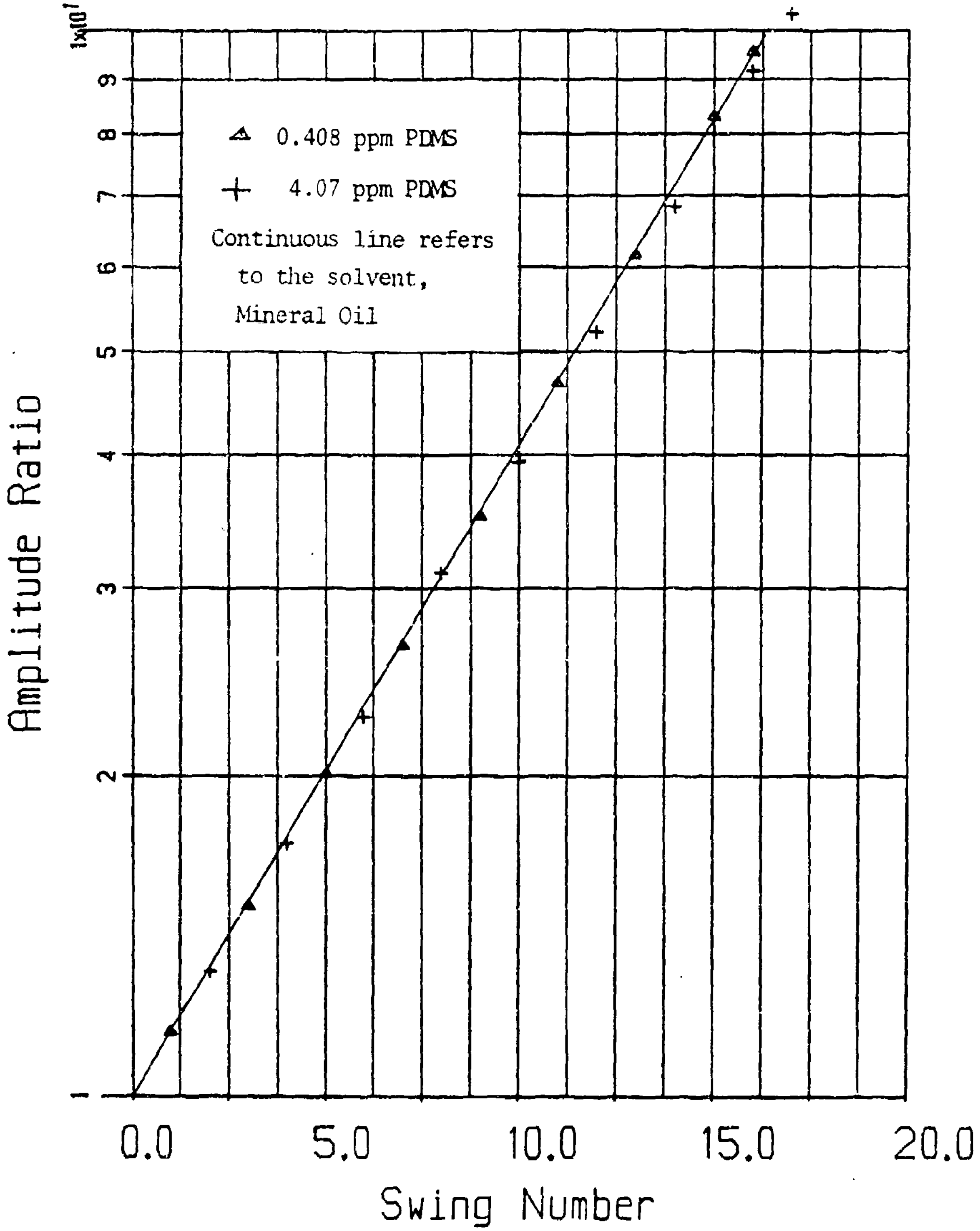

Figure 65. Damping Curve of Oscillating Disc in the Surface of Solutions of Polydimethylsiloxane in Mineral Oil at 25.0°C.

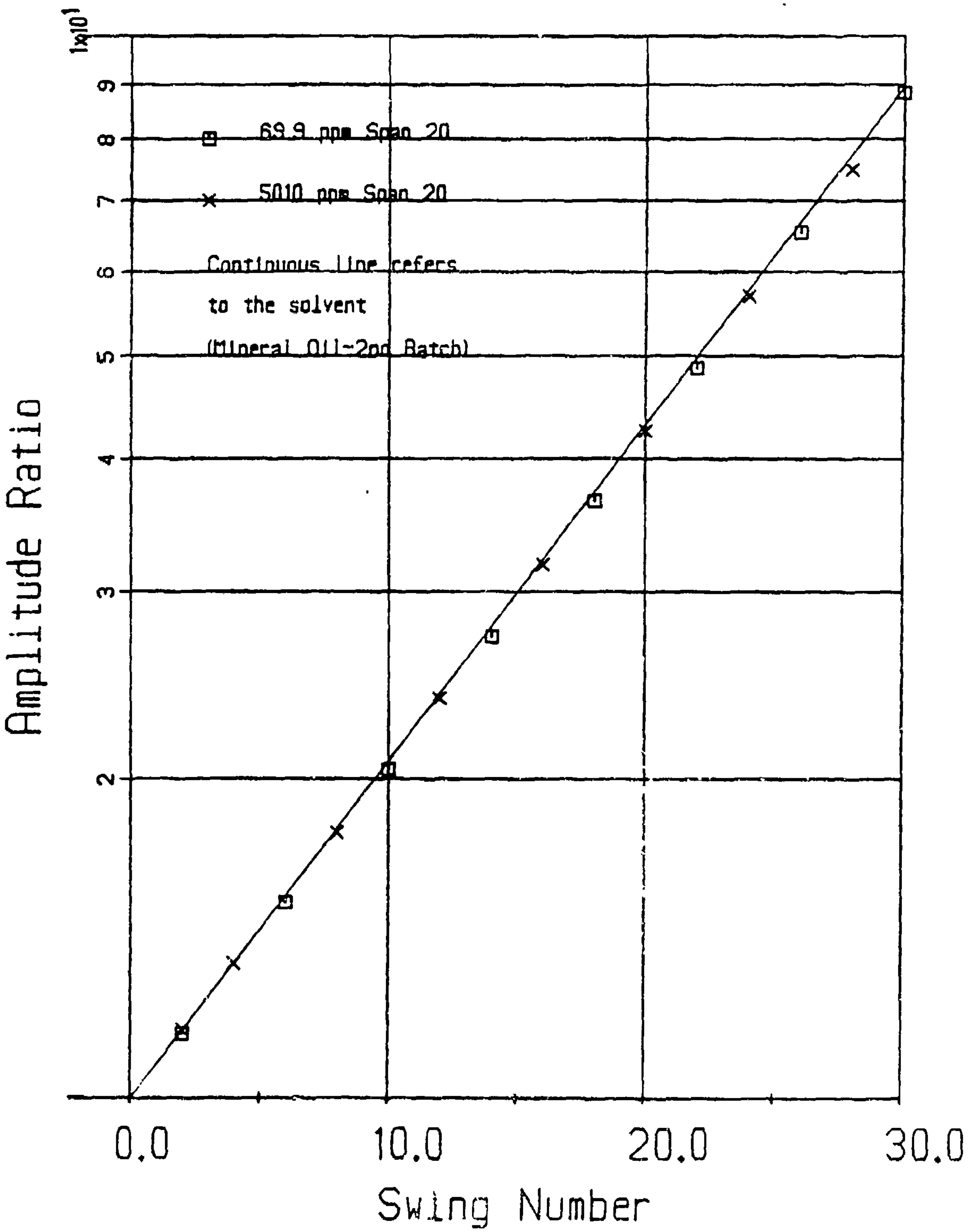

Figure 66. Damping Curve of Oscillating Disc in the Surface of Solutions of Span 20 in Mineral Oil at 25.0°C.

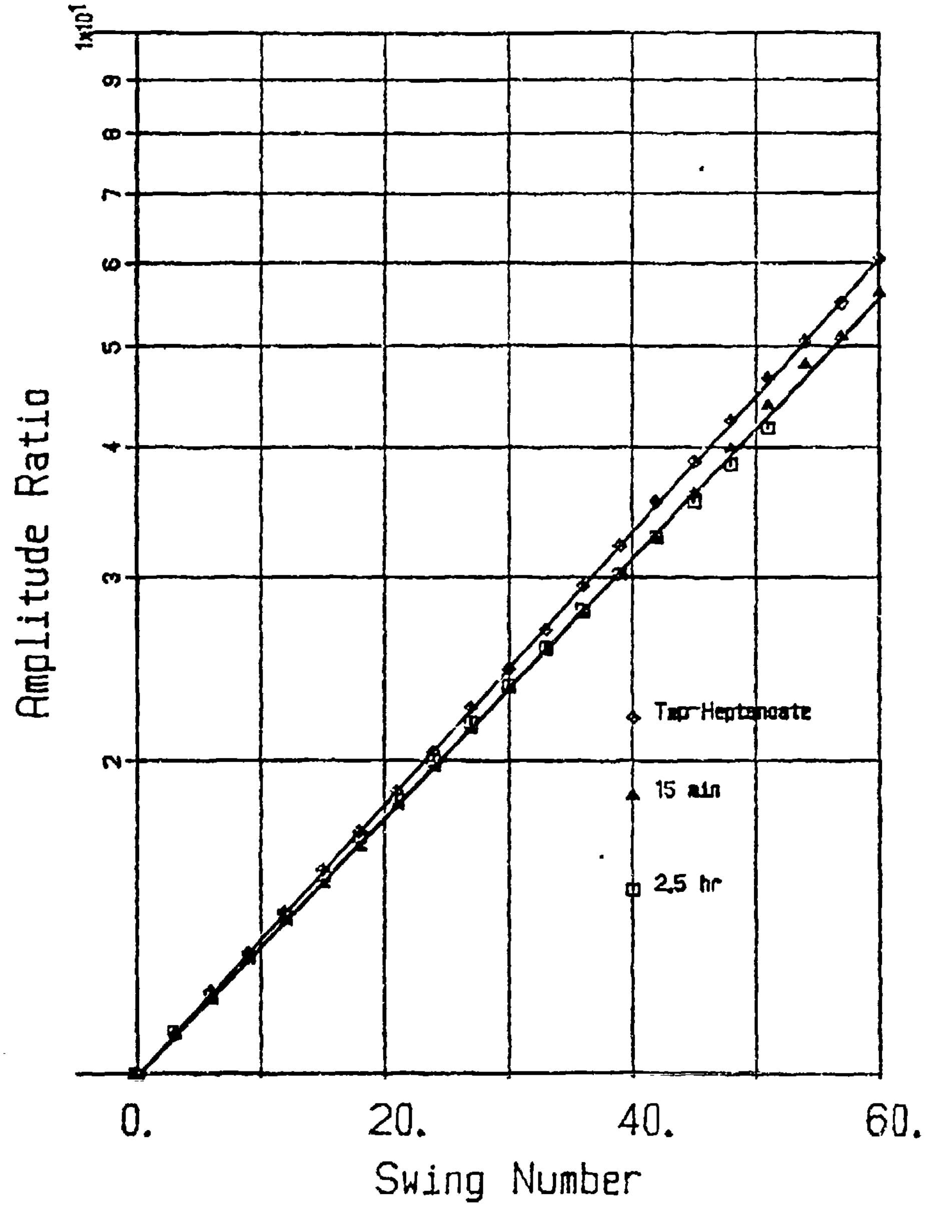

Figure 67. Linear Logarithmic Decrement of Amplitude Ratio with Time (Measured by Swing Number) for Damping of the Oscillating Disc in the Surface of Tmp-Heptanoate and of Aerosol OT (2.04% w/w) in Tmp-Heptanoate at 25°C, after Intervals of 15 Minutes and of 150 Minutes of Surface Aging.

identical with that of the solvent. To investigate this correlation further, a series of solutions were tested for foam, at 40 to 80°C using the Test Method 3213, for bulk viscosity, at 25°C using an Ostwald viscosimeter, and for surface viscosity, at 25°C using the oscillating-disc viscosimeter. In Table 13 we report:

a. The foam volumes measured at 80°C;
b. The increase (%) of the bulk viscosity of the solution, compared to the viscosity of tmp-heptanoate;
c. The increase (%) of surface viscosity relative to the surface viscosity of tmp-heptanoate.

Table 13. Correlation of Foam Volume and Surface Viscosity

Solution	Foam Volume (ml)	Bulk Viscosity increase (%)	Surface Viscosity increase (%)
2.08% A	None	3.3	5.0
2.03% B	None	3.7	5.2
1.96% D	None	-2.0	None
3.94% A	>520	10.3	20.7
4.00% B	>520	20.9	27.0
2.00% B + 2.00% D	480 to >520	4.1	15.5 to 26.0
0.98% B + 2.94% D	400 to 460	1.6	10.0
1.98% A + 1.99% D	435 to >520	7.9	8.6 to 17.2
0.99% A + 2.97% D	360 to >520	3.6	13.8

Table 13 clearly shows the correlation that exists between the measured foaminess and the presence of a surface layer of enhanced viscosity (indicated by the larger increase of surface viscosity compared to the change of the bulk viscosity) showing the importance of the formation of surface films for the production of foam.

For what may be a better evaluation of foaming propensity, we are developing an improved foam meter according to a design of R.C. Watkins.[22] (see Section XIII.9)

SECTION VIII

COMPRESSIONAL-DILATATIONAL SURFACE TENSION

1. Introduction

Dynamic surface tension is a term used to signify non-equilibrium values of the surface tension of a solution, which are produced when the surface is in a mode of motion such that new surface is being created. Pure liquids and solutions of solutes that are surface-inactive do not exhibit a dynamic, or non-equilibrium, surface tension when a new surface is created; but solutions of surface-active solutes do so. The surface tension of a solvent is reduced by the presence of adsorbed solute at the liquid-vapor interface; the more the adsorption, the lower the surface tension. The effect of expanding or contracting movements across the surface is, respectively, to decrease or increase the surface concentration of solute (moles/cm^2) and so raise or lower, respectively, the surface tension, at least momentarily. If the adsorption equilibrium with the immediately adjacent solution is established rapidly, the expanding or contracting of the surface, unless it is done still more rapidly, will have no effect upon the surface tension, which would remain at its equilibrium value; but for many oil solutions the adsorption equilibrium is far from rapid, so that expansion or contraction of the surface, even if done relatively slowly, results in appreciable changes of the surface tension. This effect, i.e., the existence of a compressional-dilatational surface tension, is connected with the propensity to foam. The hope of better understanding the nature of this connection is the reason for introducing measurements of compressional-dilatational surface tensions into the present investigation.

The Marangoni-Gibbs-Rayleigh mechanism, which we shall briefly describe, is a theory to explain the stability of foams. Figure 68A represents a horizontal cross-section of the liquid lamellae between three bubbles of a foam. Adsorbed at the interface are molecules of the surface-active solute. The X's denote areas of equal hydrostatic pressure, while the O denotes an area of lower hydrostatic pressure, located at the Plateau border, resulting from the three convex curvatures of the liquid surface. This pressure difference results in a flow of liquid, called capillary flow, into the Plateau border. The motion of the <u>liquid</u> exerts a viscous drag on the <u>surface</u> and so pulls the adsorbed molecules into the Plateau border, thus compressing the surface film, and lowering the surface tension (see Figure 68B.) This process in turn creates a surface-tension gradient, setting up a Marangoni flow, causing the surface to move away from the Plateau border. The motion of the <u>surface</u> now exerts a viscous drag on the underlying <u>liquid</u>, which is drawn back into the lamellae, thus reversing the destabilising influences of capillary and gravitational drainage.

We initiated experiments with the Cahn Dynamic Surface Tension unit as an attempt to investigate whether the foregoing theory

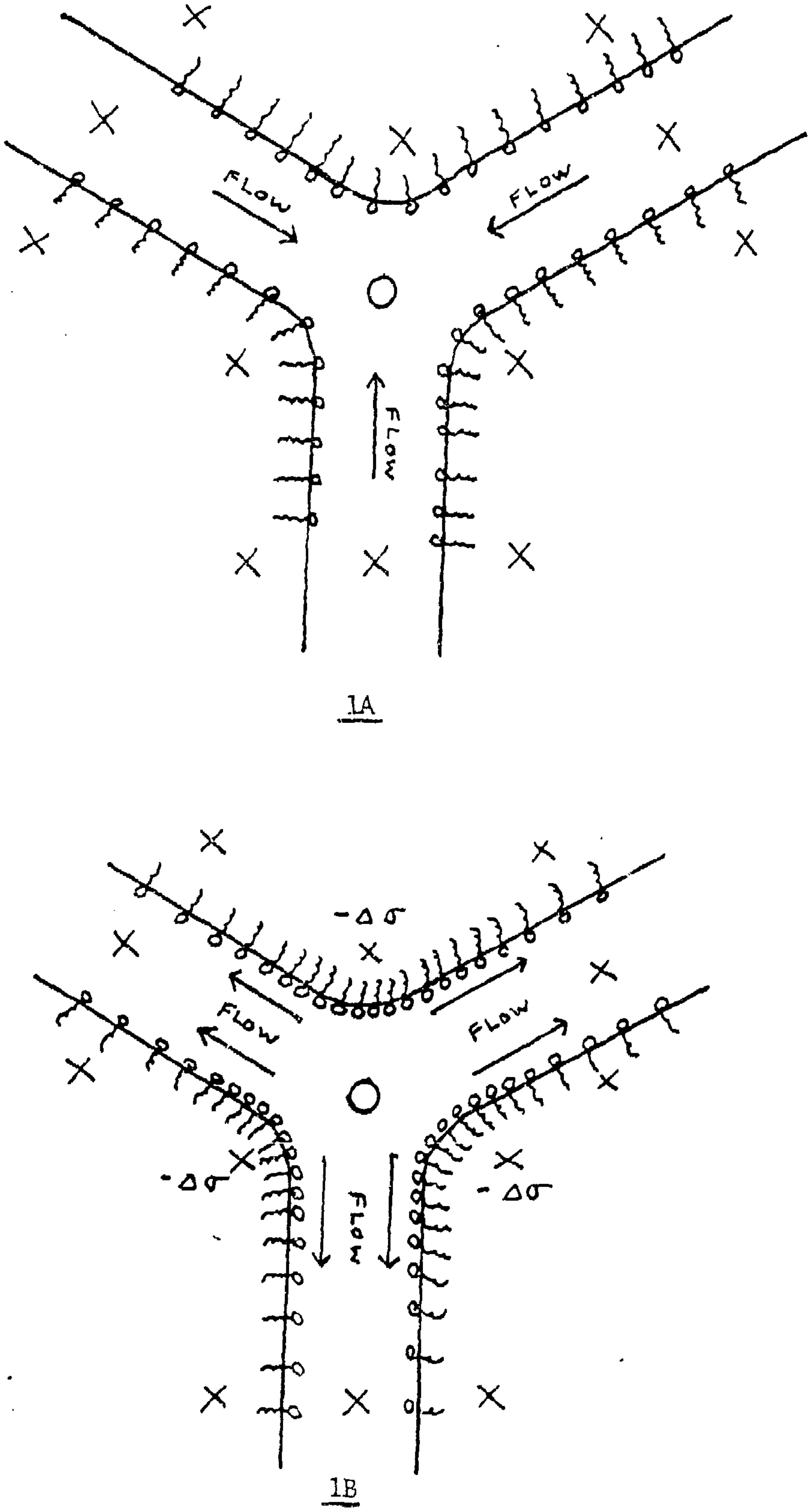

Figure 68. Schematic Explanation of the Marangoni-Gibbs-Rayleigh Theory of the Stability of Foams.
1A - Capillary Flow into the Plateau Border
1B - Marangoni Counterflow out of the Plateau Border.

applies to the foaminess of our oil systems. In this apparatus, the capillary flow part of the theorized mechanism is simulated by the mechanical action of two moving barriers that compress and decompress the adsorbed film in continuous, successive cycles; the consequent changes of surface tension are measured by a Wilhelmy plate situated between the moving barriers. With this device we observed in certain of our oil solutions changes of surface tension faithfully following contractions and expansions of the liquid surface, clearly the result of corresponding compressions and decompressions of an adsorbed layer of solute. This finding is significant, for the adsorbed film in its uncompressed state is too dilute to signal its presence in the usual way by reducing the static or equilibrium surface tension: these observations of dynamic surface tension are, however, sufficient evidence of the existence of an adsorbed film on the surface of such oil solutions. Of course, when no adsorbed film is present, as in an uncompounded oil, or if the additive is not surface active, the contractions and expansions of the liquid surface do not result in any change of surface tension. The Cahn instrument, however, having given these valuable indications, has reached its limit of usefulness: it is too crudely constructed to yield quantitative answers to the more demanding questions that we are now poised to ask.

2. Apparatus to measure Compressional-Dilatational Surface Tensions

The apparatus used is a surface, or film, balance equipped with mechanical devices for producing controlled changes of surface area with simultaneous measurement of surface tension. The instrument is commercially available as the Cahn 2000 Electrobalance with Dynamic Surface Tension Accessory (Cahn #099-002910-30,) based on a design of Mendenhall and Mendenhall, Jr.[23] The accessory equipment consists of a trough of Kel-F-coated aluminum (11.7 cm x 6.18 cm), holding 100 ml of solution. The mobile barriers of solid Teflon are driven by a synchronous motor (Model 65C, New England Gear Division of Robbins & Meyer, Inc.)

The first test of the apparatus is to obtain a horizontal line without any hysteresis on the X-Y recorder when the contraction-expansion cycle of the surface is performed on a solvent sans solute. To bring the equipment to the point where it can pass that test requires that an electric jack be added to control the elevation of the film balance until contact is just made with the Wilhelmy plate; the whole equipment is to be placed inside a shock-mounted polystyrene box; and the sides of the polystyrene box are lined with a grounded metal screen to convert it into a Faraday cage, because of the effects of static electrical charges on the response of the electrobalance. Once all these precautions against external interfering elements are duly taken care of, the equipment gives excellent performance of its function.

3. Results

a. Pure liquids do not show any measurable change of surface tension, because equilibrium is reached within microseconds, that is, far more rapidly than can be attained with any mechanical device. On the equipment described above, the X-Y tracing is a horizontal line without hysteresis. This observation agrees with Rayleigh's theory of dynamic surface tension. Liquids do not have to be absolutely pure to show this behavior; it is necessary, however, that any soluble impurity present be surface inactive.

b. The presence of a trace of surface-active impurity in a solvent can be detected by the evidence of dynamic surface tension, i.e., a value of the surface tension other than its equilibrium value, when the surface area is expanded or contracted.

c. If a surface-active solute is present, creation of new surface occurs when the mobile barriers are moving apart, and this is accompanied by an increase of the surface tension. When the barriers approach each other, the surface tension decreases.

d. Hysteretic behavior is always a sign that the system is far from equilibrium. It is produced in the present apparatus when the motion of the blades is faster than the natural mechanism of restoration of the adsorbed surface film.

e. We have discovered two well differentiated types of hysteresis obtained with this equipment. One of these occurs in solutions of polydimethylsiloxane in mineral oil, and the other in solutions of an oil-soluble, surface-active solute (Span 20) in mineral oil. The former solution yields a hysteresis loop in which the contraction branch lies above the expansion branch; the latter solution yields a hysteresis loop of the opposite character, in which the contraction branch lies below the expansion branch. These results are reported in Figures 69 and 70. Figure 69 refers to the solution of polydimethylsiloxane; the course of the hysteresis loop is counterclockwise. Figure 70 refers to the solution of Span 20; the course of the hysteresis loop is clockwise.

f. The difference in behavior described above may be traced to two different natural mechanisms by which the newly created surface is restored, and which can readily be distinguished one from another by means of this investigative technique.

4. Discussion of Results

The two different types of hysteresis loop obtained by means of the film balance can be explained as arising from the presence of two different natural mechanisms that act to restore equilibrium to a newly created surface. Two types of behavior of surface films may be understood by keeping in mind the usual shape of the isotherm of an adsorbed monolayer, shown in Figure 71, where Π, the spreading pressure in mN/m, is equal to $\sigma_0 - \sigma$, the reduction of the surface tension, and A is the area available for a fixed amount of adsorbate. In such an isotherm there exists a range of high surface concentration described by PQ in Figure 71, in which

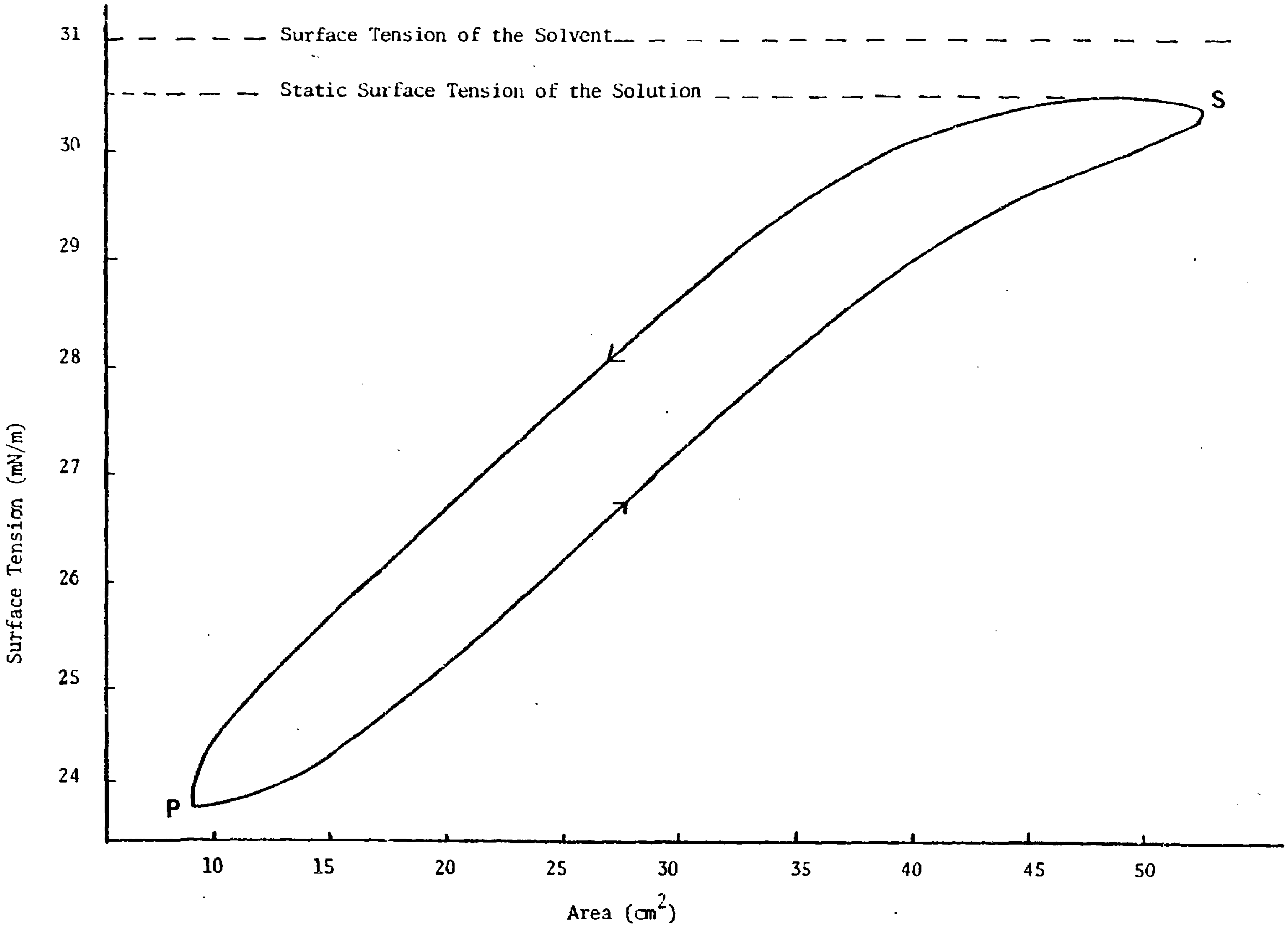

Figure 69. Surface Tension *versus* Surface Area, Showing Hysteresis at Steady State; Ten Consecutive Hysteretic Loops Recoreded One on Top of the Other. Solution of 3.5 ppm Polydimethylsiloxane in Mineral Oil at 1.5 minutes/cycle and 26°C.

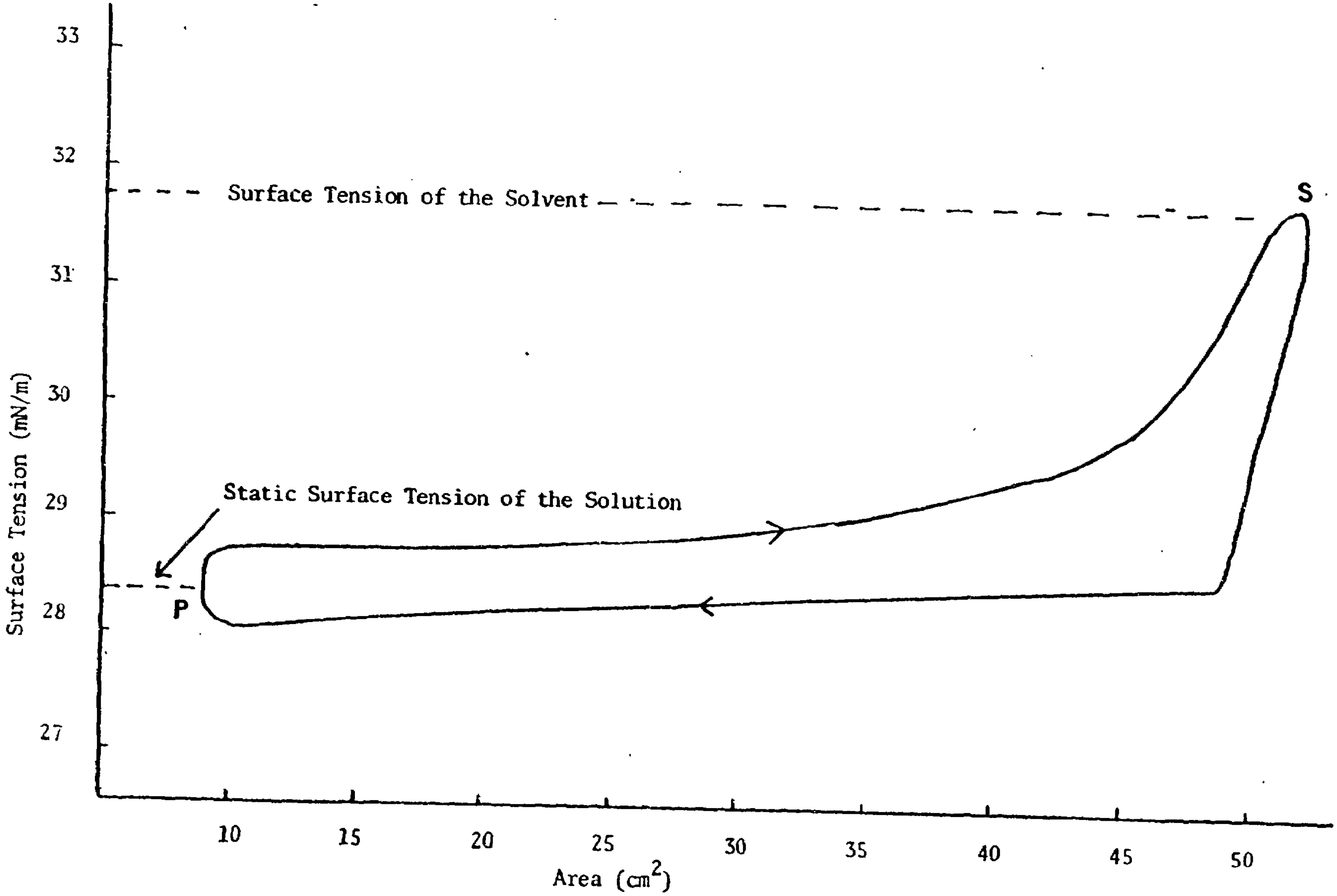

Figure 70. *Surface Tension* *versus* *Surface Area*, Showing Hysteresis at Steady State; Ten Consecutive Hysteretic Loops Recoreded One on Top of the Other. Solution of 399 ppm Span 20 in Mineral Oil at 3.0 minutes/cycle and 26°C. N.B. *The Mineral Oil Referred to in this Diagram is not the same as* that Referred to in Figure 69.

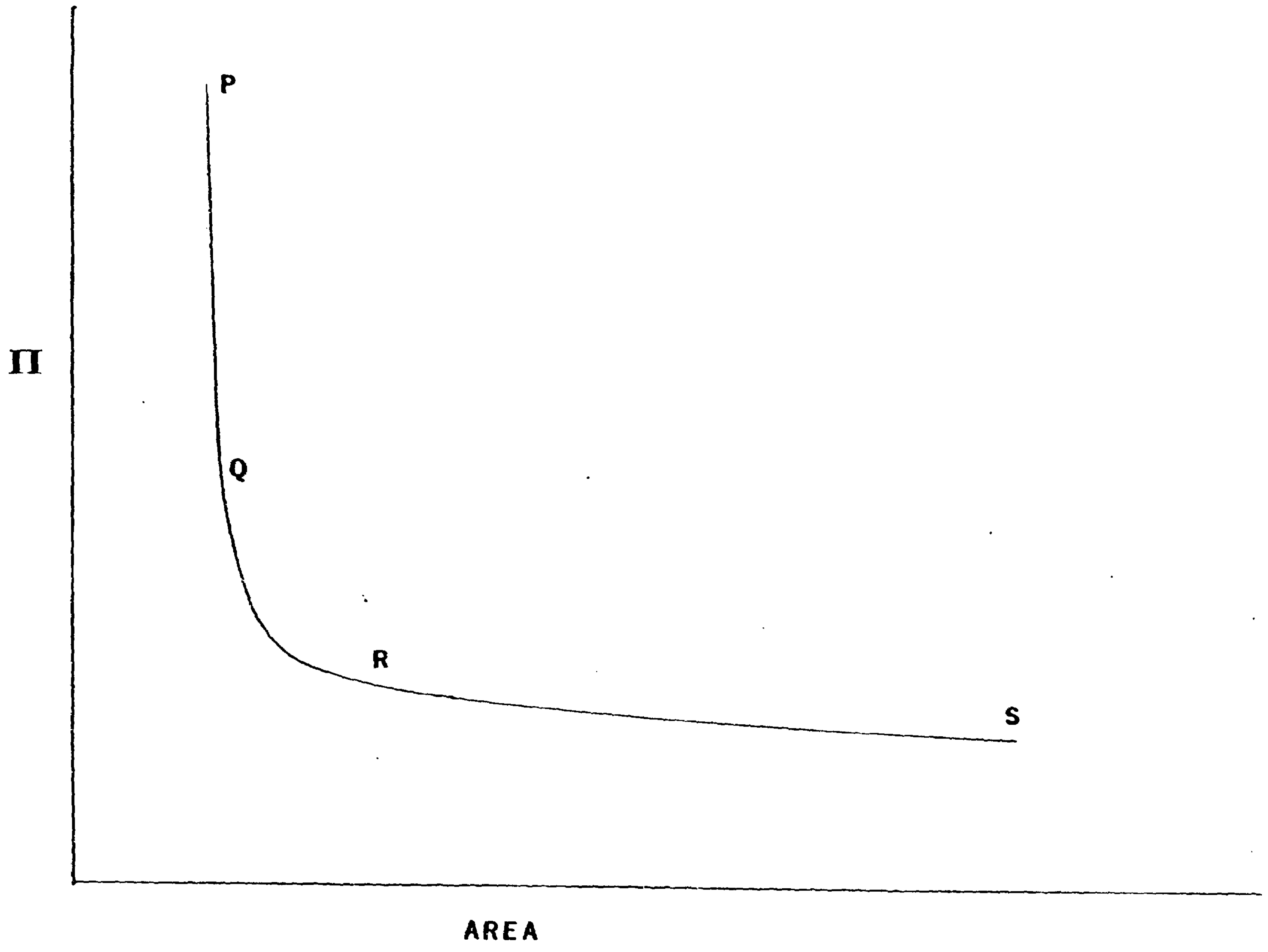

Figure 71. Typical Force-Area Isotherm of an Insoluble Monolayer, where $\Pi = \sigma_0 - \sigma$ is the Lowering of the Surface Tension and A is the Area Available for a Fixed Amount of Adsorbate.

$(d\,\sigma/dA) = -(d\,\Pi/dA)$ is large; and another range of low surface concentration, described by RS in Figure 71, in which $-(d\,\Pi/dA) = (d\,\sigma/dA)$ is small. The behavior described by Figure 71 is typical of that obtained by direct measurements of insoluble monolayers on water; and it also describes the behavior of films of adsorbed solutes in aqueous or non-aqueous solution.

Figure 69 represents the behavior of a weakly surface-active solute, which is able to reduce only slightly the surface tension of the solvent and has only a small excess surface concentration. The equilibrium surface film corresponds to the point S in Figure 71; it shows no change on expansion beyond S because it is already so dilute, but on compression it begins to respond by increasing Π (reducing σ ,) slowly at first and then more rapidly toward the end of the compression. On the return branch of the cycle the compressed film is allowed to expand. If, on the return of the blades to their original position, the rates of molecular relaxation of the compressed adsorbate plus desorption into the solution (both of which occur simultaneously) are exceeded by the rate at which the moving blades are donating new area, hysteresis follows. The lag of these processes on expansion allows a lower surface tension to be retained than would have resulted from an instantaneous response, so the expansion branch of the cycle lies below that of the contraction branch. The cycle, therefore, travels in a counterclockwise direction from the higher equilibrium surface tension of the solution to the lower nonequilibrium surface tension of the compressed soluble film.

Figure 70 represents the behavior of a strongly adsorbed solute, which markedly reduces the surface tension of the solvent. The equilibrium surface film corresponds to the point P in Figure 71. The major movement of the surface tension now occurs on expanding the surface beyond its equilibrium condition. The newly created area of liquid soon, albeit temporarily, has the character of the solvent, or at most a very dilute solution, say, at the point S: and the surface tension climbs rapidly to a value close to that of the solvent. This non-equilibrium condition of the surface cannot be maintained for long; even were the motion of the blades were to cease at this point, the surface tension would spontaneously decline to that of the equilibrium state. Accordingly we find a fairly rapid initial decrease of the tension from its high value, partly because of spontaneous adsorption but assisted by the compression of the adsorbed film, which brings the compression branch of the cycle below the expansion branch. The cycle, therefore, travels in a clockwise direction from the lower equilibrium surface tension of the solution to the higher non-equilibrium surface tension of the expanded surface.

A third type of surface film is possible: an insoluble monolayer. An insoluble monolayer may be obtained by directly depositing an insoluble material that has the ability to spread on the liquid surface. Such a film can be compressed without going into solution, so that the surface tension is brought to a value below that of equilibrium. If, on the return of the blades to their expanded position, the rate of molecular relaxation of the compressed, insoluble monolayer is exceeded by the rate at which the moving blades are creating new surface, hysteresis follows. The lag of the relaxation on expansion retains a lower surface tension than would have resulted from an instantaneous response, so the expansion branch of the cycle lies below that of the contraction branch. The cycle travels from the surface tension of the compressed film to that of the expanded film. A feature of a compressed insoluble film is that it can reduce the surface tension of water to values lower than are ever reached by soluble hydrocarbon-based detergents, which cannot give values less than about 28 mN/m. The surfactant derived from the animal lung has been reported[24] to give values of the surface tension of water of only a few mN/m. That observation alone is enough to establish the presence of an insoluble monolayer on the aqueous substrate. Another indicator of an insoluble monolayer is that the surface tension of the compressed film does not drift spontaneously upward if the motion of the barriers is stopped at that point.

The adsorption of solute takes several hours of repeated cycling to reach either a steady state or static equilibrium. This phenomenon of slow growth appears to be common to soluble types of adsorbed film. At first the cycle is a horizontal line with no hysteresis, indicating a surface indistinguishable from that of the pure solvent; but the surface tension soon begins to decline and a hysteresis loop develops. On each successive cycle the surface tension continues to decrease, indicating that adsorption out of the solution has gone further by the end of the cycle than merely to replace adsorbate that had been present at the beginning of the cycle. After cycling for several hours, a steady state is reached in which no more adsorption occurs than is required to restore the conditions that existed at the start of the cycle. At this stage the hysteretic loop repeats itself each time. Figures 69 and 70 report such steady-state loops. Figure 72 shows how the hysteresis loops develop over a period of four hours, starting with a surface that had already been aged for several hours. A genuine static equilibrium cannot be reached while the blades are in motion, as the surface is constantly being disturbed; but for every mechanically imposed speed of cycling there exists a steady state at which the rate of adsorption (not yet zero as it would be at a static equilibrium) provides just enough adsorbate in the time of the cycle to restore what had been lost by desorption during the contraction. The persistence of the hysteresis shows, however, that the natural rate of restoration still lags behind the imposed rate of the cycle. Let us reduce the imposed rate of cycling still further: the area of the hysteretic loop decreases as the lag becomes smaller; finally a steady state may be reached at which the imposed rate of cycling just equals the natural rate of restoration, at least for an appreciable portion of the cycle; at this point the hysteresis is at its minimum.

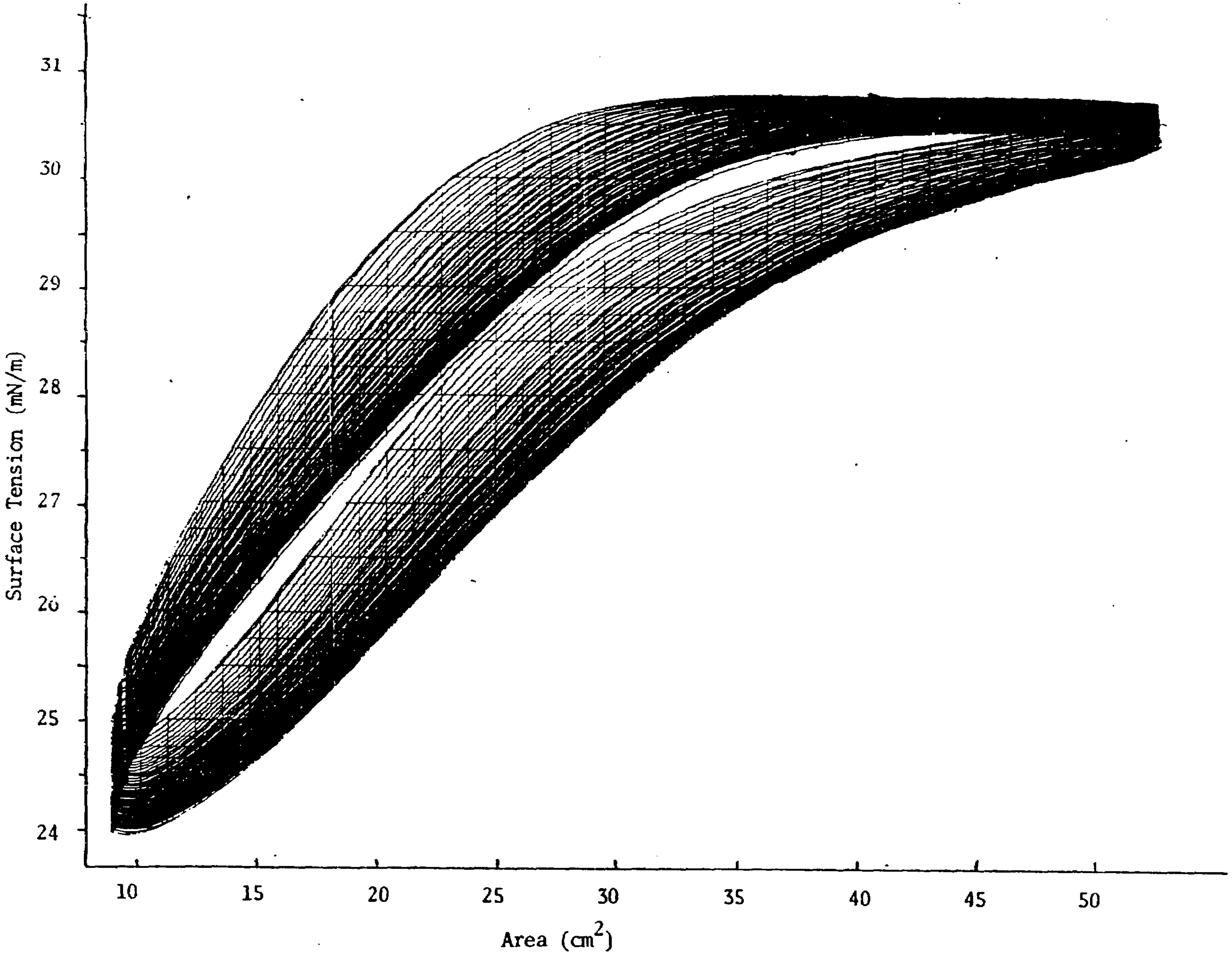

Figure 72. Compressional/Dilatational Surface Tensions of Polydimethylsiloxane (1000 cSt) in Mineral Oil at 25°C, Showing Sixty Successive Hysteresis Loops over a Period of Four Hours, as the Surface Aged from Twelve to Sixteen Hours.

5. Results of Dynamic Surface Tension with Improved Apparatus

The commercially available Cahn Dynamic Surface Tension Balance may allow the enclosed surface film to leak past the barriers. To overcome this difficulty, Mr Erik Bock suggested to us the use of a hollow funnel to confine the surface, which could then be made to contract in area as the funnel is lowered into the solution.

The schematic diagram (Figure 73) shows its basic components. Central to the design is a funnel of rectangular cross section, made of teflon-coated stainless steel, which is attached to the hydraulic cylinder (slave cylinder,) and is designed to give a linear change of area with depth of immersion. Next to the funnel is the teflon counter-volume, which compensates the volume change of the solution caused by immersing and withdrawing the funnel. Beneath the funnel is a trough, made of teflon-coated stainless steel, in which the solution is contained. It is raised into position by an optical table (not shown.) The entire unit is enclosed in a plexiglass box, which is electrostatically shielded, dust and draft proof, and vibration free. The slave cylinder is connected by hydraulic lines to a master cylinder, which is controlled by a variable-speed power station (see Figure 74.) Hydraulic operation eliminates vibrations and temperature fluctuations inside the box, and permits easy access to all the controls.

The purpose of the experiment is to measure the surface tension of the solution as the area of the surface is changed. Setting the vertical distance of travel of the funnel sets the contraction ratio of the surface. In the present experiments the contraction ratio is 5.8:1.0 and the cycling speed is 3.25 minutes/cycle. The area of the surface inside the funnel contracts and expands linearly with time. The cycles are recorded on an X-Y plotter as surface tension _versus_ area of surface. Of these cycles we need report here only the first and the final equilibrium: the first cycle is relevant to our investigation of foam, as a dynamic foam is a creation of fresh surfaces; the equilibrium cycle is included for its general interest, although too much time elapses before the surface reaches that stage for the equilibrium cycle to relate to the foaminess of these solutions.

Our first use of the new technique was to check the distinction previously drawn between dilute and concentrated surface films appearing on the surface of solutions. The result cited comes into question when the possibility is admitted of the film leaking past the barriers. The new technique with the film confined within the cone precludes this possibility. By its use, we have confirmed the correctness of the previously stated distinction. A solution of Span 20 in mineral oil, at a concentration of 474 ppm reduces the equilibrium surface tension from 31.32 mN/m (solvent alone) to 28.3 mN/m. After contracting the surface area of the solution by a factor of four, the surface tension does not change; expanding the surface, however, causes the surface tension to increase to 31.3 mN/m, which is the surface tension of the solvent; on standing, in the expanded state, the surface tension finally subsides to its

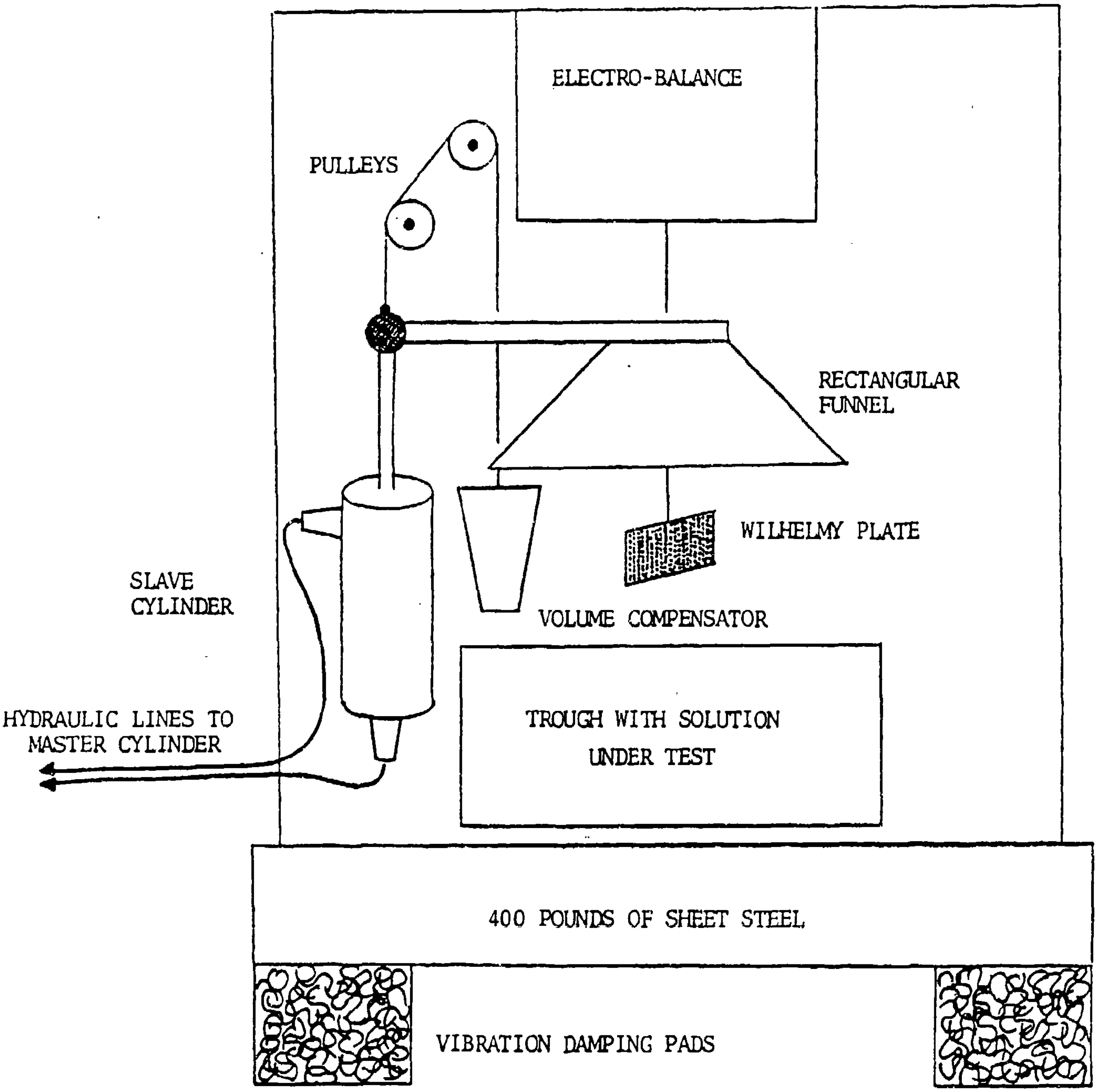

Figure 73. Experimental Chamber Used to Determine Changes of Surface Tension on Compression and /or Dilatation of Adsorbed Solute.

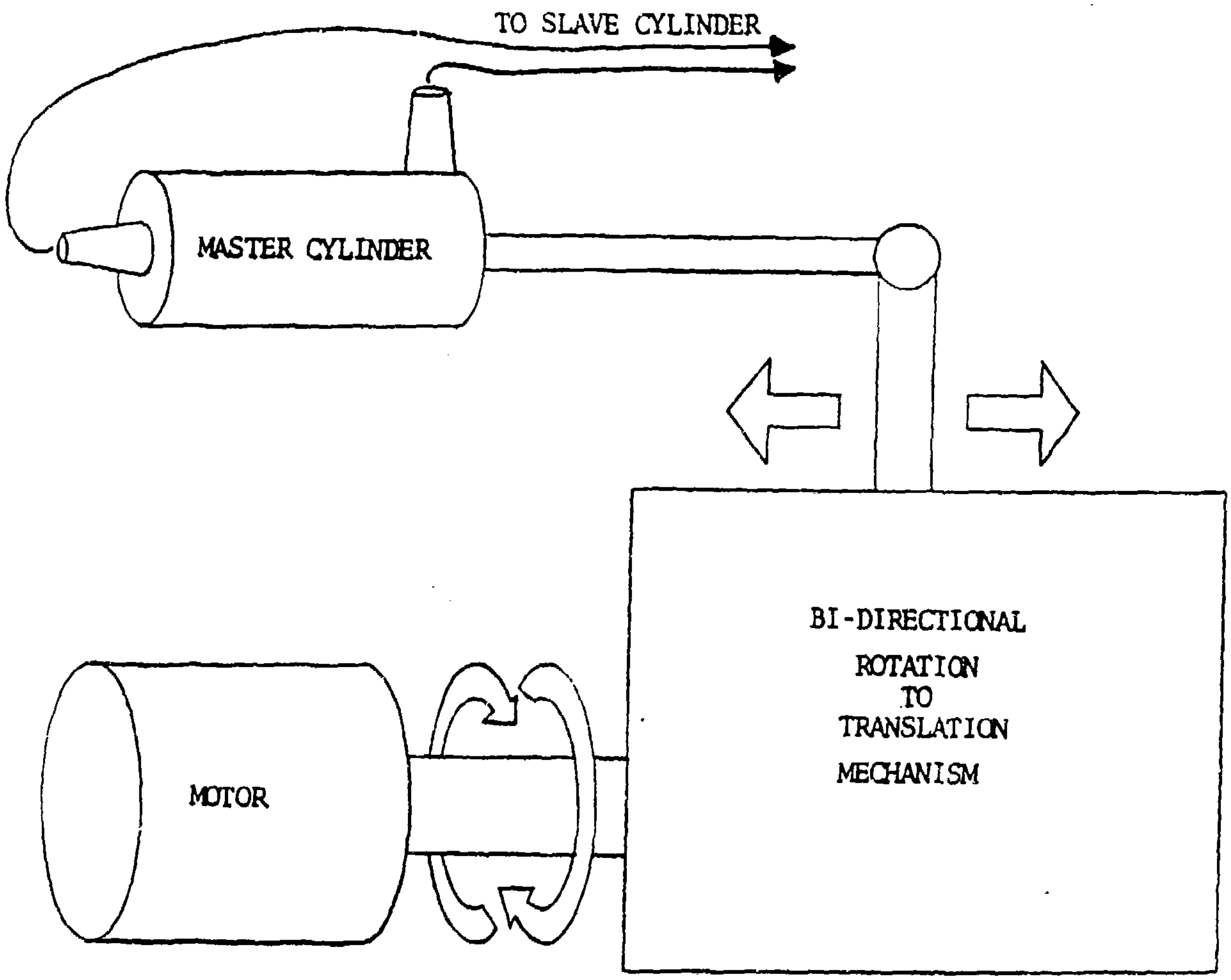

Figure 74. Hydraulic Power Station Used to Drive the Slave Cylinder in the Experimental Chamber (see Figure 73) for Compressional/Dilatational Surface Tension.

equilibrium value of 28.3 mN/m, as adsorption takes place from the bulk solution to the diluted surface. This series of observations with the leak-proof film container demonstrates that the surface film at equilibrium is concentrated: it is not concentrated further by compression because any build-up of surface concentration is rapidly dissipated by dissolution or desorption; it can, however, be diluted by expansion, at least temporarily, because the rate of adsorption is less than the rate of desorption.

The new technique with the cone also confirms our finding that solutions of polydimethylsiloxane in mineral oil give surface films of low concentration. These films are recognized by their opposite type of behavior: the surface tension decreases on contracting the surface area from its initial state, indicating that the film can be compressed; but the surface tension does not increase on expanding the film from its initial state, indicating that the equilibrium adsorbed film is exceedingly dilute; this last point is borne out by the tiny reduction of the surface tension of the solvent brought about by the presence of the solute in these solutions.

6. Dynamic Surface Tension and Foam

The condition of equilibrium, which requires a long period of time, can have no direct relevance to foaminess, as in the production of foam new surface is created as soon as a bubble is entrained within the solution. If the foaminess of solutions depends on the existence of surface films that affect surface tension, as is reasonable to assume, we must look to their state of development within, at the most, a few minutes after the creation of a new liquid surface. With this condition in mind, the difference in behavior of a solution of phenothiazine in tmp-heptanoate at 2% (w/w) concentration and at 4% (w/w) concentration is significant. The former of these solutions is essentially nonfoaming, whereas the latter foams readily and overflows the foam-meter. The presence of the solute in these solutions affects the equilibrium surface tension to a negligible degree, so that there would be no reason, on the basis of such evidence, to describe the solute as surface active. Nevertheless, a rapid contraction of the surface results in a lowered surface tension, which is definitive evidence that an adsorbed film of solute is present initially and that it becomes compressed and, as a result, concentrated on the contraction of the surface. We find that the surface tension, after contraction, of a fresh surface of the 2% solution declines from the value of the solvent very slowly; even after two hours it is still the same, after contraction, as when newly created. The surface tension of a fresh surface of the 4% solution, however, shows an immediate lowering, but again only after contraction, from 30.89 mN/m to 30.71 mN/m, and a final lowering, after aging and on contraction, to 24.48 mN/m. While these values of surface-tension lowering are small, they are greatly augmented when the film is even further compressed by a greater degree of contraction. In the production of foam by entrainment of gas, both compressions and expansions of surface films are going on throughout the foam and all the time. We therefore ascribe the nonfoaminess of the 2% solution and the foaminess of the 4% solution to the difference in initial rates of establishing a lowering of the surface tension on contraction of the surface, with its correlative and concomitant effects, the adsorption of solute and growth of the surface film.

The foregoing experiments were done with a contraction ratio of 6:1 but it is evident that compression of the film at the surface is more pronounced at the later stage of the contraction. Only the initial changes of surface tension on contraction of the surface are likely to correlate significantly with observed foam behavior, and such changes are quite small initially. These changes depend on the contraction ratio, and are greatly accentuated at ratios larger than 6:1.

7. Temperature Variation of Compressional-Dilatational Surface Tension

The apparatus to measure compressional-dilatational surface tension was modified to accomodate measurements at elevated temperatures. The solution is heated to the desired temperature prior to pouring it into trough. The air inside the box also requires to be heated, because the motion of the funnel traps warm air above the liquid surface when most of the funnel is withdrawn from the liquid, but cooler air surges in as the funnel descends, lowering the temperature of the liquid surface, thereby raising the surface tension. This causes the flat trace characteristic of the solvent alone to display a rising curve, and would cause the hysteresis loop of a solution to be reduced.

The variation with area and temperature of the change of surface tension on the first compression/dilatation cycle of solutions of N-phenyl-1-naphthylamine in tmp-heptanoate are reported in Figure 75. Curve A refers to a concentration of 3.90% (w/w) and curve B refers to a concentration of 4.40% (w/w.) Each point on the curves represents the decrease in surface tension on the initial contraction of the surface. Both solutions show a marked increase in this effect with increasing temperature; the solution of 3.90% concentration sustains its surface activity with temperature; the solution of concentration 4.40% declines in surface activity after a maximum at 60°C.

A solution of 4.0% (w/w) phenothiazine in tmp-heptanoate was measured as well. No decrease of surface tension on contraction of the surface was observed, even after continuous cycling for forty-five minutes. After standing overnight undisturbed a decrease of 2.3 mN/m was measured. At 53.6°C, after vigorous stirring, the initial decrease of surface tension on contraction was 1.6 mN/m. These changes are much less than were observed for solutions of N-phenyl-1-naphthylamine at the same temperature, although the foaminess of solutions of the two solutes in tmp-heptanoate is about the same. This observation suggests that phenothiazine solutions are stabilized electrostatically; especially as we have found that the electrical conductivity of phenothiazine solutions is also much larger than that of the solvent.

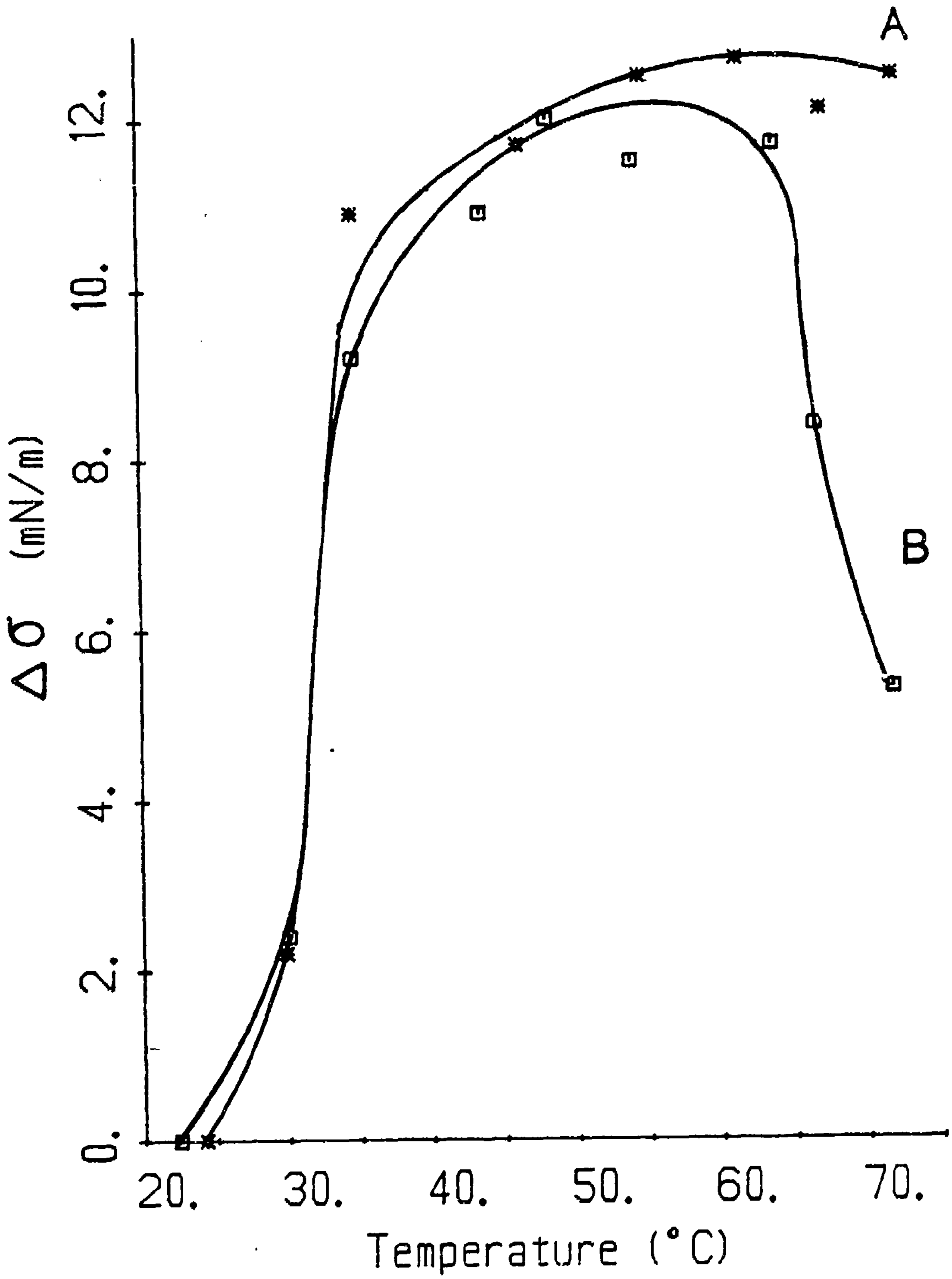

Figure 75. Variation of , the Decrease of Surface Tension on the Initial Contaction of the Surface, with Temperature.
A: N-Phenyl-1-Naphthylamine (3.90% w/w) in Tmp-Heptanoate.
B: N-Phenyl-1-Naphthylamine (4.40% w/w) in Tmp-Heptanoate.

SECTION IX

SINGLE BUBBLE STABILITY

1. Measurement of the Stability of a Single Bubble

Initial attempts to produce single bubbles were consistently defeated by the bubbles drifting, due to drafts, thermal currents, and the attraction of the meniscuses at the container wall and nearby glass capillary. The lifetime of a single bubble is not a reproducible measurement if the bubble should become attached to a meniscus or to another bubble. These experimental difficulties were overcome by containing the solution in a jacketed beaker, 12 cm in diameter, covered with a Plexiglass lid, and connected to a Haake temperature-controlled circulator. Astigmatism of the optical system was reduced by immersing the beaker in water, contained in a flat-walled Plexiglass box.

The end of a glass tube, 4mm diameter, was drawn out into a fine capillary and bent to an angle of 45° to the standing part. This conformation allows the capillary tip to be placed immediately underneath the surface of the solution in the center of the beaker. The depth of immersion of the capillary tip is kept constant by the use of a cathetometer. Control of the air injection is obtained by a micrometer-driven syringe connected to the capillary. The entire apparatus is back-lighted to make the capillary more visible.

2. Normalizing Bubble Stablities for Changes of Viscosity

The variation with temperature of the lifetime of a single bubble, averaged over at least fifteen observations, of a solution of N-phenyl-1-naphthylamine (3.5% w/w) in tmp-heptanoate, decreased continuously from a value of 13.3 minutes at 25°C to 1.56 minutes at 80°C. (See Figure 76.) The effect of increased temperature on the foaminess of a solution is largely the result of the accompanying decrease of the viscosity of the liquid. To offset that influence we have replotted bubble-stability data as the ratio of the lifetime to the kinematic viscosity *versus* the temperature; see Figure 77. A maximum value of this ratio appears at 40°C. This maximum might well be a reflection of a corresponding maximum of the surface activity of the solute at this concentration at 40°C.

Another set of data is reported in Figure 78: the temperature dependence of the stability of a single bubble in a solution of polydimethylsiloxane, 1000 cSt, in tmp-heptanoate, at a concentration of 263 ppm, in the range of temperatures of 25° to 80°C. The same data are plotted in Figure 79 as the ratio of stability to viscosity *versus* temperature, i.e., the data normalized for changes in viscosity. Figure 79 shows a decrease of the normalized stability with temperature, indicating a reduction of surface activity at higher temperatures.

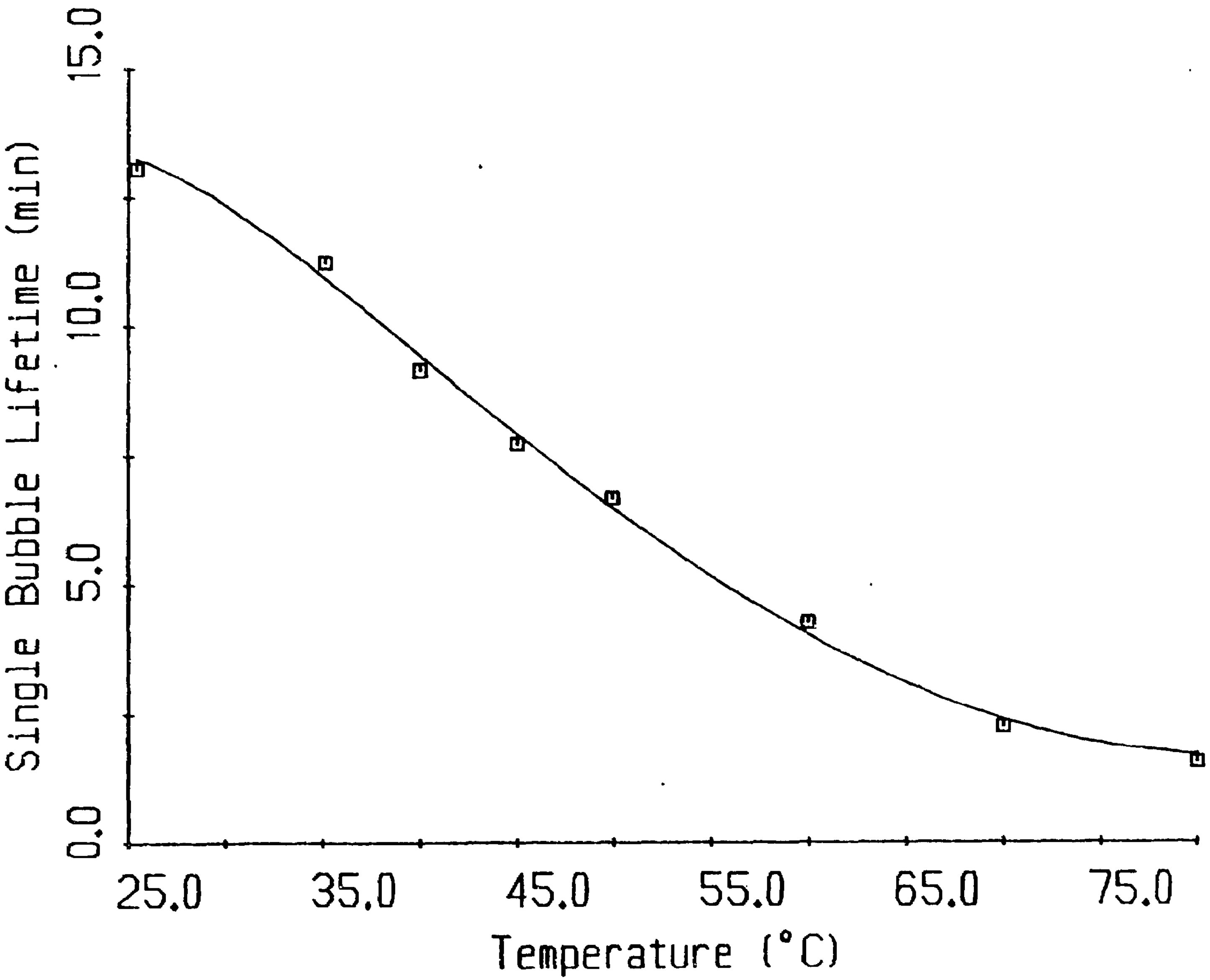

Figure 76. Variation with Temperature of the Lifetime of a Single Bubble Made from a Solution of N-Phenyl-1-Naphthylamine (3.5% w/w) in Tmp-Heptanoate.

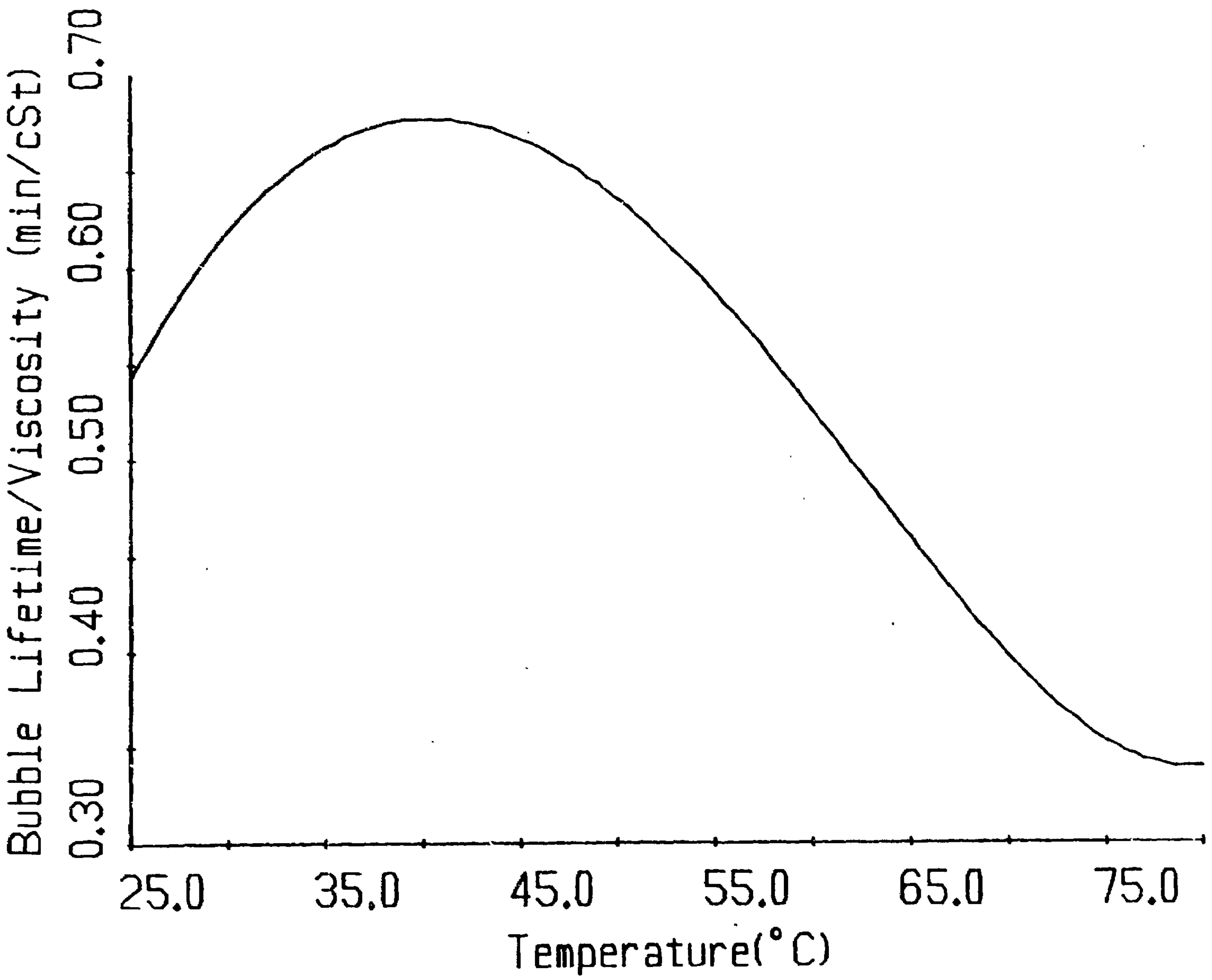

Figure 77. Variation with Temperature of the Ratio of Bubble Lifetime to Kinematic Viscosity of a Solution of N-Phenyl-1-Naphthylamine (3.5% w/w) in Tmp-Heptanoate.

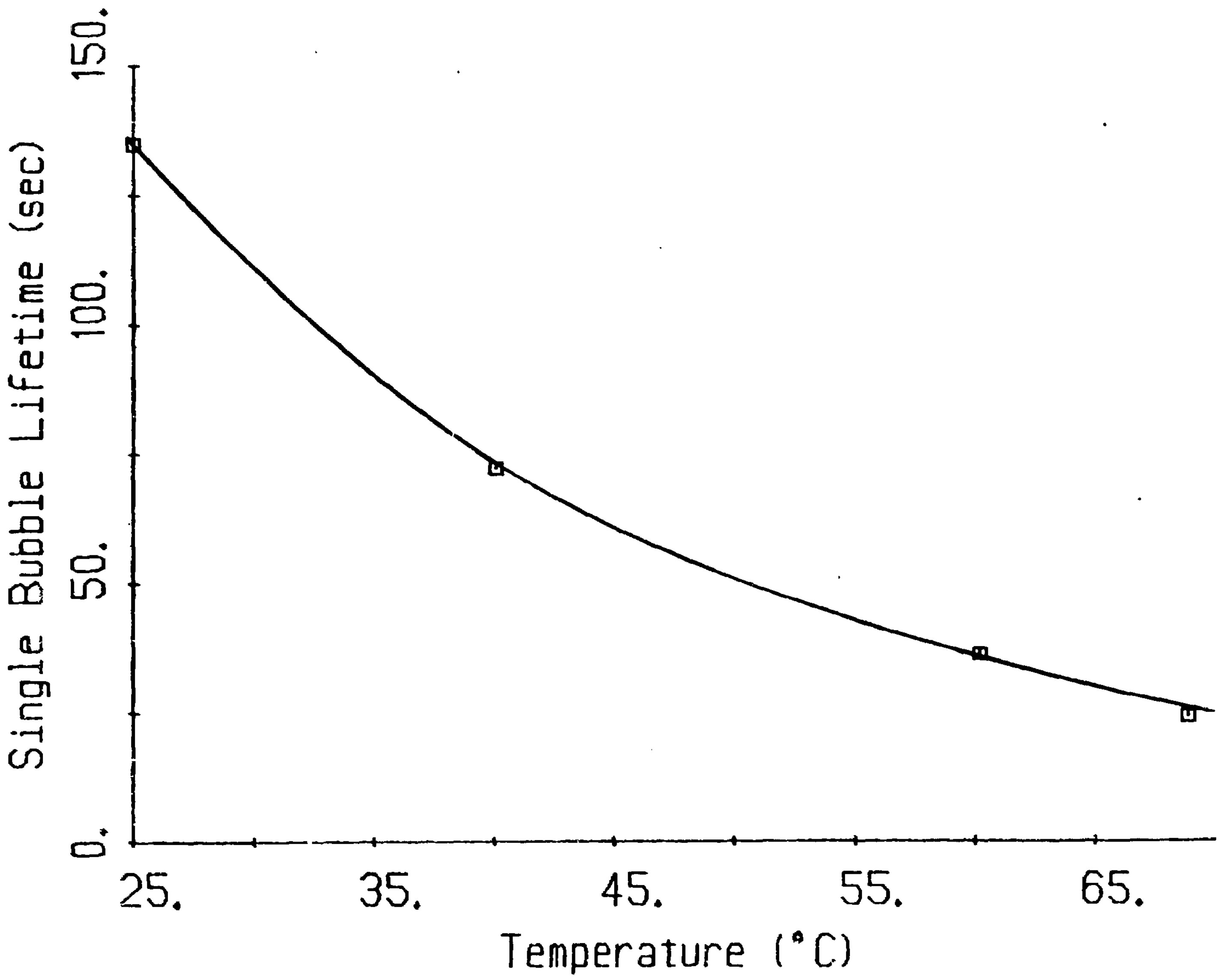

Figure 78. Variation with Temperature of the Lifetime of a Single Bubble Made from a Solution of Polydimethylsiloxane (1000 cSt) at 263 ppm in Tmp-Heptanoate.

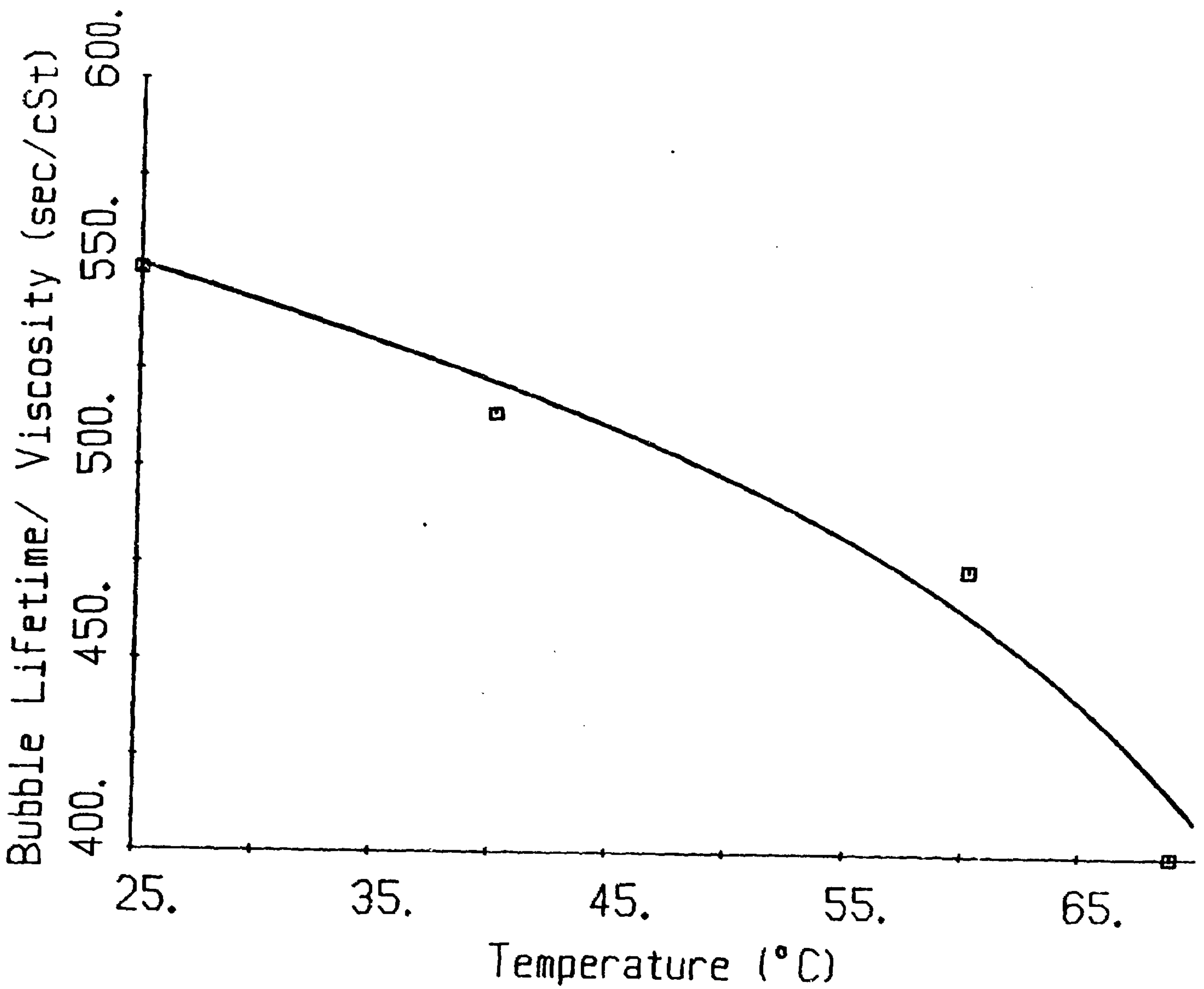

Figure 79. Variation with Temperature of the Ratio of Bubble Lifetime to Kinematic Viscosity of a Solution of Polydimethylsiloxane (1000 cSt) at 263 ppm in Tmp-Heptanoate.

SECTION X

GAS SOLUBILITY IN TMP-HEPTANOATE AND ITS SOLUTIONS

1. Apparatus to Measure Gas Solubility

A refined volumetric absorption apparatus was constructed, capable of measuring the amount of gas dissolved as a function of equilibrium pressure. (See Figure 80.) The apparatus consists of a high-vacuum pumping station (Dual-Stage Rotary Vane Pump and Turbovac, turbomolecular pump), a manifold for transferring gases, an absorption manifold and a sample thermostat. The absorption manifold contains a dosing volume and a sample chamber. The dosing volume contains a capacitance manometer, responsive to pressures up to 1000 torr. The sample chamber consists of a 10 torr manometer and a Pyrex bulb to hold the absorbing liquid. All components of the absorption system are connected with stainless steel Swagelok fittings and are vacuum tight to 10^{-7} torr.

Solubility data are obtained by loading the dosing chamber with the gas and introducing it to the sample chamber. The pressure drop in the dosing chamber and the increased equilibrium pressure over the sample are read after each addition of gas, and the moles of gas dissolved are calculated from the pressure differences in the precalibrated volumes in the usual way.

2. Vapor pressure of TMP-Heptanoate

The gas solubility apparatus was used to measure the vapor pressure of tmp-heptanoate, in the temperature range of 25 to 45°C. Prior to the measurements the liquid was degassed for 15 minutes at 25°C and pressure less than 0.01 torr. The absorption manifold was continuously heated at 45°C to prevent vapor condensation on the inner parts of the manifold. Figure 81 reports the vapor pressures obtained at the various temperatures. It shows a linear relation between log P and 1/T, according to the Clausius-Clapeyron equation.

The vapor pressure was found to be sensitive to the degassing time; the pressure at a given temperature sharply decreasing with increasing degassing time. This effect indicates the presence of some volatile substances in the tmp-heptanoate used, which are preferentially distilled out during the degassing procedure.

3. Nitrogen Solubility Isotherms

Nitrogen-gas solubilities in tmp-heptanoate were measured at 26.0°C and 34.7°C at equilibrium pressures of nitrogen up to 580 torr. Figure 82 reports the mass of nitrogen absorbed per gram of tmp-heptanoate as a function of the equilibrium pressure at the two temperatures. The two isotherms show minor variations of the amounts absorbed up to about 180 torr; at pressures greater than that, the amounts dissolved decrease significantly with rising temperature. Both isotherms deviate from linearity (Henry's law) in the pressure range examined.

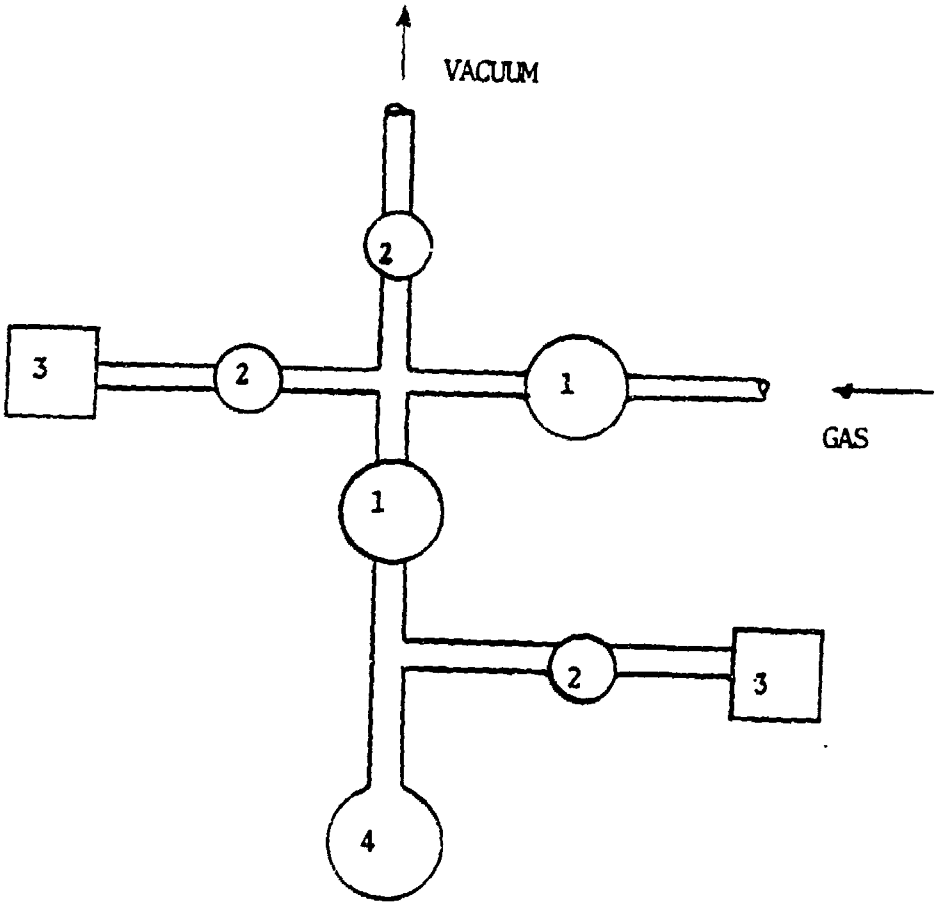

Figure 80. Schematic of the Gas Solubility Apparatus.
1. Whitey Stainless Steel Regulating Valve.
2. Whitey Stainless Steel Toggle Shut-Off Valve.
3. MKS Baratron Capacitance Manometer
4. Sample Chamber

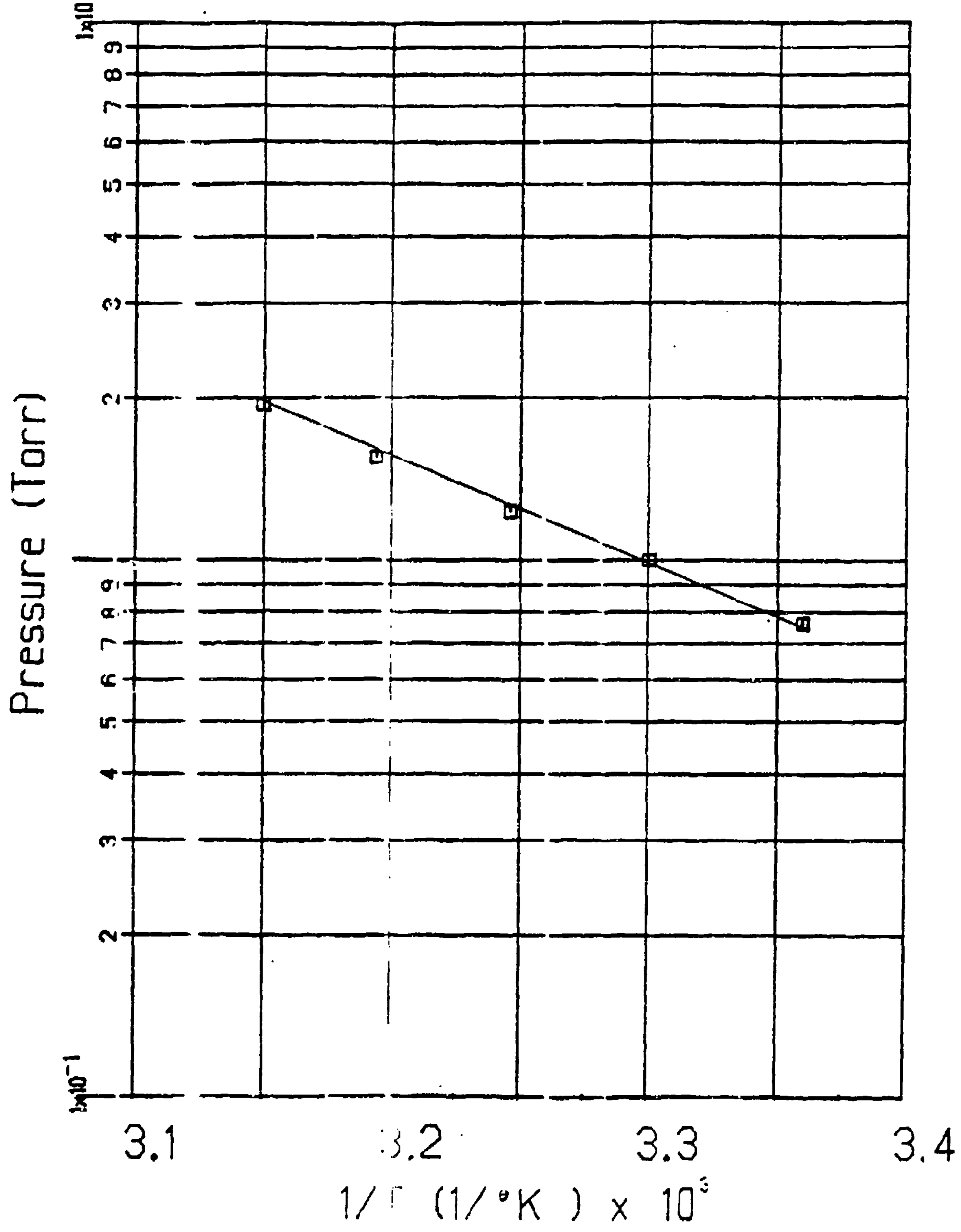

Figure 81. Clausius-Clapeyron Plot of the Variation of the Log of Vapor Pressure with Inverse Temperature for Tmp-Heptanoate.

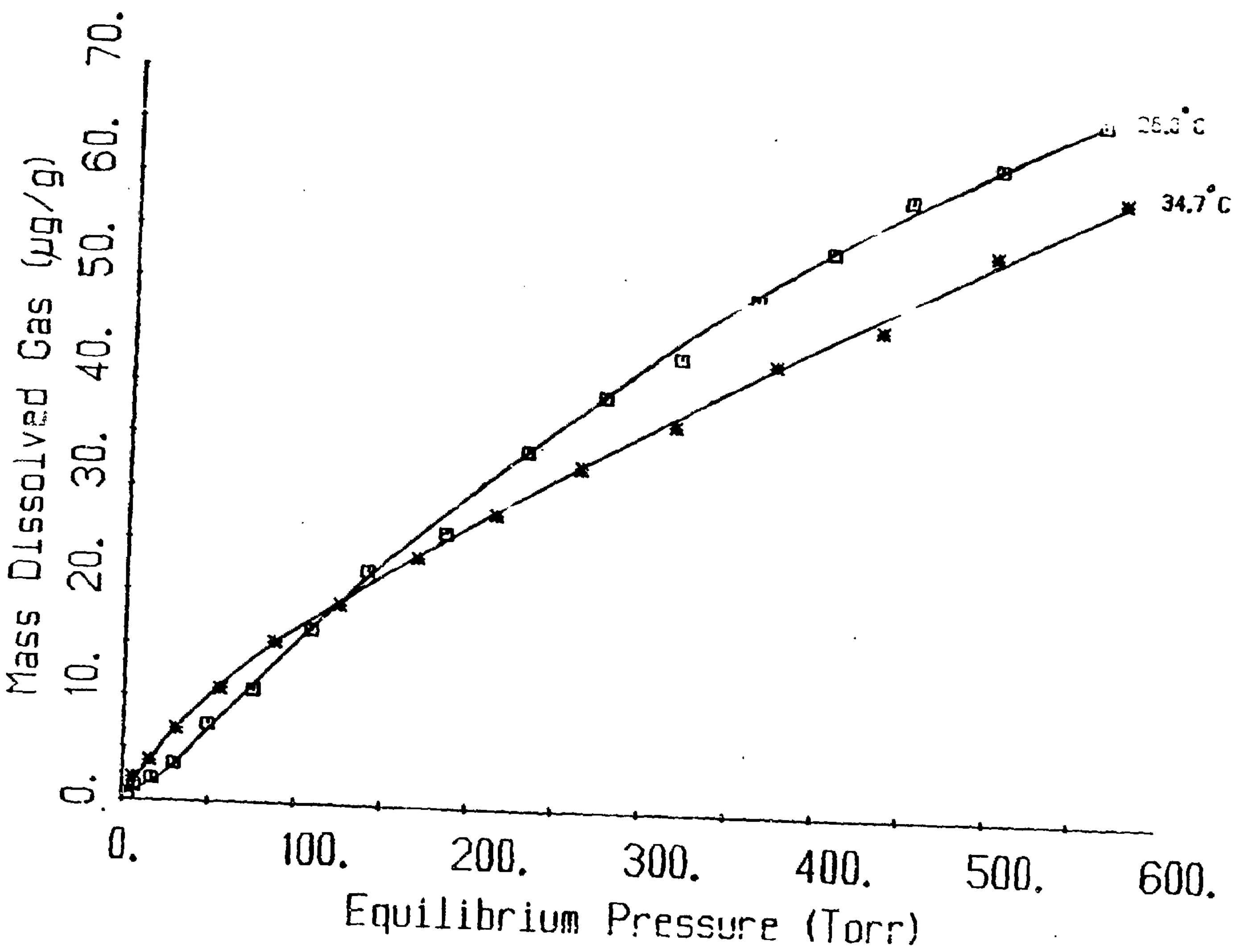

Figure 82. Solubility Isotherms of Nitrogen Gas in Tmp-Heptanoate.

4. Nitrogen and Oxygen Solubility Isotherms

The procedure previously reported was modified to obtain better reproducibility. The modifications are: (a) a more accurate measurement of the vapor pressure and more uniformity in the equilibration conditions; (b) to measure the vapor pressure, initial degassing for one hour was allowed, followed by an equilibration time of twenty-two hours; (c) the vapor pressure is taken as the average of two measurements, one at the start and the other at the end of the determination of the isotherm; and (d) the same equilibration period is allowed at each step, i.e., each change in gas pressure is followed by an equilibration time of twenty-two hours.

Figure 83 reports the isotherms at 35.1 ± 0.1°C for a solution of phenothiazine (4.20% w/w) in tmp-heptanoate, and for a solution of N-phenyl-1-naphthylamine (4.08% w/w) in tmp-heptanoate. The data show a significant increase in the volumes of gas dissolved in the solutions due to the presence of solute.

The modified procedure was used to determine the solubility isotherms at 35.1 ± 0.1°C of nitrogen gas in a solution of Aerosol OT (1.95% w/w) in tmp-heptanoate; and the oxygen-gas solubility in a solution of N-phenyl-1-methylamine in tmp-heptanoate. The results obtained are reported in Figure 84. That diagram shows:

a. Nitrogen gas is more soluble in the solution of Aerosol OT than in the solvent tmp-heptanoate.
b. The solubility isotherm of nitrogen in the Aerosol OT solution is linear.
c. The solubility isotherm of nitrogen in the Aerosol OT solution is very similar to that in the solution of N-phenyl-1-naphthylamine (4.08% w/w), both in tmp-heptanoate.
d. The solubility isotherm of oxygen in a solution of N-phenyl-1-naphthylamine (3.9% w/w) in tmp-heptanoate is much larger than that for nitrogen. Some chemical reaction between oxygen and the amine may contribute to the absorption of oxygen. Our intention in making this measurement was to find if the chemical reaction is pronounced, but the long times required to reach equilibrium show that the reaction with oxygen, if any, is neither rapid nor pronounced.

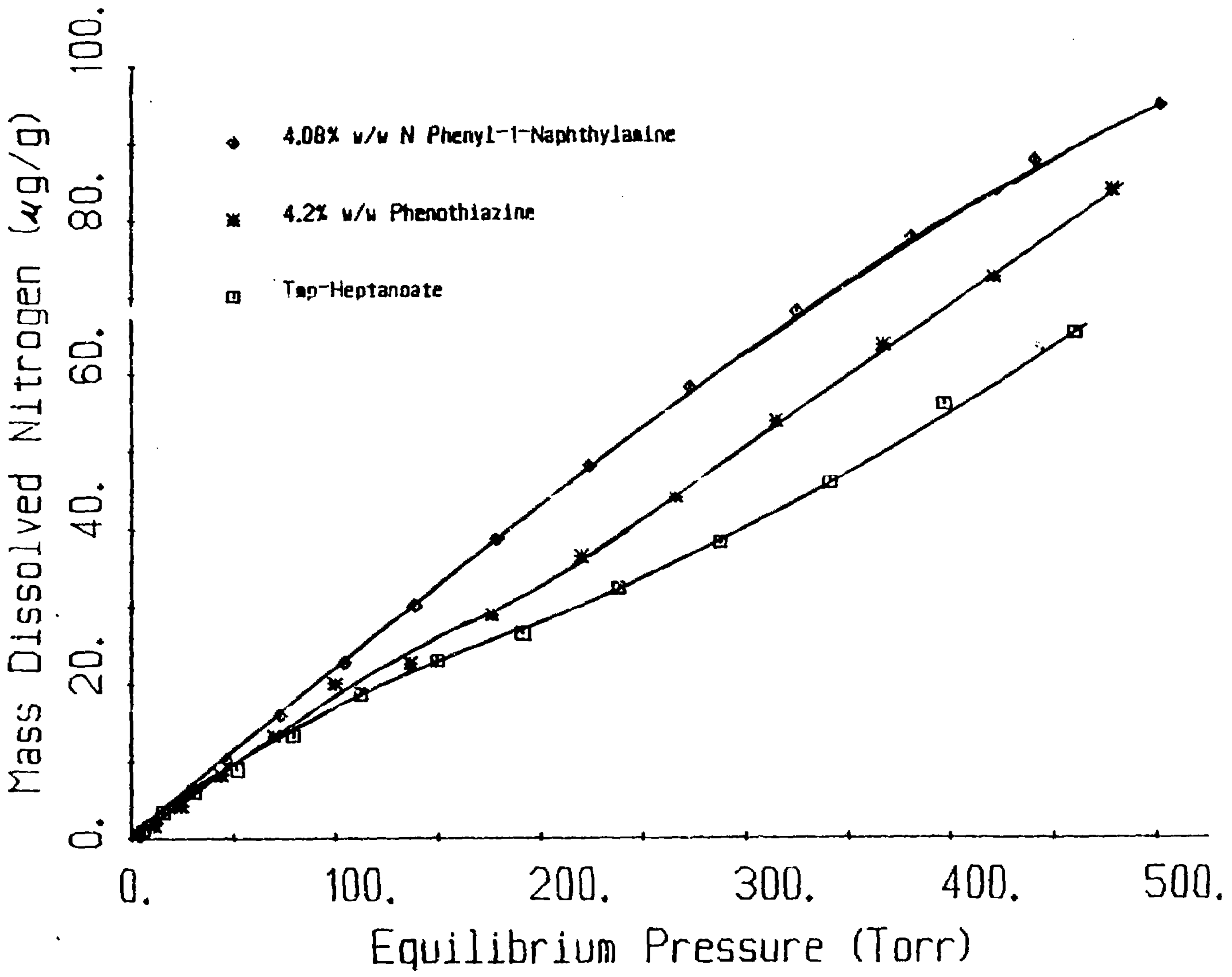

Figure 83. Solubility Isotherms of Nitrogen Gas in Tmp-Heptanoate and Solutions of Phenothiazine (4.20% w/w) and of N-Phenyl-1-Naphthylamine (4.08% w/w) in Tmp-Heptanoate at 35.1± 0.1°C.

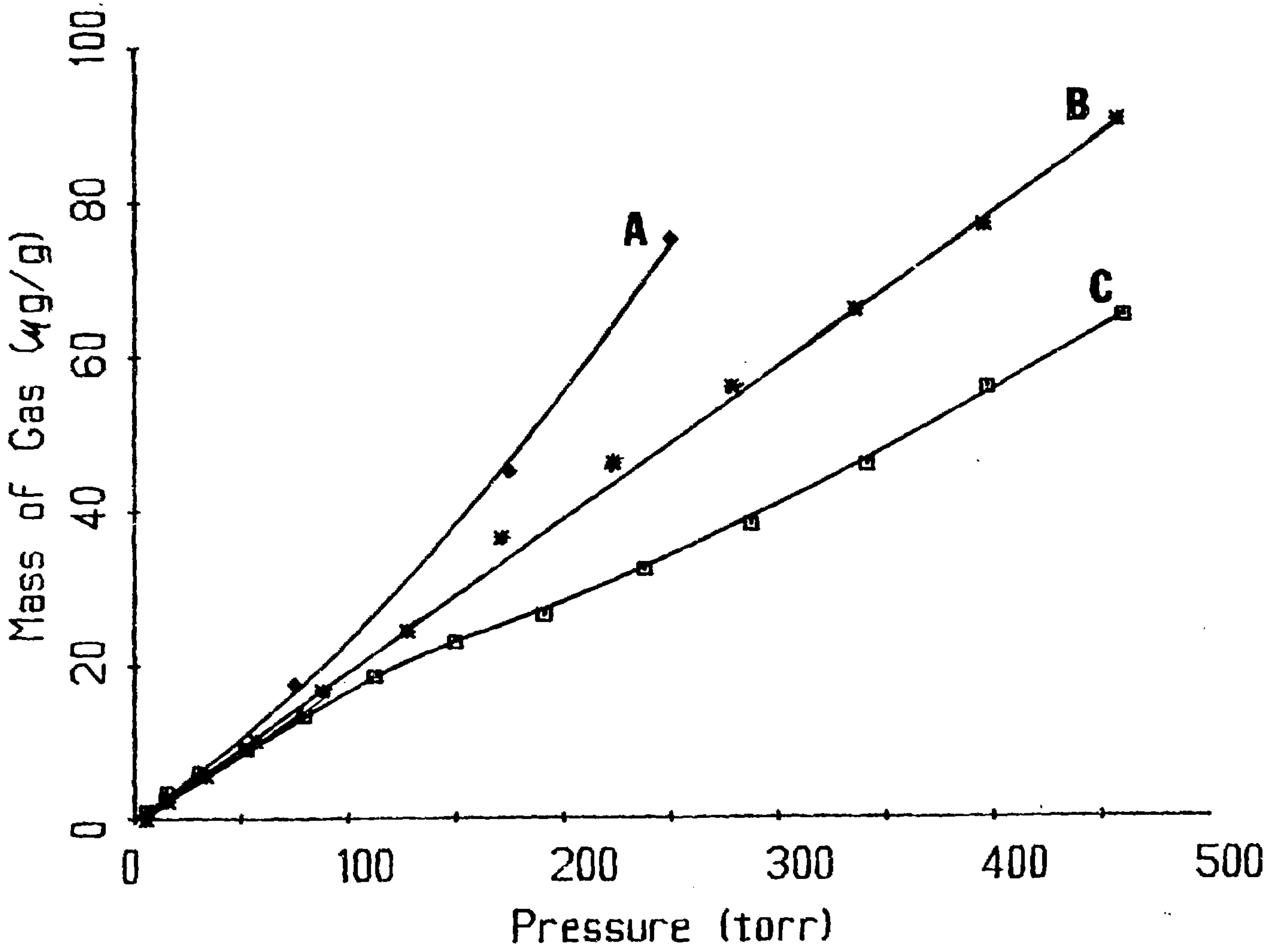

Figure 84. Gas-Solubility Isotherms at 35.1°C in Tmp-Heptanoate Solutions.
(A) Oxygen Gas in a 3.9% (w/w) Solution of N-Phenyl-1-Napthylamine in Tmp-Heptanoate.
(B) Nitrogen Gas in a 1.95% (w/w) Solution of Aerosol OT in Tmp-Heptanoate.
(C) Nitrogen Gas in Tmp-Heptanoate.

SECTION XI

ELECTRICAL PROPERTIES OF TMP-HEPTANOATE AND ITS SOLUTIONS

1. Electrical Conductivity

In connection with the possibility that electrical effects in lubricating oils may influence foam stabilities, we have measured the extremely low electrical conductivity of lubricating oils, with and without additives. The following Table reports our results for tmp-heptanoate and a few typical additives that might be present in a formulated lubricating oil (Table 14.)

Table 14. Specific Conductivity of Tmp-Heptanoate and its Solutions at 20°C.

Name of sample	Specific conductivity at 20°C in $\text{ohms}^{-1}\ \text{cm}^{-1} \times 10^{13}$
Solvent alone (tmp-heptanoate)	6.6
+ 0.2 % L5720 (Union Carbide Corporation)	9.5
+ 0.2 % L5303 (U.C.C.)	13.0
+ 0.2 % L6202 (U.C.C.)	81.0
+ 0.2 % L543 (U.C.C.)	15.0
+ 0.15% L540 (U.C.C.)	16.0
+ 0.14% silicone oil (50 cSt)	6.5
+ 0.14% polypropylene (Triol)	7.7
+ 0.15% polypropylene (Diol)	10.0
+ 0.17% carbon black	3.2
+ 1.0 % chloroform	9.0
+ 0.85% o-tritolyl phosphate	5.1
+ 0.77% phenyl naphthylamine	6.7
+ 1.0 % phenothiazine	230.0
+ 1.1 % dihydroxy anthraquinone	4.6
isooctane	0.008
JP-5	0.11

One of our objectives is to see if foaminess can be correlated with proton or electron transfer between species in the solution. So far we can say that changes in the electrical conductivity do not necessarily attend foaminess, but we are still to determine whether in some cases such changes act to augment foaminess.

The specific electrical conductivity in ohms^{-1} cm^{-1} was measured on a number of samples of oils, with and without additives, and both used and unused as lubricants in aircraft engines (Table 15.)

Table 15. Specific Conductivity of Used and Regenerated Lubricating Oils at 20°C.

Code number	Description (provided by H.A.Smith in letter of 9/11/81)	ohms^{-1} cm^{-1} X 10^{13}
L-1	Basestock Esters treated with 5% calcium hydroxide at 25°c	0.50
L-2	Basestock Esters treated with 2% wt. calcium hydroxide at 40°C.	5.11
L-3	Basestock Esters treated with 0.3% wt. calcium hydroxide at 40°C.	4.08
L-4	Basestock Esters treated with 0.3% wt. calcium hydroxide at 25°C	5.75
L-5	New Formulated Ester Lubricant	1.68
L-6	Used Lubricant MIL-L-23699	460
L-7	Used Lubricant MIL-L-23699	13.1
L-8	Used Lubricant MIL-L-23699	56.2
L-9	Used Lubricant MIL-L-7808	87.7
L-10	New MIL-L-7808	1.61
L-11	Basestock Esters prior to calcium hydroxide treatment	21.2

The results show that new and regenerated oils have lower electrical conductivities than used oils.

The experiments reported above were extended to temperatures in the vicinity of 26°C, and to a range of concentration of 0.5 to 2.0%(w/w) of additive, and to compositions of three components. The results obtained are reported in Table 16.

Table 16. Electrical Conductivities of Tmp-Heptanoate and Solutions of Additives in Tmp-Heptanoate

Solution	Concentration (%w/w)	Specific Conductivity x 10^{13} (mho-cm^{-1})	Temperature (°C)
Tmp-heptanoate fresh		9.2	25.6
		7.4	21.4
		5.9	19.3
N-Phenyl-1 naphthylamine in Tmp-heptanoate	2.00	39	25.7
	2.00	36	25.4
	1.54	36	26.3
	1.00	29	27.2
	0.51	22	26.8
Tricresyl phosphate in Tmp-heptanoate	2.01	12.8	27.2
	2.01	11.8	
	1.51	11.7	25.3
	1.00	10.0	25.3
	0.50	10.2	26.3
Phenothiazine in Tmp-heptanoate	2.01	2600	26.1
	2.01	2520	24.9
	1.51	2200	25.1
	1.00	1600	
	0.51	960	25.1
2.00% w/w N-Phenyl-1-naphthylamine + 2.00% w/w Tricresyl phosphate		39	25.1
2.00% w/w Phenothiazine + 2.00% w/w Tricresyl phosphate		3700	25.7

Table 16 shows:

a. The specific conductivity of tmp-heptanoate increases by 56% on raising the temperature from 19.3°C to 25.6°C.

b. A slight increase in specific conductivity is observed (25%) in solutions containing up to 2.0%(w/w) tricresyl phosphate. The specific conductivity is practically independent of concentration in the range 0.5 to 2%(w/w).

c. An increase in specific conductivity (by a factor of four) is obtained in solutions containing N-phenyl-1-naphthylamine up to 2.0%(w/w). The specific conductivity increases by 60% as the concentration is raised from 0.5%(w/w) to 2.0%(w/w).

d. An increase of specific conductivity by more than two orders of magnitude is observed with phenothiazine up to 2.0%(w/w). The specific conductivity increases by 270% as the concentration is raised from 0.5% (w/w) to 2.0%(w/w).

e. A synergistic increase of the specific conductivity is observed with mixtures of two solutes, phenothiazine plus tricresyl phosphate, each at 2.0%(w/w). This effect may parallel the synergism in the foam volumes observed for the same composition.

Further electrical conductivity measurements were made with a dipping conductivity cell, at room temperature. Table 17 reports the results obtained after twenty minutes of thermal equilibration. Results are reported as relative conductivity, i.e., the ratio of the conductivity of the solution being measured to that of the solvent (tmp-heptanoate) measured on the same day.

Table 17. Conductivities of Solutions of Additives in Tmp-Heptanoate at 20°C.

The Solutes	Relative Conductivity
TMP-Heptanoate (Solvent)	1
Benzotriazole (0.049% w/w)	1.32
Benzotriazole(0.049% w/w)	1.25
Benzotriazole (0.097% w/w)+ Tricresyl Phosphate (1.94% w/w)	1.56
Benzotriazole (0.12% w/w) + Tricresyl Phosphate (1.98% w/w) + Phenothiazine (.93% w/w)	76.4

2. Electrical Conductivity of Aerosol OT Solutions

The variation of electrical conductivity, measured as nano-amps at an applied potential of 1 kV, versus concentration of Aerosol OT (% w/w) at 23°C is reported in Figure 85. The data show a discontinuity at 0.14% w/w, which is interpreted as a critical micelle concentration (cmc.) The values of the conductivity for total concentrations larger than cmc in Figure 85 do not correspond to the actual concentration of micelles in the solution; if they did so the conductivity would be seen to increase manyfold on the advent of micelles in the system. This indication of the presence of conducting micelles is further circumstantial evidence for a mechanism of foam stabilization by electrostatic repulsion in these Aerosol OT solutions, which is confirmed by the measurement of surface potential (see Table 18 below.)

3. Surface Potentials

The theory of Derjaguin[13] that foam may be stabilized by charges of like sign on opposite sides of the liquid lamellae, requires us to address that question for oils susceptible to foam formation. Although measurements of electrical conductivity give

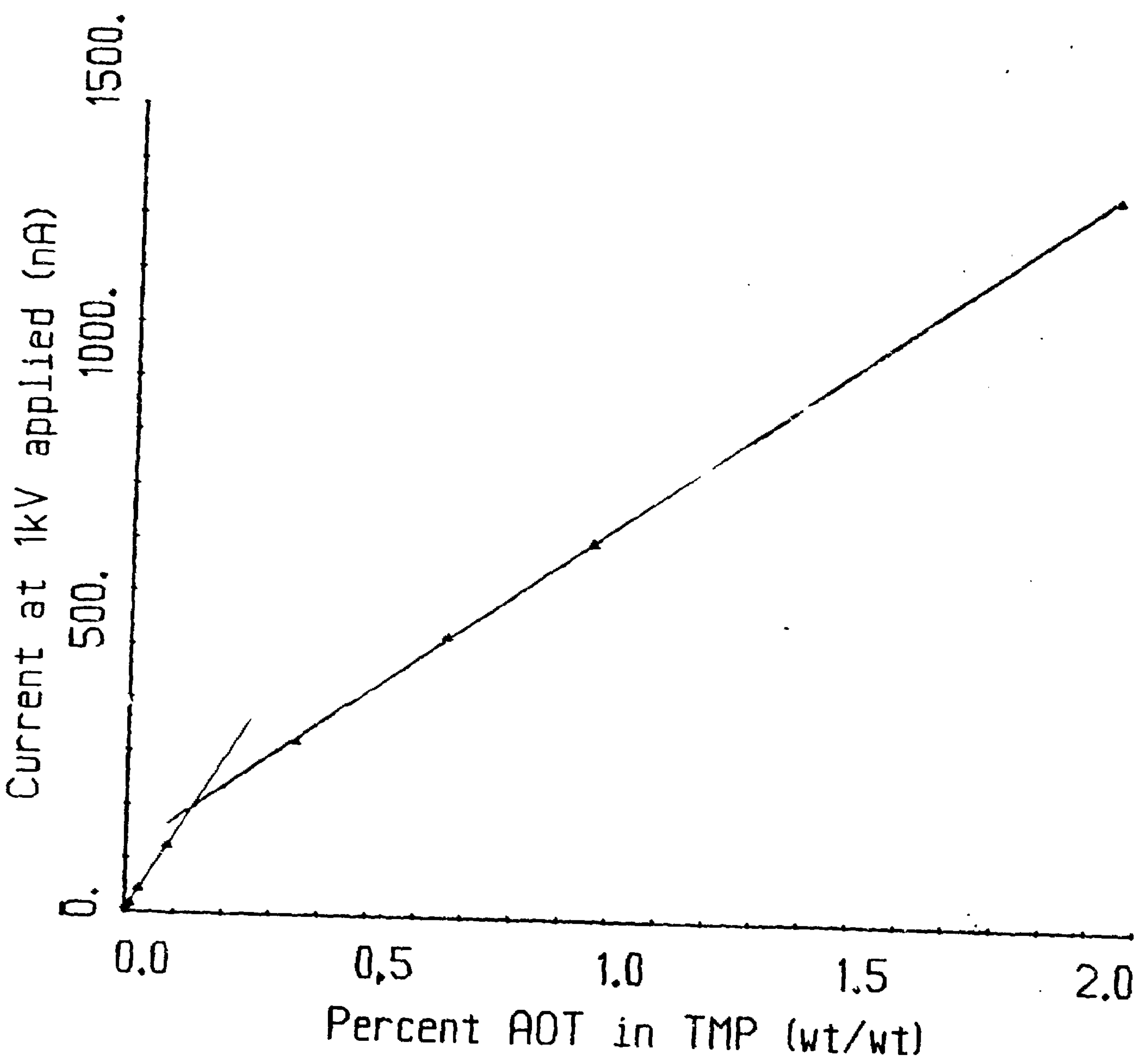

Figure 85. Variation with Concentration of Solute of the Electrical Conductivity of Solutions of Aerosol OT in Tmp-Heptanoate at 23°C.

general information about charge separation in the liquid, they do not give direct evidence of the presence or absence of adsorbed electrical double layers at the liquid surfaces. The measurement of the Volta (or surface) potential change that occurs when a charged solute segregates at the surface of the solution gives a definitive answer to this question.

The functional-block diagram for the apparatus (Figure 86) shows the components necessary for detecting surface charges or electrical fields. The sine-wave generator produces an electrical signal with an amplitude of approximately 200mV RMS. This signal is amplified and is used to drive the electro-mechanical transducer. This transducer is an audio loudspeaker. The loudspeaker has, attached to its cone, a glass rod that supports a gold plated electrode with a surface area of 12 cm^2. The surface of the solution under test is adjusted by means of an optical positioner so that the distance between the surface of the solution and the surface of the electrode is always kept constant at approximately 2mm. The gold electrode is connected to a series of high gain instrumentation amplifiers that function to magnify the small currents produced in the electrode when the apparatus is used. The output of these amplifiers is then compared with the original signal produced by the sine wave generator.

The loudspeaker vibrates the electrode in the vertical direction so as to change the spacing between the solution surface and the electrode. If a surface charge exists on the solution, or if an electric field is present in the gap, a current will arise due to the time variance of the capacity between the electrode and the surface. This current can be expressed as:

$$i = \frac{[V - E]\omega C_1 R}{\sqrt{1 + [\omega C R]^2}} \text{Sin}(\omega t) \qquad [5]$$

where E is the electric field within the gap, C_1 is the capacity between the electrode and surface when the plate is not vibrating, C is the difference in capacity between the steady state capacity and the capacity at the point when the electrode has been vibrated to the point furthest away from the solution surface, R is the input impedance of the instrumentation amplifier and is the frequency of vibration.

If a difference in electrostatic potential exists between the two plates of the condenser, a current will flow in an external circuit when one plate is moved with respect to the other. A high-gain amplifier is used to detect the alternating signal generated when the plate vibrates. The electric field produced by oriented dipoles at the surface of the liquid can be detected by the vibrating-plate technique, and its magnitude determined by cancelling the dipole field with an applied field. The field is imposed by means of a voltage applied to an inert metal electrode inside the bulk phase of the solution being measured. The field observed as the surface potential depends on this applied voltage; and if the metal electrode is grounded, reproducible values of the

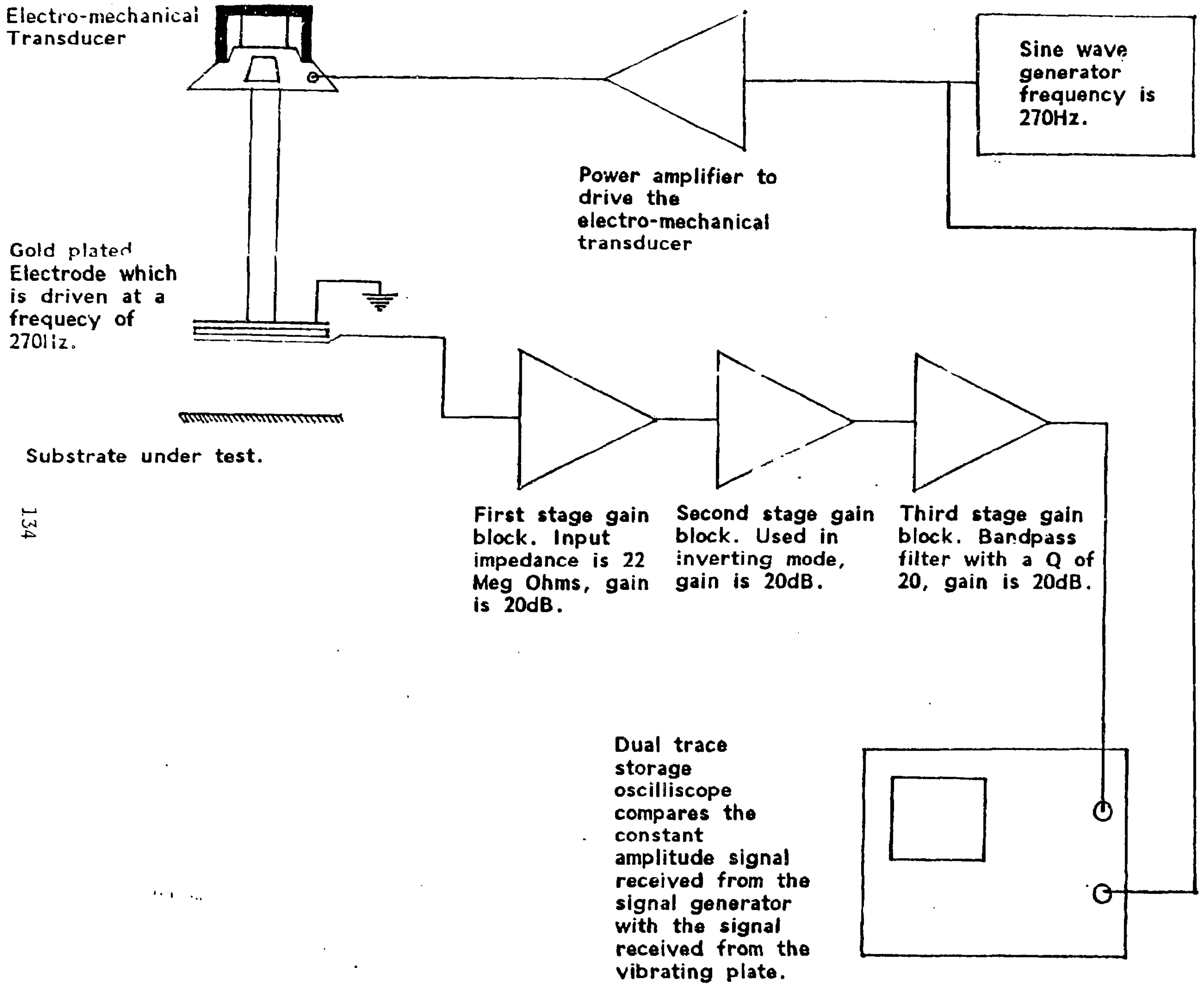

Figure 86. Schematics of the Surface Potential Apparatus.

surface potential are obtained. By disconnecting the electrode and allowing the surface potential to drift to an equilibrium voltage, a potential different from the grounded potential is obtained. The difference between the two potentials in volts divided by the voltage difference for the corresponding solvent, gives a pure number, R, that reflects the relative orientation and presence of charged species at the surface. Values close to unity denote small electrical effects at the surface; the larger the value the greater these effects. Table 18 reports values for several solutions in tmp-heptanoate, showing appreciable electrical effects for the solutes phenothiazine and Aerosol OT.

Table 18. Relative Surface Potentials of Solutes in Tmp-Heptanoate.

Solution	Concentration	R
N-Phenyl-1-Naphthylamine	2.02 (%w/w)	0.97
Polydimethylsiloxane (1000 cSt)	1.34 ppm	1.14
Phenothiazine	2.01 (%w/w)	1.73
Aerosol OT	2.54 (%w/w)	2.95

4. Electrical Properties of Single Bubbles

Two platinum electrodes were fused into the upper and lower ends of a glass tube, 70 cm in length & 26 mm internal diameter; the same tube used to measure the rate of ascent of bubbles, see Section XIV below. A potential difference of 20 kV between electrodes 58 cm apart was applied to a column of the Aerosol OT solution (2.04% w/w) in tmp-heptanoate. If the bubbles carry a net charge, their rate of ascent would be increased or decreased according to the polarity of the applied potential field. The rates of ascent were measured and showed no change with the polarity of the field; but calculations, assuming a zeta potential of 100 mv at the surface of the bubble and a bubble diameter of 1 mm, show that the expected change of velocity is less than the experimental error of the measurement. The experiment ought to be repeated with a larger potential gradient.

SECTION XII

EFFECTS OF AGING

1. Effects of Aging on Foaminess of Tmp-Heptanoate Solutions

To find out if thermal treatments have an effect on the ester's chemical stability and foam quality, the ester was treated in three consecutive cycles as follows: Each cycle consisted of a 30 minute heating at 80°C, followed by 30 minutes of bubbling nitrogen gas at 1 liter/minute at 80°C, followed by 60 minutes of cooling at room temperature. Two solutions of 1000 cSt polydimethylsiloxane in the aged ester were tested at various temperatures and compared to solutions of the same concentrations, prepared with fresh tmp-heptanoate. Figures 87 and 88 show the results obtained for solutions of 119 ppm and 200 ppm respectively, with the fresh (A) and the aged (B) esters as solvents. The results illustrate a significant reduction of foam volume with the aged tmp-heptanoate.

Further investigation of the possible effect of aging on the foaminess of solutions in tmp-heptanoate was carried out with certain additives as solutes. N-phenyl-1-naphthylamine (1% w/w) and tricresyl phosphate (3.03% w/w) combined together in solution were prepared in fresh and in aged tmp-heptanoate. In Figure 89 the smooth curve shows the average of two duplicate measurements of solutions made up in fresh tmp-heptanoate; and the open circles show similar measurements of solutions prepared with aged tmp-heptanoate. The same concentrations were used in both solvents; the aging process is as described above. Figure 89 reports large deviations between duplicate samples, therefore a definitive conclusion about the effect of aging of the solvent is not forthcoming from these data.

2. Changes of Physical Properties of Tmp-Heptanoate on Exposure to Room Atmosphere

We suspect the occurrence of changes in bulk and surface properties of tmp-heptanoate as a result of its being exposed to room-atmosphere conditions, i.e., 25°C and 50-70% relative humidity. The kinematic viscosities (by Ostwald viscosimeter) of unexposed tmp-heptanoate and of tmp-heptanoate exposed for twenty-four hours to room atmosphere, in a glass dish of diameter 95 mm containing a sample of 150 ml, were compared. The comparisons also included a series of solutions of polydimethylsiloxane (1000 centiStokes) in tmp-heptanoate, which were exposed to the room atmosphere for at least fourteen days, and were unequally handled. The results of the viscosity measurements are reported in Figure 90, which demonstrates that:

a. The bulk viscosity of tmp-heptanoate is significantly reduced after protracted times of exposure;

b. The viscosity *versus* temperature curves of the various solutions of polydimethylsiloxane (1000 centiStokes) in tmp-heptanoate, curves C to G in Figure 90, do not correlate with the concentration of solute, but rather reflect variations in

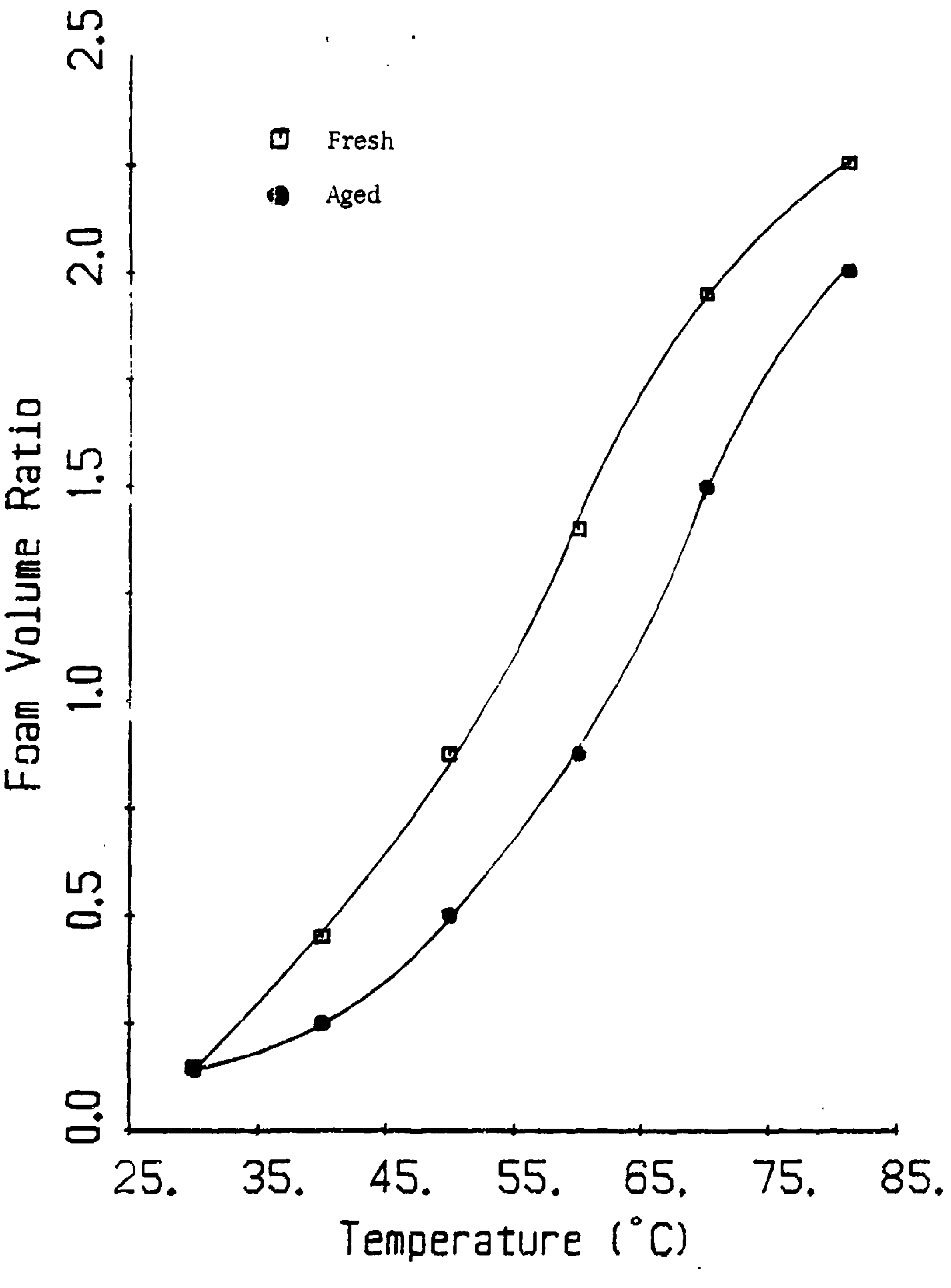

Figure 87. Foam Volume Ratio of Solutions of Polydimethylsiloxane (1000 cSt) in Fresh and Aged Tmp-Heptanoate. Concentrations of both Solutions are 119 ppm.

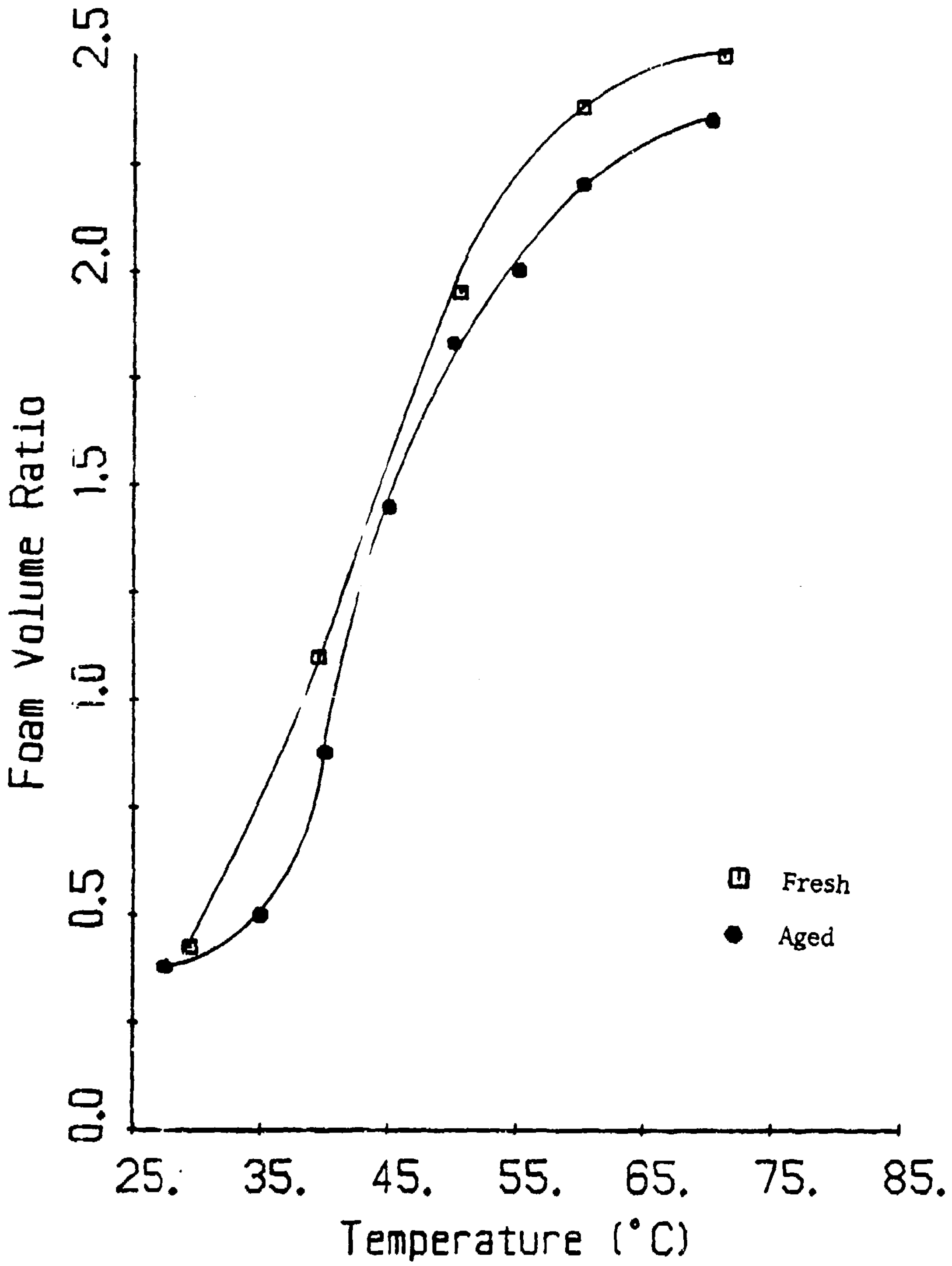

Figure 88. Foam Volume Ratio of Solutions of Polydimethylsiloxane (1000 cSt) in Fresh and Aged Tmp-Heptanoate. Concentrations are 193 ppm and 201 ppm Respectively.

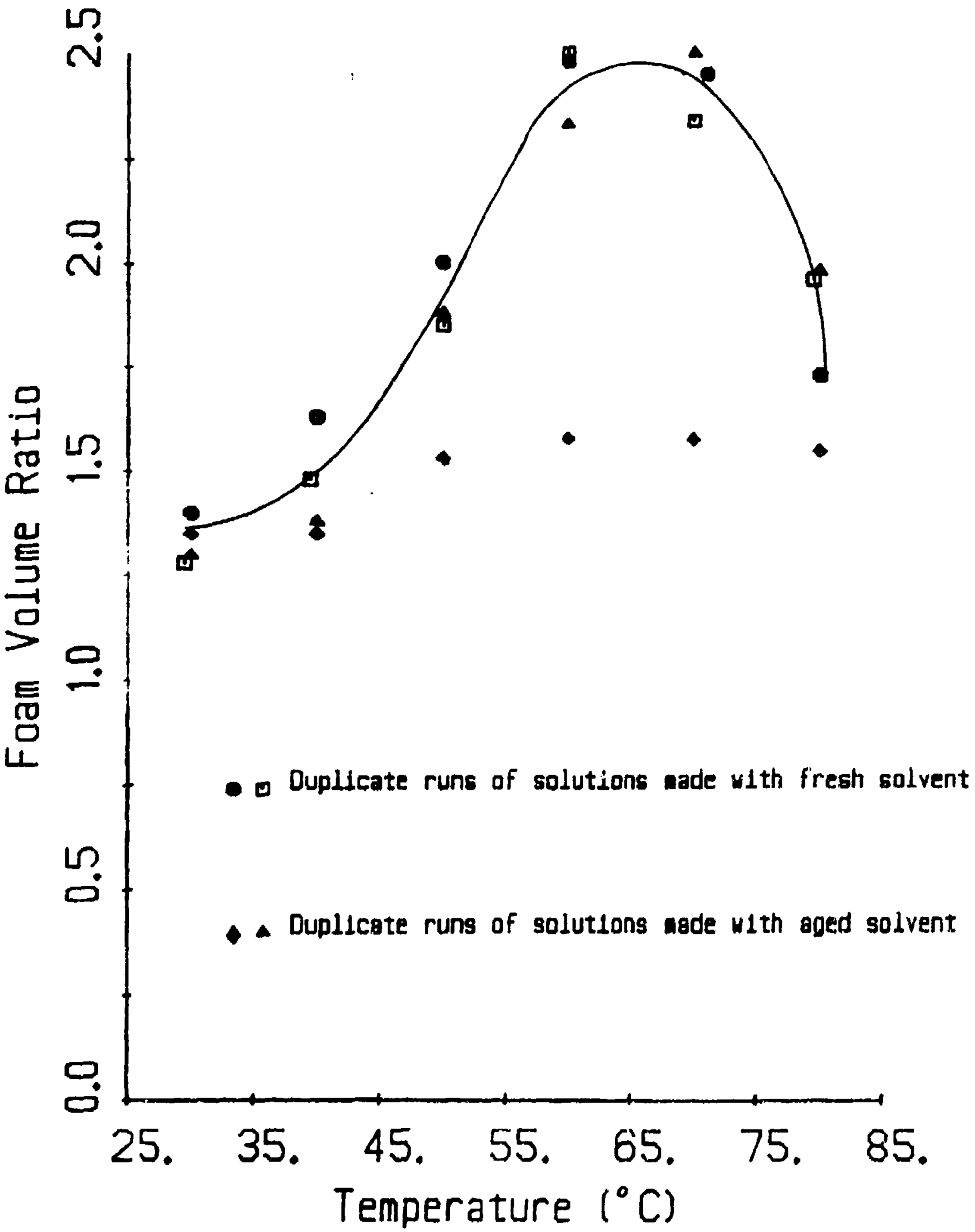

Figure 89. Foam Volume Ratio of Solutions Containing both N-Phenyl-1-Naphthylamine (1.00% w/w) and Tricresyl Phosphate (3.03% w/w) in Fresh and Aged Tmp-Heptanoate.

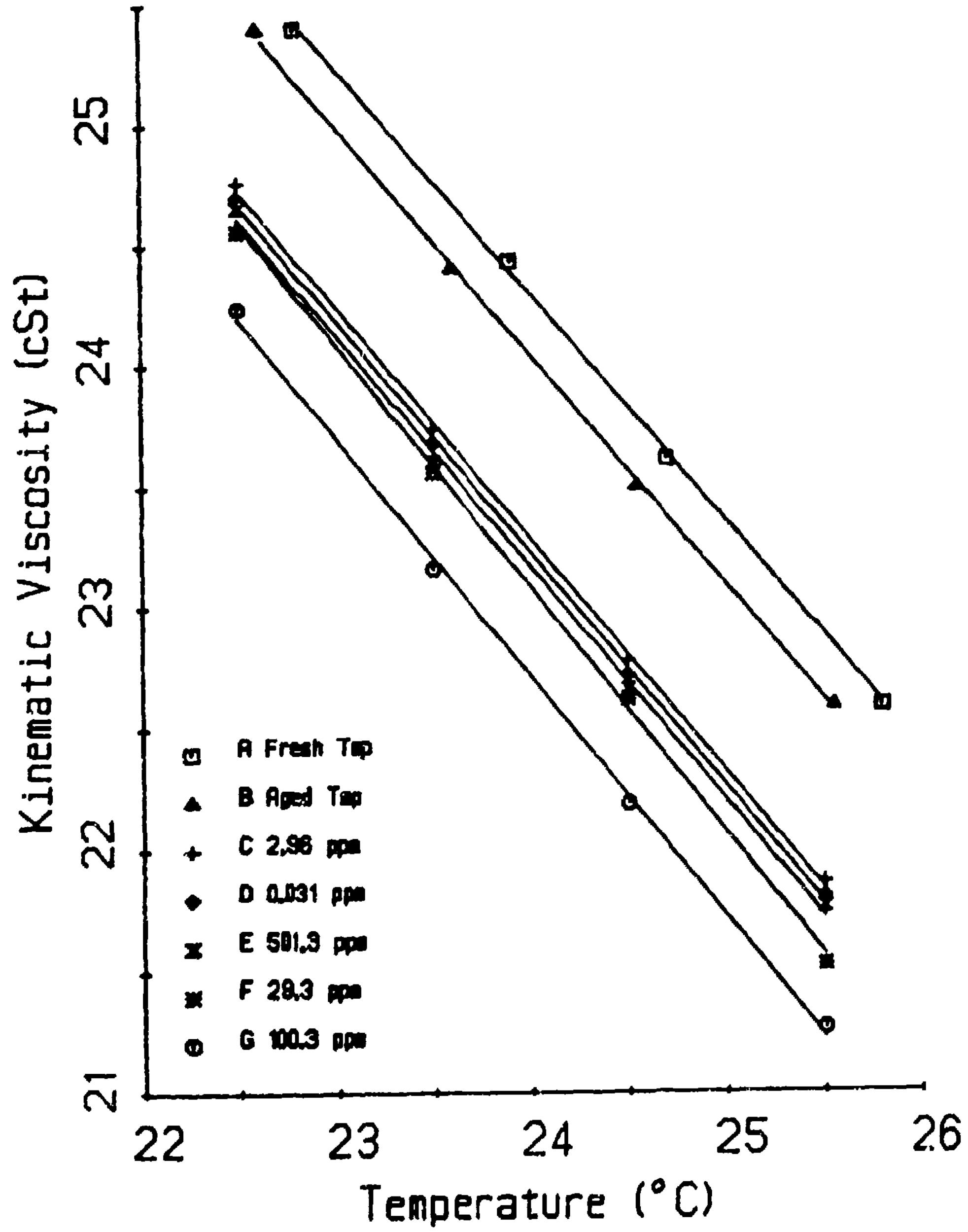

Figure 90. Kinematic Viscosity <u>versus</u> Temperature of Tmp-Heptanoate (Freshly Exposed A; after Twenty-Four Hours Exposure B) and of Various Solutions of Polydimethylsiloxane (1000 cSt) in Tmp-Heptanoate, after Various Handling and Exposure Time of at least Fourteen Days.

handling and exposure time.

c. A reduction of 6.5% in bulk viscosity is to be expected as a result of a period of exposure of fourteen days.

Electrical conductivity measurements also show a slight change as a result of exposure to room atmosphere and with variation in handling procedure. The specific conductivities of unexposed tmp-heptanoate, of tmp-heptanoate exposed for a period of three days, with and without stirring prior to the measurement, are reported in Table 19.

Table 19. Conductivity of Tmp-Heptanoate after Different Handling at Room Atmosphere

Treatment	Conductivity x 10^{13} (mho-cm^{-1})	Temperature (°C)
Tmp-hepatanoate fresh	9.2	25.6
Tmp-heptanoate exposed 3 days	11.2	24.8
Tmp-heptanoate exposed 3 days and stirred	12.5	25.7

Figure 91 illustrates the results obtained in identical experiments carried out with solutions of phenothiazine (1% w/w) and tricresyl phosphate (3.06% w/w) combined together in fresh (smooth curve) and aged (open circles) tmp-heptanoate. As before, the deviations of duplicate runs are too large to allow us to draw a definitive conclusion about the possible effect of aging of the solvent. So far, pronounced indications of aging effects have been found with silicone solutions only.

3. Possible Effects of Aging of Solutions on their Properties

In tests reported previously, an aging of the solution was carried out, and its effects investigated by comparing the properties of solutions prepared from fresh and from aged tmp-heptanoate. A more realistic way to investigate the chemical stability of the lubricant is to perform the aging process with the various additives present initially in the solvent tmp-heptanoate.

A solution of 2.0%(w/w) phenothiazine plus 2.0%(w/w) tricresyl phosphate was thermally treated as described in Section XII.1. Foam volumes at 40°C, 60°C, and 80°C; surface viscosities and electrical conductivities at room temperature, were measured and compared to those of the fresh solution of the same content. The results are summarized in Table 20 below.

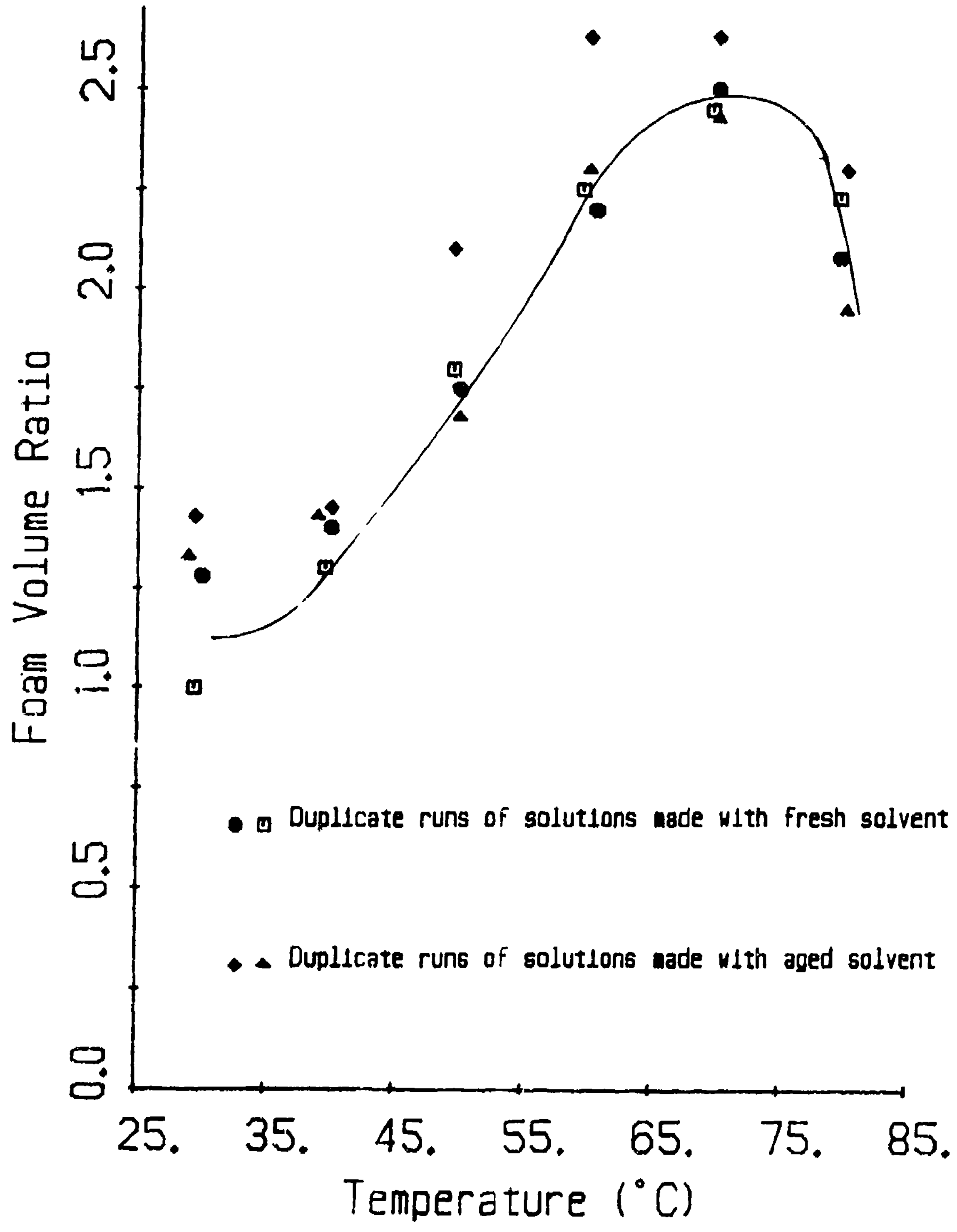

Figure 91. Foam Volume Ratio of Solutions Containing both Phenothiazine (1.00% w/w) and Tricresyl Phosphate (3.03% w/w) in Fresh and Aged Tmp-Heptanoate.

Table 20. Effect of Aging on Foam Volume, Surface Viscosity and Electrical Conductivity.

	Foam		Surface Viscosity (slope)	Relative Electrical Conductivity
	Temp (°C)	Volume (cm^3)		
Fresh Solution	40.0 60.5 79.3	365 455 480	0.122	94.3
Aged Solution	39.6 60.6 79.3	410 475 460	0.122	62.6

Table 20 shows only minor differences between the fresh and aged solutions, the only exception being the 34% reduction of electrical conductivity with aging.

We have investigated the effects of the aging of the solvent upon the properties of the solutions (foaminess, electrical conductivity, surface viscosity) of various additives in tmp-heptanoate. We have also reported the effects of aging of a <u>solution</u> (phenothiazine + tricresyl phosphate in tmp-heptanoate) upon its properties. Following are the results of the tests carried out with an additional solution, 2.01% (w/w) <u>N</u>-phenyl-1-naphthylamine <u>plus</u> 2.01% (w/w) tricresyl phosphate, that was thermally treated (as described in Section XII.1.) Foam volumes at 40°C, 60°C, and 80°C, and surface viscosities at room temperature, were measured and compared to those of the fresh solution of the same composition and concentration in Table 21.

Table 21. Effect of Aging on Foam Volume and Surface Viscosity

	Foam		Surface Viscosity (slope)
	Temp (°C)	Volume (cm^3)	
Fresh Solution	39.8 60.3 80.1	345 515 435	0.110
Aged Solution	39.8 60.8 80.0	410 500 435	0.110

Table 21 shows that no significant changes take place in the properties of the solution tested, which is the same result we obtained with other aged solutions of additives in tmp-heptanoate.

4. Foaminess of Solutions of Phenothiazine in Tmp-Heptanoate after Aeration with Dry or Moist Air

During some measurements with solutions of phenothiazine in tmp-heptanoate, a variation of the surface tension was noticed that depends on how long the solution is exposed to the atmosphere. A change of surface tension indicates a possible effect on the foaminess of the solution, which therefore has to be investigated. Chemical changes that could have taken place on exposure to atmosphere are oxidation of phenothiazine, or absorption of water vapor. Two series of experiments were made.

a. A solution of phenothiazine, 2.98% w/w, in tmp-heptanoate was tested for foaminess after 150 liters of dry air had been bubbled through it at a rate of 1.0 liters/minute, at a temperature of 40°C.

b. A solution of the same concentration was tested for foaminess after bubbling through it the same volume of moist air at the same temperature. To prevent any loss of water content, the second series of foam measurements was done with moist air, of the same humidity as used for pre-aeration, instead of with dry nitrogen gas.

Table 22 shows the volume ratio obtained at four temperatures, for the two series of solutions. The results show a slight increase of the volume ratios for the solution treated with dry air; but because of the poor reproducibility of these tests, this point is to be further investigated.

Table 22. Volume Ratios of 2.98% (w/w) Phenothiazine Solutions after Bubbling with Dry and Moist Air.

Temp. (°C)	Volume Ratios		
	Original Solution	After Bubbling Dry Air	After Bubbling Moist Air
25.	0.225; 0.300	0.439	0.324
40.	0.400; 0.625	0.732	0.324
60.	1.225; 1.500	1.390	1.486
80.	1.200; 1.200	1.415	0.973

5. The Effect of Water Content on Foaminess of Solutions

Foaminess increases with temperature in some of the solutions that we have investigated, e.g., polydimethylsiloxane (1000 cSt) in mineral oil, polydimethylsiloxane (1000 cSt) in tmp-heptanoate, phenothiazine in tmp-heptanoate. An explanation that has been suggested[25] for such an effect is that the presence of water in the surface film reduces its cohesion, so that an increase of temperature, by driving off water, gives a stronger surface film, which increases the foaminess. We have tested this hypothesis by measuring the foaminess and the surface viscosities of three samples of mineral oil:

a. mineral oil as received;
b. mineral oil containing 500 ppm water;
c. mineral oil dried by bubbling 150 liters of dry nitrogen gas at a rate of one liter per minute through 200 ml of oil.

Foam volumes were measured by Test Method 3213. With sample (b) we used clean, humid air instead of dry nitrogen gas to avoid reducing the water content of the oil. Surface viscosities were measured with the oscillating-disc viscosimeter, with a flow of dry nitrogen gas maintained across the surface. The surface viscosity is reported as the slope of the straight line that relates the amplitude ratio to the swing number.

Table 23 shows the results obtained. We observed no reduction of the foaminess with the presence of water, as the hypothesis postulated; nor did the surface viscosity show a clear trend of being reduced by water content, at either of the two temperatures. At least for this solution, therefore, the hypothesis is not confirmed.

Table 23. Foam Volumes and Surface Viscosities of Mineral Oil Samples Containing Various Amounts of Water

	Mineral Oil + 500 ppm Water		Mineral Oil		Dried Mineral Oil	
	Foam Volume (cm^3)	Surface Viscosity (Slope)	Foam Volume (cm^3)	Surface Viscosity (Slope)	Foam Volume (cm^3)	Surface Viscosity (Slope)
25°C	375	0.29	385	0.29	300	0.33
40°C	425	---	440	---	475	---
50°C	>550	0.093	>550	0.097	>550	0.097

SECTION XIII

EFFECT OF VESSEL SHAPE ON FOAM FLOODING

1. Introduction

The term foam flooding signifies the carriage of liquid by means of foam into spaces intended for the passage or reception of gas or vapor. Of common occurrence, foam flooding is a problem in the chemical industries, the food industries, and the pulp and paper industry. The formation of foam in these applications is most frequently controlled by adding chemical foam inhibitors, such as silicone polymers, which promote the coalescence of bubbles and consequent separation of the gas from the liquid. But this mode of solving the problem may not be desirable, either because of the expense or because of subsequent harmful effects introduced by the foam inhibitor. The problem may sometimes be solved by redesigning the internal geometry of the vessel in which foam is generated, either to provide more space for a head of foam, or, preferably, to so alter conditions at key points that foam production is reduced. Any guiding principle toward this end is valuable knowledge. Recently an attempt to improve standard tests for measuring foam introduced a concept of foam decay that directs attention to the possible influence of vessel shape on the build up of foam.

A dynamic foam is one that has reached a state of dynamic equilibrium between rates of formation and decay. A static foam is one in which the rate of foam formation is zero; the foam once formed is allowed to collapse without regeneration by further agitation or input of gas. The typical measurement of a dynamic foam is the volume of foam at equilibrium; the typical measurement of a static foam is the rate of foam collapse. Dynamic-foam measurement is applicable to evanescent or transient foams, such as these of the present work; static-foam measurement is applicable to foams of high stability such as are generated from solutions of detergents or proteins.

Standard methods of measuring dynamic foam stability, generate and contain the foam in a cylindrical vessel. Watkins[22] postulated a model of foam decay that explains why a cylindrical container, or indeed any container with a cross-sectional area invariant with height, may be a poor design for such an instrument. He showed that the substitution of a conical shape would, at least, avoid the disadvantage he had pointed out pertaining to the cylinder. The postulates of Watkins' foam model have not been tested. Such a test of the hypothesis is of more than academic interest, because foam problems in industry are almost all associated with cylindrical vessels; so that exploring the implications of such a shape is a worth-while undertaking. This is especially true when the conclusion based on the tenets of the hypothesis condemns that shape completely, as conducive to foam flooding.

We present here an experimental test of Watkins' hypothesis, in which foam is generated under precisely the same conditions in both cylindrical and conical vessels. The predictions afforded by the theory are not corroborated in detail, but two main conclusions of the utmost practical importance are confirmed, namely, the positive influence of the shape of the vessel on foam flooding and the propensity toward flooding of cylindrical vessels in particular.

2. Two Theories of Dynamic Foams

Watkins proved by statistical analysis and experimentation that foam-measuring devices using cylindrical containers for foam are intrinsically prone to a lack of reproducibility, casting doubt on the quantitative aspects of these methods. By assuming that the gas loss from a foam is a function of the exposed top area of the foam and some intrinsic property of the liquid, the following equations were developed with respect to a vessel of any shape:

Let the surface of the exposed top area of the foam = A_f;

The gas injection rate (ml/minute) = $\dot{V}$;

The foam volume (cm^3) = V_f.

Watkins assumed that the rate of gas loss from the foam's surface in ml/minute is directly proportional to A_f, i.e., equal to kA_f. In a dynamic foam at equilibrium, the rate at which gas, on emerging from the diffuser, is converted into foam equals the rate of loss of gas out of the foam at its top surface. Therefore:

$$\dot{V} = kA_f . \qquad [6]$$

Equation [6] makes clear the disadvantage of the cylindrical shape. $\dot{V}$ and k are constants set before the start of the test, and if the vessel is a cylinder then A_f is also fixed. Three conditions are then possible:

a. If $\dot{V} > kA_f$, then V_f increases to infinity.

b. If $\dot{V} = kA_f$, then V_f is constant;

c. If $\dot{V} < kA_f$, then V_f reduces to zero.

This analysis points out a fundamental weakness of cylindrical containers used as part of a foam-measuring device, namely, that they will give values that are too high or too low depending on a fine balance of properties. In some practical instances, using a method[19] that requires a cylindrical vessel (AFAPL-TR-75-91,) this conclusion is supported. We have observed the volume of foam in a cylinder, measured at a constant rate of injection of gas, jump abruptly with concentration of solute from zero to a value beyond the capacity of the instrument. That result seems to be in accord with Watkins' analysis. But it is not always so: Bikerman's method[26], which requires a cylindrical vessel, has been in use for several years and, though often unsatisfactory, is not always so. We must therefore take into account that the k in equation [6] may not remain constant at all rates of injection of gas.

Equation [6] suggests that the cylindrical device is unsound as the source of a quantitative measurement of foaminess, because of the inflexibility of the parameters $\dot{V}$ and A_f. To overcome this disadvantage, one of the constants has to vary with foam height. The area available for foam breakdown, A_f, may be increased in a regular way with foam height by providing a cone-shaped container for the foam.

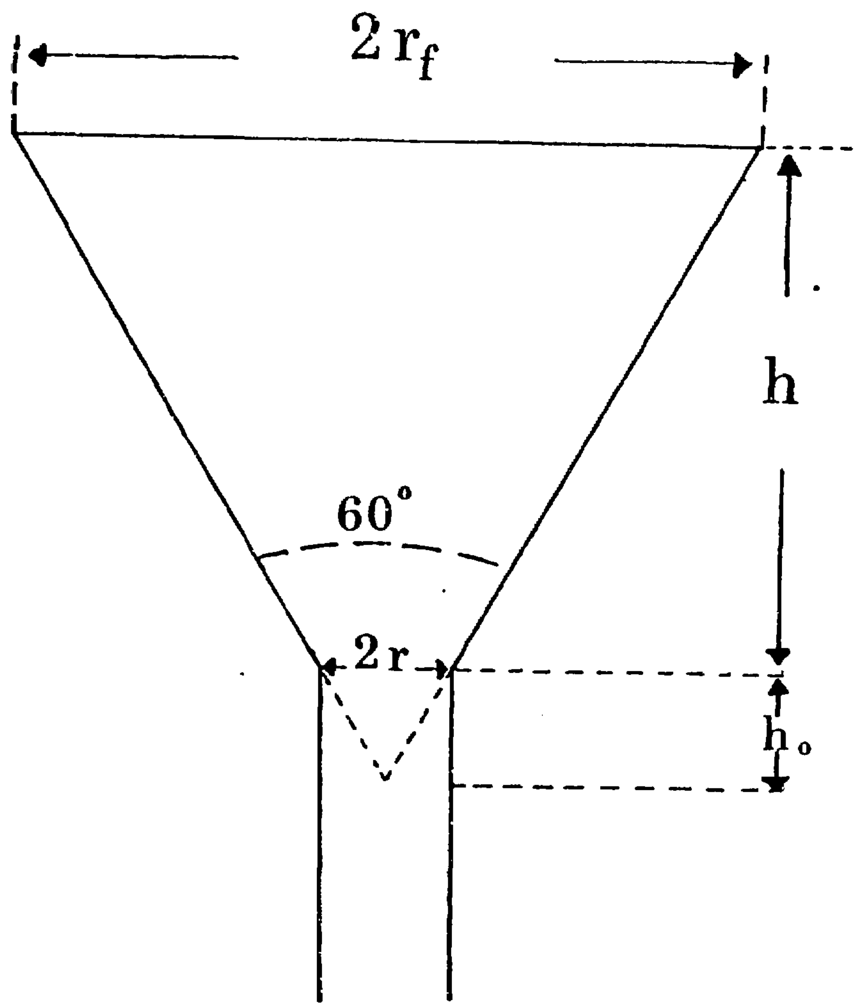

Figure 92. Principlas of Conical Foam Meter.

As illustrated in Figure 92, for a 60° cone,

$$A_f = 1.047\ (h_f + 1.732\ r)^2. \qquad [7]$$

where r is the radius at the base of the truncated cone. At equilibrium:

$$\dot{V} = kA_f = 1.047\ k\ (h_f + 1.732\ r)^2 \qquad [8]$$

Therefore, for a given solution and a fixed gas-injection rate the foam height is constant. Let the rate of gas injection be raised and the foam height increases, k remaining constant; 1/k (cm^2 foam surface per cm^3 sec^{-1} of gas flow) equals the maximum area of foam/air interface attained by a given solution at a rate of gas injection of 1 cm^3 sec^{-1}. The value of k is, nevertheless, NOT a characteristic property of the solution to be taken as a measure of its "innate foaminess." As we have seen such a concept leaves out of account the properties of the foam itself, which vary with the means used to generate it.

If the foregoing analysis is correct, this theory of the dynamics of foam cannot be reconciled with that of Bikerman, who disregarded the possibility that vessel geometry might affect the stability of the foam contained therein. Using a cylindrical vessel, Bikerman believed he had established a characteristic unit of foaminess of a solution, designated Σ , which equals the average lifetime of a bubble. But, if Watkins is correct, cylinders of different cross sectional area would endow the same solution with different values of Σ , and so negate its claim to be a characteristic property of a solution. Indeed Watkins' postulates, when applied to a cylindrical container, deny the proportionality of V_f to $\dot{V}$, and so would even deprive the Bikerman method of its mode of evaluating Σ as the ratio $V_f / \dot{V}$. To resolve the question, Watkins' postulates are best tested by investigating foams in conical containers rather than by the less direct and less certain route of measuring the possibly unattainable Σ in cylindrical vessels. The present Section is directed to that end. Its implications pertain less to the production of an improved foam meter than to a highly practical question of foam control; for we have observed that the volume of foam arising from a given amount of liquid, under fixed conditions of temperature and gas flow, is affected by the shape of the container. A container with vertical sides lacks an essential feature to facilitate release of the gas from the foam; whereas if the sides are flared so that the top surface of the foam expands in area as the volume of foam increases, the release of gas from the foam is promoted. This deduction from the theoretical analysis, which we find to be borne out, should have a significant bearing on the design of distillation and fractionation towers in the chemical industries, of kettles in the food industries, and of digesters in the pulp and paper industry. These possibilities depend on whether the assumptions underlying the theoretical model are valid. The model has hitherto lacked experimental confirmation, which we now provide.

3. Design of the Conical Foam-Meter

The conical foam meter was constructed from a large Pyrex filtering funnel with a bowl at a 60° angle and a top diameter of 150mm (Fisher Scientific Co., Catalog No. 10-373B,) fused to a cylinder 20 mm in diameter, 55 mm long, which has a fritted glass disc of coarse-grade porosity (Lab Glass, Inc., Catalog LG-8675, Coarse code -152) attached to its lower end. The function of the fritted glass is to disperse the injected nitrogen into bubbles of small diameter (< 1 mm). To the upper part of the funnel is connected a glass pipe fitted with a flange, on which a flanged cap may be seated. The cap is pierced with two tubular openings, one of which is for attachment of a gas flowmeter and the other, which remains closed during operation of the instrument, is a convenience port for inserting additional liquid to maintain the liquid/foam interface at the datum level, i.e., the level where the cylinder is attached to the cone. (See Figure 93.)

Essential to the instrument are a controlled flow of dry nitrogen gas and a thermostat bath able to maintain a constant temperature to within 0.2°C. The nitrogen, from a cylinder of the compressed gas at a regulated pressure, is preheated by passing through a copper coil inside the thermostat bath before passing through the liquid sample. A soap-film flowmeter measures the flow rates of gas output from the top of the foam. The foam meter is situated inside the thermostat bath. The flow rate of the gas is set at approximately 10 ml/minute, to prevent the liquid sample, when added, from leaking downwards through the fritted-glass diffuser. The liquid sample is then added through the convenience port up to the predetermined mark. When thermal equilibrium is reached, the flow rate is regulated and the corresponding foam height noted. The procedure is repeated for various flow rates and temperatures for each liquid sample under investigation.

4. Tests of Watkins' Postulates

Our first test of Watkins' theory is to find the relation between the rate of injection of nitrogen gas and the exposed area of foam-air interface at equilibrium. These measurements were made on a white mineral oil, which as purchased was found to possess foaminess and so did not require further solute to be added. The observed relations are reported in Figure 94 for temperatures of 22.5°C, 40.2°C, and 58.0°C. The curves do not pass through the origin but have a common point of intersection on the y-axis at an area of interface equal to 3.7 cm^2, which is quite reasonable as the cone in use is truncated where it is connected to the cylindrical base: there is, therefore, a real area of interface , namely, the liquid surface, even at zero flow of injected gas. The value of 3.7 cm^2 is a little larger than the area of the cylinder at its junction with the cone, which is 3.14 cm^2, but there cannot be any doubt that that area is the physical significance of the intersection point shown on Figure 94. The three curves shown in the diagram are all linear at flow rates less than 14.3 ml/minute. At larger flow rates the linearity no longer obtains; but under

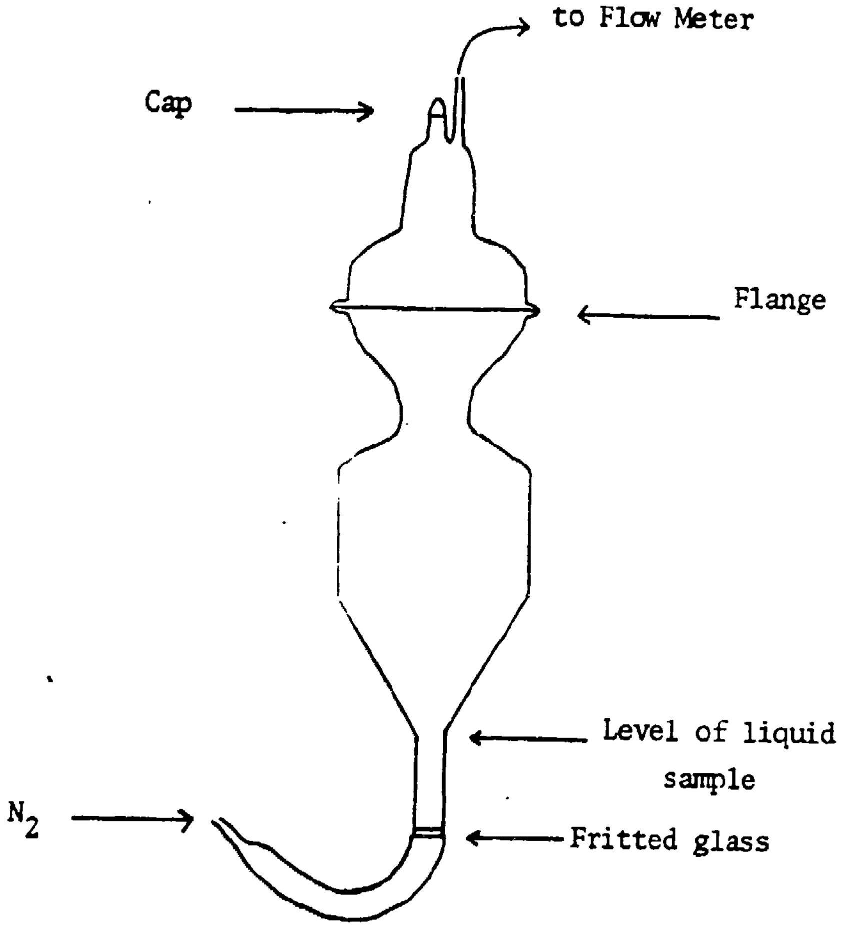

Figure 93. Conical Foam-Measuring Device.

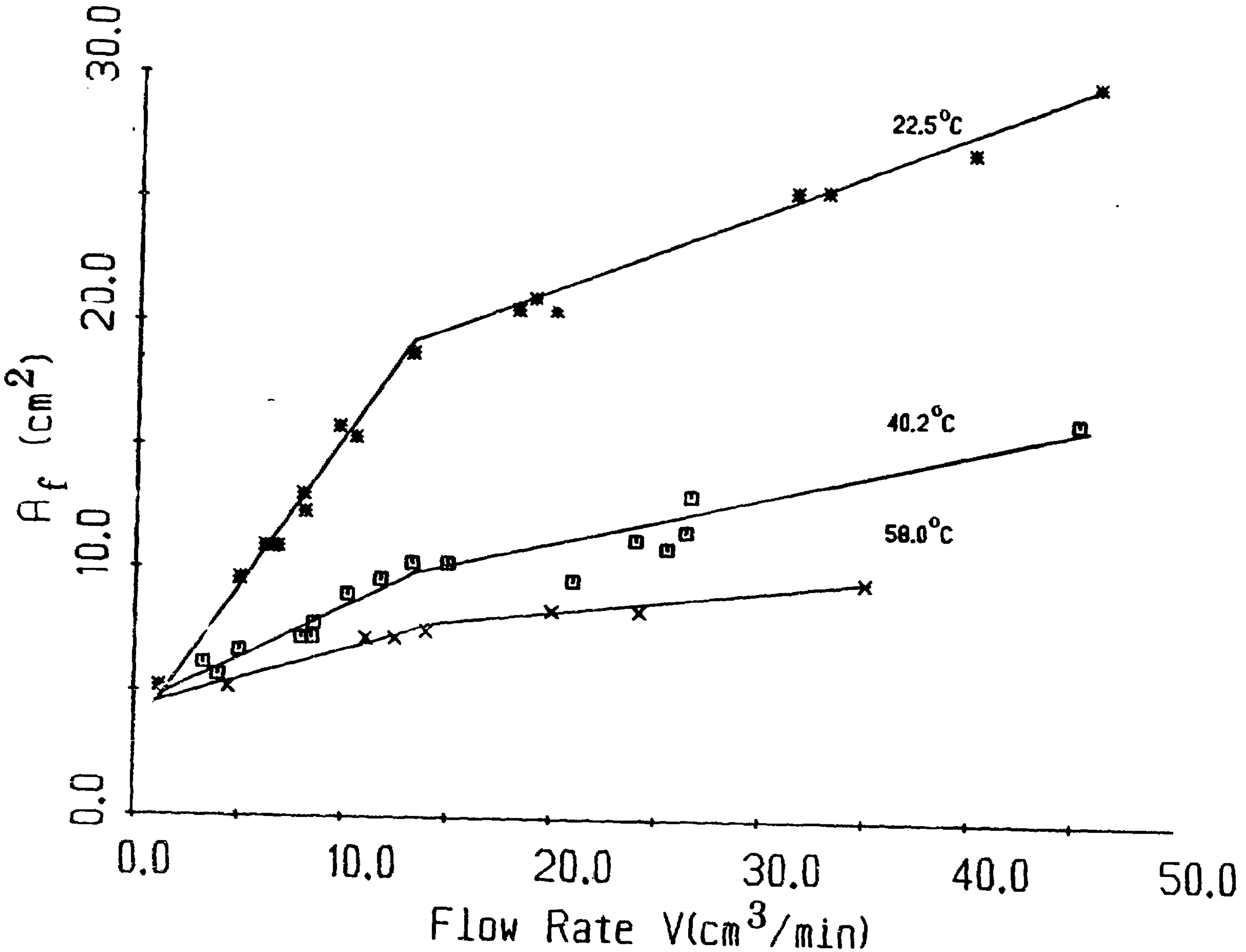

Figure 94. Areas of Foam/Air Interface at Equilibrium for Various Rates of Gas Injection in *Watkins' Type Foam Meter* (Figure 97A) for Mineral Oil (as is) at Three Different Temperatures.

Figure 95. Two Conical Foam Containers showing the Same Equilibrium Area of Foam/Air Interface.
Solute: Span 20 Solvent: Mineral Oil
Concn.: 601.2 ppm Temp.: 22.5°C
Volume flow rate: 20cm^3/minute
Linear flow rate: 0.106 cm/second

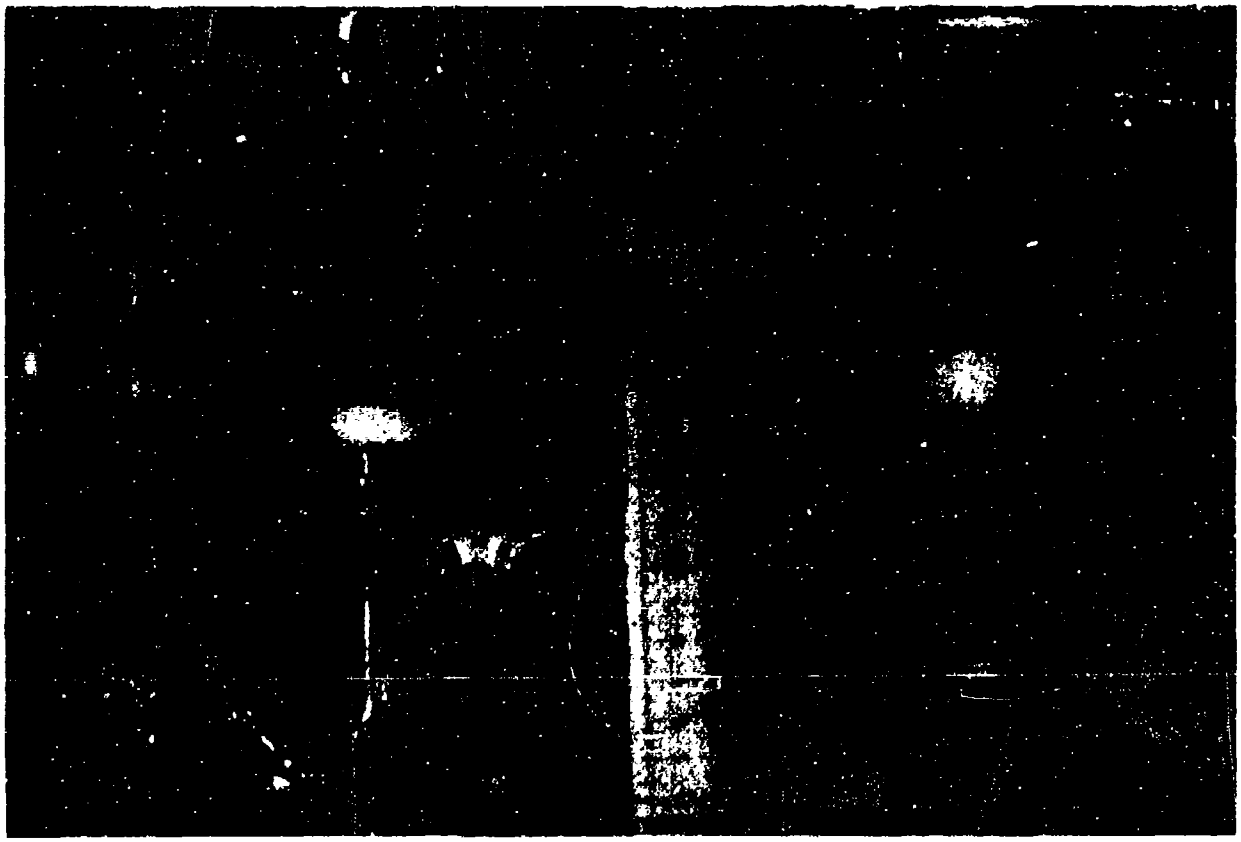

Figure 96. Two Conical Foam Containers showing the Same Equilibrium Area of Foam/Air Interface.
Solute: Span 20 Solvent: Mineral Oil
Concen.: 601.2 ppm Temp.: 22.5°C
Volume flow rate: 26.4 cm^3/minute
Linear flow rate: 0.140 cm/second

these conditions of increased pressure behind the fritted disc, smaller pores that are sealed at lower pressures begin to transmit gas and so change the size distribution of the pores creating the foam. A similar series of tests, with similar results, were undertaken by Gibson and McElroy[27], using various hydrocarbon lubricating oils as liquid samples.

Another test of Watkins' theory is shown in Figures 95 and 96. Each of these photographs shows two conical containers of different angles, 60° and 40°, equipped with similar glass-fritted discs, containing the same solution, and turned into foam by the same gas at the same rate of gas injection. The foam produced reaches its equilibrium volume at the same area of foam-air interface in each case. Figure 95 shows the comparison made at a relatively low rate of gas injection; Figure 96 shows the comparison at a higher rate. Both photographs confirm the prediction based on Watkins' postulates, inasmuch as the foam reaches dynamic equilibrium when it attains an area of exposed surface that is the same in each cone.

5. The Effect of Vessel Shape on Volume of Foam Produced

According to Watkins' theory, equilibrium conditions of rate of foam production equal to rate of foam disappearance can be obtained in a cylindrical vessel only for the unique case where $\dot{V} = kA_f$, where $\dot{V}$ = rate of gas flow, A_f = area of the exposed top surface of the foam, and k is a proportionality constant characteristic of the solution and of the foam. If $\dot{V} > kA_f$, then the column will flood; if $\dot{V} < kA_f$, no volume of foam occurs. In a cone-shaped vessel, in which A increases with the height of foam in the vessel, an equilibrium height of foam may be obtained.

The theory suggests a simple principle that may be useful to control volume of foam produced in any vessel, merely by paying attention to its shape. The results predicted by the theory were tested with two sets of containers of different diameter, each set comprised of a straight cylinder and of a conical container with a cone angle of 60°. The first set (Figure 97) has a tube diameter of 20mm and the second set (Figure 98) has a tube diameter of 46 mm. Both the cylindrical and conical containers of the smaller set were made from the same glass tubing and have identical sintered disks sealed inside. With respect to the larger set, the diameter of 46mm corresponds to the specification for AFAPL-TR-75-91,[19] and was made by sealing a cone to a standard graduated cylinder. The gas is dispersed by means of a porous ball; and the tests were made with one vessel at a time, using the same gas disperser.

Comparison measurements were made with a solution of Span 20 (601.2 ppm) in mineral oil, and with a solution of phenothiazine (3.92% w/w) in tmp-heptanoate. The experimental conditions and numerical results in terms of Phase-Volume Ratio (PVR) are reported in Table 24, and in a series of photographs, Figures 99 to 102.

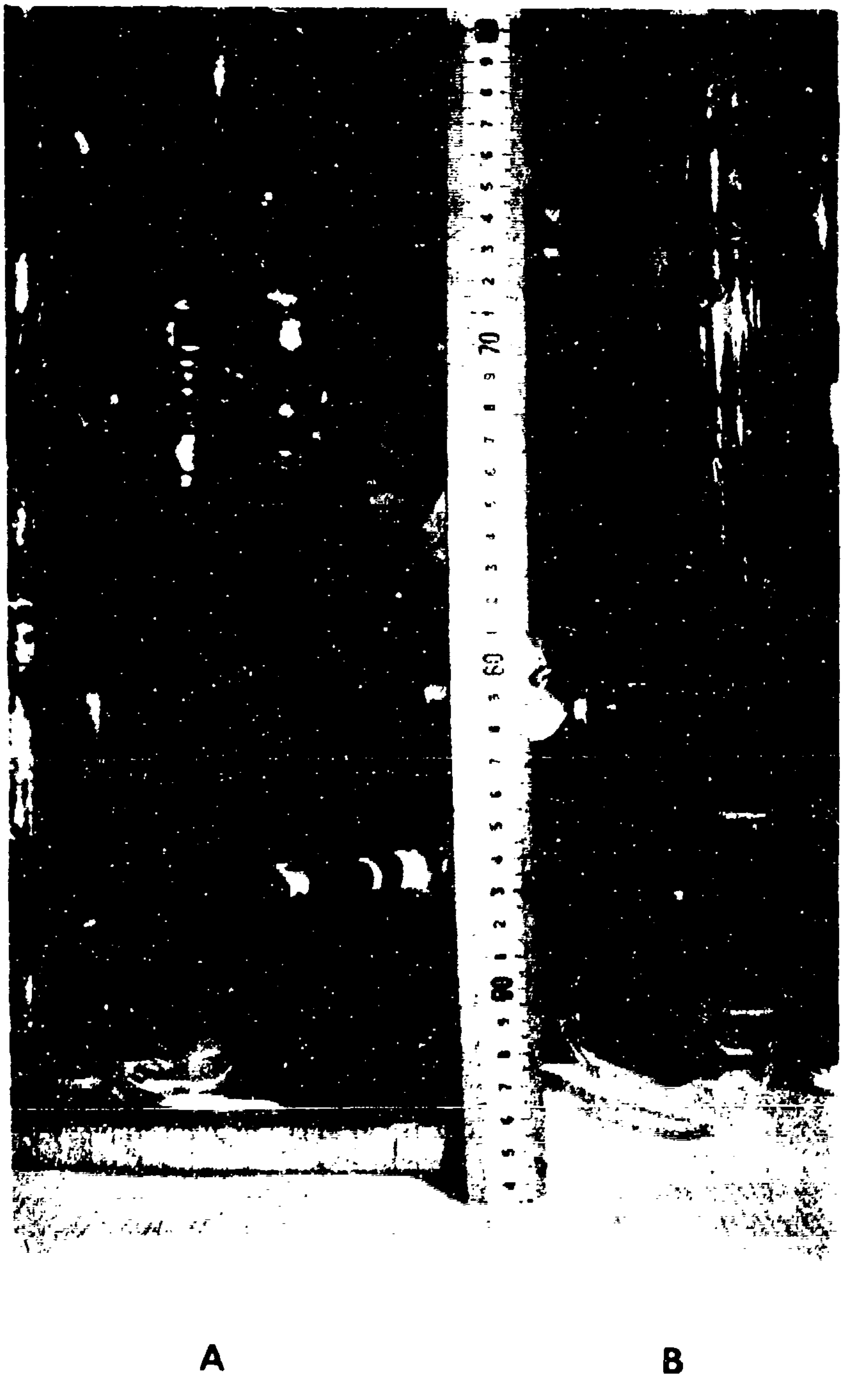

Figure 97. Two Foam Containers of the Same Diameter (20 mm), with the Same Height of Solution (63 mm) in Each, Fitted with a Glass Frit of the same Porosity. A has a 60° Cone Attached; B is a Continuous Cylinder.

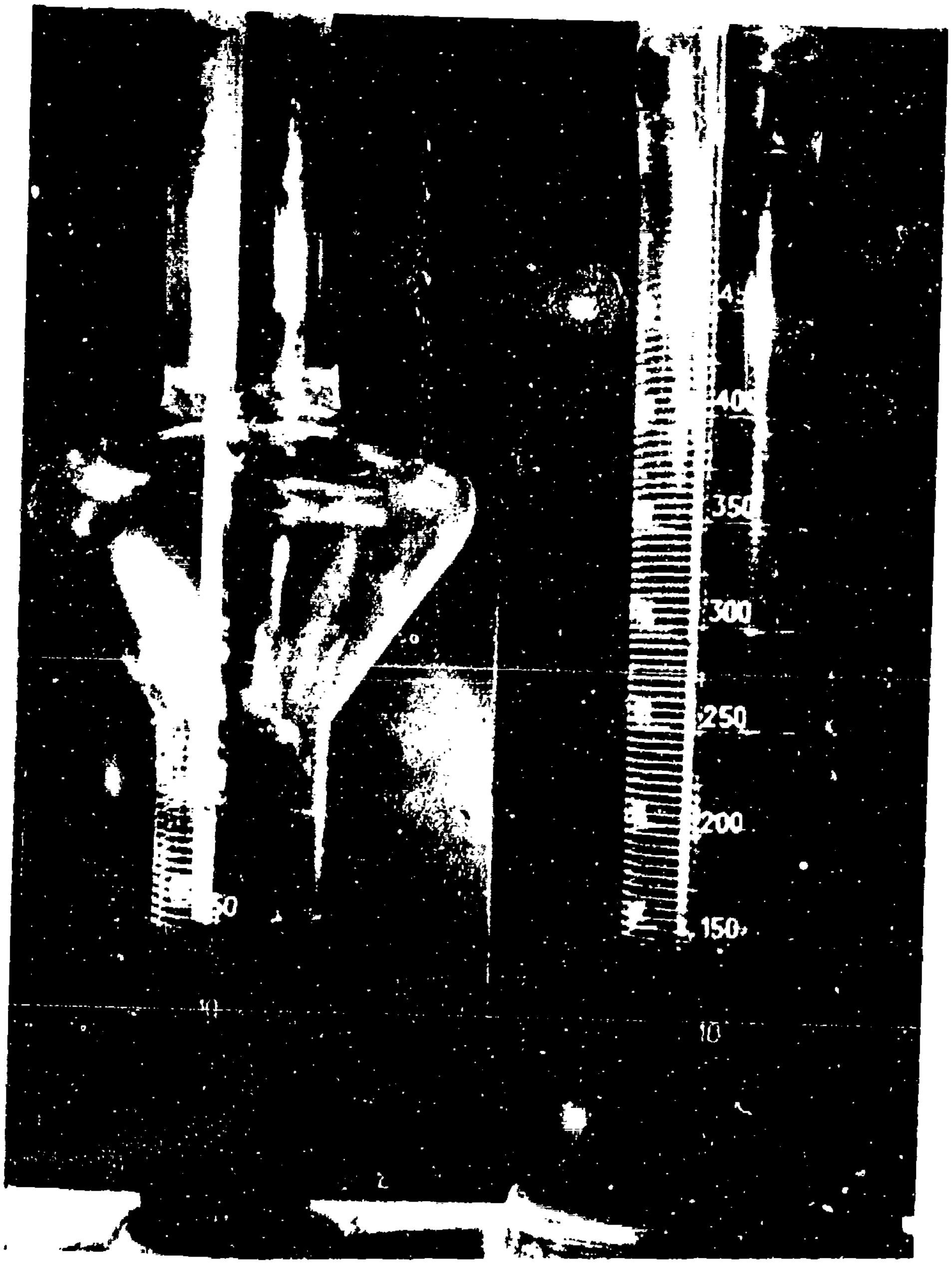

Figure 98. Two Foam Containers of the Same Diameter (46.2 mm), with the Same Height of Solution (63 mm) in Each, Equipped with the Same Porous Ball to Generate Foam.

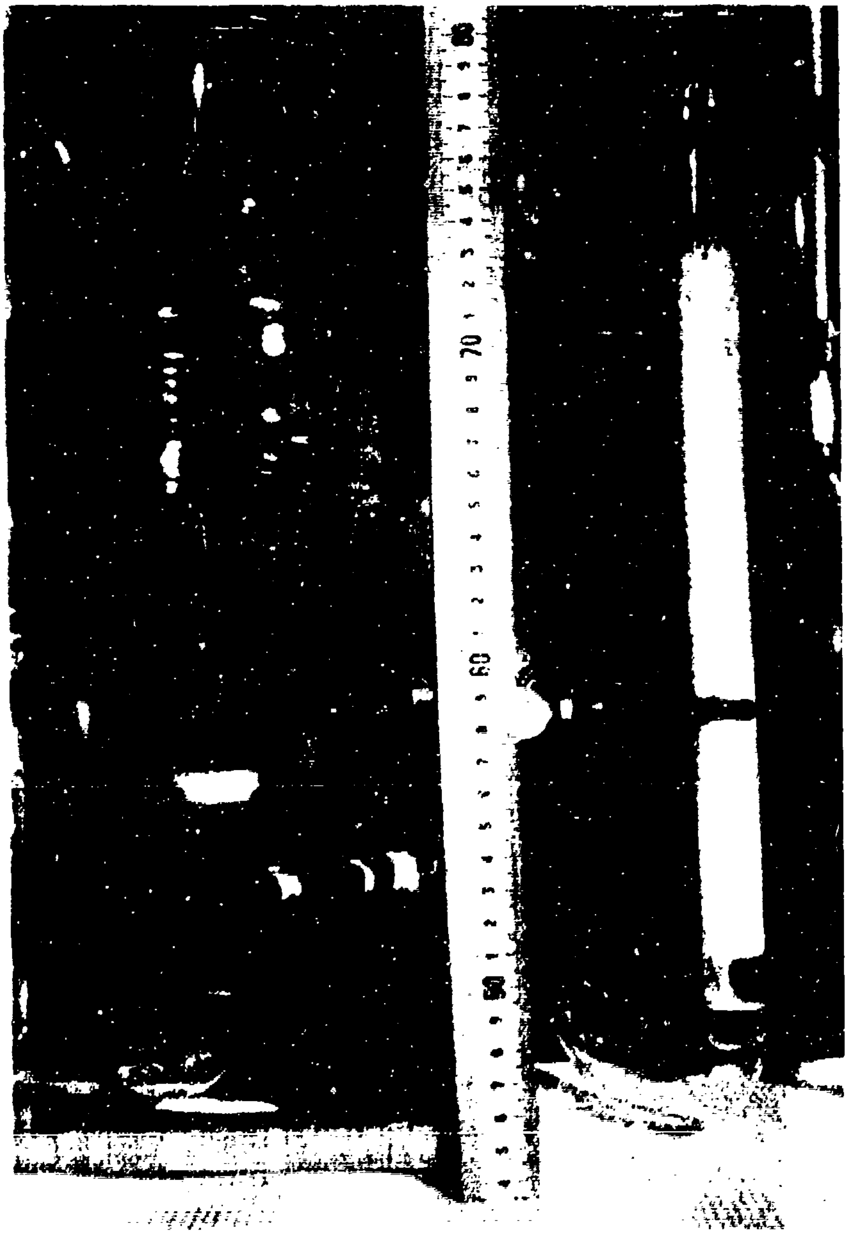

Figure 99. Comparison of Volume of Foam Production in a Conical and in a Cylindrical Foam Container.
Solute: Span 20 Solvent: Mineral Oil
Concn.: 601.2 ppm Temp.: 22.5°C
Volume flow rate: 20 cm^3/minute
Linear flow rate: 0.11 cm/second

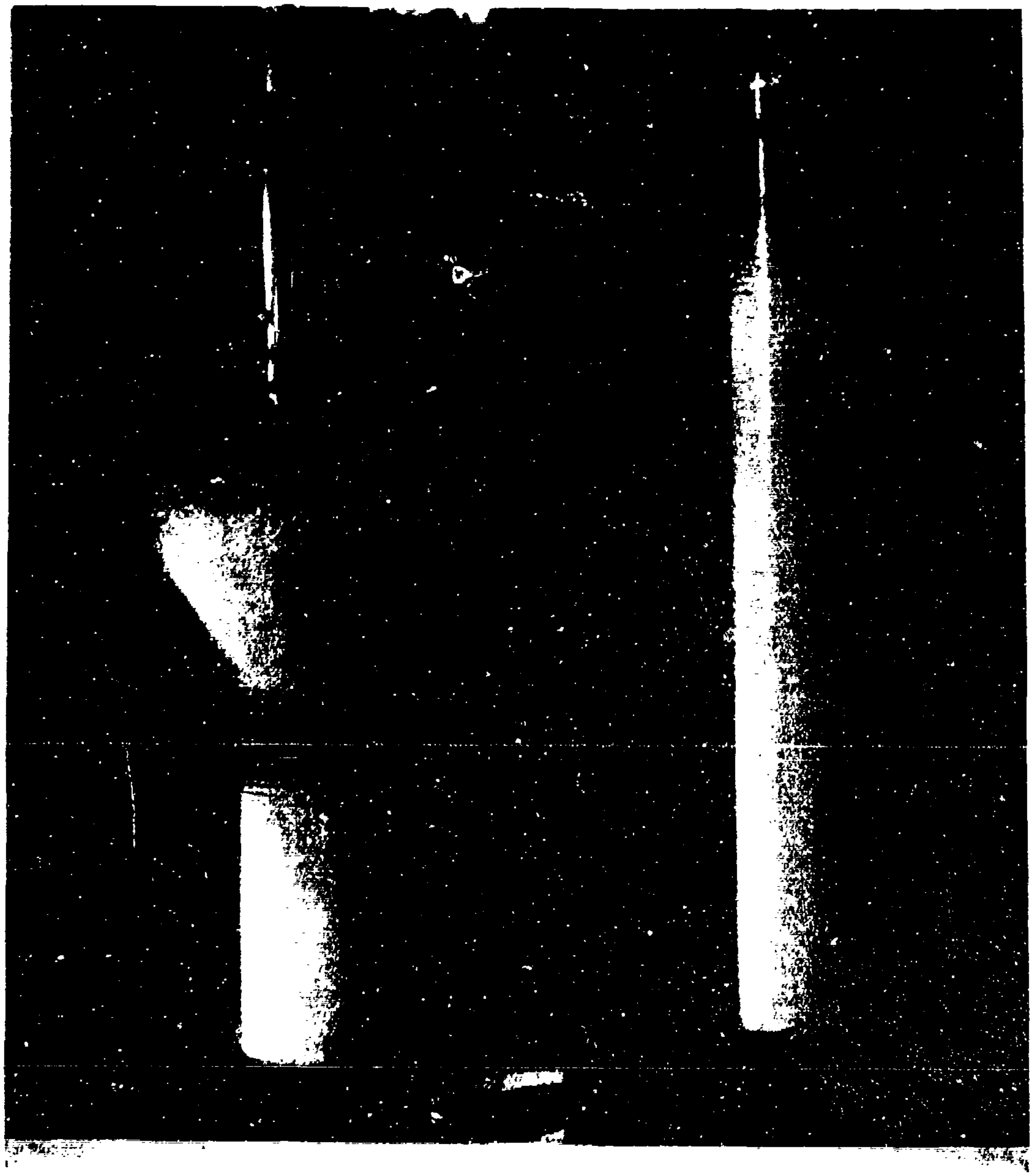

Figure 100. Comparison of Volume of Foam Production in a Conical and in a Cylindrical Foam Container.
Solute: Span 20 Solvent: Mineral Oil
Concn.: 601.2 ppm Temp.: 22.5°C
Volume flow rate: 100 cm³/minute
Linear flow rate: 0.100 cm/second

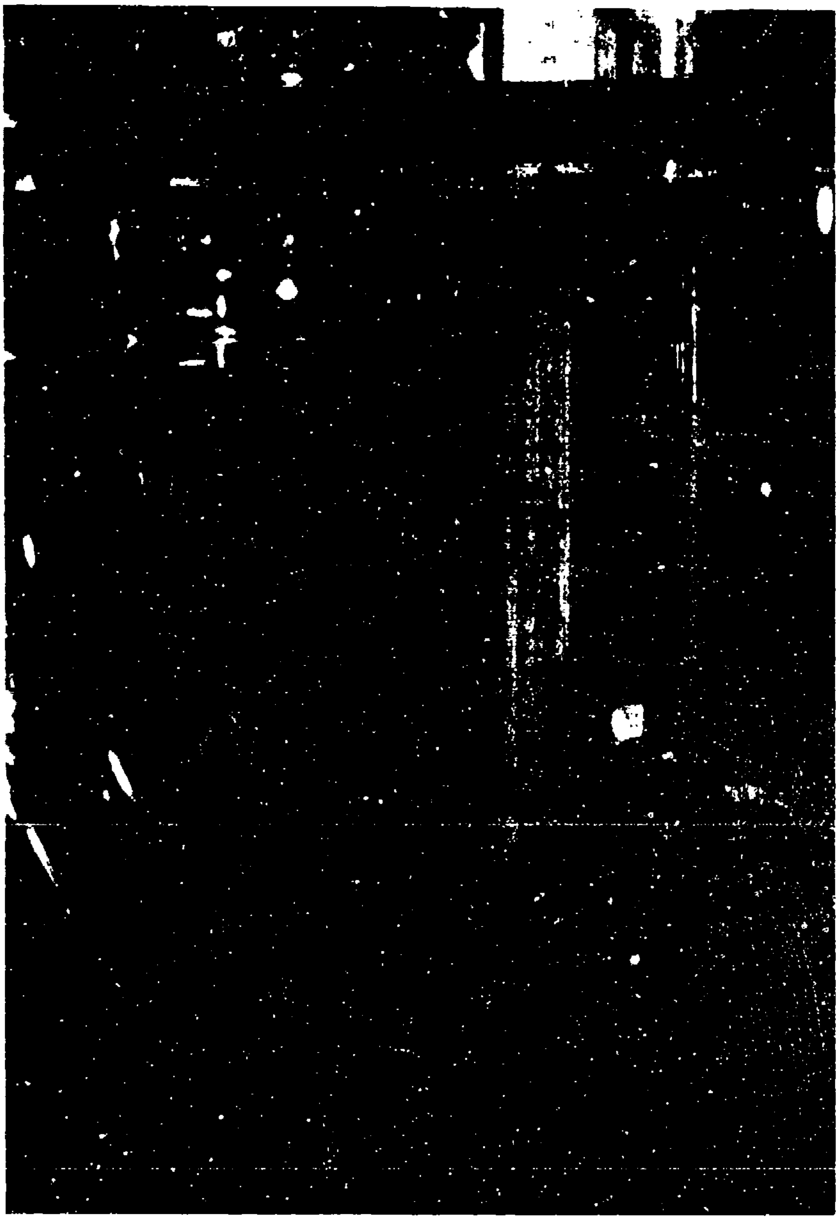

Figure 101. Comparison of Volume of Foam Production in a Conical and in a Cylindrical Foam Container.
Solute; Phenothiazine Solvent; Tmp-Heptanoate
Concn.: 3.92% (w/w) Temp.: 60°C
Volume flow rate: 187.5 cm^3/minute
Linear flow rate: 0.99 cm/second

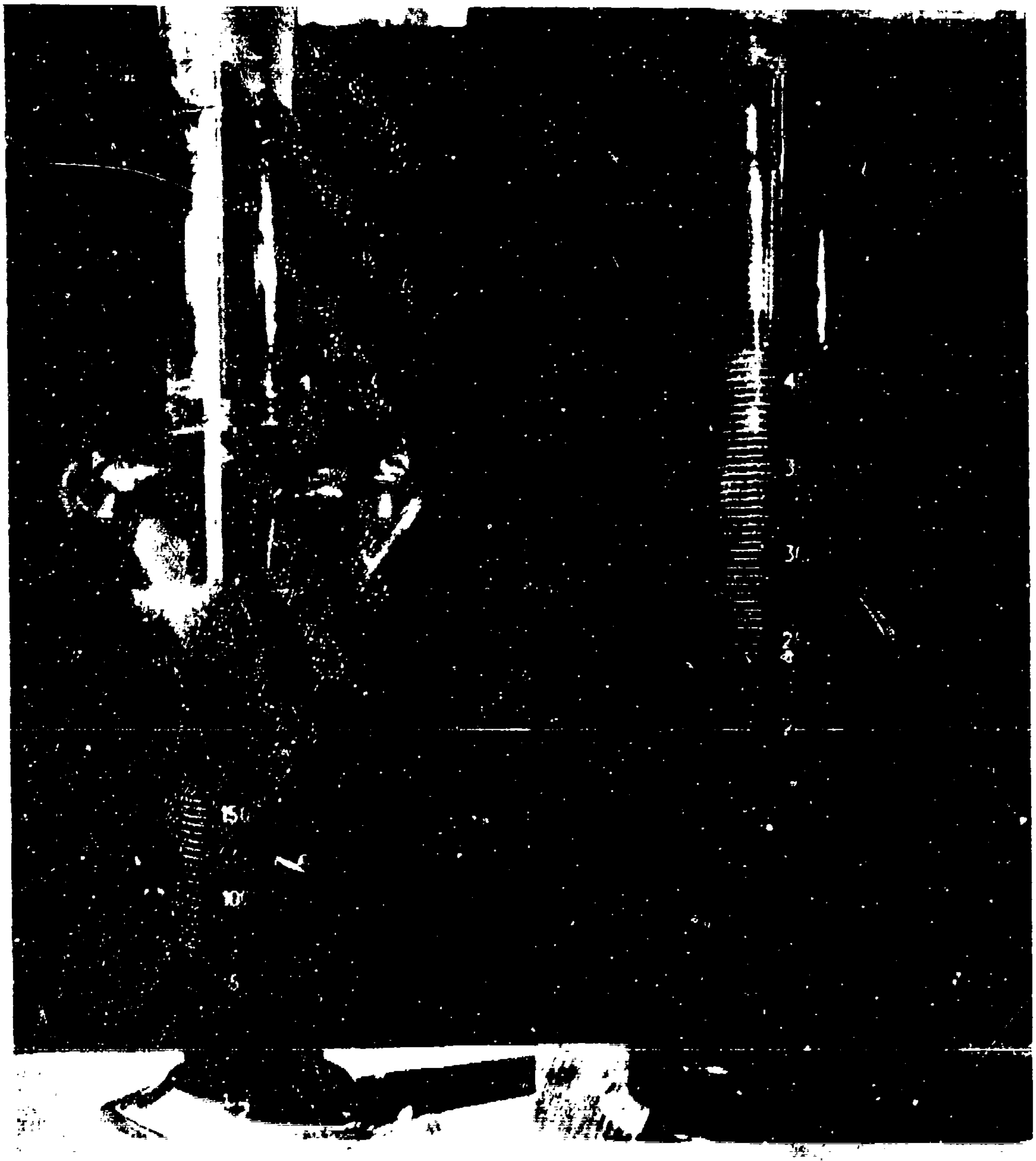

Figure 102. Comparison of Volume of Foam Production in a Conical and in a Cylindrical Foam Container.
Solute: Phenothiazine Solvent: 1mp-Heptanoate
Concn.: 3.92% (w/w) Temp.: 60°C
Volume flow rate: 1000 cm^3/minute
Linear flow rate: 1.00cm/second

Table 24. Experimental Conditions and Volume Ratio Values in Containers of Various Shapes and Diameters.

Solution	Temp (°C)	Flow Rate (cm/sec)	Volume Ratio			
			Small Cyl.	Small Cone	Big Cyl.	Big Cone
601.2 ppm Span 20 in Mineral Oil	22.5	0.10-0.11	>2.7	0.31	>2.4	3.0
3.92% w/w Phenothiazine in Tmp-Heptanoate	60.0	0.99	1.57	0.45	2.9	1.3

Table 24 shows that the Volume Ratios are considerably smaller in the cone-shaped vessel than in the cylinder, both in the smaller and larger diameter tubes. These results follow the prediction of Watkins' theory. The value of the Volume Ratio for the same solution and identical conditions of temperature and rate of gas flow also depends on the size of the vessels, the larger ones giving larger volumes of foam. The photographs provide convincing evidence of the effect of the shape of the container on the volume of foam produced.

We have observed, with a certain solution, that foam will be created in a narrow tube but not in a wider tube. This is another effect of vessel shape on foam volume. It may be called a wall effect, but that phrase is descriptive without being explanatory. The effect may be ascribed to the presence of a meniscus, which is produced when the liquid has a low angle of contact with the wall, i.e., wets the wall. The curvature of the meniscus creates a capillary (or Laplace) pressure that prevents hydrodynamic drainage. A bubble inside the meniscus is stabilized, since the liquid surrounding the bubble cannot drain away. The presence of the bubble increases the volume of the meniscus and causes it to extend farther from the wall. In a cylinder sufficiently narrow, the meniscus may, in this way, extend across the diameter of the cyclinder; and so foster the stability of the bubbles within a finite volume. Inside a wider tube, the reinforcement of the effect by overlapping of the meniscus from opposite sides of the tube would not occur, and no build-up of the bubbles into a foam would be observed.

6. The Effect of Vessel Shape on Foam Flooding during Degassing and Distillation

We have reported above the effect of the shape of the vessel on the volume of foam produced when gas is bubbled through various solutions. Under these conditions the volume of foam produced is

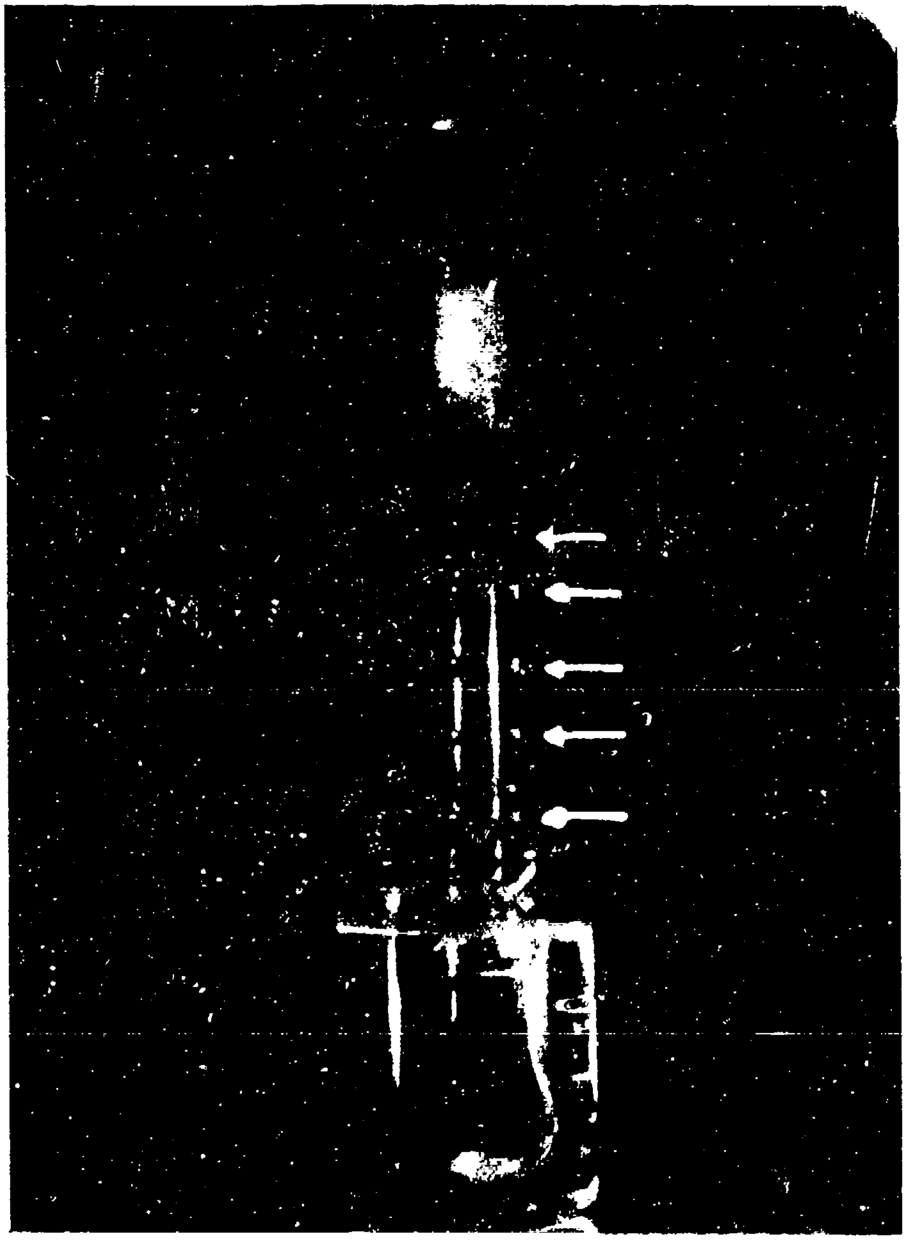

Figure 103. Boiling Solution in a Cylindrical Vessel, showing Foam Flooding.

Figure 104. Boiling Solution in a Conical Vessel, showing Foam Flooding.

remarkably reduced in a conical vessel compared to a cylindrical vessel. When foam is produced during the boiling of a liquid, would the same alteration of the shape of the containing vessel have the same effect? The answer is of potential significance in the design of distillation and fractionation towers, kettles, flash evaporators, degassing units, and digesters.

Standard distillation systems were connected to a cylindrical vessel (20 mm external diameter, 250 mm height) and to a 60° conical vessel. The experiments were carried out with 10 ml of an aqueous solution containing 500 ppm of detergent, at a reduced pressure of 65 mm of mercury and at temperatures in the range of 45 to 50°C.

Before distillation starts, a short degassing period is observed during which a column of foam is produced. In the cylindrical vessel the foam is pushed by rising vapor to the upper end of the column and overflows or "floods;" (see Figure 103) whereas in the conical vessel the foam does not rise much above the surface of the liquid (see Figure 104.) As boiling continues, a series of circular liquid films, spanning the whole cross-section of the cylindrical column, is pushed by the escaping vapor all the way to the top of the column, and floods (see Figure 105.) In the conical container, large single bubbles appear, which burst in the lower part of the cone, without any flooding (see Figure 106.)

These results show that the conclusions of Watkins' theory may be extended to additional industrial applications.

7. Variation of Foaminess with Temperature-- The Effect of Vessel Shape

We have previously reported the variation with temperature of the foaminess of solutions in tmp-heptanoate and in mineral oil as solvents. We observed that the foam volumes increase with temperature in solutions of phenothiazine or N-phenyl-1-naphthylamine in tmp-heptanoate, with or without added tricresyl phosphate, and in solutions of Span 20 or of polydimethylsiloxane (both 100 cSt and 1000 cSt) in mineral oil. An explanation suggested for the solutions of polydimethylsiloxane was based on the increase of solubility with temperature, which would more than make up for the decrease of foaminess expected from the lower viscosity of the solution at higher temperatures. The same explanation could hold for other solutes of low solubility such as phenothiazine, but would not apply to solutions such as N-phenyl-1-naphthylamine in tmp-heptanoate or to Span 20 in mineral oil, which are completely soluble even at the lowest temperature tested (25°C). Another attempted explanation was based on the change of water content with temperature, but that was not confirmed either.

When testing the relation between the rate of injection of nitrogen gas and the exposed area of foam/air interface, we observed that foam volumes in the small conical vessel decreased with temperature, contrary to the variation observed in the cylindrical container, used according to Foam Test 3213. That discrepancy

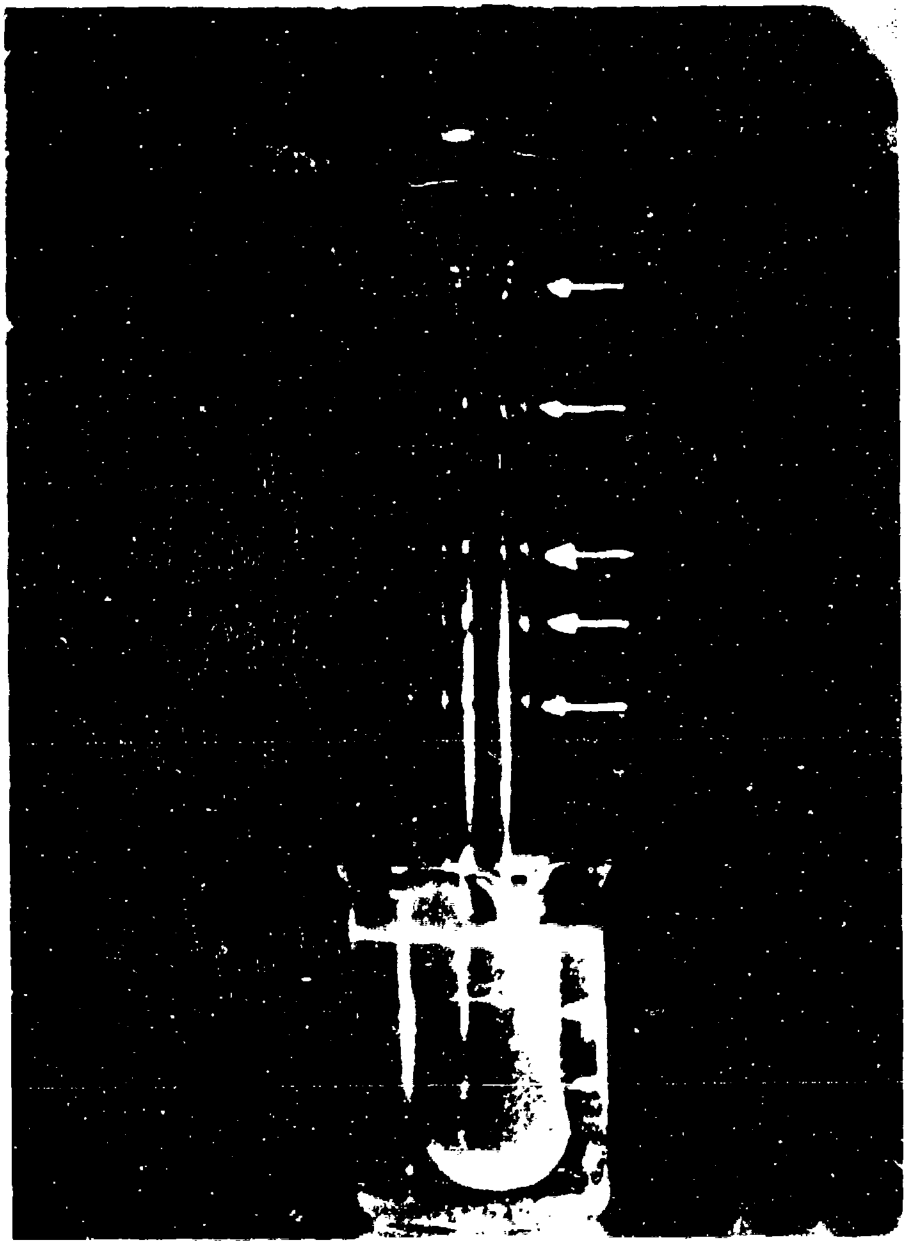

Figure 105. Boiling Solution in a Cylindrical Vessel, showing Flooding by Liquid Films (Arrows.)

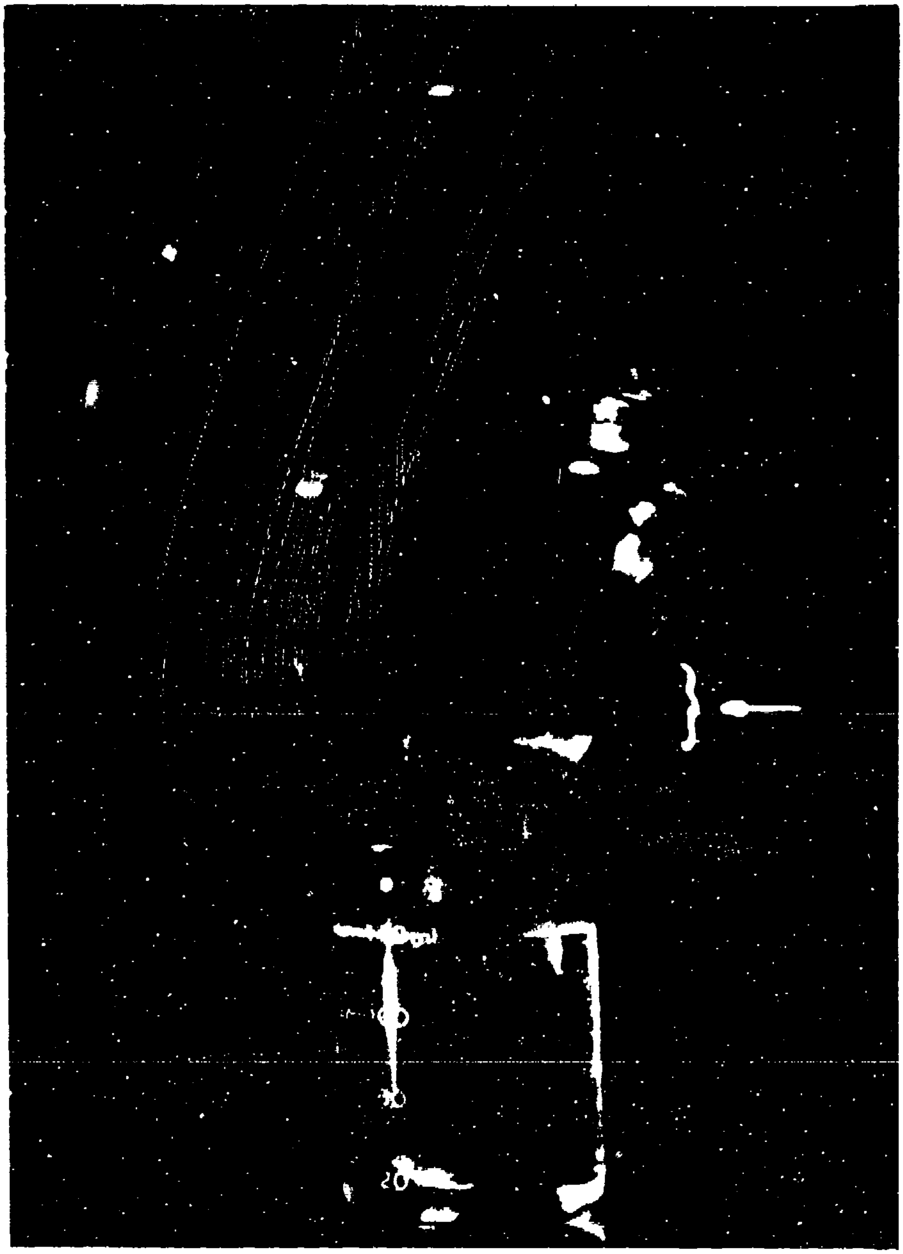

Figure 106. Boiling Solution in a Conical Vessel, showing Control of Flooding. Uppermost Bubble indicated by Arrow.

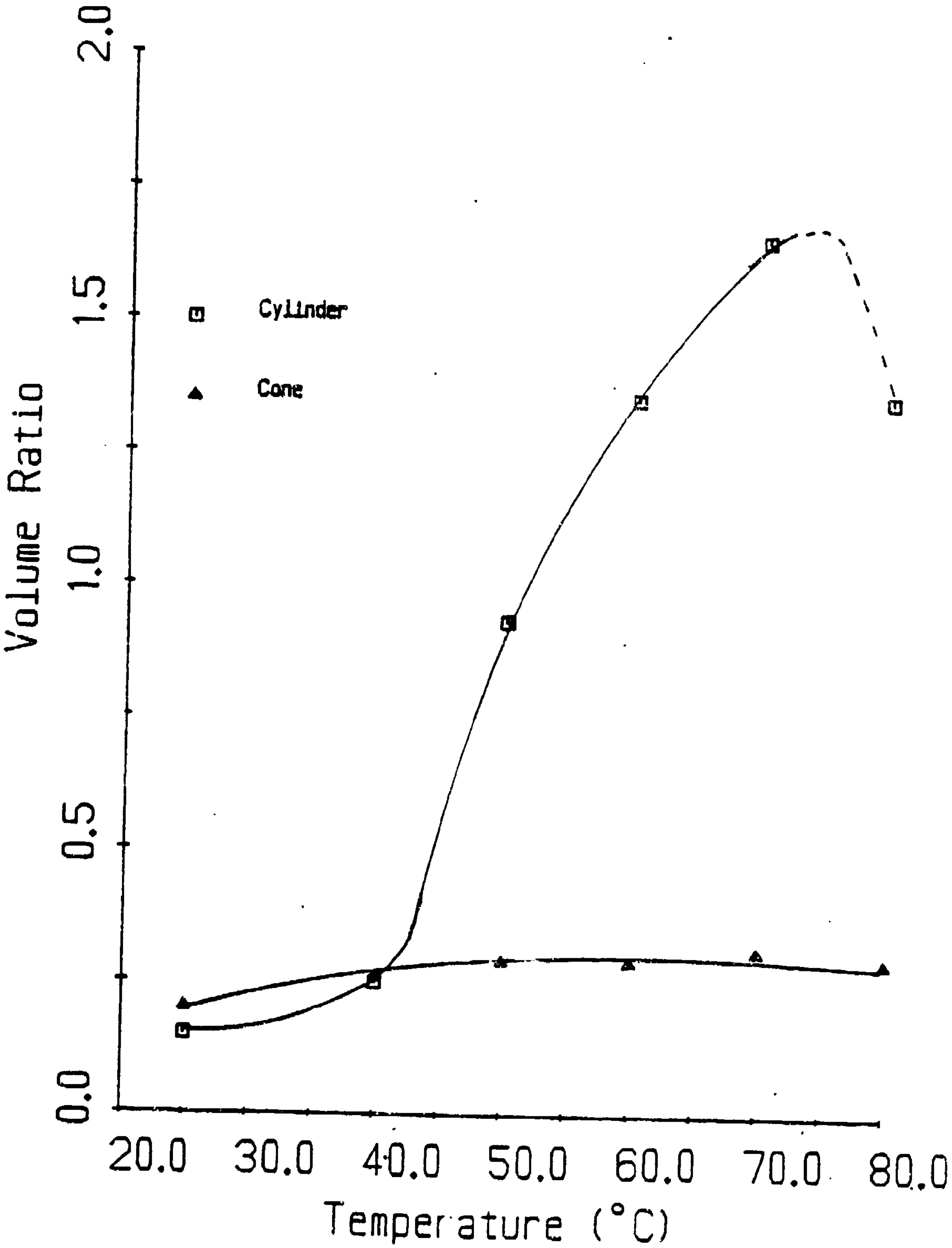

Figure 107. Variation of the Volume Ratio, with Temperature, for a Solution of 2.0% (w/w) N-Phenyl-1-Naphthylamine and 2.0% (w/w) Tricresyl Phosphate in Tmp-Heptanoate as a Function of Vessel Geometry.

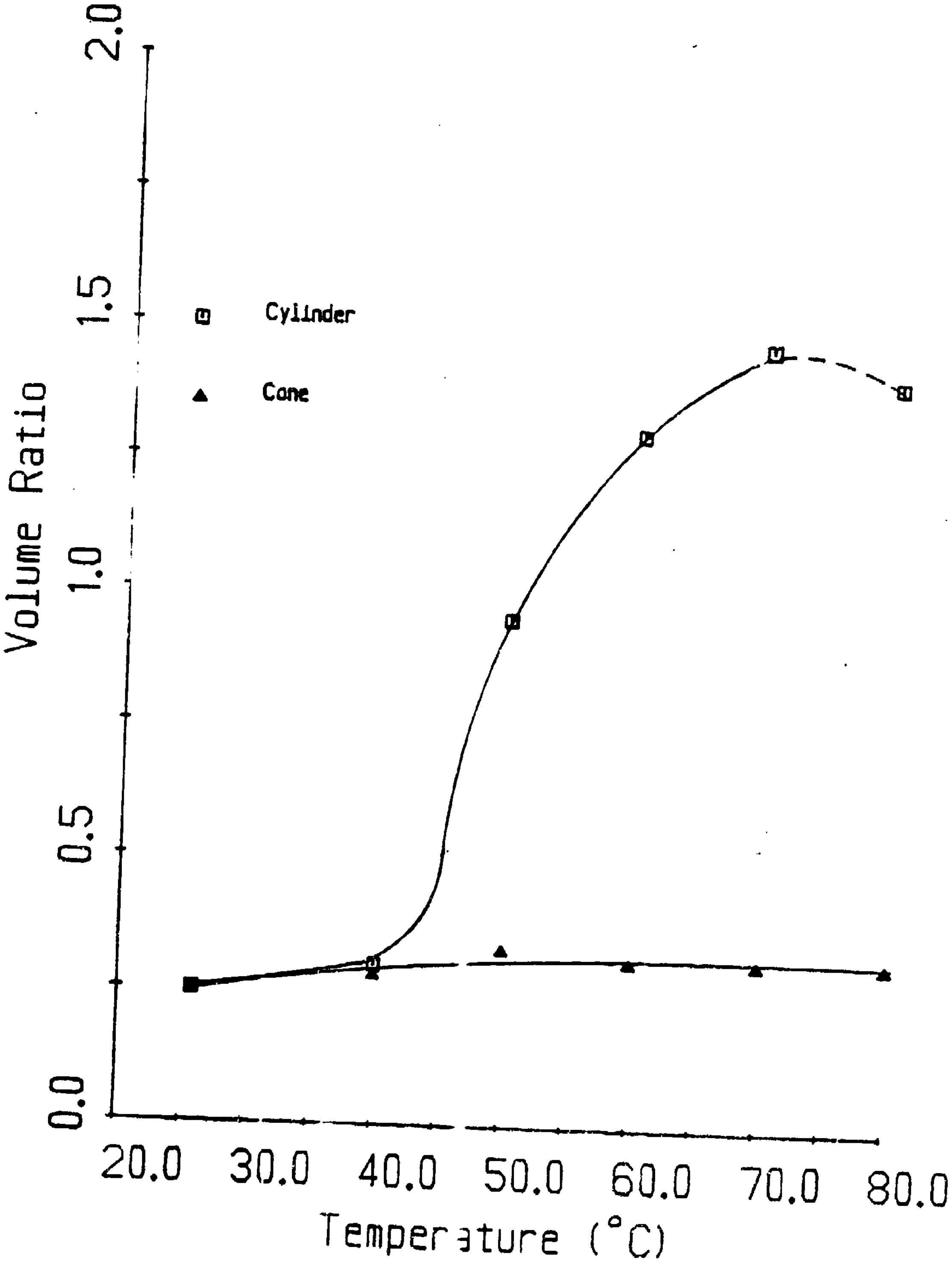

Figure 108. Variation of the Volume Ratio, with Temperature, for a Solution of 2.0% (w/w) Phenothiazine and 2.0% (w/w) Tricresyl Phosphate in Tmp-Heptanoate as a Function of Vessel Geometry.

indicated that the changes of foam values with temperature are not entirely an intrinsic property of the solution under test but depend also on the shape of the foam container.

To investigate this inference further we tested several solutions for foaminess over a range of temperature, from 25°C to 80°C, using the conical and cylindrical foam containers of 46 mm diameter already described ("Big Cylinder and Big Cone.")

Figure 107 shows the volume ratios of the foams measured in the two containers with a solution in tmp-heptanoate of
2% w/w N-phenyl-1-naphthylamine + 2% w/w tricresyl phosphate

Figure 108 shows the results observed with a solution in tmp-heptanoate of
2% w/w phenothiazine + 2% w/w tricresyl phosphate.

Both Figure 107 and Figure 108 show a nearly constant and very low volume ratio of the foam in the conical container (0.30 and 0.32 for Figure 107 and Figure 108 respectively,) and, in the cylindrical container, a large increase of volume ratio of the foam with temperature. A maximum volume ratio of the foam occurs between 70 and 80°C. (The exact point is unknown, since the foam volumes in that range are above the measurable limits of the cylindrical meter.)

The next two diagrams report the results of similar comparative tests made with polydimethylsiloxane (1000 cSt): a solution of 262 ppm in tmp-heptanoate (Figure 109,) and a solution of 0.111 ppm in mineral oil (Figure 110.) The results of these tests show a significant increase in the volume ratios of the foam with increasing temperature, even in the conical container, but certainly more pronounced in the cylindrical container. This increase is most probably due to the increase of the solubility of polydimethylsiloxane in these solvents with temperature. Nevertheless, the volume ratios of the foams in the cylindrical container are much larger than those, obtained under the same conditions, in the conical container, confirming that vessel shape plays a major role in determining the quantity of foam produced from a given solution and the variation of that quantity with temperature.

8. Variation of Foaminess with Temperature and Flow Rate of Gas Input.

If any correlation between foaminess and any other property of the foamable solution is to be found, a foam test that is influenced by peculiarities of the test method must be avoided. We have evidence to indicate that the results obtained for foaminess of a solution when measured in a cylinder does not reflect the intrinsic surface activity of the solution. We have previously reported the variation with temperature of the foaminess of oil solutions in the range 25-80°C, as measured in cylindrical and in conical containers. For example, the gas volume ratios, which we use as our measure of

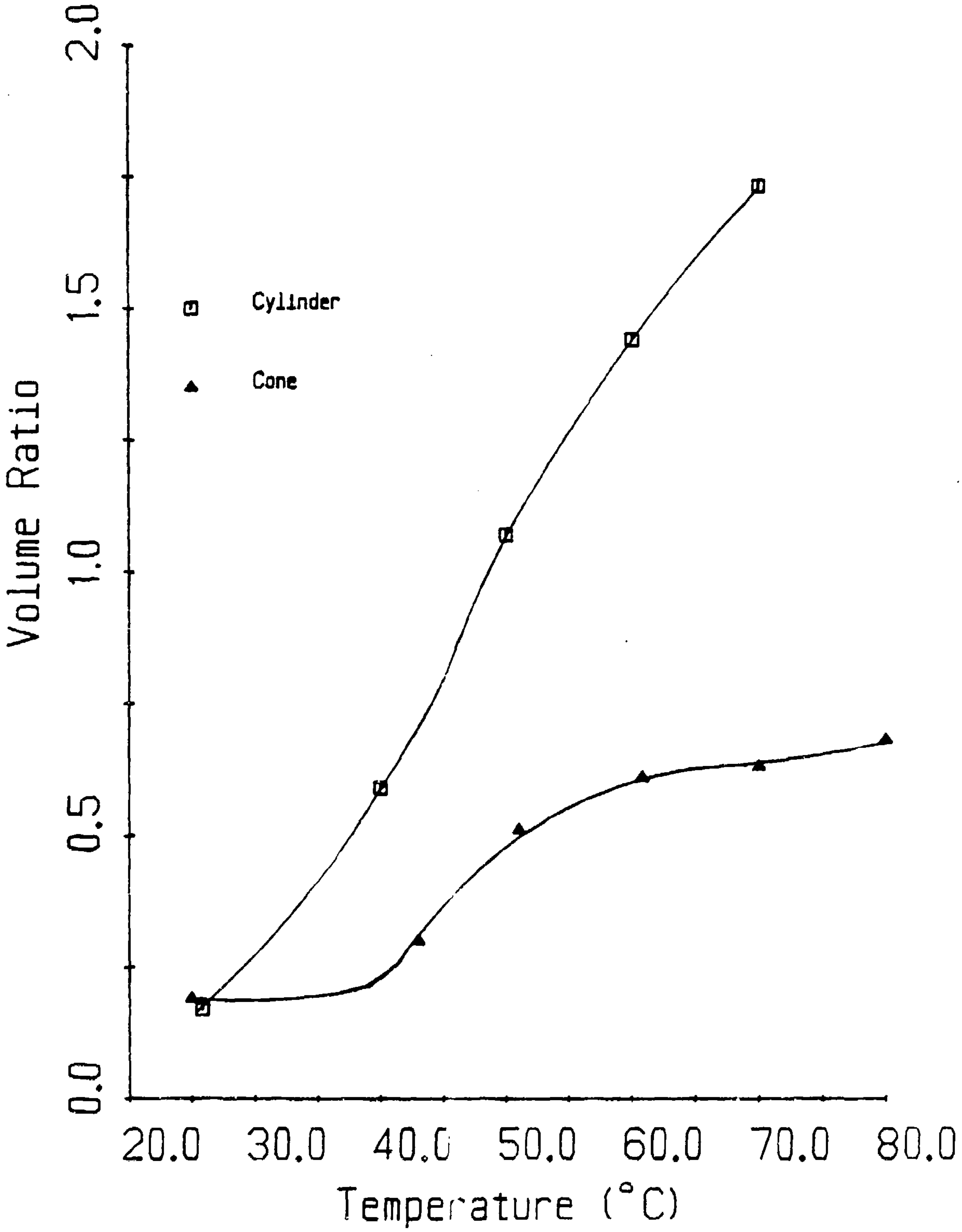

Figure 109. Variation of the Volume Ratio, with Temperature, for a Solution of 262 ppm Polydimethylsiloxane (1000 cSt) in Tmp-Heptanoate as a Function of Vessel Geometry.

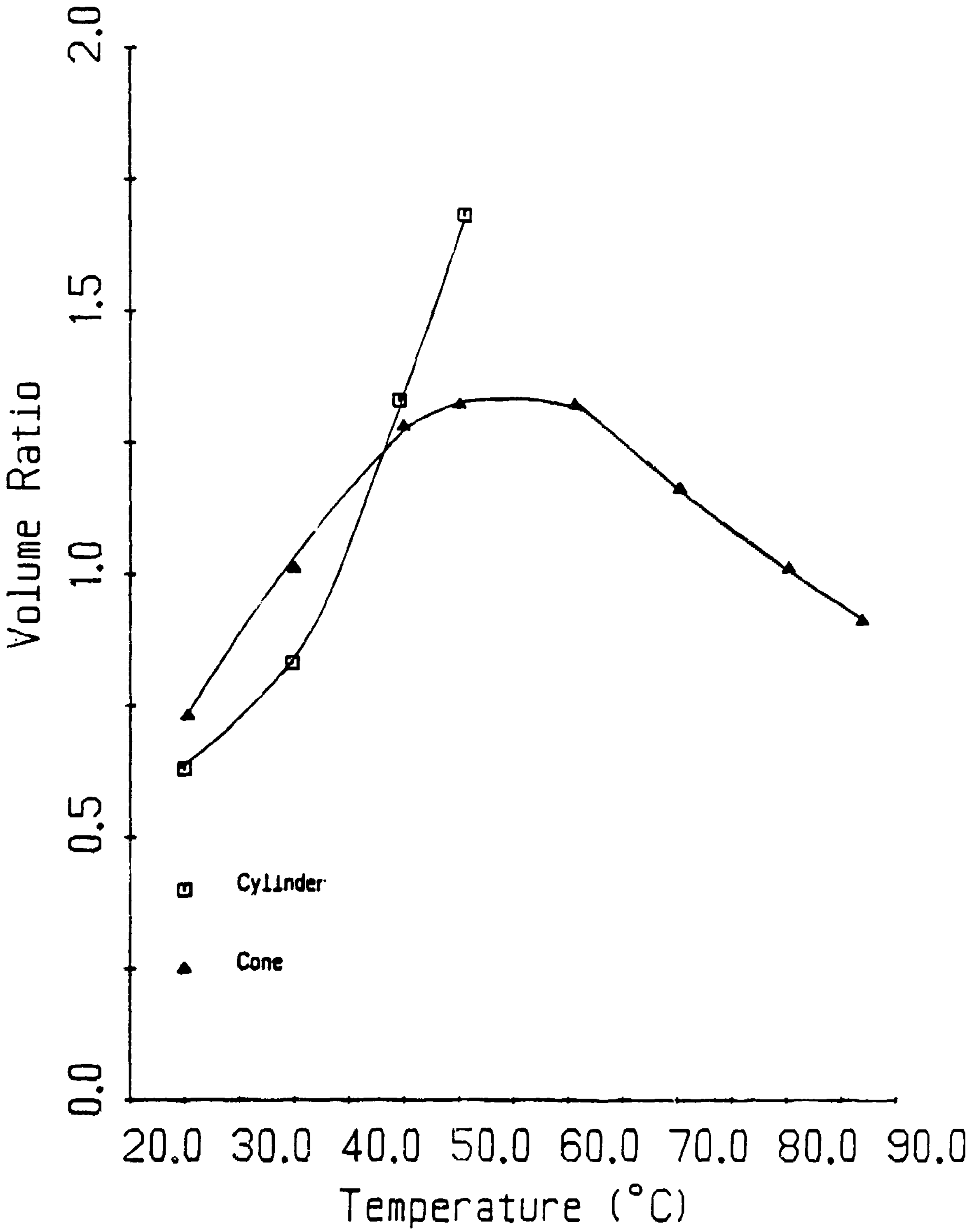

Figure 110. Variation of the Volume Ratio, with Temperature, for a Solution of 0.111 ppm Polydimethylsiloxane (1000 cSt) in Mineral Oil as a Function of Vessel Geometry.

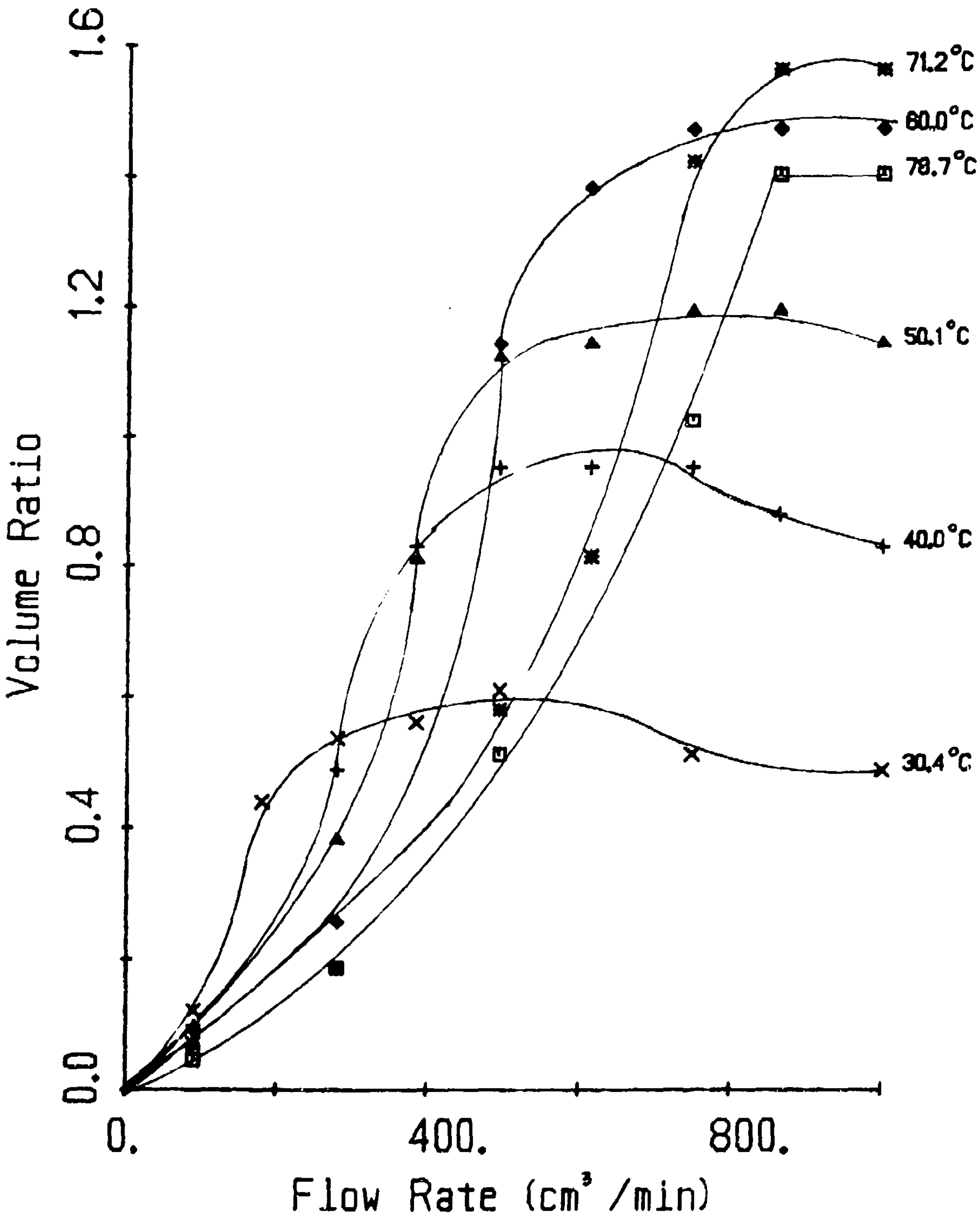

Figure 111. Variation of the Volume Ratio with Various Flow Rates of Gas Input at Various Temperatures for a Solution of Phenothiazine (4.20% w/w). Measured in a Cylindrical Container.

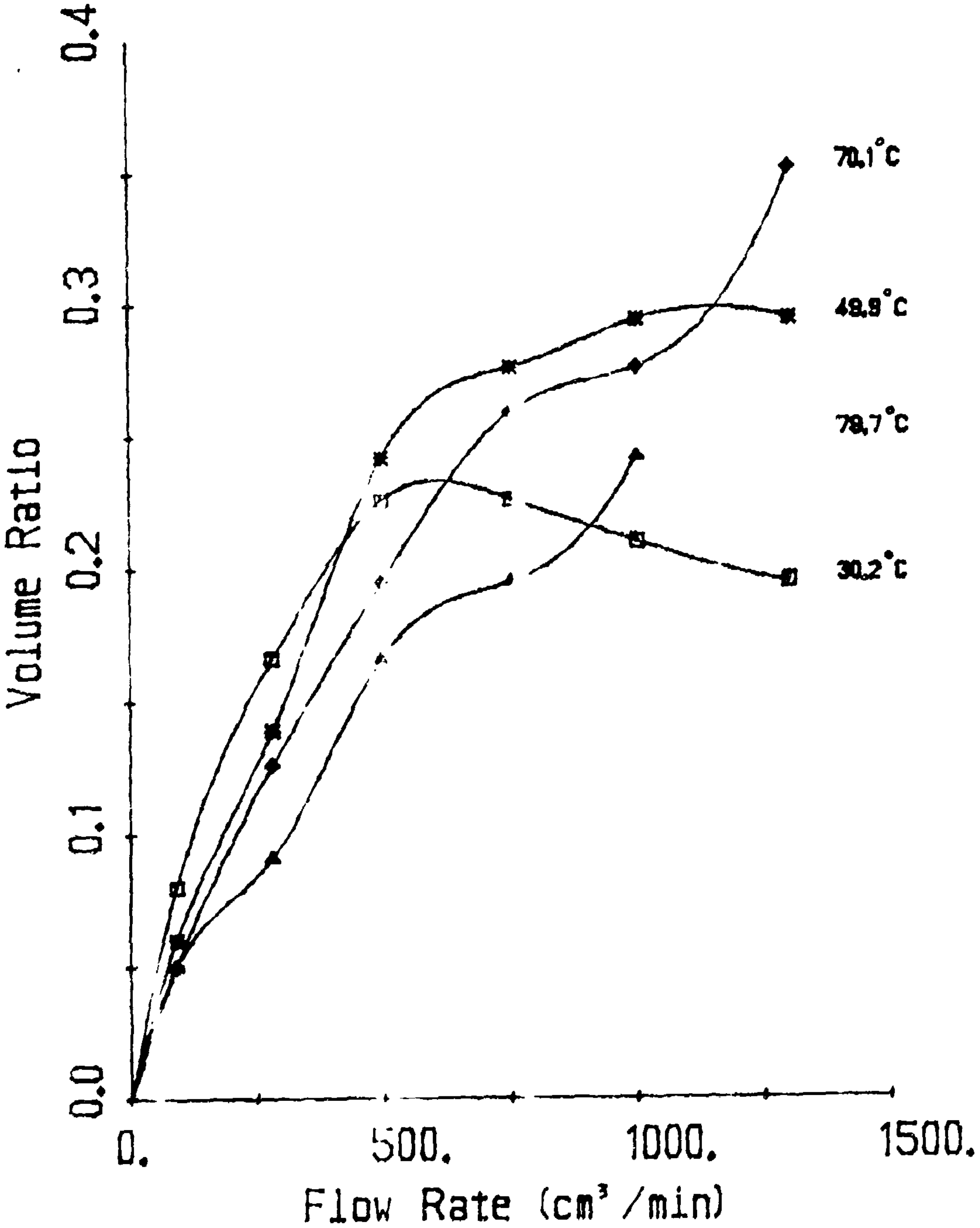

Figure 112. Variation of the Volume Ratio with Various Flow Rates of Gas Input at Various Temperatures for a Solution of Phenothiazine (4.20% w/w). Measured in a Conical Container.

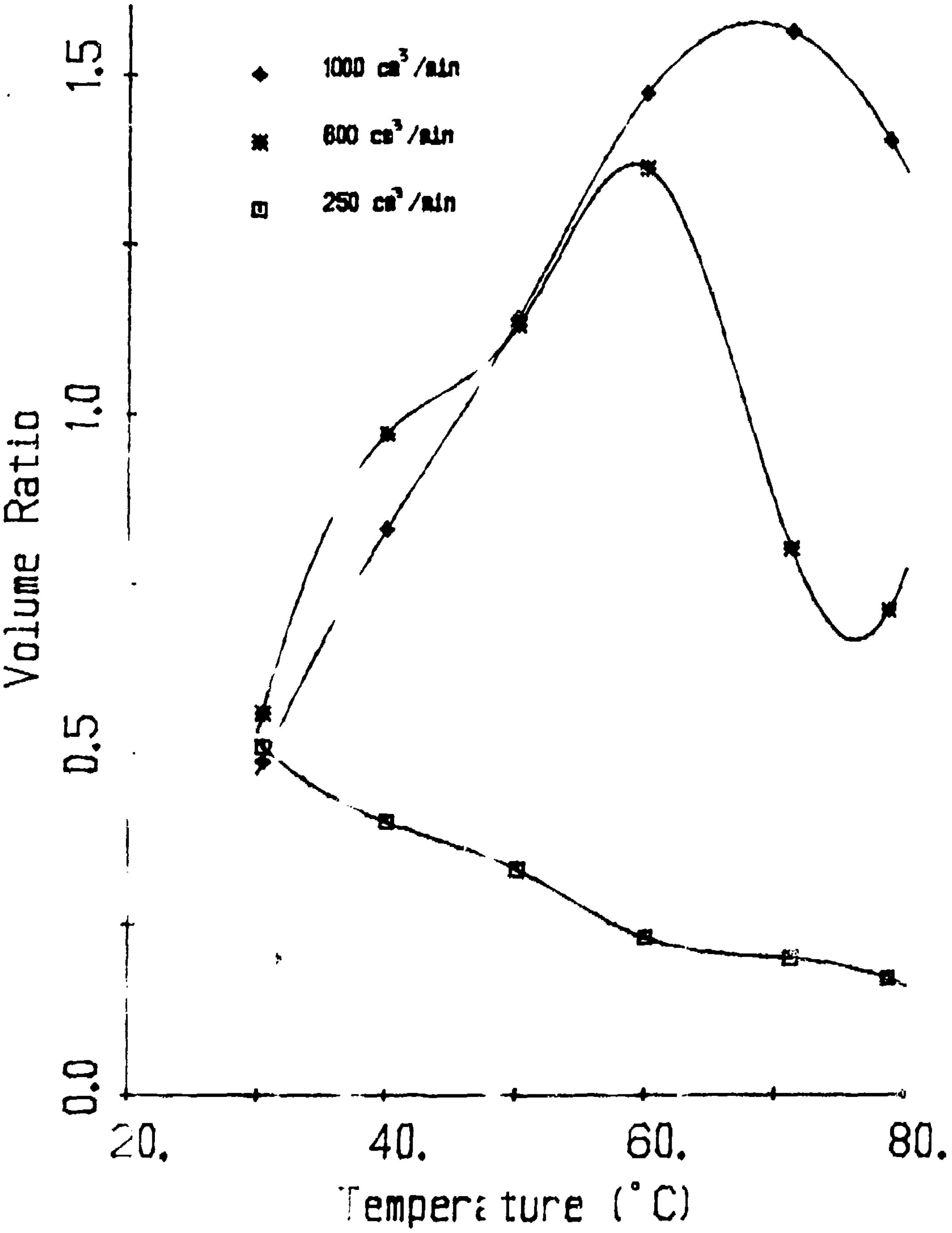

Figure 113. Variation of the Volume Ratio with Temperature at Various Rates of Gas Input for a Solution of Phenothiazine (4.70% w/w).
Measured in a Cylindrical Container.

foaminess, in the various oil solutions that we have tested, increase with temperature to a maximum at about 70°C and then decline with further increase of temperature. Are these temperature effects on the foaminess real, or are they a function of the method of measuring foam ? That behavior, if shown to be an intrinsic property of the solution tested, is highly significant and warrants further investigation and a search for correlations with surface activity as a function of temperature. To find out if the behavior observed is affected by adventitious factors such as the arbitrary parameters of the test method, we compared a number of the conditions that are normally held constant in the standard Test Method 3213, namely, the rate of gas flow, the shape of the foam container, and the temperature. We report the results of tests with a solution of phenothiazine, 4.20% w/w, in tmp-heptanoate, at different temperatures, different flow rates, and in containers of two different shapes.

Figures 111 and 112 show the gas-volume ratios as a function of volumetric flow rate in the cylindrical and in the conical containers, respectively. Figure 111 shows that the foaminess in the cylinder decreases continuously with temperature, in the range of flow rates up to 280 ml/minute. At higher flow rates the functional dependence of foaminess upon temperature may appear to be quite different, depending on what flow rate is used for the comparisons. Thus Figure 113 shows how the variation of foaminess with temperature would appear for the flow rates of 250, 600, and 1000 ml/minute, if these rates were used with the Test Method.

A similar result is obtained on substituting the conical foam container for the cylindrical one, although, as reported earlier, the foam volumes in the cone are much less than in the cylinder under the same conditions. With the conical container, the foaminess decreases with temperature up to a flow rate of 500 ml/minute, and at higher rates begins to increase. These higher rates of gas flow, both in the cylinder and the cone, are believed to introduce turbulent flow in the volume of foam, and so affect its stability in a different way.

Figure 114 compares the variation of gas-volume ratio with temperature in the two types of foam container, at a fixed rate of flow of 1000 ml/minute. The results closely resemble those previously reported (Figures 107 and 108) for solutions in tmp-heptanoate of N-phenyl-1-naphthylamine(2% w/w) + tricresyl phosphate (2% w/w) and of phenothiazine (2% w/w) + tricresyl phosphate (2% w/w.)

The conclusion reached from these results is that changes of foaminess with temperature vary with the container geometry of the foam-meter, and with the flow rate selected for the prosecution of the test; and so cannot be relied on as genuine reflections of whatever changes in the surface activity of the solution may occur with temperature. Another conclusion drawn from these experiments is that the linear relation between foam volume and rate of gas flow found by Bikerman for some aqueous solutions is not observed in the solutions of the present study.

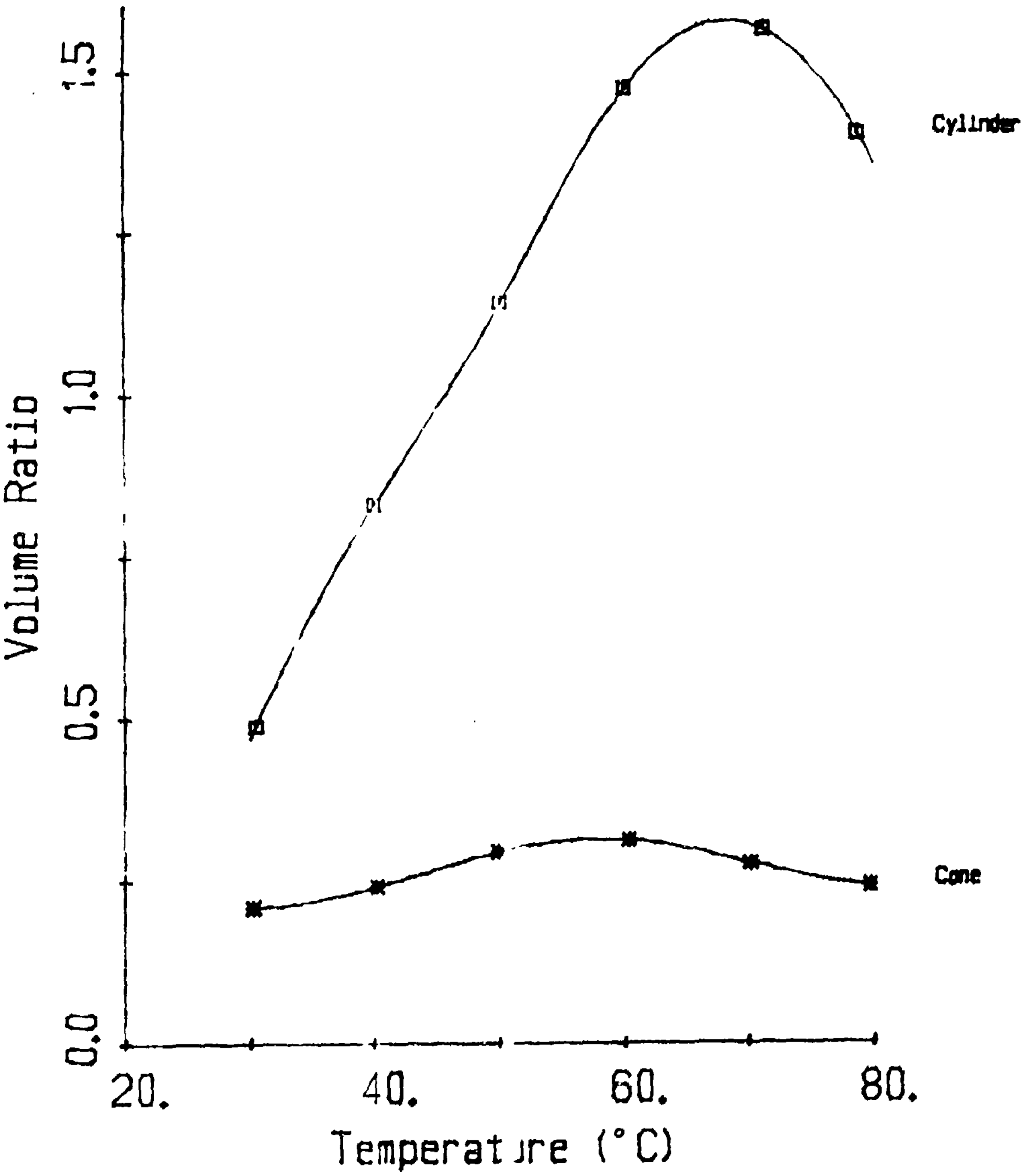

Figure 114. Variation of the Volume Ratio with Temperature at a Fixed Rate of Gas Input of 1000 cm^3/min for a Solution of Phenothiazine (4.20% w/w). Comparison of Cylindrical and Cone as Foam Vessels.

The propensity of a solution to form foam may be tested by measuring the lifetime of single bubbles; and that test is less influenced by extraneous factors introduced by the bubbling-type methods. Deryagin and Gutop[28] have shown that the use of a life of a single bubble as the measure of film stability is justified; and Gleim et al.[29] have found that the behavior of a single bubble is a sufficient characteristic of films in a foam. We have already found a significant correlation between single-bubble lifetimes and dynamic surface tensions (see Section IX.2,) which was not brought out as clearly by means of the standard foam-stability method.

9. The Effect of Vessel Shape

Although the conical foam meter prevents flooding, except when the volume of foam produced exceeds the dimensions of the cone provided, Watkins' prime equation [6], does not include any reference to a parameter relating to the characteristic foaminess of the solution, such as the Σ introduced by Bikerman.[26] This quantity, however, may readily be introduced. The volume of foam created in a dynamic apparatus is determined by the volumetric rate of gas injection and limited by the duration of the foam:

$$V_f = \int_0^{\Sigma} \dot{V}\, dt = \dot{V}\Sigma \qquad [9]$$

Taking into account the geometry of a 60° cone, truncated at a distance h from its apex by a normal cross-section of area A_o, and containing a volume of foam, V_f, contained between the two normal cross-sections A_o and A_f, we get:

$$V_f = (1/\sqrt{3\Pi})\, A_f^{3/2} - (h_o A_o/3) \qquad [10]$$

Eliminating V_f between equations [9] and [10], gives

$$A_f^{3/2} = m\dot{V} + c \qquad [11]$$

where $m = \Sigma\sqrt{3\Pi}$ and $c = h_o A_o \sqrt{\Pi/3}$
Equation [11] has not been suggested before: it only remains to put it to the test of experiment.

The data reported in Figure 94 are for the areas A_f of foam/air interface at dynamic equilibrium for various rates of gas injection in a conical foam meter at three different temperatures. Replotting the same data according to equation [11] above gives the results shown in Figure 115. The solution to which these data refer is a refined mineral oil, which as purchased was found to possess foaminess and so did not require to have any solute added to it. From the initial linear portion of the curves, the foaminess of the solution can be expressed in terms of the characteristic unit Σ, which has the physical meaning of the duration of the gas within the foam from its initiation at the lower part of the column to its release at the top surface of the foam. In Table 25 are reported the results obtained by the application of equation [11] to the replotted data shown in Figure 115.

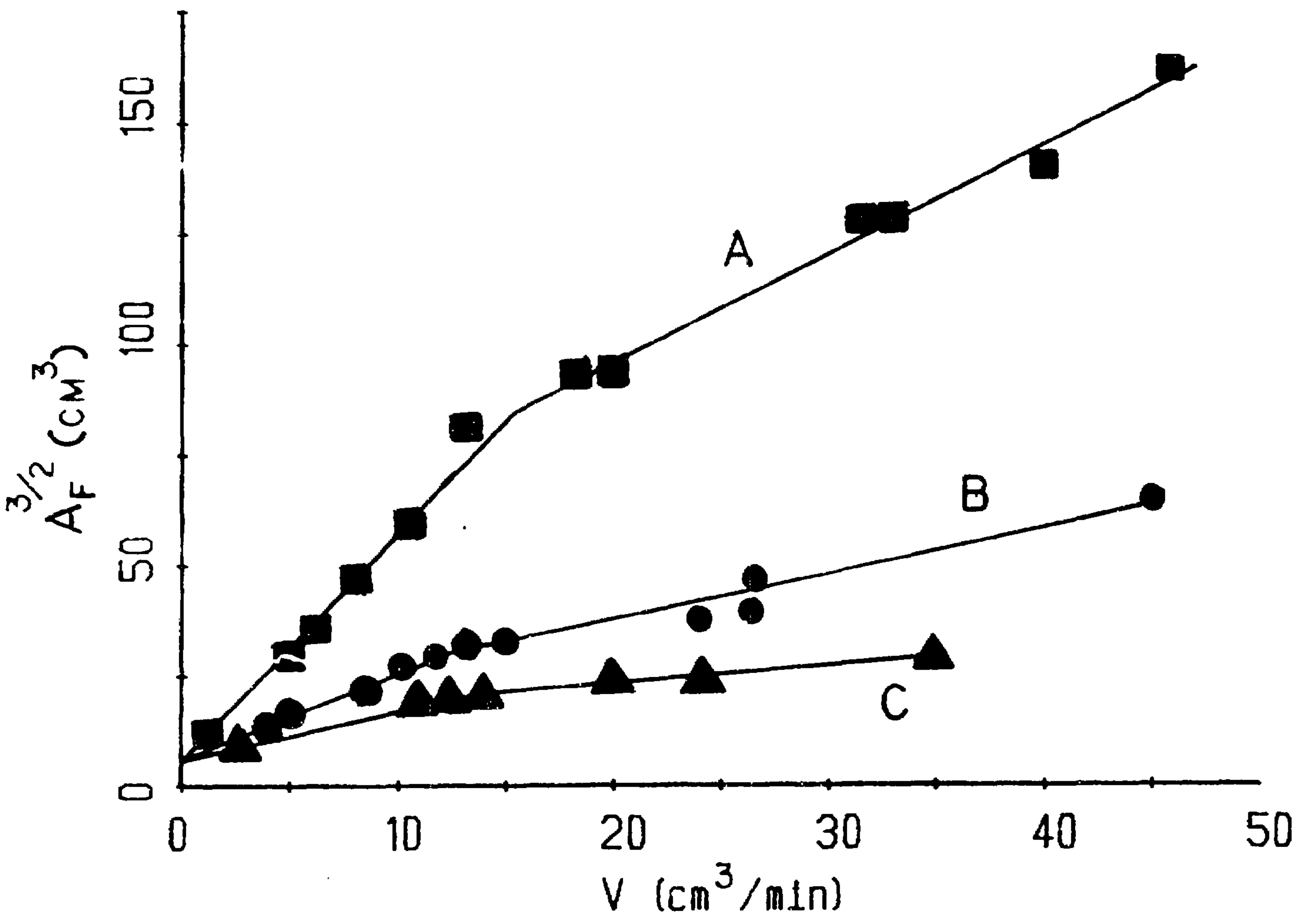

Figure 115. Results of Foam Measurements of Mineral Oil (as is) in Conical Foam Meter (r = 10 mm) at Various Temperatures. See Figure 94.
A = 22.5°C
B = 40.2°C
C = 58.0°C

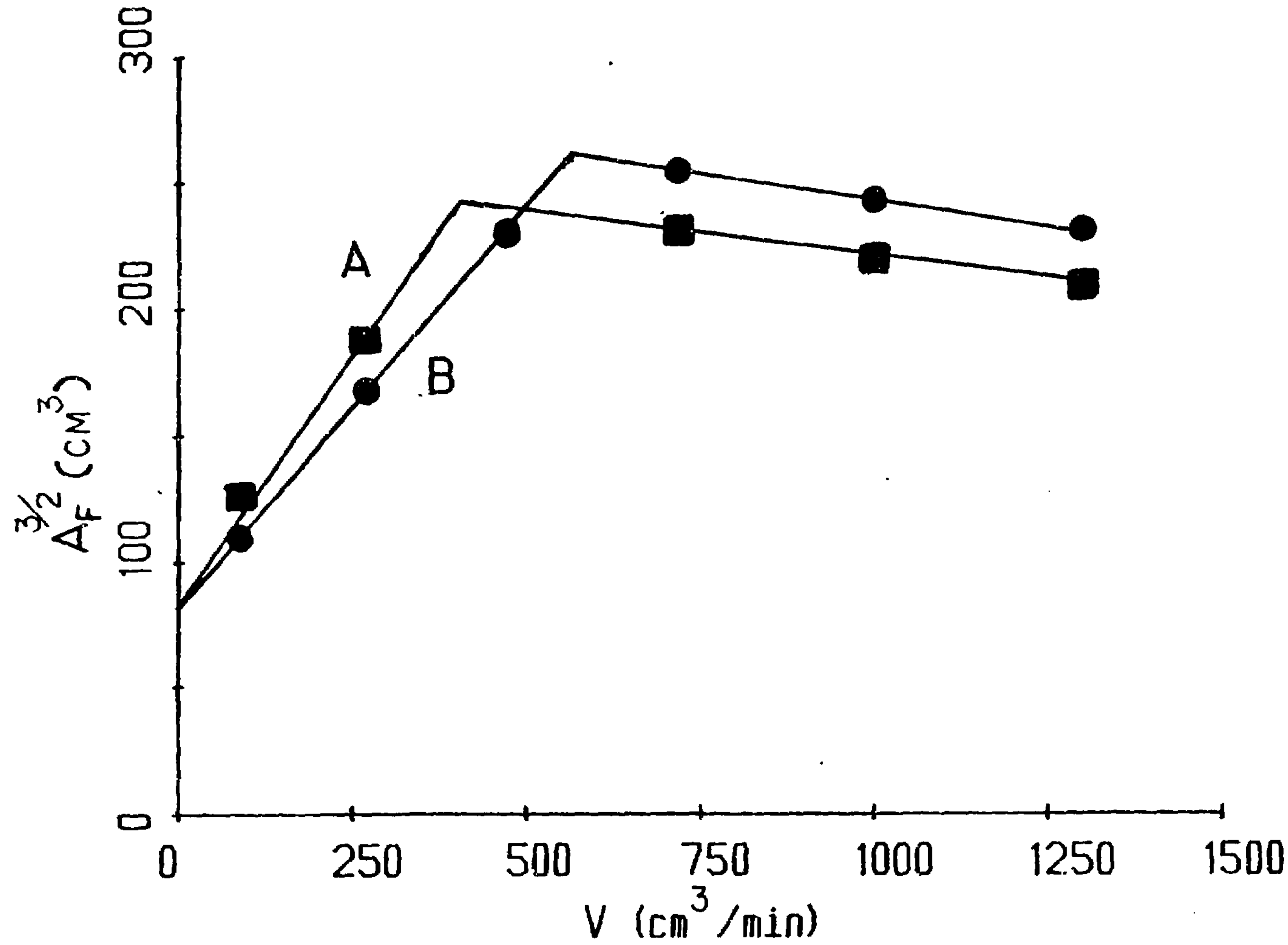

Figure 116. Results of Foam Measurements of Phenothiazine (4.20% w/w) in Tmp-Heptanoate in Conical Foam Meter (r = 23.1 mm) at Various Temperatures.
A = 30.2°C B = 40.2°C

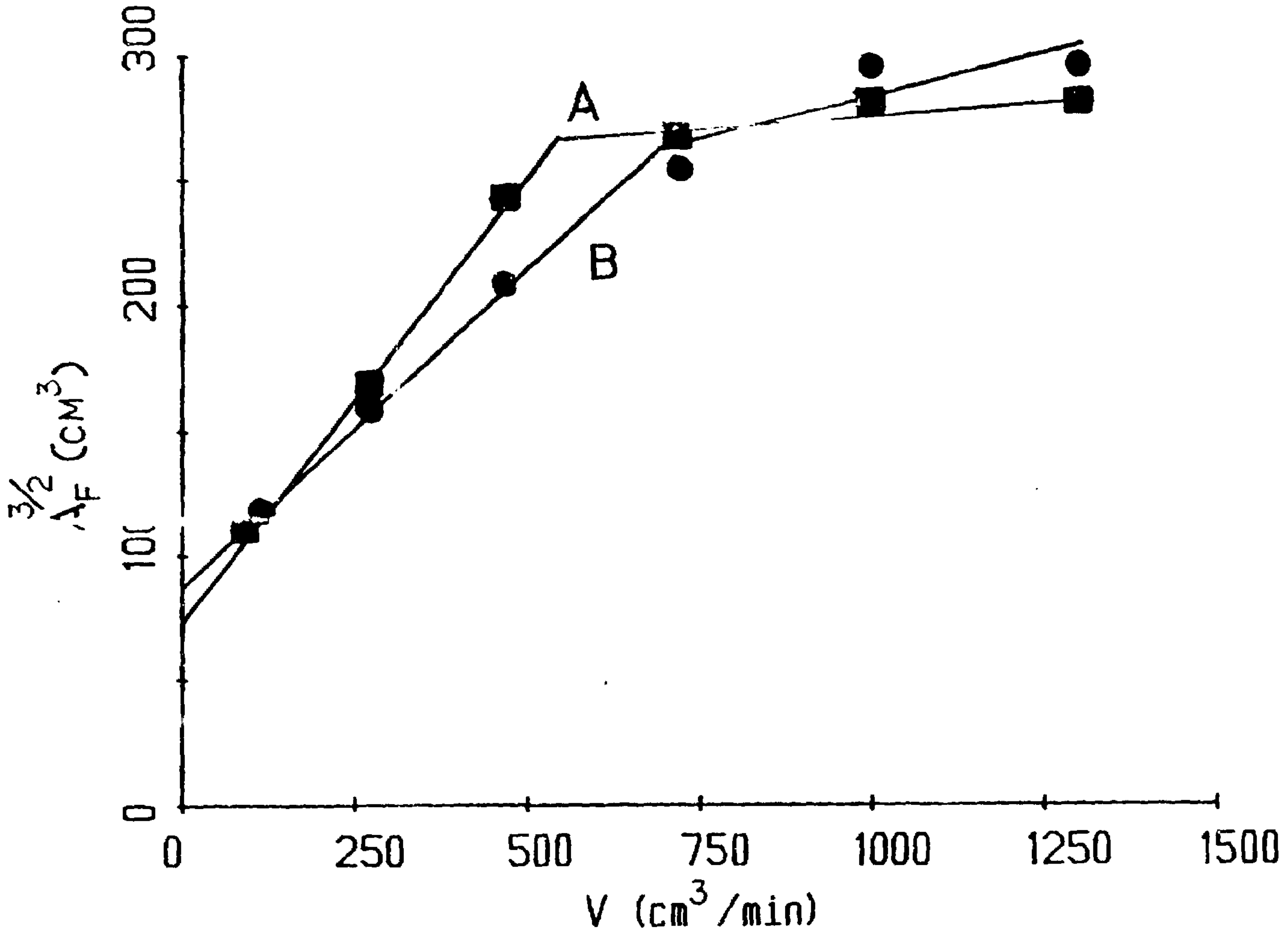

Figure 117. Results of Foam Measurements of Phenothiazine (4.20% w/w) in Tmp-Heptanoate in Conical Foam Meter (r = 23.1 mm) at Various Temperatures.
A = 49.9°C B = 60.3°C

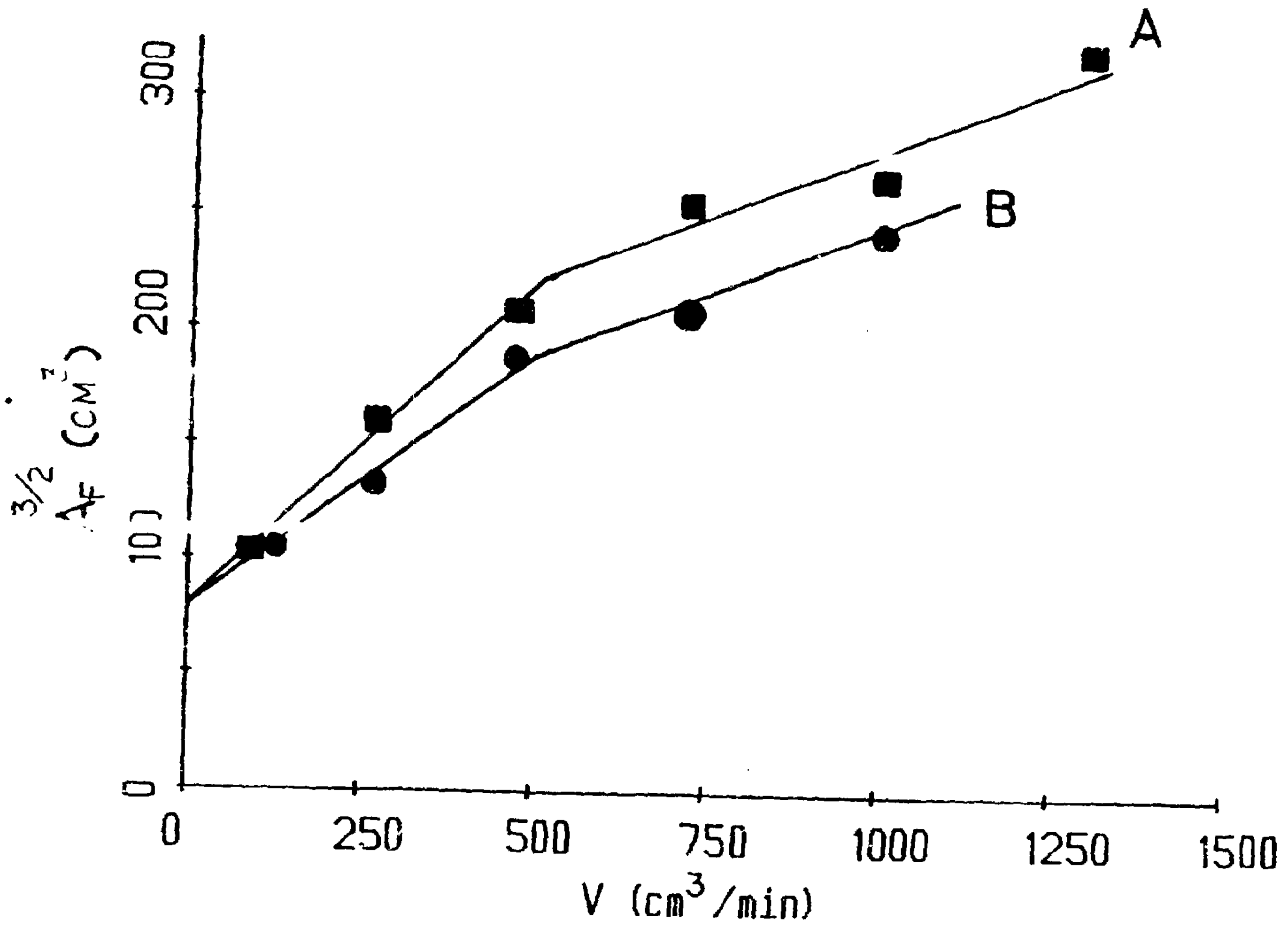

Figure 118. Results of Foam Measurements of Phenothiazine (4.20% w/w) in Tmp-Heptanoate in Conical Foam Meter (r = 23.1 mm) at Various Temperatures.
A = 79.1°C B = 79.7°C

Table 25. Foaminess of a Refined White Mineral Oil

Temp. °C	Σ seconds	Intercept cm³
22.5	104	5.0
40.2	38	6.0
58.0	22	6.0
		5.6 (theor. for r_0=1.0 cm)

The data reported in Figure 112 are for the foam-volume ratios of a solution of phenothiazine (4.20 % w/w) in tmp-heptanoate at various flow rates of gas input and at various temperatures, measured in a conical foam meter. These data are replotted according to equation [11] as $A_f^{3/2}$ versus volume flow-rate of gas, $\dot{V}$, ml/minute; and are displayed in Figures 116, 117, and 118. The initial portion of the data at each temperature gives a straight line from which the characteristic unit of foaminess Σ can be derived. The results are given in Table 26.

Table 26. Foaminess of Phenothiazine (4.2% w/w) in Tmp-heptanoate

Temp. °C	Σ seconds	Σ / μ * sec²/m²	Intercept cm³
30.2	7.92	40	76
40.2	6.48	46	76
49.9	6.84	66	76
60.3	5.22	70	83
70.1	5.64	99	76
79.7	4.56	95	76
			68.6 (theor. for r_0=2.31 cm)

* Foam stability Σ divided by kinematic viscosity μ .

According to an analysis of dynamic foams by D'yakonov[30], the initial linear portion of foam curves, such as those shown in Figures 115 to 118, corresponds to low values of the Reynolds number and is characterized by a linear relation between the volume of the foam created and the rate of gas injection. The Reynolds number, Re, isgiven by:

$$Re = vd/\mu \qquad [12]$$

Where v is the linear flow rate of gas in m/sec; d is the diameter of the vessel in meters; μ is the kinematic viscosity in m²/sec. Equation [11] is valid for this region, where the volume of foam created is independent of the Reynolds number. At greater flow rates of injected gas, the foam created is no longer independent of Reynolds number, and the stability of the foam now depends on the kinematic conditions of the foaming process. These conclusions are illustrated by D'yakonov for a cylindrical foam container; the data reported here for a conical foam container also correspond to the terms of his analysis.

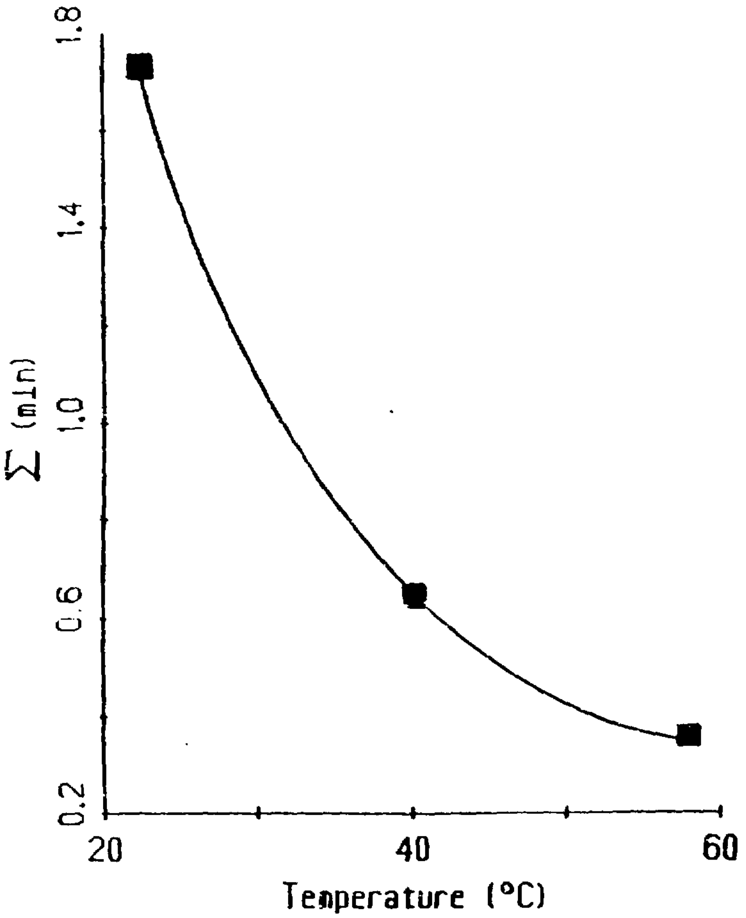

Figure 119 Variation of Foam Stability (Σ in seconds) of Mineral Oil (as is) with Temperature.

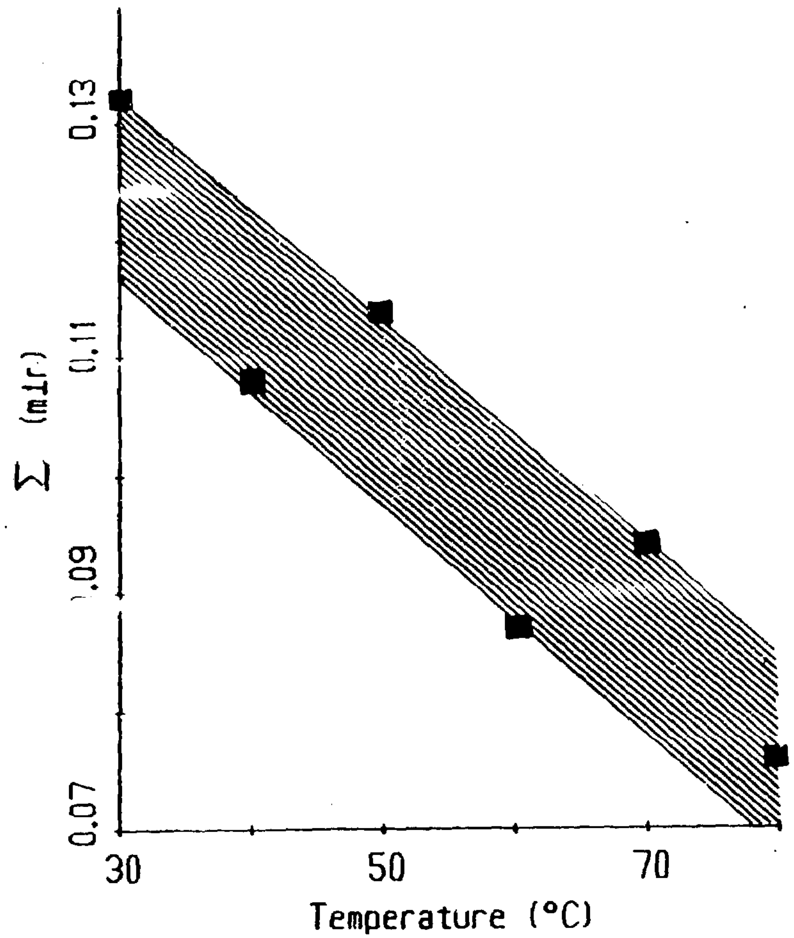

Figure 120 Variation of Foam Stability (Σ in seconds) of Phenothiazine (4.20% w/w) in Tmp-Heptanoate with Temperature.

A comparison of our results for the same solution and the same kinematic conditions applied to the cylindrical and conical foam meters, using the appropriate equations for each, shows that the portion of the relation between foam volume and gas flow that is independent of the Reynolds number is more extended in the cone than in the cylinder. For practical purposes that fact establishes the superiority of the conical form of foam meter to determine the innate foaminess of a solution, which is the nearest approximation yet devised to the ideal "unit of foaminess," as characteristic of a liquid as its density, viscosity, etc.

The variation of the foaminess with temperature is depicted in Figure 119 for the mineral-oil solution and in Figure 120 for the solution of phenothiazine in tmp-heptanoate. These stabilities decrease at higher temperatures, but a factor in this decrease of foaminess is the concomitant decrease of the bulk viscosity of the solution.

In conclusion, therefore, we have distinguished several factors that go to make up the dynamic foaminess and its variation with temperature as measured by Test Method 3213. These are:

a. Compressional/dilational or kinematic surface tension of the solution, rather than its static surface tension;
b. Kinematic viscosity of the solution;
c. Geometric shape of the container;
d. Flow regime of the injected gas.

Factor a. is measured by the compression-dilatation cycles of our surface tensiometer. Factor b. is measured by conventional instruments, such as the Ostwald viscosimeter. Factor c. was investigated by means of our cylindrical and conical foam meters. Factor d. is a variable that we have studied (see Figures 111 and 112.) Isolating the effects of these variables requires correlative results on the same solutions measured by the various instruments listed above.

10. Normalizing Foam Stabilities for Changes of Viscosity

The effect of normalizing for changes of viscosity was determined for the family of curves obtained with a solution of phenothiazine (4.2 % w/w) in tmp-heptanoate, previously reported in Figure 111. These data were extended by measuring foam volumes at additional temperatures. Figure 121 shows that the value of the ratio of foam volume to kinematic viscosity is now independent of temperature for flow rates up to 280 ml/minute. At higher flow rates the ratio is temperature dependent, which may be more the result of a change in the flow regime than of a change in the surface activity of the solution.

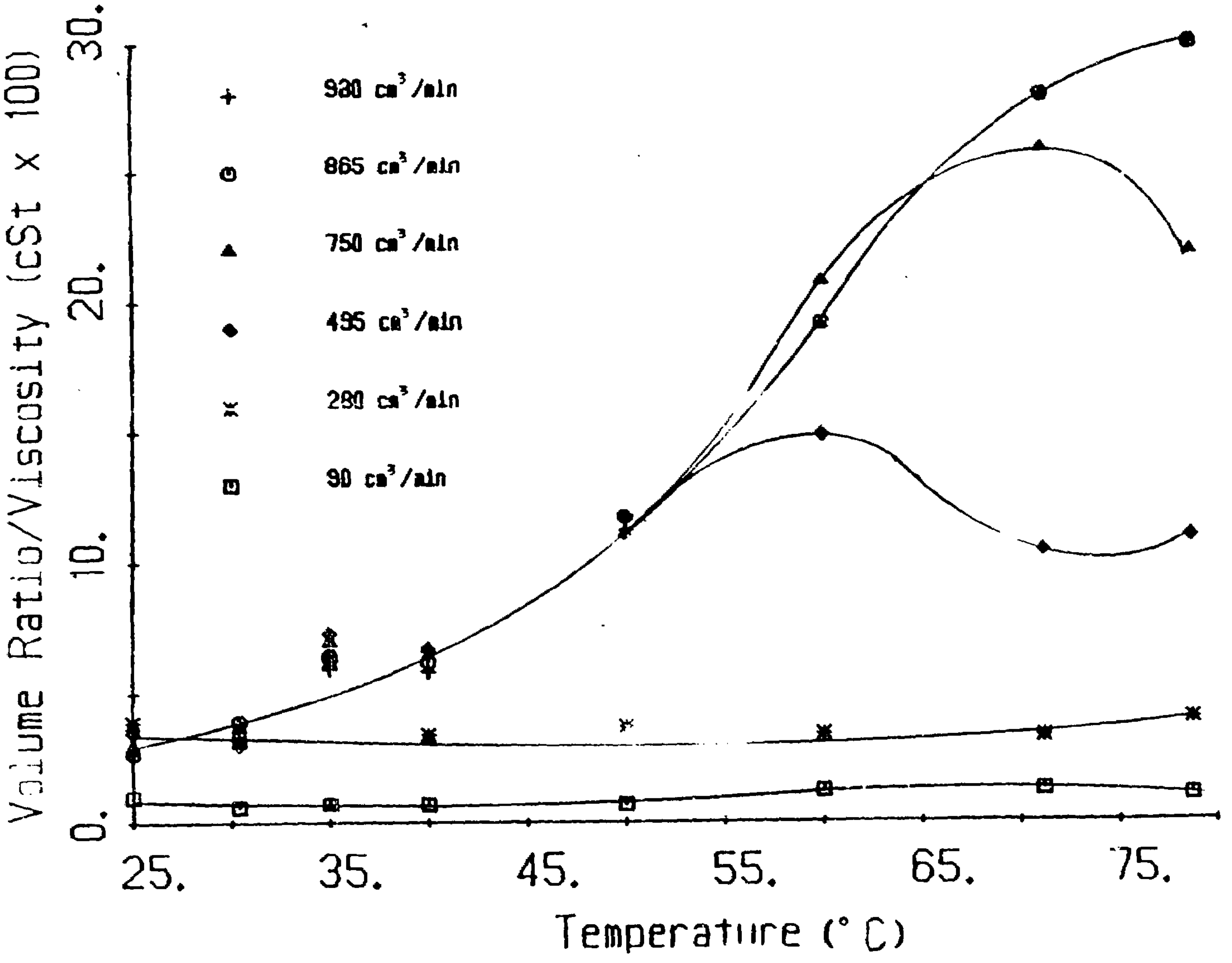

Figure 121. Variation with Temperature of the Foaminess-Viscosity Ratio of a Solution of Phenothiazine (4.20% w/w) in Tmp-Heptanoate at Different Rates of Flow of Nitrogen Gas.

SECTION XIV

RETARDATION OF THE ASCENT OF GAS BUBBLES BY SURFACE-ACTIVE SOLUTES IN NON-AQUEOUS SOLUTIONS

1. Introduction

Many interfacial phenomena, such as emulsification, dispersion, foaming, and wetting, are active chiefly under dynamic or non-equilibrium conditions. The stability of a single bubble produced from various solutions and the velocity of rise of a single bubble in these solutions are both related in different ways to dynamic properties of the interface. Several studies of these phenomena have been reported pertaining to aqueous solutions of surface-active solutes, but few of non-aqueous systems. Water is an atypical solvent, however, and offers special difficulties of inadvertent contamination: one part of a surface-active solute in ten million parts of water stabilizes a single bubble and retards its rate of rise through the solution. Non-aqueous solvents are much less susceptible to these effects on contamination and besides are worth study on their own account and for comparison with what is known of the behavior of aqueous systems.

The rate of rise of single air bubbles in a solution and the stability of a single air bubble on the surface of a solution are both determined by the behavior of newly formed interfaces that are subject to forces of dilatation and compression. In a pure liquid, a rising bubble moves faster than predicted by Stokes' law, since mobility of its interface allows lower velocity gradients in the liquid than those that develop at an immobile, or solid, interface. When surface-active solute is adsorbed at the interface, however, the circulation at the surface and inside the bubble is restricted; the velocity gradients at the interface are increased; until at the limit the surface of the bubble acquires the properties of a rigid sphere, and its rate of rise is reduced to that given by Stokes' law. The stability of a single bubble also depends on the presence of an adsorbed solute at an interface that is subject to forces of dilatation and compression. Comparing these two effects in the same series of solutions, reveals similarities of behavior, that can be described or explained by the theory of bubble rise as given by Levich [31]; and by rather similar considerations to explain bubble stability. Thus we have an hypothesis that of itself and without adjustment for the purpose gives us the rule and reason of a class of facts not contemplated when it was first framed. That is one criterion of a good hypothesis.

2. Theories of Rate of Bubble Rise in Viscous Media

a. Rise in Pure Liquids: Stokes' theory for the terminal velocity of solid spheres in a viscous medium was extended by Rybczynski [32] and Hadamard [33] to fluid spheres. For a liquid drop or a gas bubble of radius r, density ρ_1, and viscosity η_1, moving through an infinite volume of a medium of density ρ_2, and viscosity η_2, the terminal velocity is given by:

$$V_s = \frac{1}{K}\left(\frac{2}{9}\ \frac{(\rho_1 - \rho_2)\mathbf{g}\,r^2}{\eta_2}\right) \qquad [13]$$

where K, the Rybczynski-Hadamard correction factor, has the value:

$$K = \frac{3\,\eta_1 + 2\,\eta_2}{3\,\eta_1 + 3\,\eta_2} \qquad [14]$$

The derivation of equation [14] postulates that the medium exerts a viscous drag on the surface of the bubble or liquid drop, and so sets up a circulation of the fluid contained inside, whether gas or liquid. According to the equation, bubbles containing a circulating gas, with $\eta_1 << \eta_2$, would move fifty percent faster ($K = 2/3$) than those in which the gas, for any reason, does not circulate; for in the latter case the Rybczynski-Hadamard factor does not apply, and the velocity of the fluid sphere is given by the unmodified form of Stokes' law.

Garner[34, 35] demonstrated experimentally the existence of the circulation inside air bubbles and examined the effects of bubble size and shape. He showed that the validity of the above equations is limited to the range of Reynolds' number, Re, less than one {Re < 1}, and to conditions where Stokes' law would hold, including the requirement that the gas bubbles be spheres.

b. Effect of Surface-active Solutes: Levich was the first to provide a satisfactory explanation of the retardation of the velocity of a rising bubble caused by surface-active solutes in the medium. He postulated that adsorbed solute is not uniformly distributed on the surface of a moving bubble. The surface concentration on the upstream part of the bubble is less than the equilibrium concentration, while that on the downstream part is greater than equlibrium. This disequilibration of the concentrations is brought about by the viscous drag of the medium acting on the interface, which in turn creates a disequilibrium of interfacial tensions, with the lower tension where the concentration of adsorbate is greater. The liquid interface then flows from the region of lower tension to that of higher tension, and the direction of this flow offsets the flow induced by the viscous drag of the medium acting on the interface. The internal circulation of fluid is thereby inhibited to a greater or lesser degree; if completely inhibited, the terminal velocity of rise is reduced to that given by Stokes' law.

Another mechanism was introduced by Robinson[36] for the effect of surface-active solutes on the terminal velocity of bubble ascent in a viscous medium. He related the observed retardation to the presence of an immobilized layer of the medium accompanying the bubble during its rise and so changing its effective density. He assumed that Stokes' law still applied, K = 1, and used it to calculate the effective density of the bubble from its measured rate of rise. The effective density was translated into terms of the thickness of the accompanying shell of the medium that accompanies the bubble. Unlike the Levich theory, in which the least velocity of rise is given by the Stokes value (with K = 1 for the more concentrated solutions,) and the greatest velocity of rise is given by 1.5 times the Stokes value (with K = 2/3 for the more dilute solutions,) Robinson's theory predicts that the upper limit of velocity is given by the Stokes value, while the lower velocity is not limited to any theoretical value but is determined by the presence of an adherent immobilized layer and its increase of thickness with concentration of solute.

3. Experimental

a. Apparatus and Procedure for Measuring Rate of Bubble Rise: By means of an extended syringe, single bubbles of air were released at a capillary orifice into oil contained in a graduated cylinder, 70 cm high and 26 mm internal diameter. The volume of air in each bubble was measured before its release, while the air was still contained inside a capillary tube of known diameter (0.397 mm,) by measuring the length of the air slug with a cathetometer, with a precision of ± 0.01 mm. The diameter of the bubble is obtained from this measured volume, and the Stokes' velocity of rise calculated by use of equation [12], with K put equal to unity. The actual rate of rise of each released bubble was measured with stop watches (± 0.1 seconds) at three different points along its upward path inside the cylinder. The measured velocities are corrected for the effect of the presence of the confining walls of the cylinder by the Ladenburg equation: [35, 37]

$$V_c = V_m (1+2.1\, d/D) \qquad [15]$$

where V_c = corrected rate of rise;
V_m = measured rate of rise;
d = bubble diameter;
D = diameter of cylinder.

For bubbles of an average diameter of 1.1 mm, rising in a tube of 26 mm diameter, this equation gives a correction of 8.9%. For each bubble, the observed Rybczynski-Hadamard correction factor was obtained from the relation:

$$K = V_c / V_s \qquad [16]$$

All measurements were made at 21 ± 1°C.

b. Measurement of the Stability of a Single Bubble: The method of measurement has been described above, see Section IX.1.

c. Measurement of Physical Properties: Densities of solutions in the range of temperature 18°C to 27°C were measured with a pycnometer (capacity 27.7 ml) placed in a water thermostat bath with temperature control ±0.1°C. Viscosities of solutions in the same temperature range and temperature control were measured with an Ostwald viscosimeter. Surface viscosities were measured with a torsional-pendulum viscosimeter, for which see Figure 49. The semi-logarithmic decrement of its oscillations was determined with and without solute, at 25±0.1°C, with dry nitrogen gas flowing across the surface to prevent sorption of water vapor. Each solution was stirred for at least fifteen minutes and then allowed to remain at rest for thirty minutes before each measurement. Measurements were repeated after one hour and again after two hours.

d. Materials:

White mineral oil -- lubricant laxative grade;
Trimethylolpropane heptanoate (Base Stock 704), practical grade -- Stauffer Chemical Co.
Sorbitan monolaurate (Span 20) -- ICI Americas Inc.
Polydimethylsiloxane, 1000 centiStokes -- General Electric Co.
N-phenyl-1-naphthylamine -- Eastman Kodak, No.351

4. Results

In Table 27 are reported the experimental conditions, physical properties of the solutions measured, and the range of Reynolds numbers ($R = ur/\mu$,) and of Bond number ($B = \rho r^2 g/\sigma$,) which are used as criteria of the spherical shape ($B < 0.1$) and of the transition from fluid to solid behavior ($B > 1$ is fluid; $B < 1$ is solid) [37, 38, 39]. The Reynolds numbers show that the systems were in the regime of viscous flow required for the valid application of Stokes' law. The spherical shape was verified experimentally by photographing the rising bubble in the same focal plane as a steel ball-bearing (diameter 1.46mm.) Figure 122 shows a bubble perfectly spherical in one of these photographs. The same result was obtained in all the solutions measured, with air bubbles of diameter $d = \leq 1.3$mm. The slug of air from which a bubble is formed is also visible in Figure 122.

The velocity of ascent of bubbles was measured in four series of solutions:

Sorbitan monolaurate (Span 20) in white mineral oil;
Polydimethylsiloxane in white mineral oil;
Polydimethylsiloxane in tmp-heptanoate.
N-phenyl-1-naphthylamine in tmp-heptanoate.

The results of a few tests to find the change of velocity with height in the column are reported in Table 28. The lengths of the air slugs, given in column e, are used to calculate diameters of the bubbles formed from them (column f,) taking into account the meniscus volumes. The velocity of each ascending bubble (column j) was measured at each of three sections of 20.0 cm length along the column, namely, 10 to 30 cm, 25 to 45 cm, and 40 to 60 cm from the orifice. The measured velocities were corrected for wall effects according to equation [15] and are reported in column k.

Table 28 shows:

In the mineral-oil solvent the value of K obtained is 1.53, which is within the experimental error of the theoretical value of K = 1.50; this finding and the invariability of the velocity of ascent with height indicate that the solvent is free of surface-active contaminants.

In the solutions of highest concentrations of Span 20 and of polydimethylsiloxane, the measured velocities of ascent of bubbles are equal to the Stokes' velocities (K = 1) and no variation with height is observed, which indicates that adsorption at the bubble surface takes place rapidly.

Table 27. Experimental Conditions, Physical Properties of Solutions, and Dimensionless Groups

Solvent	Temp. °C	Bubble Diameter m $\times 10^{-2}$	Density kg/m^3 $\times 10^{-3}$	Solvent Surface Tension mN/m	Kinematic Viscosity m^2/sec $\times 10^6$	Bubble Velocity m/sec $\times 10^2$	Re	B
Mineral Oil	20-22	0.095-0.130	0.873-0.874	31.7	2.00-2.27	0.28-0.60	0.0056-0.020	0.054-0.113
Tmp-Hept.	20-22	0.090-0.130	0.960-0.961	30.6	0.28-0.31	1.0-3.0	0.15-0.70	0.063-0.131

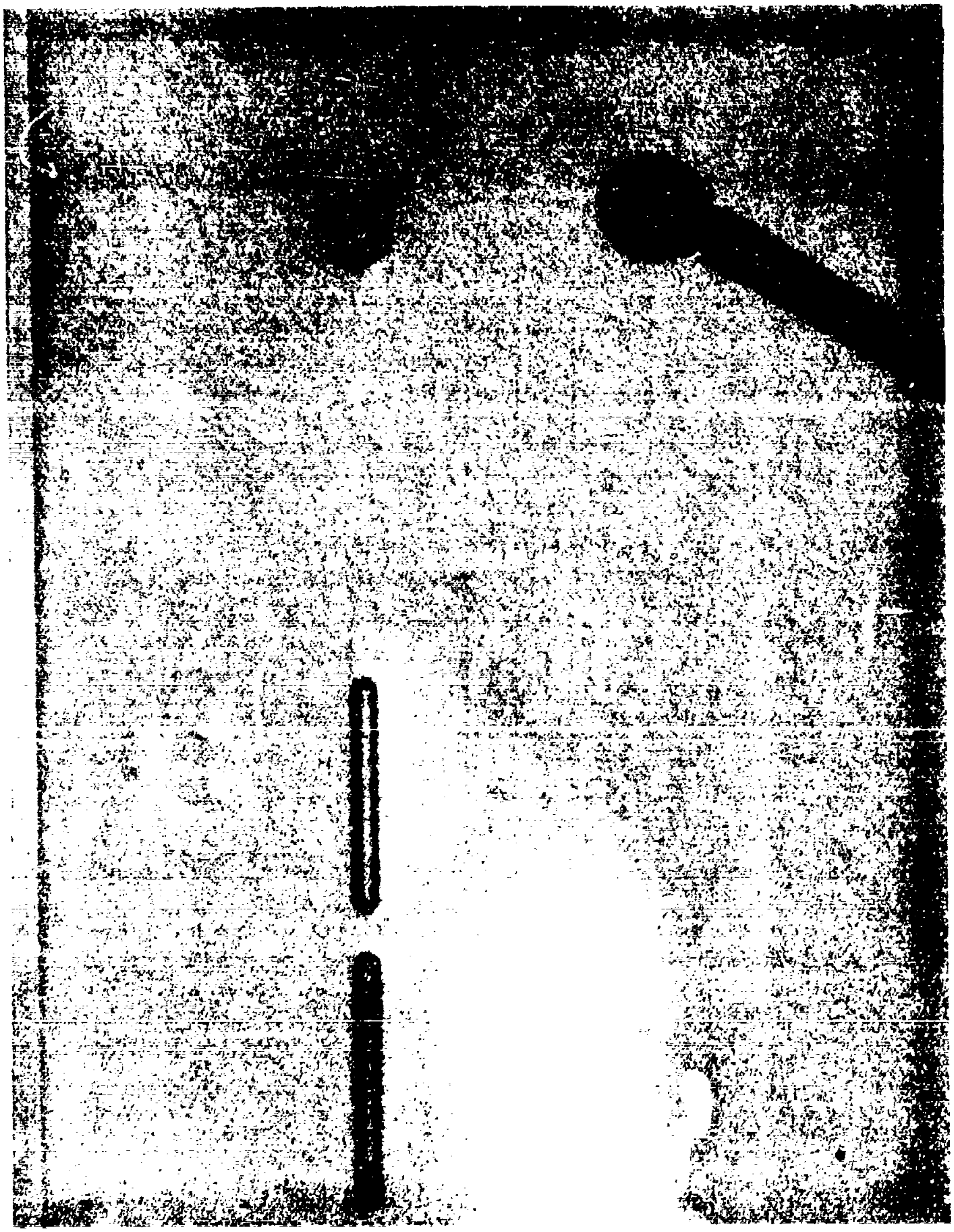

Figure 122. Photograph of a Bubble and a Steel Ball Bearing.

Table 28. Bubble Velocities at Various Column Heights for Solutions of Selected Solutes in Mineral Oil

Solution in Mineral Oil	Conc. (ppm)	Temp. (°C)	Kinematic Viscosity (cSt)	Air Slug Length (cm)	Bubble Diameter (cm)	Stokes' Velocity (cm/sec)	Column Section	Time of Rise (sec)	Velocity (cm/sec)	Corrected Velocity (cm/sec)	K
a	b	c	d	e	f	g	h	i	j	k	l
Span 20	7160	20.9	213	0.660	0.115	0.338	1	64.4	0.311	0.340	1.01
							2	64.2	0.312	0.341	1.01
							3	63.6	0.314	0.343	1.02
	226	21.2	209	0.560	0.109	0.310	1	48.4	0.413	0.449	1.45
							2	53.6	0.373	0.406	1.31
							3	57.6	0.347	0.378	1.22
Pure Mineral Oil		20.4	221	0.561	0.109	0.293	1	48.4	0.413	0.449	1.53
							2	48.2	0.415	0.452	1.54
							3	48.4	0.413	0.449	1.53
PDMS	3.23	21.7	204	0.750	0.120	0.387	1	38.6	0.518	0.568	1.47
							2	41.6	0.481	0.528	1.36
							3	43.0	0.465	0.510	1.32
	61.7	20.7	218	0.515	0.106	0.280	1	75.8	0.264	0.287	1.02
							2	76.0	0.263	0.286	1.02
							3	75.6	0.265	0.288	1.03

At intermediate concentrations of solute in mineral oil, the velocity of ascent of a bubble becomes significantly less as the bubble rises. This effect is not caused by adsorption of solute continuing to occur during the ascent. The rate of adsorption at a freshly created surface of these solutions is so slow that in the forty or so seconds during which the bubble rises through the column the surface tension does not depart from that of the solvent. The growth of the retardation of the rate of ascent of the bubble during its ascent is therefore to be ascribed to the time required for the dynamic equilibrium between viscous drag and Marangoni flow to be established at the bubble surface. Ideally for this situation the column provided would have to be of sufficient length so that the velocity of ascent reaches a constant value in the upper stretches of the column; lacking that, we take for future use the lowest measured velocity (in the highest part of the column.) The significance of the data reported is to identify the range of concentration at which the transition occurs in each solution, rather than to provide accurate values of K in the transitional range.

The values of the Rubczynski-Hadamard correction factor, K, are averaged for at least five repeated measurements for each solution. The dependence of the value of K on concentration of solute is reported in Figures 123, 124, and 125. In Figure 123, K is reported: (A) for solutions of polydimethylsiloxane (1000 cSt) in mineral oil in the range of concentrations 0.1 to 60 ppm; and (B) for for solutions of Span 20 in mineral oil in the range of concentrations of 50 to 7200 ppm. In Figure 124A, K is reported for solutions of polydimethylsiloxane (1000 cSt) in tmp-heptanoate in the range of concentrations of 0.1 to 30 ppm; and in (B) the stability of single bubbles in these solutions for the same range of concentrations at the same temperature. Figure 125A reports the values of K for solutions of N-phenyl-1-naphthylamine in tmp-heptanoate in the range of concentrations 0.01 to 5% (w/w); and in (B) the stability of single bubbles in these solutions for the same range of concentrations at the same temperature.

In Figure 126 are reported the measurements of surface viscosity of two solutions of Span 20 in mineral oil, concentrations of 69.9 ppm and 5010 ppm (A;) and of two solutions of polydimethylsiloxane in tmp-heptanoate, concentrations of 0.31 ppm and 29.3 ppm (B.) In the diagram, the damping of the oscillation of the disc in the surface, expressed as the ratio of the lengths of the first to the nth amplitude, is plotted *versus* the swing number. Figure 126 shows that the surface shear-viscosities of the two solutions in each solvent are the same; and indeed do not differ from that of the solvent alone in each system.

5. Discussion

Figures 123, 124, and 125 show that the ratio of the observed velocity of ascent of a bubble to the calculated Stokes' velocity varies between the limits $0.99 < K < 1.52$ for the solutions in mineral oil, and the limits $0.95 < K < 1.47$ for the solutions in

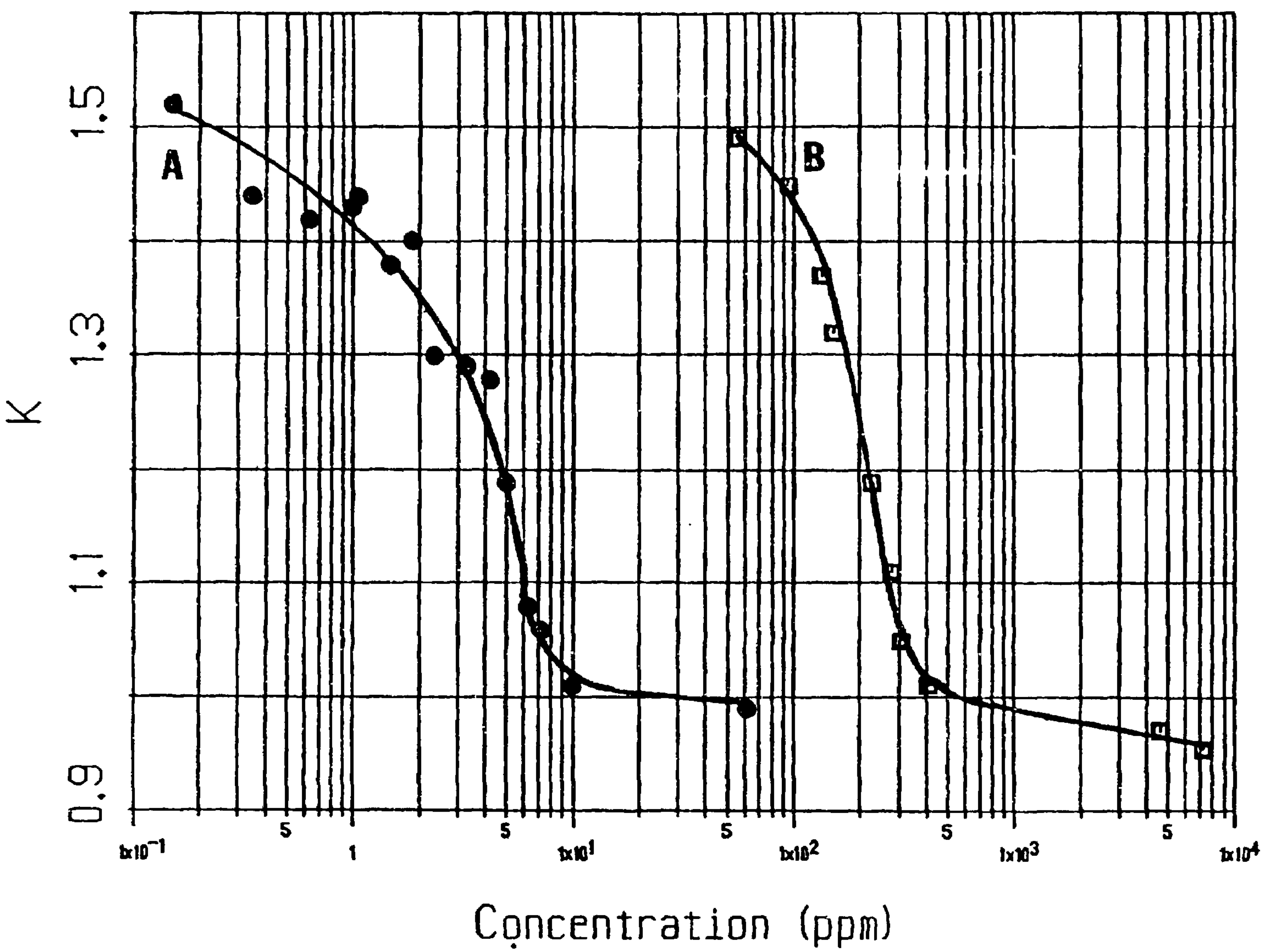

Figure 123. Comparative Rates of Ascent (Corrected for the Effect of the Wall) of Air Bubbles in Mineral Oil at 22°C Containing
(A): Various Concentrations of Polydimethylsiloxane (1000 cSt);
(B): Various Concentrations of Span 20 (Sorbitan Monolaurate).

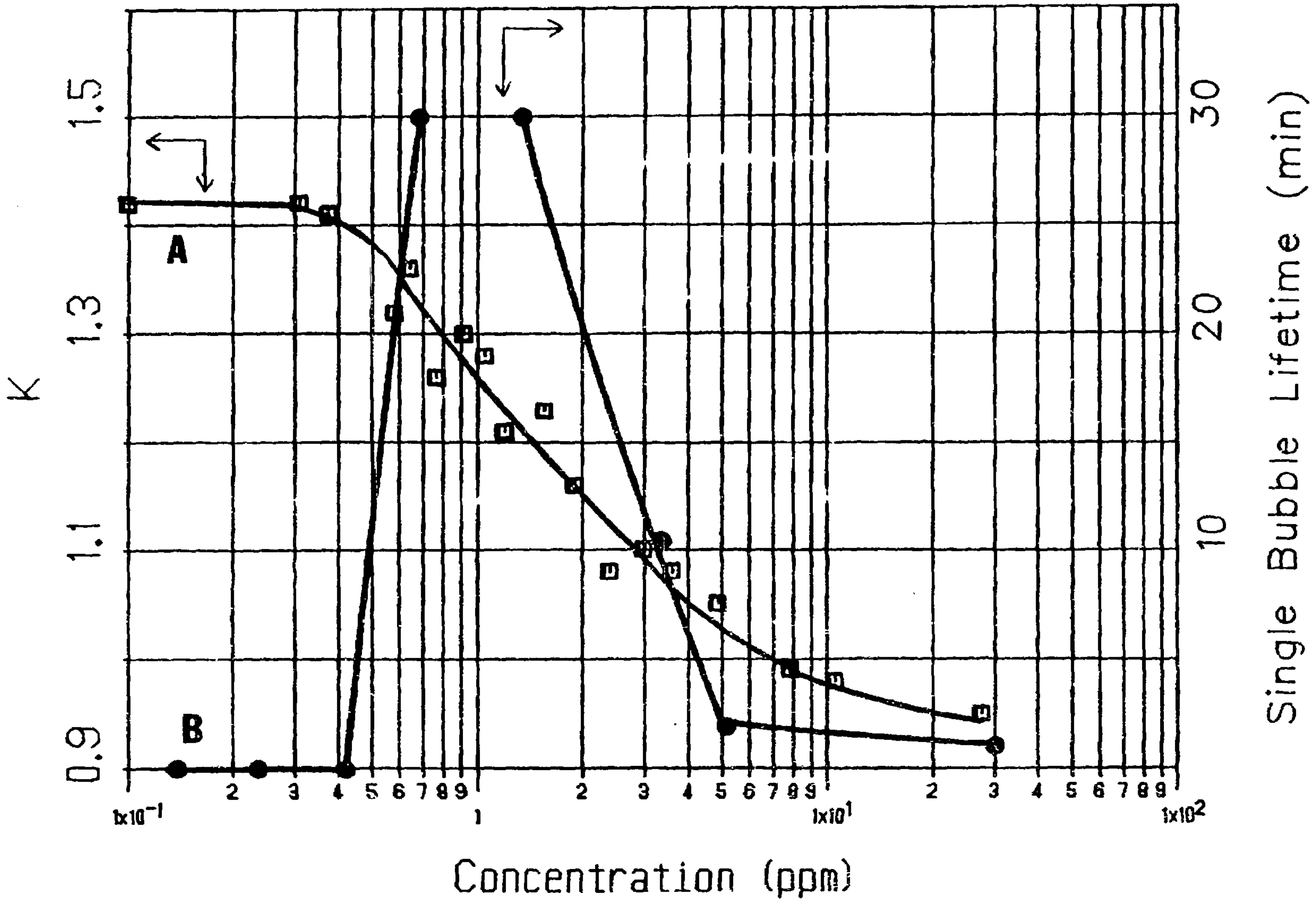

Figure 124. (A) Comparative Rates of Ascent (Corrected for the Effect of the Wall) of Air Bubbles in Tmp-Heptanoate at 22°C Containing Various Concentrations of Polydimethylsiloxane (1000 cSt.)
(B) Stability of Single Bubbles in the Same Series of Solutions at the Same Temperature.

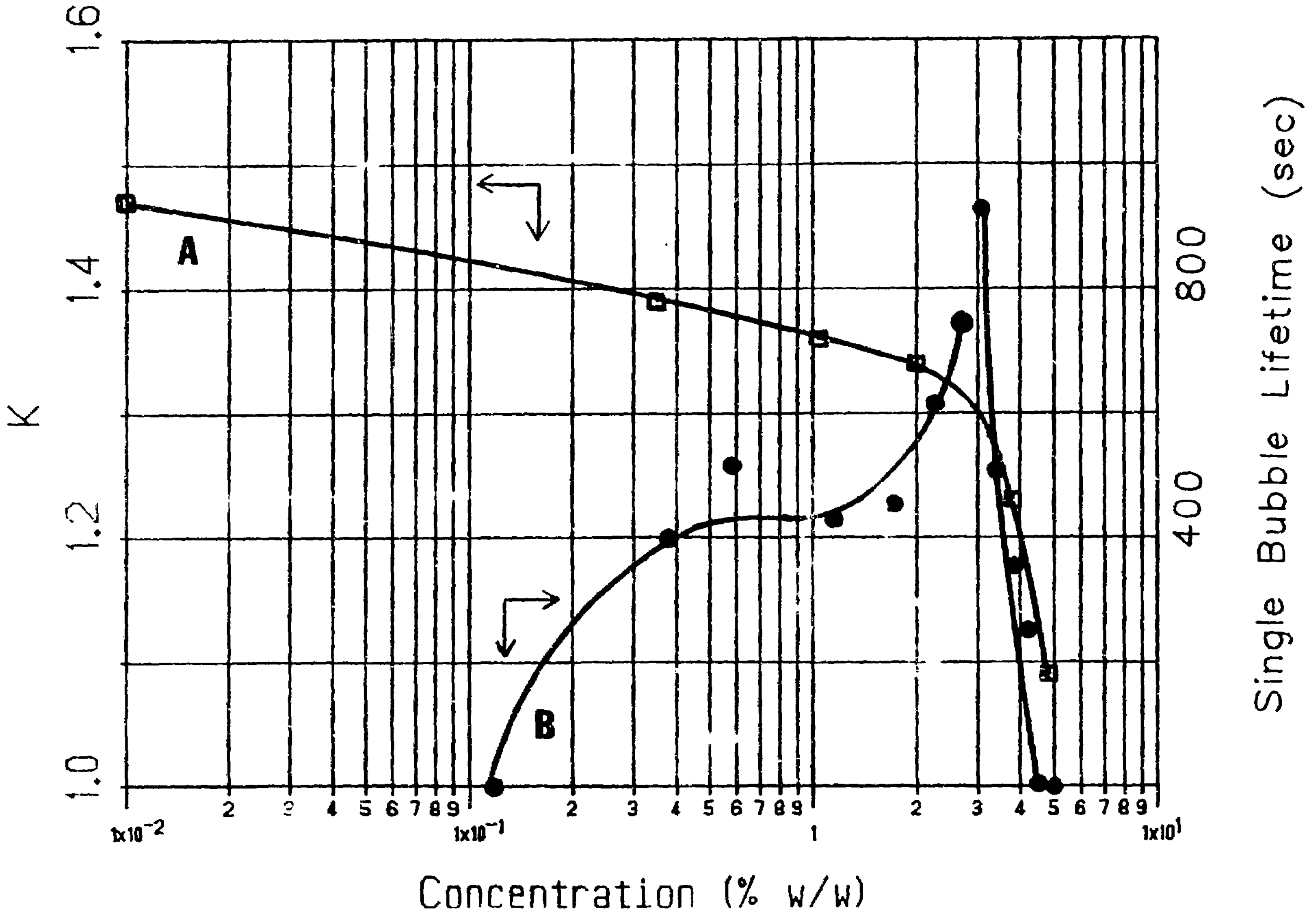

Figure 125. (A) Comparative Rates of Ascent (Corrected for the Effect of the Wall) of Air Bubbles in Tmp-Heptanoate at 26°C Containing Various Concentrations of N-Phenyl-1-Naphthylamine.
(B) Stability of Single Bubbles in the Same Series of Solutions at the same Temperature.

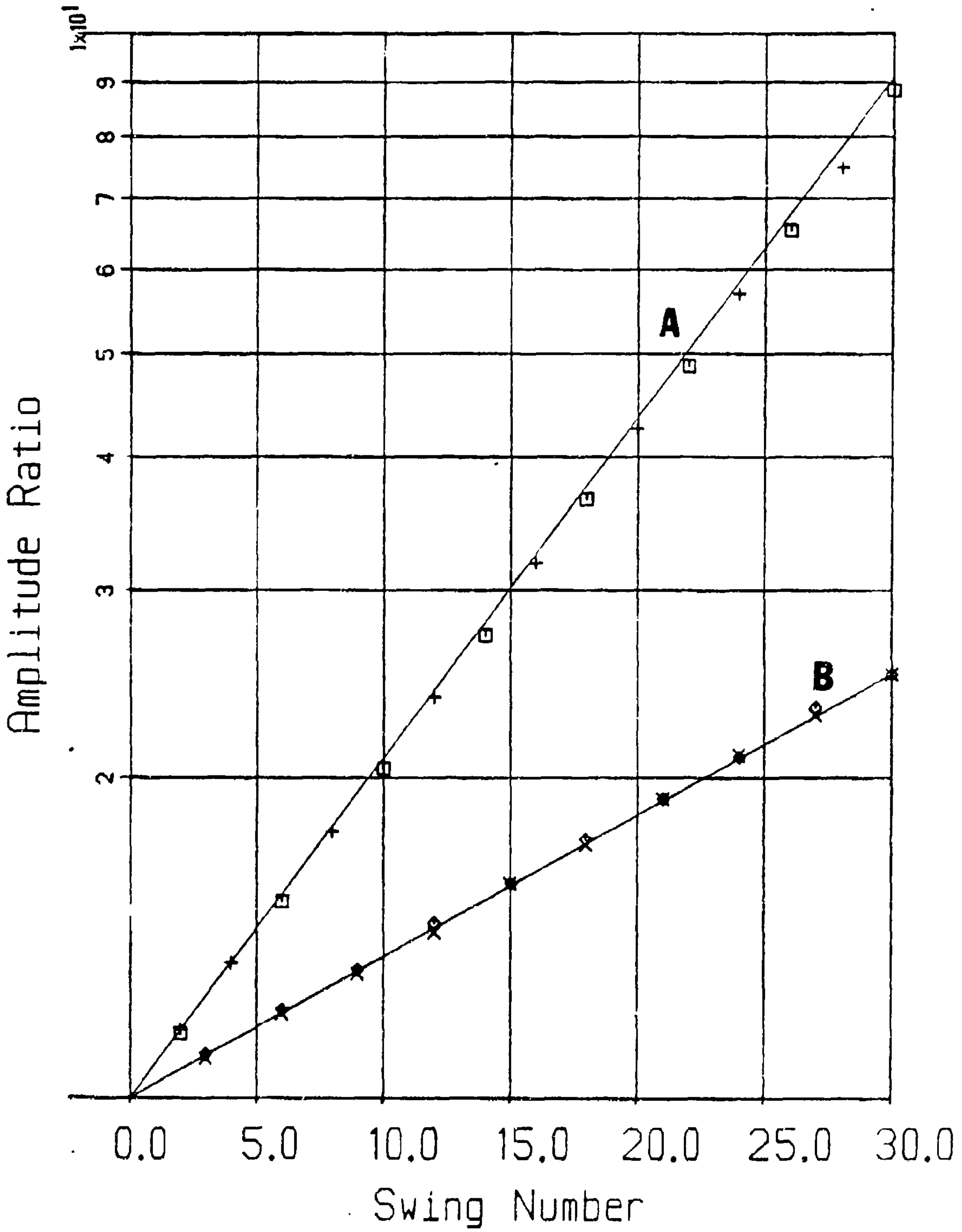

Figure 126. Semi-Logarithmic Decrement of Amplitudes of Torsional-Pendulum Surface Viscosimeter.
(A) Mineral oil Solutions of Span 20 at Concentrations of 70 ppm and 5010 ppm at 22°C.
(B) Tmp-Heptanoate Solutions of Polydimethylsiloxane (1000 cSt) at Concentrations of 0.31 ppm and 29.3 ppm at 26°C.

tmp-heptanoate. The value of K = 1.52 obtained for the mineral oil and 1.47 for the tmp-heptanoate demonstrates the absence of any surface-active contaminant therein. No significance is attached to the difference of 0.05 units from the theoretical value at the lower limit, K = 1.00, as fluctuations of that magnitude at that limit are within the experimental error. Figure 124 also shows that the range in which K is concentration dependent is 0.1 ppm $< \underline{c} <$ 20 ppm for solutions of polydimethylsiloxane both in mineral oil and in tmp-heptanoate. For solutions of Span 20 in mineral oil, the lowest concentration for any measurable variation in the value of K is 500 times greater; but the range of concentration through which the variation of K takes place is narrower, i.e., 50 ppm $< \underline{c} <$ 500 ppm. The solute N-phenyl-1-naphthylamine in tmp-heptanoate requires still greater concentration before its effect is found, showing that it is only slightly surface active in this solvent.

Adsorption equilibrium was certainly not attained in the various solutions that were tested. Equilibration is rapid at higher concentrations, but is slow with the more dilute solutions. The adsorbed layer of solute is very dilute in these oil solutions. Although the equilibrium surface tension is less than that of the solvent, the time required for these solutions to reach equilibrium is several hours; therefore, the rise of the bubble and the lifetime of the single bubble at the surface are phenomena too fleeting to be referred to equilibrium surface concentrations of solute. During the whole time period of their existence the surface tension of the solution is not altered from that of the solvent; nevertheless the interpretation of the phenomena displayed by the bubble argues that traces of positively adsorbed solute are indeed present; enough, when subjected to a force of compression, to establish the local difference of surface tension that is the basis of Marangoni flow and of the retardation of the rate of bubble rise.

Various theories and criteria for this process have been put forth by different authors. Bond's criterion for the transition from fluid to solid behavior, namely B > 1 for fluids, B < 1 for solids, was not confirmed in these studies. Values of K of 1.5, indicating fluid behavior, were found at B = 0.055, as for example with small bubbles of d = 0.9 mm in mineral oil at 21°C. The criterion for spherical shape, namely B < 0.1, was also not confirmed; bubbles up to the largest value of d = 1.3 mm, were all found to be perfect spheres.

In these studies, measurements of surface shear-viscosity did not reveal any evidence for higher viscosity in any of the solutions studied; therefore, no positive evidence is adduced to favor the supposition that a plastic skin accounts for the rigidity of the bubble surface.

The inhibition of circulation at the surface and inside the bubble is accepted as the explanation of the remarkable retardation of the ascending velocity of the bubble. Okazaki et al.[40] found that a concentration of sodium dodecyl sulfate (SDS) in water as low as 10^{-5} molar will retard the rate of ascent of a bubble in that solution, and also confers stability to a single bubble at its surface, even though the static properties of the liquid, i.e., the density, the bulk compressibility, the viscosity, and the surface tension, all remain unchanged from those of pure water. The dynamic surface tension, i.e., the time dependence of the surface tension, is also absent in 10^{-5} molar SDS in water; and no measurable increase of the shear viscosity of the surface of a solution so dilute was observed.

Our oil solutions behave in many respects as do these very dilute aqueous solutions of SDS in water at concentrations of 10^{-6} to 10^{-4} molar, investigated by Okazaki et al. In our systems as in theirs, what would appear to be static and dynamic properties of the solution pertinent to surface activity show no change from those of the solvent, yet both the rate of rise and the stability of a single bubble are greatly affected by the presence of the solute.

Robinson [36] ignores the Rubczynski-Hadamard correction and assumes the Stokes' velocity for bubbles at all concentrations of solute. His theory is therefore unable to explain our finding velocities larger than Stokes' velocity; nevertheless it would account for observed velocities less than the Stokes' velocity, although we observed none such.

6. Rate of Ascent of a Bubble in Solutions of Aerosol OT in Tmp-Heptanoate

The rate of bubble rise was measured in a solution of 1.94% w/w Aerosol OT in tmp-heptanoate at room temperature (23°C.) The retardation of the velocity of rise was much less than expected, considering the high concentration of solute (see Table 29 below.) The reason may be a slow rate of adsorption, or it may be a low surface activity of this solute in oil. Only further experiments can determine which of these alternatives is more likely. Something more could be done with the present experiments, however, bearing on this question. Bubbles may be released from the capillary tip immediately after being formed; or they may be retained for a time at the tip, to allow more adsorption to occur. To test the hypothesis of slow adsorption at the liquid-gas interface, bubbles were kept at the tip for some additional minutes before disconnection. The average values of K (ratio of measured velocity to Stokes-law velocity) are presented in Table 29.

Table 29. Values of K in a Solution* of Aerosol OT (1.94% w/w) in Tmp-Heptanoate at 23°C.

After immediate release	After 5 minutes	After 15 minutes
1.30	1.26	1.22

The results reported in Table 29 show an increased retardation of bubble rise velocity with increasing time of retention at the tip before release, thus lending weight to the hypothesis of a slow rate of adsorption of solute at the liquid-gas interface. The variation of K with time is small, perhaps because the bubbles are located in an unstirred liquid in which mass transfer occurs by a slow process of diffusion.

These experiments allow a comparison to be drawn between foaminess and dynamic surface tension as expressed indirectly by the bubble-rise measurements. In the previous results, pertaining to solutions of polydimethylsiloxane in tmp-heptanoate and to solutions of Span 20 in mineral oil, the rate of bubble rise is completely retarded to the Stokes-law value at concentrations of solute several orders of magnitude less than for the Aerosol OT solutions; and at these low concentrations there is no measurable foaminess. The solutions of Aerosol OT in tmp-heptanoate, on the other hand, do show a strong tendency to foam, along with a small, but detectable, effect of adsorbed solute on the rate of bubble rise. Our search for a correlation between the rate of bubble rise in a solution, which reflects somewhat indirectly the play of dynamic tensions on the surface of a single bubble, and the measurement of foaminess of the solution by standard test methods, has not been successful. In some solutions the retardation of the rate of bubble ascent is fully developed without the development of the ability to foam; and in other cases the retardation has barely begun at a concentration where the foaming ability is fully developed. We see the need here for a more extended range and better control of the measurement of the dynamic surface tension, which our new apparatus now provides; and equally the need for a test of foaminess that is less subject to idiosyncrasies of the test method, for which we propose the measurement of the lifetime of single bubbles, see Section IX.

7. Foaminess and Rate of Ascent of a Bubble in Solutions of Span 20 in Tmp-Heptanoate

We wished to find out if properties like those observed for solutions of Aerosol OT in tmp-heptanoate occur with another amphipathic solute, for which purpose we selected Span 20. Foaminess (by Test Method 3213) and rates of ascent of a bubble were measured with solutions of Span 20 in tmp-heptanoate in the range of

---

* The solution used might be slightly contaminated as it had been used previously for foam testing. Measurements of bubble rise velocities with new solution, immediate release, gave K = 1.40 compared with K = 1.47 for the solvent.

concentrations 0.52 to 2.11 % (w/w). No foaminess in the range of temperatures 24.6 to 80.1°C, and no significant retardation of the rate of bubble ascent at room temperature were observed. Two comparisons are worth notice: Span 20 reduces the rate of ascent of bubbles when dissolved in mineral oil (a hydrocarbon) but not when dissolved in tmp-heptanoate, i.e., it is surface active in a hydrocarbon solvent but not in an ester solvent; and the lack of surface activity of Span 20 in tmp-heptanoate correlates with the lack of foaminess of that solution, whereas the lack of surface activity of Aerosol OT in tmp-heptanoate does not entail a nonfoaming solution. We have investigated the electrical properties of these two solutes in tmp-heptanoate, to discover whether electrical charge is, as we suspect, the operating mechanism that stabilizes foam in the Aerosol OT solutions; and found evidence that indeed it is so (see Section XI.3, Table 18.)

It follows that positive evidence of some surface activity is not by itself a necessary condition for the production of foam. We see the need here for a direct measurement of the surface elasticity of a solution, to discover what degree of elasticity is required to produce a foam under specified conditions of a foam test, such as Method 3213, which is known to correlate with the problem as it occurs in aircraft engines.

8. Correlations between Bubble Stability, Retardation of Bubble Rise, and Foaminess

The stability of single bubbles in solutions of polydimethylsiloxane (1000 cSt) and of N-phenyl-1-naphthylamine in tmp-heptanoate were determined, to find if surface activities as indicated by that property and by retardation of the rate of bubble rise, can be correlated. The procedure for measuring single-bubble stability is described in Section IX.1. Figures 124 and 125 compare the concentration dependence of K (the ratio of the observed rate of rise to that derived from Stokes' law) and the single-bubble lifetime for polydimethylsiloxane (1000 cSt) and N-phenyl-1-naphthylamine solutions respectively. (The solutions in mineral oil were no longer available for the measurement of bubble stability.) Both diagrams show an interesting relation between the two phenomena: the stability of the bubble increases in the same range of concentration as the occurrence of the retardation of the rate of rise. The stability of the bubble reaches a maximum and declines to zero at the same concentration at which the retardation of the rate is reduced to that of a rigid sphere. The maximum of single-bubble stability occurs at K = 1.3 and the zero stability occurs at K = 1.0: neither the perfectly fluid interface (K = 1.5) nor the completely rigid interface (K = 1.0) appear to have the requisite elasticity to stabilize a bubble.

The results of foaminess, as measured by Test Method 3213 are also reported in Figures 124 and 125, and show that no necessary correlation exists between the stability of a single bubble and the stability of a foam as measured by this Method.

As shown in Figures 124 and 125 the stability of single bubbles at the surface of these oil solutions becomes perceptible and gradually increases at the same concentrations of solute at which the retardation of the rate of ascent of the bubble likewise becomes perceptible and gradually increases. A common underlying cause is strongly indicated. The excess surface concentration of solute must be small, too small to reduce the surface tension, yet enough to be swept up by the action of liquid flow around the rising bubble and compressed at its lower surface. These consequences follow: the local difference of surface tension around the bubble stimulates a Marangoni flow in the direction opposite to that of the flow of liquid attendant on its ascent; this counterflow in its turn retards the velocity with which the bubble is rising. A similar action occurs within the lamella of a stabilized bubble: the lamella flows from a convex region to a concave region of the bubble surface, carrying the two surfaces along with it. In such a movement there may be both a dilatational increase of surface tension near the apex of the bubble and a compressional reduction of surface tension around its base; or either type of change may occur without the other. The more concentrated adsorbed solute thus produced in the Plateau borders creates a spreading pressure, which in turn sets up a counterflow and so retards draining and thinning of the lamella. This resistance to flow in the lamella is equivalent in effect to a surface viscosity that is brought into action by the compression of the adsorbed film: it should therefore be termed "compressional surface viscosity." It is similar in its effect to the "dilatational surface viscosity" of Lucassen and van den Tempel[41] on surfaces of aqueous solutions of surface-active solutes, which has its source (of course, only at much higher concentrations) in the increase of surface tension on dilatation of a surface; the compressional surface viscosity arises from the reduction of surface tension on contraction of a surface. Extremely dilute aqueous solutions of surface-active solutes, where the lowering of the static surface tension is undetectable, cannot manifest dilatational surface viscosity, but if the adsorbed film is sufficiently compressed may develop a non-equilibrium reduction of the surface tension.

To obtain a more complete picture of the various possible correlations, Figures 127, 128, and 129 show a comparison between the K values of the ratios of bubble-rise rates and foaminess measured by Test Method 3213 as expressed by gas-volume ratios. These diagrams show that no correlation exists between the concentration ranges at which these two effects occur: the rate of rise of a bubble may be fully retarded at a concentration of solute where there is still no development of foaminess by Test Method 3213, as is shown in Figures 127 and 128; or the solution may have a strong propensity to foam without there being any significant retardation of the rate of rise of a bubble, as is shown in Figure 129 for solutions of Span 20 in mineral oil, or as reported in Table 29 for solutions of Aerosol OT in tmp-heptanoate.

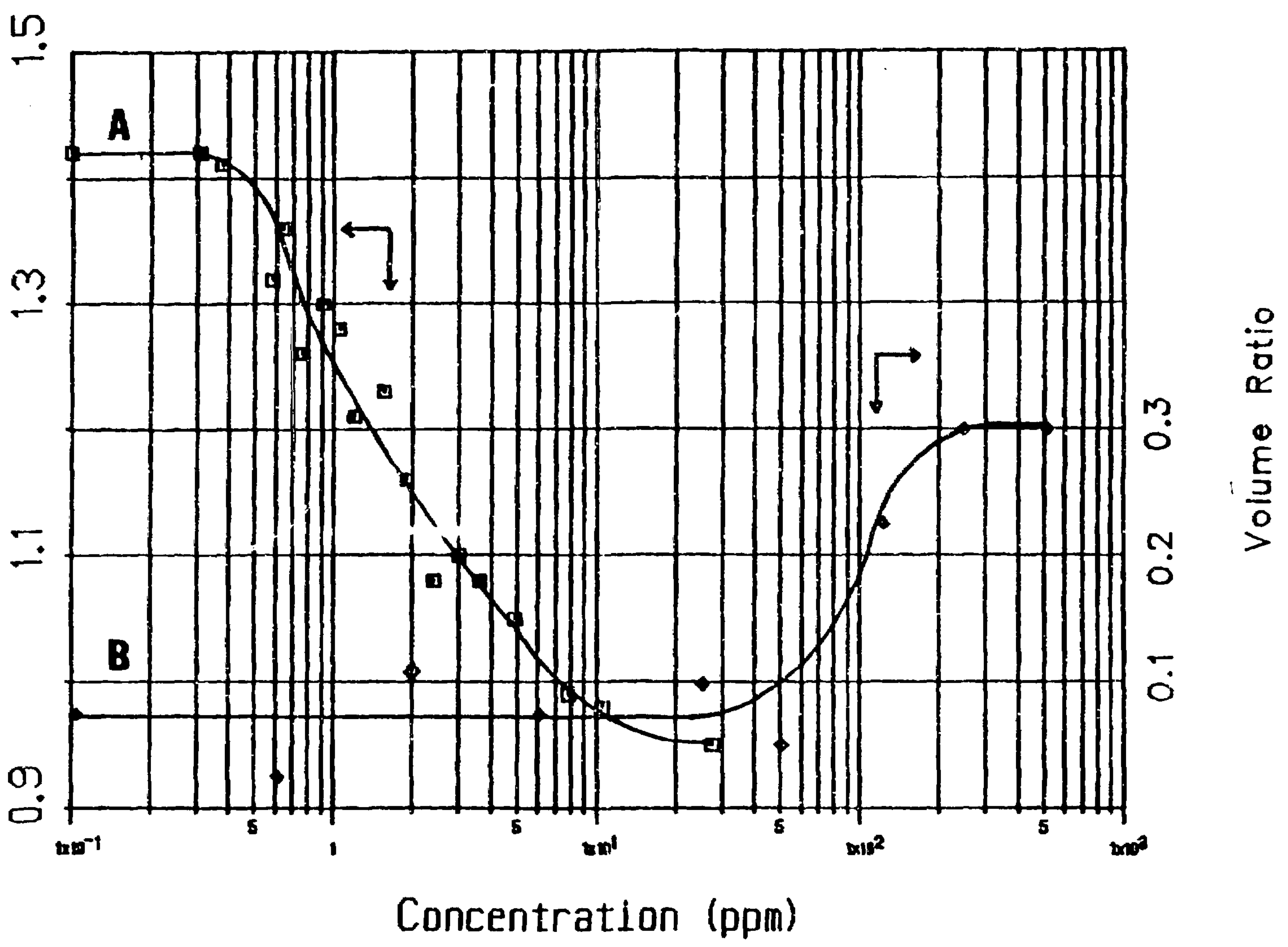

Figure 127. (A) Comparative Rates of Ascent (Corrected for the Effect of the Wall) of Air Bubbles in Tmp-Heptanoate at 22°C Containing Various Concentrations of Polydimethylsiloxane (1000 cSt)
(B) Foaminess by Test Method 3213 of the Same Series of Solutions at the Same Temperature.

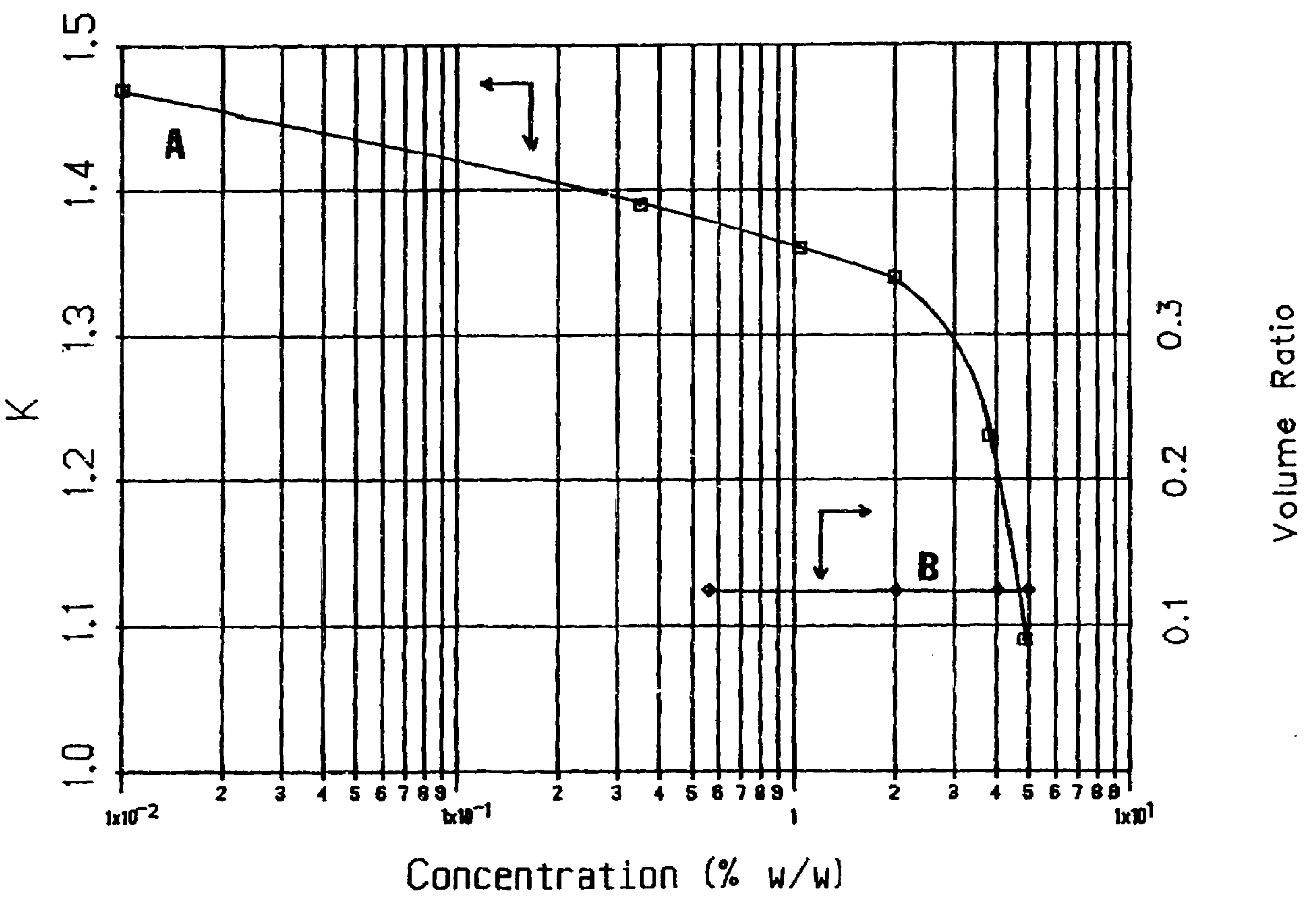

Figure 128. (A) Comparative Rates of Ascent (Corrected for the Effect of the Wall) of Air Bubbles in Tmp-Heptanoate at 22°C Containing Various Concentrations of N-1-phenyl-1-Naphthylamine.
(B) Foaminess by Test Method 3213 of the Same Series of Solutions at the Same Temperature.

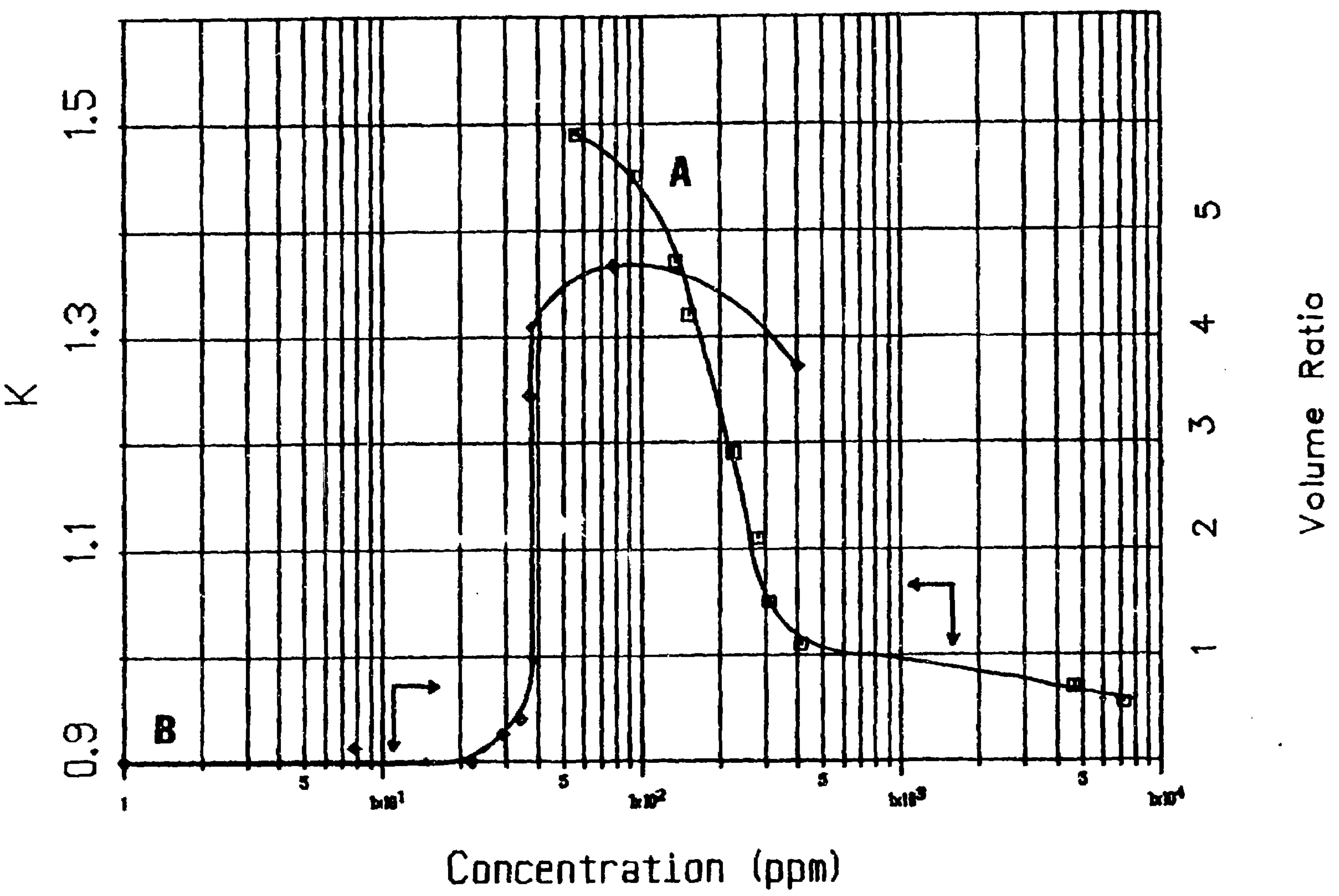

Figure 129. (A) Comparative Rates of Ascent (Corrected for the Effect of the Wall) of Air Bubbles in Mineral Oil at 22°C Containing Various Concentrations of Span 20.
(B) Foaminess by Test Method 3213 of the Same Series of Solutions at the Same Temperature.

SECTION XV

CONCLUSIONS

1. Surface activity of silicone polymers in synthetic lubricants: (See Section III)

Silicone polymers are more soluble in synthetic lubricants than in hydrocarbon oils. Unlike hydrocarbon-based solutes, which hardly affect the surface tension of organic liquids, silicone polymers are strongly surface-active when dissolved; and can reduce the surface tension by several mN/m (milliNewtons per meter.) This surface activity explains the tendency of such solutions to foam. The foam-inhibiting action of silicone polymers above their solubility point, which is pronounced in hydrocarbon oils, is absent in tmp-heptanoate, perhaps because the lowered surface tension of the oil, resulting from the silicone polymer already in solution, does not allow the undissolved silicone to spread on the foam lamellae; which spreading is a requisite for a foam inhibitor.

2. Foam induced by oil additives and mixtures thereof. (See Section IV)

Tricresyl phosphate is not by itself a foam-inducing solute in tmp-heptanoate, but when combined with certain other oil additives, such as N-phenyl-1-naphthylamine or phenothiazine, a synergism occurs with respect to foam. We find that the tricresyl phosphate promotes the rate of adsorption of its co-additives without affecting their ultimate equilibrium.

3. Effects of oil additives on compressional surface tension. (See Section VIII)

An oil without any additive shows no change of its surface tension when its surface is made to contract; but the presence of a surface-active additive can be detected by this means, as the solute adsorbed at the surface is compressed on contraction and a lowering of the surface tension results. This test is more sensitive to detect such an additive than a mere measurement of the equilibrium surface tension, which, for most nonaqueous solvents, shows almost no change even in the presence of a surface-active solute: compression of the adsorbed film is required to bring its surface concentration up to the detectable level. We find that the ability of an oil to foam correlates with a lowering of the surface tension on contracting the surface, except in these cases where we have reason to suspect the operation of an alternative mechanism of foam stabilization (see paragraph 8 below.)

4. Effects of oil additives on the rate of ascent of a bubble. (See Section XIV)

Another sensitive diagnostic test for the presence of surface activity in an oil solution is the reduction of the rate of ascent of a single bubble in the solution. As the bubble rises, the adsorbed film (if one exists) is swept to the rear of the bubble, where it is concentrated. The ultimate effect is a reduction of the rate of ascent of the bubble by a factor of up to two-thirds. We find that in the range of concentrations where this effect takes place, single bubbles floating on the surface of the liquid are stabilized, although large volumes of foam are not obtained until the concentration of solute is much greater.

5. Effects of oil additives on gas entrainment. (See Section V)

Measurements of the entrainment of nitrogen gas by oils and oil solutions reveal parallel behavior with measurements of foaminess. The more productive of foam is the oil solution, the more gas is entrained on aeration and the slower is its rate of escape from the oil.

6. Effects of oil additives on gas solubility. (See Section X)

Oil additives that stabilize oil foam also increase the solubility of nitrogen in the oil. The solubility of nitrogen increases with pressure and decreases with temperature. The increase of nitrogen solubility in these solutions also increases their propensity to foam expansion on reduction of pressure, e.g. with altitude, in an aircraft engine.

7. Effects of oil additives on surface viscosity.
(See Section VII)

The effect here is small, so that foams of great stability, such as are produced by soaps or detergents in water, the stabilities of which are ascribed to a viscous or plastic skin, are not produced in oil foams by the customary additives. The foams that are produced fall into the class of transient or evanescent foams, like the foam on a glass of champagne, with stabilities measured in seconds or at most a few minutes. In spite of these low stabilities, the oil retains gas long enough to cause various problems in the functioning of the lubricant.

8. Effect of oil additives on electrical surface potential.
(See Section XI)

Some solutes (e.g. Aerosol OT, phenothiazine) in tmp-heptanoate give solutions that foam, yet show no sign of surface activity on contraction of their surface. These solutions, however, when tested for electrical surface potential, yield appreciable values, demonstrating the presence of electric charges at the liquid surface. These findings indicate the functioning of the electrostatic mechanism of Derjaguin[13], i.e., that foam may be stabilized by charges of like sign on opposite sides of the liquid lamellae, preventing, by their mutual repulsion, any thinning of the liquid film that would normally take place, whether by hydrodynamic drainage or capillary flow. The electrostatic mechanism is not usually suspected as operative in oil solutions.

9. The influence of container shape on foam flooding.
(See Section XIII)

A vessel with outwardly flared sides promotes the molecular diffusion of gas through the liquid lamellae, and so accelerates destabilization of the foam. Foam flooding that would occur in a cylindrical container may be controlled by so designing vessel shape to allow the foam/air interface to increase in area as the foam expands in volume.

SECTION XVI

RECOMMENDATIONS FOR FURTHER INVESTIGATIONS

The work reported here has settled upon two mechanisms out of the many that have been attributed by theorists as explanations for foam stabilization. These are:

(a) The Gibbs-Rayleigh mechanism that ascribes local differences of surface tension in the lamella as the causative factor in its stability; and

(b) The Derjaguin mechanism of electrostatic repulsion between opposite sides of the lamella as the causative effect.

The former mechanism is demonstrated (see Section VIII above) by the results obtained on contraction of the surface of the oil solution, where a difference of surface tension is observed if surface activity is one of the properties of the oil solution. The device we used is slow in functioning compared to the rapid contractions and expansions that occur in the actual units of a foam; but it compensates for its slowness by the large factor of area contraction that it performs on the liquid surface. An apparatus that would come closer to matching the model of the Gibbs-Rayleigh mechanism would reverse the emphasis, relying on a rapid rate of contraction-expansion cycling to compress and decompress the adsorbed solute before the processes of desorption and adsorption, respectively, have time to act; and therefore not requiring a large contraction-expansion ratio to elicit the effect.

A means to this end may be provided by the study of capillary surface waves. A close relation exists between the properties of surface waves and the dynamic response of an interface to a disturbance of its equilibrium.[42] Both production and stabilization of bubbles and foam depend on the same dynamic surface properties that govern the propagation and damping of surface waves. An analysis of the hydrodynamics and mass transfer interactions at the liquid/gas surface gives the surface viscoelastic properties in terms of surface elasticity (dyne/cm) and surface viscosity (surface poise.)

Another technique to determine viscoelastic properties of the liquid surface is the pulsating-bubble method.[43] [44] [45] The method is based on the following principle:

A bubble of definite size is formed at the tip of a small capillary, dipped into a liquid. The bubble is forced by a special electromechanical system to radial harmonic pulsations of definite amplitude. The force necessary to obtain the required pulsations of the bubble is measured as a function of the pulsation frequency and the concentrations of solution. The magnitude of this driving force depends on the viscoelastic properties of the liquid surface surrounding the bubble.

These techniques are worth developing for oil solutions, to which they have not yet been applied, because they measure viscoelastic properties of the surface, which, for some <u>aqueous</u> solutions at least have been shown to be related directly to foam stability.[6] Viscoelasticity is not measured directly by our technique of detecting surface activity by contracting the surface, as described in Section VIII above, although the property can be inferred if changes of surface tension on compression are observed. But viscoelasticity need not be occasioned solely by these changes of the surface tension; it might be the result of other causes as well, such as electrical charges at the surface, which, on expansion or contraction of the surface of a solution that carries like charges, would tend to initiate reverse movements of the liquid surface, and so would damp ripples by an electrostatic mechanism. Viscoelasticity engendered in this way would account for the foaminess of aqueous solutions of electrolytes, which have higher surface tensions than the solvent, so that the Gibbs-Rayleigh mechanism of bubble stabilization would not explain the foaminess of such salt solutions. In the same way, oil solutions that show no surface tension change on surface contraction may yet foam by an electrostatically induced mechanism.

One of the results of the present work is the similarity of behavior that it reveals between the oil solutions that foam and aqueous solutions of weakly surface-active solutes, or even of strongly surface-active solutes at dilutions so great that the effect of the solute on the surface tension of water is barely perceptible. Presumably, like the oil solutions that foam, they too would show a decrease of surface tension on compression of their surface. Such comparisons have not yet been made, but should be part of the continuing investigation.

REFERENCES

1. J.W. Gibbs, Scientific Papers, Vol. 1, Longmans, Green, and Co., London, 1906, pp 300-314.

2. J.W. Strutt (Lord Rayleigh,) Scientific Papers, Vol. 3, Cambridge University Press, Cambridge, 1902, pp 351-362.

3. W.E. Ewers and K.L. Sutherland, Aust. J. Sci. Res. Ser. A, 5, 1697 (1952).

4. M. van den Tempel, J. Lucassen, and E.H. Lucassen-Reynders, J. Phys. Chem. 69, 1798, (1965).

5. A.I. Rusanov and V.V. Krotov, Prog. Surf. Membr. Sci., 13, 418 (1979).

6. K. Malysa, K. Lunkenheimer, R. Miller, and C. Hartenstein, Colloids and Surfaces, 3, 329 (1981).

7. A. Sheludko, C.R. Acad. Bulg. Sci. 9, (1), 11 (1956).

8. R.J. Mannheimer and R.S. Schechter, J. Colloid Interface Sci. 32, 212 (1970).

9. T.Yasukatsu, K. Saburu, and T. Nobuyuki, ASLE Trans., 21, 351 (1978).

10. N.L. Jarvis, J. Phys. Chem., 70, 3027 (1966).

11. J.J. Bikerman, Foams, Springer-Verlag, New York, 1973, p. 106.

12. H.C. Maru, V. Mohan, and D.T. Wasan, Chem. Eng. Sci., 34, 1283 (1979).

13. B.V. Derjaguin and A.S. Titijevskaya, Proc. 2nd Intnl Congr. Surface Activity, Butterworths (London), 1, 210 (1957).

14. R.H. Ottewill, D.L. Segal, and R.C. Watkins, Chem. Ind. (London), 17 January 1981, 57.

15. G. Nishioka, L. Lacy, and B.R. Facemire, J. Colloid Interface Sci., 80, 197 (1981).

16. S. Ross and D.F. Townsend, Chem. Eng. Commun., 11, 347 (1981).

17. R.S. Drago, G.C. Vogel, and T.E. Needham, J. Am. Chem. Soc., 93, 6014 (1971).

18. A.J.Barry, "Viscometric investigation of dimethylsiloxane polymers," in High Polymer Physics, H.A.Robinson, editor, Chemical Publishing Co., Brooklyn, N.Y., 1948, pp 144-154.

19. "Foaming Characteristics of MIL-L-7808 Turbine Lubricants," AFAPL-TR-75-91; Standard Test Method for Foaming Characteristics of Lubricating Oils.

20. Air Release Value, Institute of Petroleum 313/74. This method is technically identical with DIN 51381.

21. D.W. Criddle and A.L. Meader, J. Appl. Phys. 26, 838 (1955).

22. R.C. Watkins, J. Inst. Petroleum, 59, 106 (1973).

23. R.M. Mendenhall and A.L. Mendenhall, Jr., Rev. Sci. Instrum., 34, 1350 (1963).

24. R.M. Mendenhall, Arch. Environ. Health, 6, 74 (1963).

25. R.J. Mannheimer and R.S. Schechter, J. Colloid Interface Sci., 32, 212 (1970).

26. J.J. Bikerman, Trans. Faraday Soc., 36, 634 (1938); Idem, "Foams," Springer-Verlag, New York, 1973, pp 78-80.

27. Gibson, H. and McElroy, R., "Air Release from Mineral Oils," Ph. D. dissertation, University of Strathclyde, Glasgow, 1980.

28. B.V. Deryagin and Yu.V. Gutop, Kolloidn. Zh.,24, 431 (1962); Colloid J. USSR (Engl. Transl.) 24, 370(1962).

29. V.G. Gleim, V.M. Vilenskii and S.G. Tereshchenko, Kolloidn. Zh., 32, 849 (1970); Colloid J. USSR (Engl. Transl.) 32, 713 (1970).

30. G.K. D'yakonov, Zh. Tekhn. Fiz. [Journal of Technical Physics,] 12, 302 (1942); Chemical Abstracts, 37, 5299-5300 (1942).

31. V.G. Levich, Physicochemical Hydrodynamics, Prentice-Hall, Inc.,New York, N.Y., 1962, pp 395,432,448.

32. W. Rybczynski, Bull. Acad. Sci. Cracovie (1911), 40.

33. J. Hadamard, Compt. rend., 152, 1735 (1911).

34. F.H. Garner and A.R. Hale, Chem. Eng. Sci.,2, 157 (1953).

35. F.H. Garner and D. Hammerton, Chem. Eng. Sci.,3, 1 (1954).

36. J.V. Robinson, J. Phys. Colloid Chem., 51, 431 (1947).

37. R.M. Griffith, Chem. Eng. Sci., 17, 1057 (1962).

38. F.H. Garner, Trans. Inst. Chem. Eng., 28, 88 (1950).

39. J.T. Davies, Adv. Chem. Eng., 4, 33 (1963).

40. S. Okazaki, Y. Miyazaki and T. Sasaki, Proc. 3rd. Intern. Congr. Surface Activity, Mainz, Germany, 2, 549 (1961).

41. J. Lucassen and M. van den Tempel, J. Colloid Interface Sci., 41, 491 (1972).

42. E.H. Lucassan-Reynders and J. Lucassan, Adv. Colloid Interface Sci., 2, 347 (1969).

43. G. Kretzschmar and K. Lunkenheimer, Ber. Bunsenges. Phys. Chem., 74, 1064 (1970).

44. K. Lunkenheimer and G. Kretzschmar, Z. Phys. Chem. (Leipzig), 256, 593 (1975).

45. K.D. Wantke, R. Miller and K. Lunkenheimer, Z. Phys. Chem. (Leipzig), 261, 1177 (1980).

☆ U.S. GOVERNMENT PRINTING OFFICE 759-062/791